The Change in the Horizontal Position of the Dune Toe and Vegetation Line on Beaches Within the Waikato Region

A thesis

submitted partial fulfilment

of the requirements for the degree

of

Master of Science (Research) in Earth Sciences

at

The University of Waikato

by

Celeste Jade Davies-Calway

THE UNIVERSITY OF

WAIKATO

Te Whare Wānanga o Waikato

2020

Abstract

Beaches are highly variable landscapes that are constantly changing in response to a range of climatic variables. For example, local wind can cause the movement of sand across the beach and accretion, whilst storms that occur far from the beach create waves and surges which also changes the shape and morphology of the beach. The lower beach face is inundated for longer during a tidal cycle and therefore is subjected more often to wave action conversely, the upper part of the beach is inundated less often and therefore is less affected by wave energy. When storms occur, water levels are higher along the beach, waves are brought into contact with the upper beach face and erosion occurs. This erosion causes escarpment of the dune face and landward movement of the beach face, where sand is transported to offshore bars in the surf zone. Changes also occur during fair weather conditions where accretion occurs across the beach face and dune area and sand is transported back up onto the beach and sand dunes.

Beach morphology has traditionally been monitored using beach profiles, however new methods are emerging that provide more information with the potential for greater spatial and temporal data collection. In New Zealand the vegetation line and the position of the dune toe is often used as a proxy for the shoreline and setback distances are measured relative to this feature. Beach morphodynamics have been studied extensively but typical monitoring and predictive methods are not optimised to track and predict changes in the dune toe position. Beach profile surveys are the most common and reliable monitoring method used for monitoring beaches and they are used extensively throughout the world. Although beach profiles give valuable information on several different aspects of beach processes, they may not be the optimal method for tracking dune toe movement and there are other methods that might be more effective.

The aim of the research was to provide information to help optimise the monitoring and prediction of changes in the dune toe by determining: (i) the horizontal and vertical variation of the dune toe to establish how often the horizontal and vertical position of the sand dune toe changes, (ii) the alongshore variation of the dune toe along the beach length, (iii) what causes the changes in

the dune toe, (iv) compare using the dune toe for beach monitoring with traditional beach monitoring methods, (v) testing different methods to measure the dune toe and vegetation line, (vi) predicting the dune toe in the future using a model. The main study sites for the research were Whangapoua Beach, Matarangi Beach, Buffalo Beach, Hot Water Beach and Tairua beach of eastern Coromandel Peninsula, and Ngarunui Beach, Raglan, where field surveys were conducted. An historical dataset of beach profiles from 20 Eastern Coromandel beaches were analysed for long term patterns. A new method for measuring dune toe using video analysis and a model for predicting the future dune toe changes was tested at Tairua Beach, Coromandel Peninsula.

The results show that, from the field survey of beach profiles, there was low variability at the dune toe compared with further down the beach. The range of distribution of the vegetation line was larger than the range of distribution for the dune toe and the dune toe was generally more seaward than the vegetation line. The vegetation line was generally not at the same location as the dune toe which has strong implications for using vegetation as a measure of dune movement. The alongshore dune toe underwent small changes throughout the survey period and there was alongshore variation of the dune toe, along with changes in the dune toe horizontal position and height of the dune toe throughout the year survey period, which was expected. Video analysis was shown to be a potential new technique for measuring the vegetation line which could be used for beach monitoring. A model was used to predict the change in the dune toe, and it predicted that there was no change in the dune toe between 1998 and 2011; however, the analysis of the imagery showed there were numerous occasions where water reached the dune toe and therefore erosion of the dune toe occurred.

Acknowledgements

Table of Contents

List of Figures

List of Tables

Chapter One

Introduction

1.1 Importance and Motivation of the Study

The vast coastline of the Waikato Region includes the beaches of eastern Coromandel Peninsula in which are popular holiday destinations and have a high amenity value to the public. However, coastal developments resulting from the popularity of Coromandel beaches has caused a greater potential for erosion and poor beach states, due to modification of the sand dunes within the region. Coastal developments of building houses on top of sand dunes that are far too close to the beach, cause the inability of natural processes, including the movement of sand dune landward and seaward to occur over long time periods, resulting in damage to property, the need for seawall and other protective structures to be constructed along the coast and loss of amenity value. Naturally, well established sand dunes also protect the areas behind the coastline from flooding and inundation, which will become more of a focus due to future sea level rise (Splinter & Palmsten, 2012).

Beach profiles have been a reliable beach monitoring tool that gives valuable information on several different beach aspects, however beach profiles can be expensive to use for beach monitoring and provide a small range of spatial and temporal data. There are a number of other techniques that are now present which can provide valuable multipurpose datasets with a high temporal frequency. Measuring the dune toe is a new technique that could be a useful beach monitoring tool in the future where valuable information of how often the sand dunes move, relates directly to the setbacks of houses and flooding protection of the sand dunes. Due to the high importance of risk management along coastal beaches and areas, including the setback distances for coastal developments along beaches and the potential risk of coastal flooding, measuring the vegetation line and dune toe of sand dunes could provide more useful information for determining the risks within the coastal beach environment and making risk management decisions (Healy, 2002; Splinter & Palmsten, 2012). By

1

giving recommendations to Waikato Regional Council (WRC) on how often the horizontal position of the dune toe moved along Coromandel Beaches, along with the frequency and spatial distribution necessary for effective and efficient beach monitoring using the vegetation line and dune toe, risk management for Coromandel beaches may be improved within the future, along with future coastal settlement planning.

1.2 Research Aims and Objectives

The aim of the research was to provide information to Waikato Regional Council to help optimise the monitoring and prediction of changes in the dune toe by determining: (i) the horizontal and vertical variation of the dune toe to establish how often the horizontal and vertical position of the sand dune toe changes, (ii) the alongshore variation of the dune toe along the beach length, (iii) what causes the changes in the dune toe, (iv) compare using the dune toe for beach monitoring with traditional beach monitoring methods, (v) testing different methods to measure the dune toe and vegetation line, (vi) predicting the dune toe in the future using a model.

1.3 Thesis Outline

Following on from this chapter, this thesis is separated into chapters based on different methods and measurements of the vegetation line and dune toe.

Chapter 2: Study site descriptions

Chapter 2 consists of the study site descriptions for the Coromandel Beaches used for analysis from both the historic beach profile dataset and the field surveys completed of beach profiles and alongshore dune toe, showing the detail of each analyses and range of data sources used.

Chapter 3: Traditional Methods of Using Beach Profiles to Measure Dune Toe and Beach Morphology

In Chapter 3, the short-term change in the dune toe and beach morphology of five Coromandel Beaches and Ngarunui Beach, Raglan is analysed. The chapter shows the information gained from using the traditional method of beach profiles to

measure beach morphology and highlights how often the dune toe moves compared with other areas of the beach face.

Chapter 4: Frequency and Magnitude of Changes to the Alongshore Dune Toe and Vegetation line

Chapter 4 presented the historic change in the horizontal position of the dune toe and vegetation line, and the change in the alongshore dune toe over a one-year period. The distribution of the dune toe compared with the vegetation line was assessed.

Chapter 5: Video Analysis of the Horizontal Position of the Vegetation line

Chapter 5 presented a new method used to measure the vegetation line using video analysis. A new technique was formed and tested on imagery of Tairua Beach and an analysis of changes to the beach morpohology is undertaken to a high level of detail.

Chapter 6: Using a Simple Model to Predict Observed Dune Toe Changes

An existing dune toe erosion model was produced and tested at Tairua Beach. Where predictions from the model were compared with observations of water reaching the dune toe of imagery taken at Tairua Beach.

Chapter 7: Conclusions and Recommendations

A summary of the key results and findings showing the different methods in measuring the vegetation line and dune toe was provide in Chapter 7. This chapter outlined the future areas of research in order to measure the vegetation line dune toe more effectively and also provides recommendations for future beach monitoring using the vegetation line and dune toe.

Following the main results and analyses, a full reference list was provided and further information supporting the understanding of the movement of the dune toe and vegetation line are as follows:

Appendix A: Aerial photographs of field survey profile sites at 5 Coromandel Beaches and Ngarunui Beach Raglan.

Appendix B: Historic beach profiles for beach profiles along 20 Coromandel Beaches and Ngarunui Beach, including the field surveys for 5 Coromandel Beaches.

Appendix C: The alongshore dune toe for the magnitude and frequency of change in the vegetation line and dune toe, which includes the time series of vegetation line and dune toe for the 20 Coromandel Beaches and the vertical distribution and vertical position of the vegetation line and dune toe for 5 Coromandel Beaches.

Chapter Two

Study Site Descriptions

2.1 Study Sites

The chapter describes the physical aspects of each beaches in this research study, and the historic beach profile dataset that has been collected over the past 40 years across the eastern Coromandel beaches. A range of data and datasets were used in the study, with varying levels of analysis, ranging from an overview to in-depth analysis. Tairua Beach was used for the in-depth analysis of a single beach to show the mechanisms and variability of changes in great detail, where measurements of the vegetation line position were taken every month throughout the 20-year period. A slightly lower level of detail was used for the field sites, where an in-depth analysis of measurements taken every 6 weeks to 3 months, across a one-year time period. Lastly, the historic beach profile dataset has an overview of changes, that were shown from the beach profile measurements, throughout the last 40-year time period.

2.2 Eastern Coromandel Peninsula

The eastern Coromandel Peninsula is situated on the North Island of New Zealand (Figure 2.1). The predominate wave direction for Coromandel Peninsula is from the North East and the tidal range is 1.8 m (Gorman et al., 2003; Wood et al., 2009). All of the beaches across the Coromandel Peninsula are white sand pocket beaches that generally have intermediate or reflective beaches states (Wright and Short, 1985; Wood et al., 2009).
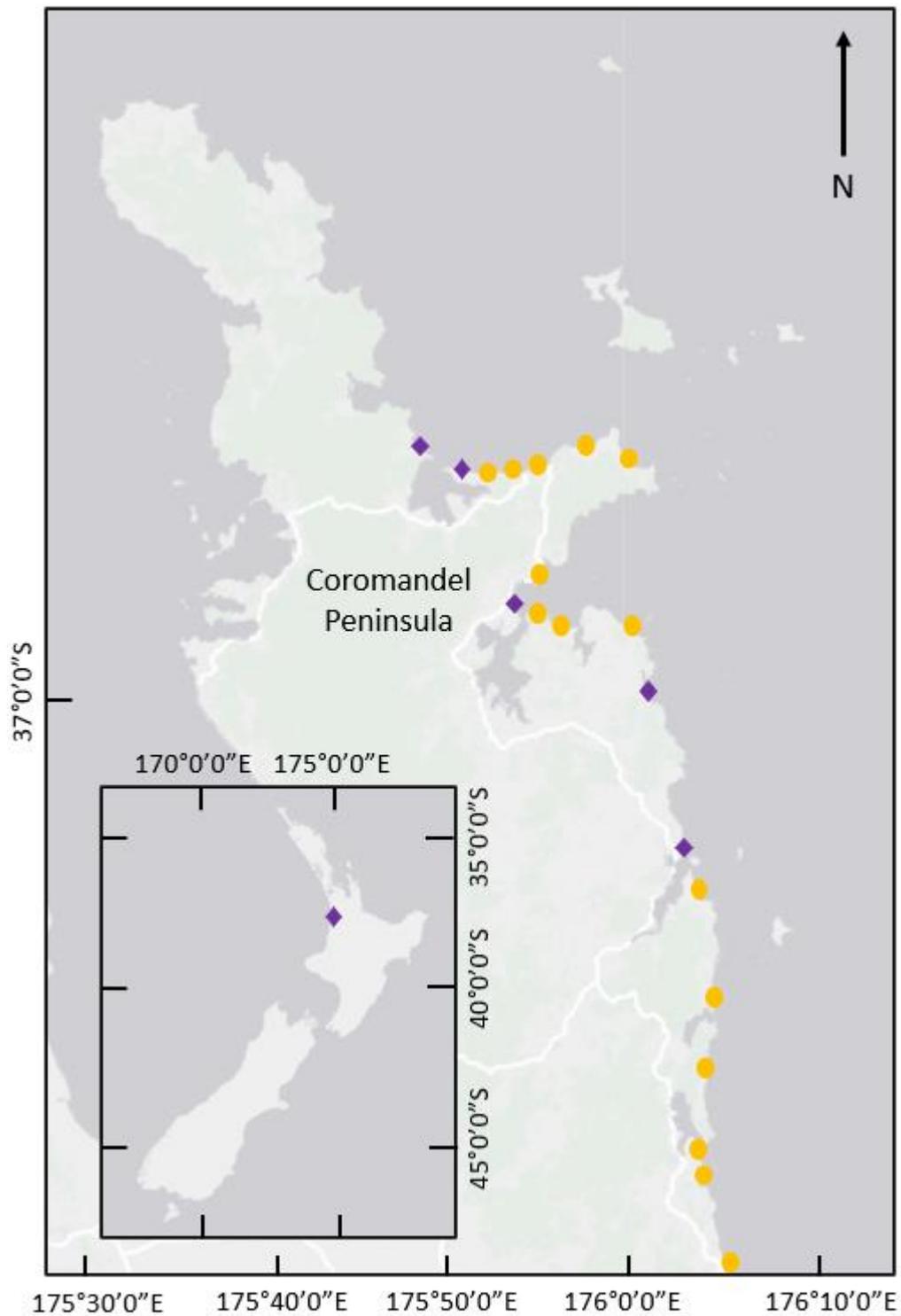
Figure 2.1. Study site map showing the location of Coromandel Peninsula on the North Island of New Zealand (inset). The six field surveyed beaches, of five Coromandel Beaches and Ngarunui Beach, Raglan (purple diamond). The historic beach profile dataset including 20 Coromandel beaches (orange circles and purple diamonds). The purple diamond in the inset represents Ngarunui Beach Raglan.

2.2.1 Historic Beach Profile Dataset

There are 20 Coromandel beaches within the historic beach profile dataset (Figure 2.1), which are listed below in geographical order from North to South:

- Whangapoua Beach
- Matarangi Beach
- Rings Beach
- Kuaotunu West Beach
- Kuaotunu East Beach
- Otama Beach
- Opito Beach
- Wharekaho Beach
- Buffalo Beach
- Maramaratotara Beach
- Cooks Beach
- Hahei Beach
- Hot Water Beach
- Tairua Beach
- Pauanui Beach
- Opoutere Beach
- Onemana Beach
- Whangamata North Beach
- Whangamata South Beach
- Whiritoa Beach

The historic beach profile dataset was provided by the Waikato Regional Council and consists of 40 years of beach profile data for the 20 eastern Coromandel Beaches, and 10 years of data for Ngarunui beach, Raglan. The first 10 years of data for the Coromandel Beaches was sporadic, however the last 30 years of data has been collected every 2 months to 6 weeks for the majority of the profile sites. The historic beach profile dataset was used to determine the beach morphology and how often the dune toe and vegetation line moved. Comments from the beach profile datasets were used to determine the historic vegetation line and

dune toe for each of the profile sites. The location of benchmarks is shown in Appendix A for the field surveys and on the WRC website for the Historical beach profile locations.

2.2.2 Field Survey Beaches

Five Coromandel Beaches were selected for field surveying throughout out the one-year period of between December 2018 and December 2019. The five beaches that were chosen for field surveys were Whangapoua Beach, Matarangi Beach, Buffalo Beach, Hot Water Beach and Tairua Beach. Theses beaches are considered to be indicator beaches (Wood et al., 2009) and have undergone different levels of human modification, where for example Buffalo Beach is heavily modified and Hot Water Beach only slightly modified. Field Surveys were taken every 6 weeks, however due to field surveying restrictions there was period of up to 11 weeks between surveys in some instances throughout the year. A total of 7 field surveys were completed at each of the five beaches throughout the year survey period. A site description for each of the five field surveyed Coromandel beaches are given below:

2.2.2.1 *Whangapoua Beach*

Whangapoua beach is approximately 1500 m long with a small river mouth present at the North end of the beach, and the Harbour entrance to Whangapoua Harbour to the South of the beach. Where there is a rocky headland situated between the beach and Harbour entrance. There is also a small rocky outcrop present at the North of the beach. There are three beach profile sites located along Whangapoua Beach that are 375 m and 500 m apart from one another, from the North to the South of the beach. There are houses situated on the top of the frontal sand dunes along the length of the beach, with a small setback of houses along the length of the beach.

2.2.2.2 *Matarangi Beach*

Matarangi Beach is approximately 4240 m long, where the harbour entrance is situated to the North of the beach. There are five beach profile sites located along Matarangi Beach that are 941 m, 690 m, 476 m and 1133 m apart from one

another. There are houses situated behind the frontal sand dune along the majority of the length of the beach, with a smaller setback of the houses situated on the frontal sand dune at the east end of the beach.

2.2.2.3 Buffalo Beach

Buffalo Beach is approximately 3720 m long, where there is a harbour entrance at the south of the beach, and two small river mouths at the middle and north of the beach. There are fifteen beach profile sites along the length of Buffalo Beach that are 541 m, 104 m, 186 m, 397 m, 511 m, 300 m, 206 m, 96 m, 57 m, 143 m, 114 m, 111 m, 105 m and 135 m apart from one another from the North to the South end of the beach. There is a sandbag-wall present along the north end of the beach between the end of the beach and the river mouth at the north of the beach. There are also two seawalls present, where one is situated at the northern end of the beach, where houses are present behind the seawall and one at the south end of the beach, where a road is situated. Through the middle of there is an area of open sand dunes present.

2.2.2.4 Hot Water Beach

Hot Water Beach is approximately 1925 m long, where are small river mouths present at both the north and south end of the beach. There are three beach profile sites along the length of Hot Water Beach that are 812 m and 493 m apart from each other from the north to the south of the beach. There are no houses situated on the sand dunes at Hot Water beach and the sand dunes are in a natural state.

2.2.2.5 Tairua Beach

Tairua Beach is approximately 1212 m long and there are headlands present at both ends of the beach, where the Tairua Harbour entrance is to the south of the beach. There are houses situated along the length of Tairua Beach, where at the northern and southern end of the beach, houses are situated on top of the frontal sand dunes. Through the middle of the beach, the houses are situated behind the frontal sand dunes and the setback of the houses is large.

2.2.3 A Detailed Analysis of Tairua Beach

A more detailed analysis was undertaken at Tairua beach, where the CamEra dataset of imagery taken at Tairua beach was used. The CamEra system takes a series of images every half an hour and these images are averaged to produce one 'exposure' image. There is one exposure image produced for each daylight hour.

Monthly images from 2002 and to 2019 were used for the analysis of the horizontal position of the vegetation line. Shoreline data was used to compare the vegetation line with other areas of the beach, the shoreline data can be accessed from Shoreshop dataset (Available at https://coastalhub.science/data). Tairua Beach was also used to validate a simple model produced for measuring dune toe erosion. The CamEra images were used for a quantitative analysis of whether observations of water hitting the dune toe water occurred, in order to validate the model. Significant wave height, tide and storm surge data also from Shoreshop data was used within the model.

2.2.4 Ngarunui Beach, Raglan

Ngarunui Beach, Raglan is situated on the West Coast of the North Island New Zealand. The predominant wave direction for Ngarunui beach and Raglan is from the South West and the spring tidal range at Nagrunui beach is between 2 and 3 m (Simarro et al., 2015; Gorman et al., 2003). Ngarunui Beach is a dissipative beach that has a large arbour entrance situated at the northern end of the beach. Ngarunui Beach is approximately 2920 m long and there are 6 beach profile sites along the beach length of the beach, these profile sites are 1052 m, 501 m, 270 m, 191 m and 256 m apart from one another. There are no houses situated along the sand dunes of the beach and the sand dunes are not modified.

Chapter Three

Traditional Methods of Using Beach Profiles to Measure Dune Toe and Beach Morphology

3.1 Introduction

The morphology and the shape of beaches are constantly changing due to a range of climatic variables that influence the coastal area. Accretion is caused by local wind forcing sand to move across and along the beach. Erosion is generally caused by storms that occur far away, which create waves and surges that also change the morphology of the beach (Davis & Fox, 1972; Hayes & Boothroyd, 1969). The duration of exposure to water across the beach face varies greatly, where the lower beach face is inundated every tidal cycle and for a longer duration each tide, and the upper beach face is inundated less often and for a shorter duration (Larson & Kraus, 1993; Ruz & Meur-Ferec, 2004). Water levels reach higher along the beach when storms occur, and waves reach the upper beach face more often causing erosion to occur across the upper beach face and occasionally the sand dunes. Erosion at the dune toe causes escarpment of the dune face and landward movement of the beach face, where sand is transported to offshore bars in the surf zone or to other areas of the beach (Castelle et al., 2015). Beach morphology also changes during fair weather conditions when accretion often occurs across the beach face, where sand is transported back up onto the beach and sand dunes (Winant et al., 1975).

Beach profile surveys are a traditional survey technique used for coastal monitoring to determine beach morphology and health. A subaerial beach profile is a cross-sectional transect which measures the elevation of the beach face across the transect, from the benchmark (usually located within the sand dunes) to the water's edge. Beach profiles give valuable information for a number of different beach processes, which include erosion and accretion of the cross-sectional area, sand volume changes and different temporal changes such as short-term changes from individual storm events and seasonally, along with long-term changes over

years to decades (Copper et al., 2000). Due to the beach profiles being a low-cost well-established technique used since the 1960's, there are now long beach profile datasets for many beaches allowing detection of long-term patterns. The Emery method was the first instance in which the beach profile technique was used and the reason why beach profiles are widely used and can be relied upon in the present day (Emery, 1961). The Emery method is a simple method in which the horizon and a known benchmark is used as a reference point for measuring the elevation across the beach face (Emery, 1961). The use of the 'Global Positioning System' GPS, in particular RTK-GPS (Real-Time Kinematic Global Positioning System), is now commonly used for measuring beach profiles and has replaced the Emery method due to its higher accuracy and precision, where the Emery method had an much higher error than using RTK-GPS (Harley et al., 2011; Emery, 1961; Andrade & Ferreira, 2006). The RTK-GPS method also measured the distance and height from a known benchmark to determine the cross-section of the beach face.

For this chapter, field surveys of beach profiles were taken at five Coromandel Beaches: Whangapoua Beach, Matarangi Beach, Buffalo Beach, Hot Water Beach and Tairua Beach, along with Ngarunui Beach at Raglan. The field surveys were taken over the over span of one year from December 2018 to December 2019, where seven field surveys were taken throughout the one year. The Waikato Regional Council benchmarks were used for the benchmarks of the beach profiles so that field surveys could be compared with Waikato Regional Council historic beach profile datasets. The field survey beach profiles show a high level of detail of short-term patterns throughout one year and the Waikato Regional Council historic dataset showed the general long-term patterns of beach morphology throughout a much larger range of Coromandel beaches and Ngarunui Beach, Raglan. All beach profiles from both datasets are relative to the Moturiki 1953 datum which is 0.014 m above mean sea level.

The aim of this chapter is to use beach profiles in order to determine changes of beach morphology for Coromandel Beaches and Ngarunui Beach, Raglan. The main focus of the chapter is determining the frequency of changes to beach morphology and understand its spatial distribution, for example comparing how and how often the sand dunes have moved above the dune toe, how the dune toe

has moved, along with how the beach face and intertidal area has also moved. Different time spans were investigated. The 2019 field surveys were analysed in depth throughout the year, determining where erosion and accretion has occurred. The Waikato Regional Council historic beach profile datasets were analysed for general trends over longer time periods, with a particular focus on long term trends at the dune toe and surrounding areas of the upper beach and sand dunes. Large erosion events were investigated and identified in order to determine potential frequencies of large sudden changes to the dune toe. This chapter represents the traditional and current method used for beach monitoring before other methods are explored for future use.

3.2 Expected Outcomes

The expected outcomes for this chapter are that the frequency of change observed in the beach profile will be related to the elevation of the beach and therefore the length of inundation during a tidal cycle and the likelihood of inundation during a storm. Specifically, a low frequency of change is anticipated on the upper beach area, where the water does not reach often, and high frequency of change is anticipated lower down the beach face, where water reaches often (Larson & Kraus, 1993). The beach profiles should show the sand dunes and above the sand dune toe does not move often at all and only small changes occur over time. It is expected that the dune toe will change with a slightly higher frequency than the sand dunes (Larson & Kraus, 1993; Houser, 2013). The dune toe is expected to go through large sudden landward movement when erosion events occur from storms and high tides, and slow incremental seaward changes of accretion during fair weather conditions. It is also expected that the large sudden landward movement of the dune toe will be during large storm events likely occurring during winter. Seawards movement of the dune toe during incremental accretion is likely to occur over the summer period each year (Dissanayake et al., 2015; Castelle et al., 2015; Winant et al., 1975). Lower down the beach on the lower beach face and across the intertidal area, the frequency of change will be much higher and more variable, where erosion and accretion will happen more frequently and at much high magnitude of change. The difference in variability is expected to be due to water reaching this area of the beach

significantly more often that further up the beach (Larson & Kraus, 1993; Ruz & Meur-Ferec, 2004).

3.3 Methods

3.3.1 Field Survey of Beach Profiles

The RTK GPS (GS16 GNSS receiver with CS20 controller network corrections using SmartFix ©) unit was used for field surveying of Coromandel beaches and Ngarunui Beach, Raglan. Fieldwork was completed on mostly sunny days, as changes in weather between the field location and the base station interferes with the workings of the RTK GPS. Beach Profiles were completed within two hours either side of low tide (+ or -2 hours of low tide).

3.3.2 Technical Methods of Using RTK GPS Unit

A new job was created, and the unit was adjusted to the correct datum and coordinate system. The coordinate system used was Mt Eden 2000 and the vertical datum used was Moutiriki 1953. A dataset of pre-existing coordinate systems for the benchmarks were loaded into the RTK GPS unit prior to going into the field, in order to have reasonable knowledge of the approximate location of the benchmarks for the beach profiles. The correct internet server used was GHST for Ngarunui Beach, Raglan and CORM for all of the Coromandel Beaches. The coordinate area used was for all the survey sites was Waikato 3817.

Once out in the field, ten points were taken at a known geodetic mark. Geodetic marks were taken from the LINZ Geodetic database (http://apps.linz.govt.nz/gdb/?mode=gmap). The list of the survey marks used for each beach are:

- BE1G (3/1V) (Ngarunui Beach-Raglan)
- EJUF (5/3V) (Whangapoa-Coromandel)
- F2TU (4) (Matarangi-Coromandel)
- BUGN (4/2V) (Buffalo Beach-Coromandel)
- BVVW (3/1V) (Hot Water Beach-Coromandel)
- DJQQ (5/3V) (Tairua-Coromandel)

The geodetic marks were measured with the height set of the survey pole at 2.000 m, before and after the survey of the beaches, to see if the there was any changes in the survey before and after the measurements of the beach.

3.3.3 Technique for Measuring the Beach Profiles

Once the geodetic marks were measured, beach profiles and the dune toe/vegetation line of the beach were measured. The RTK GPS receiver was mounted onto a pole attached to the top of a backpack and the height of the receiver was set at 1.738 m for all of the surveys.

The beach profile benchmark location was located. The survey was started by standing directly on the location of the beach profile benchmark, facing the ocean, and the first point of the profile was measured on this point. Each point measured was labelled with the site/benchmark of the beach profile being measured, and labelled with ascending numbers, i.e. 17ccs01, 17ccs02, 17ccs03. Once the first point was measured, a couple of steps were taken towards the ocean and perpendicular to the beach length, where the next point was measured from. Points were then taken, at every morphological change in the landscape (change in vertical height along the transect) or every couple of meters if there were no significant changes, until the ocean was reached, in which the beach profile is complete. Care was taken to stand upright and in a similar position when each point was taken to decrease the amount of error in measurement. Once the field survey was completed and the geodetic marks were measured after the field survey and the data was exported from the RTK GPS unit into an ASCII file and KML file and saved.

3.3.4 Benchmarks of Beach Profiles

The benchmarks used for the measured beach profiles were established benchmarks used by Waikato Regional Council over the last 40 years. There were a number of sites where the benchmarks have been destroyed and new benchmarks have been created which is shown within the historic beach profiles dataset. The location of the benchmarks was measured in relation to the Moturiki 1953 datum by Waikato Regional Council, and benchmark locations were

converted to the coordinate system of Mt Eden 2000, so that the benchmarks were found for the field survey profiles.

3.3.5 Data Analysis of the Beach Profiles

3.3.5.1 Field Survey Beach Profile Data Analysis

The field survey beach profiles were analysed using Matlab software. The field survey beach profiles data contained a label, coordinates, and a vertical height. The data was separated into each individual profile based on the label and the coordinates were converted into a horizontal distance from the benchmark location. An accurate and precise benchmark location was chosen from the field surveys and used as the reference point for which is considered the benchmark and the reference point beach profiles based from. The benchmark coordinates provided by Waikato Regional Council were in the form of a different coordinate system than Mt Eden and the accuracy and precise location of the benchmark was lost when converted. Therefore, the reference point from field surveys were used as the benchmark location. The beach profiles were checked, the outliers removed, and the profiles were plotted. A horizontal and vertical offset was then added to the beach profiles in order for the beach profiles to match the historic beach profile dataset. The horizontal and vertical offsets used were provided by Waikato Regional Council, in which was part of the BPAT software data process. Manual adjustment was necessary for some of the field survey beach profiles in order for the profiles to match the historic beach profiles accurately and precisely.

3.3.5.2 Historic Beach Profile Data Analysis

The historic beach profiles provided by Waikato Regional Council were previously processed in the BPAT software and provided in the form of an ASCII file. The data was formatted and exported into the Matlab software for processing. The data was then further edited, by taking out the vertical spikes that were present within the data and were likely caused by BPAT processing and the beach profiles plotted. The field survey beach profiles were then matched to and plotted against the historic beach profiles.

3.4 Results

3.4.1 Field Survey Beach Profiles

Figure 3.1-3.36 showed the beach profile for each profile location, the graph shows the cross-sectional beach contour where the horizontal axis represents the horizontal distance from the benchmark and the y-axis represents the vertical height.

3.4.1.1 *Whangapoua Beach*

Throughout the survey period from December 2018 to December 2019, there was little to no movement of the majority of the sand dune area behind the frontal sand dune at all three of the beach profile survey location of CCS11, CCS11-1 and CCS12 (Figure 3.1, 3.2 & 3.3). There was slight erosion below the dune crest at CCS11 and slight accretion above the dune toe at CCS12.

Throughout the summer period from early December to early March, there was slight accretion that occurred at the dune toe where the dune toe moved horizontally towards the sea and vertically upwards at CCS12 and vertically upwards at CCS11, whilst staying in the same position at CCS11-1. Across the beach face from below the dune toe to the intertidal area, accretion occurred at all three profile locations, where a small berm formed high on the beach face at CCS12, except for some erosion on the mid beach face at CCS11-1 where a berm disappeared.

From the time period of March to mid-May the dune toe did not move at any of the three locations and the small berm formed mid beach face at all three locations, where the berm was most pronounced at CCS12 (Figure 3.1). From May to early July, the dune toe accreted slightly at all three locations and across the lower beach face and intertidal area large amounts of erosion occurred. The small berm present disappeared also. During early July to the August, dune toe position does not move at any of the three locations. At CCS12 there is accretion that occurred across the mid beach face, there is slight erosion that occurred in the intertidal area of CCS11 and a large berm has formed at the lower beach face of CCS11-1, at the south end of the beach. Between August and the End of October

17

there are large amounts of erosion that occurs at all three locations of CCS12, CCS11 and CCS11-1. Where the berm disappears at CCS11-1 and at all of the locations the beach face was eroded the most at this time of year, during the end of winter, as shown in Figure 3.3. However, there was a small amount of accretion at the dune toe at the locations of CCS12 and CCS11-1. From the end of October to early December of 2019, the dune stayed in the same position and there were large amounts of accretion at all three locations. A large berm formed at CCS12 high on the beach face and a smaller berm was present lower on the beach face at CCS11-1.

From comparing the morphology of the Whangapoua beach from December 2018 to December 2019, the north of beach at CCS12 accreted with a big berm present, the middle of the beach at CCS11 experienced no net change where the upper beach face was lower and the lower beach face slightly higher. At the south end of the beach there were berm present at both time, however in 2019 the berm is less pronounced and lower on the beach face.
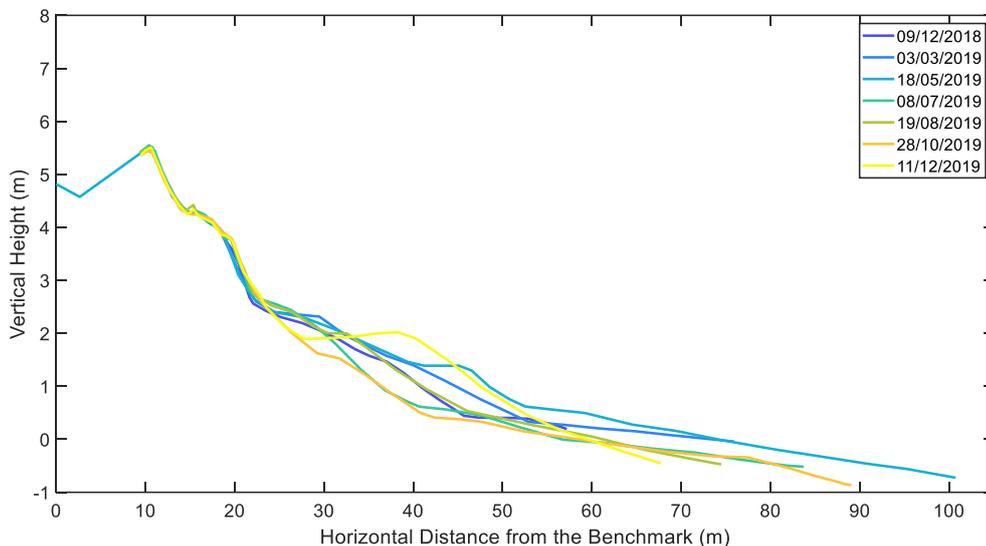
Figure 3.1. Beach profile of CCS12, Whangapoua Beach. Field surveys were taken 9th December 2018, 3rd March 2019, 18th May 2019, 8th July 2019, 19th August 2019, 28th October 2019 and 11th December 2019.
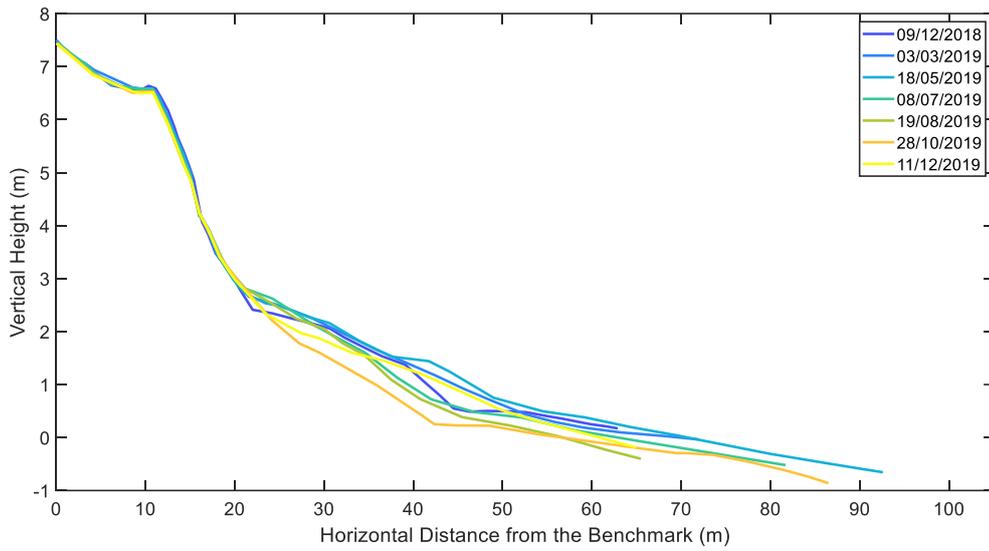
Figure 3.2. Beach profile of CCS11, Whangapoua Beach. Field surveys were taken 9ᵗʰ December 2018, 3ʳᵈ March 2019, 18ᵗʰ May 2019, 8ᵗʰ July 2019, 19ᵗʰ August 2019, 28ᵗʰ October 2019 and 11ᵗʰ December 2019.
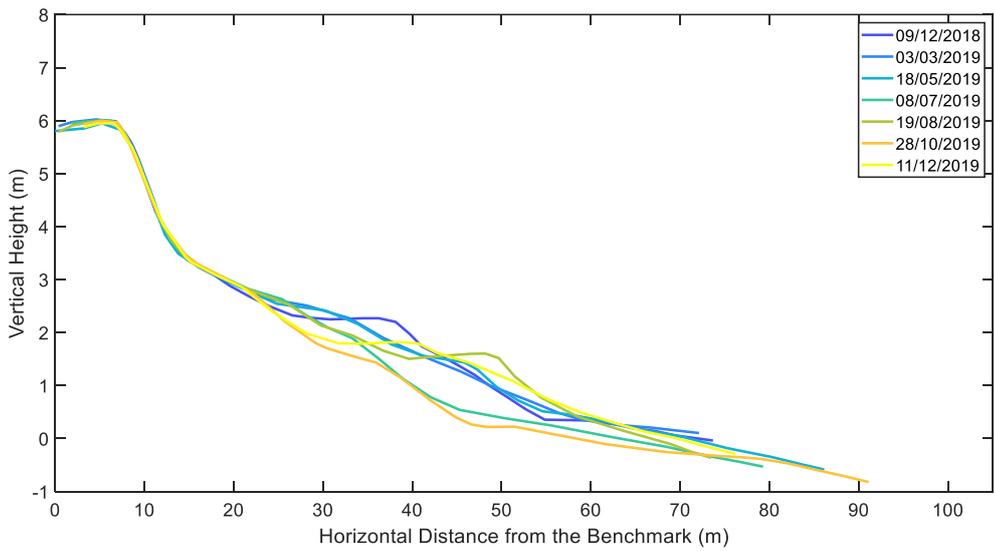
Figure 3.3. Beach profiles of CCS11-1, Whangapoua Beach. Field surveys were taken 9ᵗʰ December 2018, 3ʳᵈ March 2019, 18ᵗʰ May 2019, 8ᵗʰ July 2019, 19ᵗʰ August 2019, 28ᵗʰ October 2019 and 11ᵗʰ December 2019.

3.4.1.2 *Matarangi Beach*

Throughout the survey period from December 2018 to December 2019, there was little to no movement of the sand dune area at Matarangi except for a small amount of erosion at CCS13 and CCS17 below the dune crest, a small amount of erosion on the dune crest and the first frontal dune at CCS14 and accretion at the dune crest at CCS16. From March 2018 to December 2019, there was accretion of the frontal dune area at CCS17.

During the summer period from early December to early March there was accretion at the dune toe and across the beach face at CCS13, CCS14 and CCS15 where a small berm has increased in size at all three locations over the summer period. At CCS16, the small berm has stayed and there is a small amount of accretion above and below the berm. At CCS17, there was a small mound of sand formed at the dune toe position and accretion at the upper beach face. At the lower beach face and intertidal area, the large berm and mass of sand present in December underwent a large amount of erosion over the summer period.

During the time period of March to mid-May, accretion occurs at the dune toe at CCS13, CCS14 and CCS15 whilst staying in a stable position at CCS15 and eroded at CCS17. There was accretion at CCS13, CCS14 and CCS15, where the berm became more pronounced at CCS13 and CCS15 and moved landward at CCS14. The berm at CCS16 became more pronounced but there was slight erosion that occurred above and below the berm present on the beach face. At CCS17 which is located in the harbour entrance, there was erosion that occurred at the upper beach face and a large bank of sand formed seaward of the beach face with a large runnel forming in between the bank and beach face.

During the time period from May to early July, there was accretion of the dune toe at all locations along the beach with a small mound of sand forming in front of the dune toe at CCS13, CCS14 and CCS16. The largest amount of erosion during the survey period occurred from below the dune toe to the intertidal zone between May and early July for CCS13, CCS14, CCS15 and CCS16. At CCS17, the runnel present between the upper beach face and the sand bank, narrowed and the sand bank increased in size.

From July to the end of August, the ridge present in front of the dune toe has disappeared at CCS13 and CCS14, accretion of the dune toe has occurred at CCS5 and CCS16 and a small amount of accretion at the dune toe at CCS17. Accretion has occurred and a small berm has formed on the mid beach face at the locations of CCS13, CCS14, CCS15 and CCS16. At CCS17 there was erosion at the upper beach face and accretion across the lower beach face and intertidal zone where the runnel between the upper beach face and the sand bank has closed, and there has been accretion on the north side of the sand bank.

From August to the end of the October, accretion occurred at the dune toe of CCS13, CCS14, CCS15, CCS16 and CCS17. Erosion occurred from the upper beach to the intertidal zone at CCS13, CCS14, CCS15 and CCS16, where the berms decreased and moved further up the beach at all of the mentioned locations. Accretion occurred at the upper beach face at CCS17 and more sand filled into the area where the runnel was previously present. However, there was erosion on the north side of the sand bank.

From October to December, there was accretion at the dune toe at all of the locations along Matarangi beach, where there was new mound of sand present above the dune toe at CCS14 and CCS16. There was accretion across all of the locations of CCS13, CCS14, CCS15, CCS16 and CCS17 across the beach face and intertidal zone, with exceptionally large amounts of accretion at CCS15, CCS16 and CCS17. Berms that were present at CCS13 and CCS14 have disappeared, the berm present at CCS15 has become less pronounced and berm at CCS16 has increased in magnitude. AT CCS17 accretion has occurred on the northside of the prior sand bank.
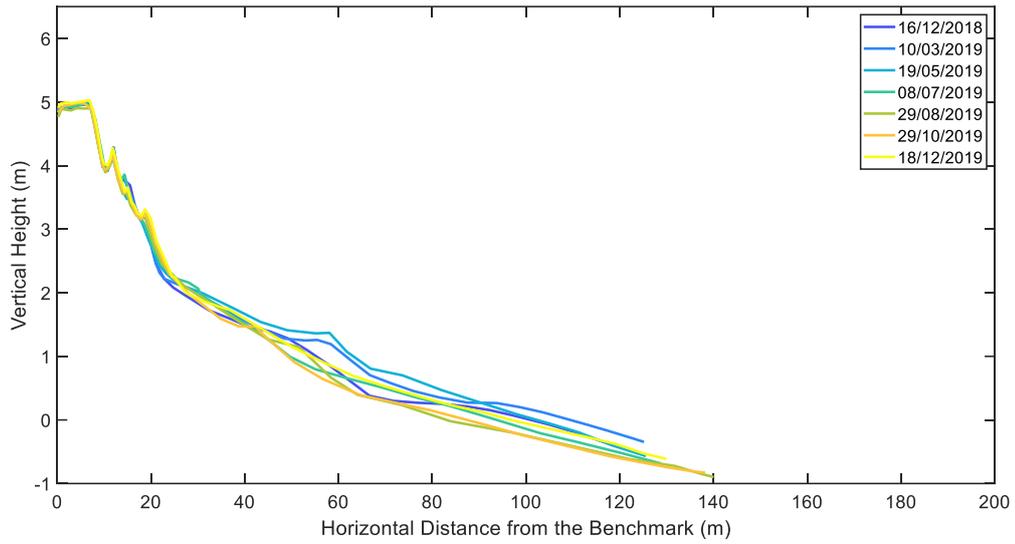
Figure 3.4. Beach profile of CCS13, Matarangi Beach. Field surveys were taken 16th December 2018, 10th March 2019, 19th May 2019, 8th July 2019, 29th August 2019, 29th October 2019 and 18th December 2019.
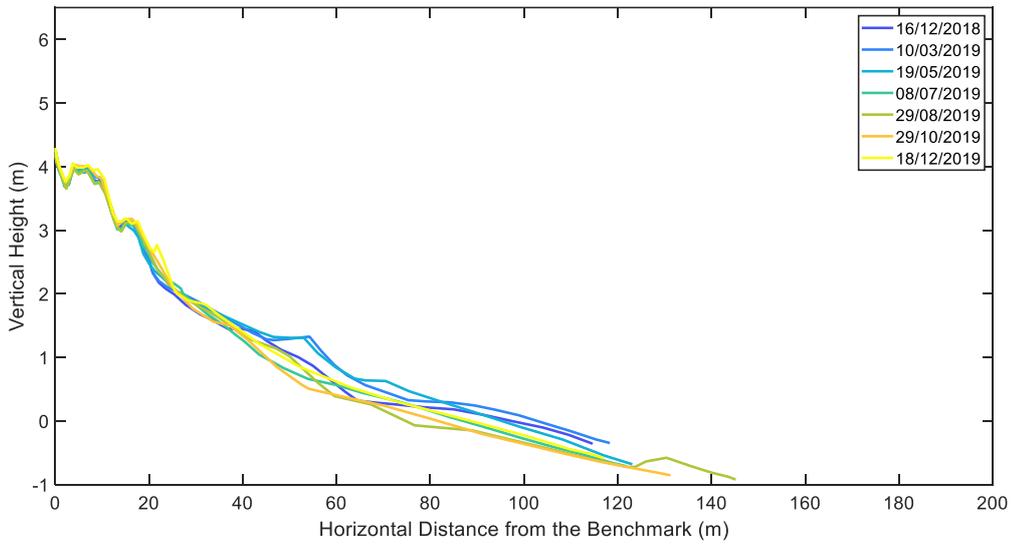
Figure 3.5. Beach profile of CCS14, Matarangi Beach. Field surveys were taken 16th December 2018, 10th March 2019, 19th May 2019, 8th July 2019, 29th August 2019, 29th October 2019 and 18th December 2019.
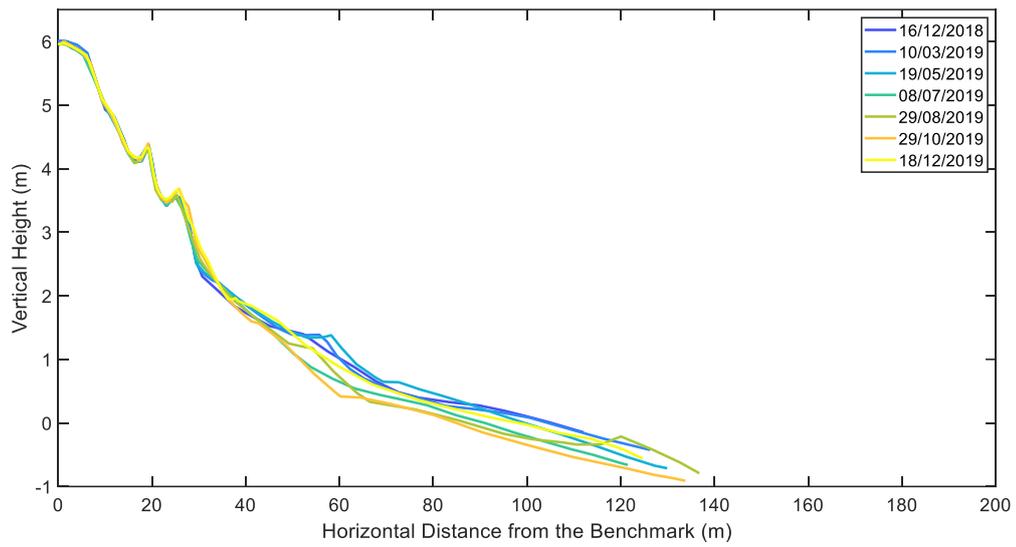
Figure 3.6. Beach profile of CCS15, Matarangi Beach. Field surveys were taken 16th December 2018, 10th March 2019, 19th May 2019, 8th July 2019, 29th August 2019, 29th October 2019 and 18th December 2019.
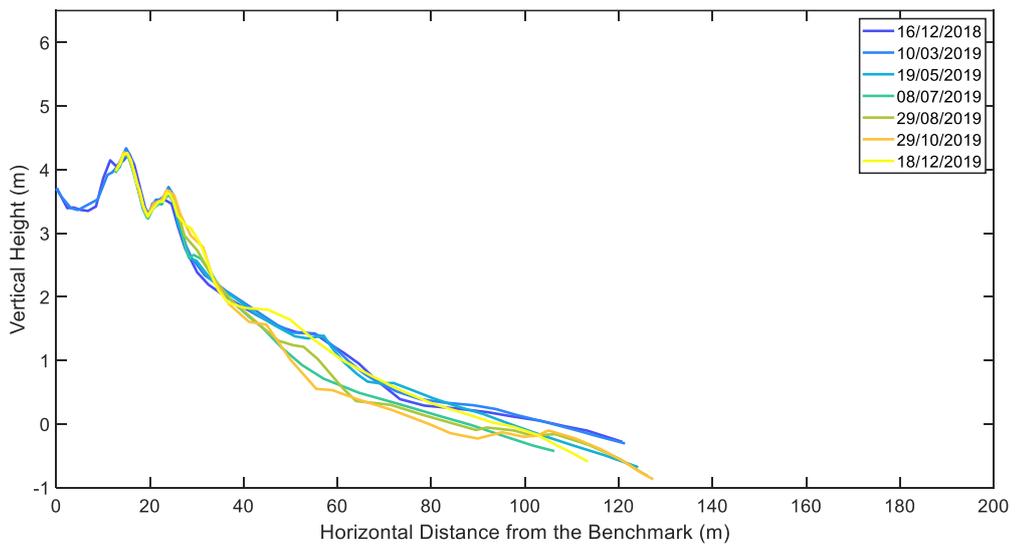
Figure 3.7. Beach profile of CCS16, Matarangi Beach. Field surveys were taken 16th December 2018, 10th March 2019, 19th May 2019, 8th July 2019, 29th August 2019, 29th October 2019 and 18th December 2019.
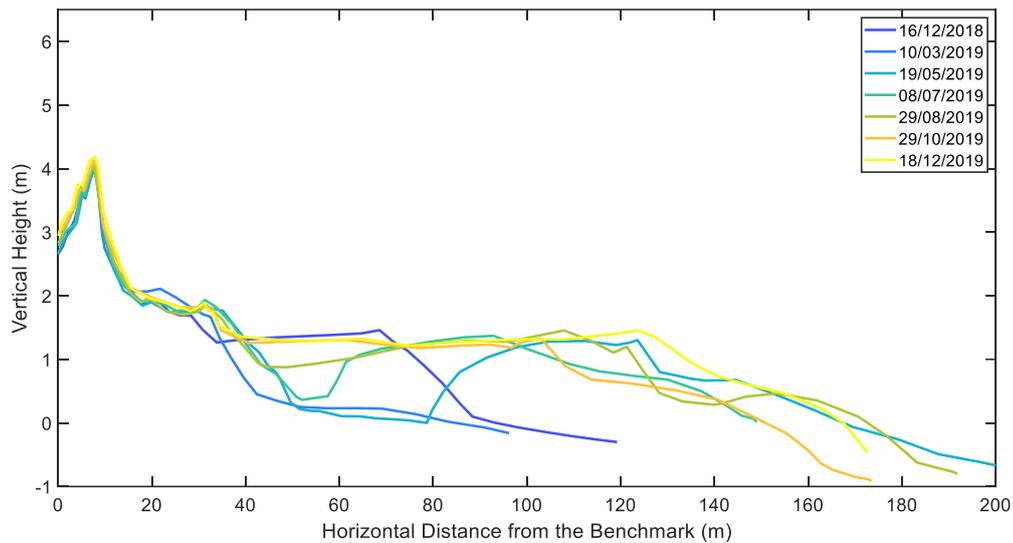
Figure 3.8. Beach profile of CCS17, Matarangi Beach. Field surveys were taken 16th December 2018, 10th March 2019, 19th May 2019, 8th July 2019, 29th August 2019, 29th October 2019 and 18th December 2019.

3.4.1.3 Buffalo Beach

The analysis of the beach profiles for Buffalo have been separated into beach profile locations at the north of Buffalo Beach which consisted of CCS24, CCS25, CCS25-2, CCS25-3 and CCS25/1 and at the south of Buffalo Beach which consisted of CCS26, CCS26/1, CCS27, CCS27/10, CCS27/8, CCS27/6, CCS27/2, CCS27/3, CCS27/4 and CCS27/5.

North of Buffalo Beach

Throughout the survey period there was no movement of the above the dune toe at CCS24, CCS25-2 and CCS25-3 (3.9, 3.11 & 3.12). There was a small amount of erosion at the location of CCS25 between December 2018 and March 2019 and August to October 2019, as shown in Figure 3.10. There was also landward movement that occurred at CCS25/1 in the sand dune area from between July and October (Figure 3.13).

During the time period from the end of December to early April, there was accretion of the dune toe at profiles CCS24, CCS25-2 and CCS25-3. There was erosion of the dune toe at CCS25 and CCS25/1 (Figure 3.10 & 3.13). Accretion that occurred across the beach face and intertidal area for CCS24 and CCS25. However,

at CCS25-2, the berm that was present disappeared and there was accretion at the upper beach face (Figure 3.11). Erosion occurred at both CCS25-3 and CCS25/1, situated south of the other profiles.

During the time period from April to May, there was slight erosion of the dune toe at CCS25 and CCS25-2. The dune toe was stable at CCS24 and CCS25/1, and the dune toe was accreted at CCS25-3. At CCS24 at the north end of the beach, there was erosion across the beach face and a small berm has formed in the intertidal area (Figure 3.9). A small amount of erosion has occurred on the beach face of CCS25/1. There was a large amount of accretion at the beach face and intertidal area at the locations of CCS25, CCS25-2 and CCS25-3, where a berm has form on the upper beach faces.

From May to mid-July, the dune toe was stable at CCS25 and CCS25/1 and accreted at CCS25-2 and CCS25-3, whilst there was erosion of the dune toe at CCS24. Further down the beach there was erosion at CCS24, CCS25, CCS25-2 and CCS25-3, where the berm became less pronounced at CCS25 and CCS25-2 and disappeared at CCS25-3 where there was accretion on the upper beach face. There was accretion of the beach face and intertidal area at CCS25/1.

From July to August, there was accretion of the dune toe at CCS24, CCS25, CCS25-2 and the dune toe was stable at CCS25-3. There was accretion of the beach face and intertidal area at the location of CCS24, CCS25, where a berm high on the beach face became more pronounced at CCS25. At CCS25-2 there was erosion across the beach face where a small berm formed, and accretion within the intertidal area. There was also a berm that formed at CCS25-3 in the same location on the beach face, where there was erosion across the beach face and intertidal area (Figure 3.12).

During the time period of August to the end of October, there was erosion of the dune toe at all of the beach profile locations of CCS24, CCS25, CCS25-2, CCS25-3 and CCS25/1. At CCS24, there was some erosion of the upper beach face and accretion of the lower beach face and intertidal area. At CCS25, CCS25-2 and CCS25-3, there was a large amount of erosion on the beach face which reached the lowest elevation of the beach face for the survey period, and there was

accretion in the intertidal area. Where at CCS25 there was a small berm that formed on the beach face and at CCS25-3 a berm formed in the intertidal area. At CCS25/1 there was also erosion from July to October time period.

From October to December, there was erosion of the dune toe at CCS24, and accretion of the dune toe at CCS25, CCS25-2, CCS25-3 and CCS25/1. Further down the beach, there was erosion of the beach face and intertidal area at CCS24. At the location of CCS25, there was a large amount of accretion that occurred and the berm became more pronounced, where a small amount of erosion occurred at in the intertidal area. There was accretion that occurred across the beach face and intertidal at CCS25-2. Whilst at CCS25-3, large amounts of accretion occurred at the upper beach face and a small amount of erosion at the intertidal area where the berm disappeared. At CCS25/1, there was a small amount of erosion at the dune toe and accretion lower down the beach.
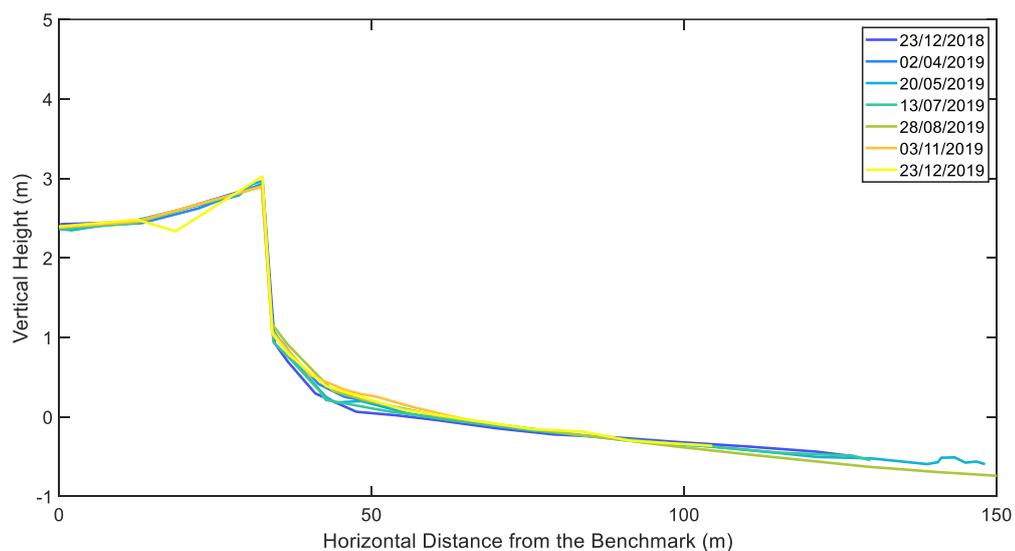
Figure 3.9. Beach profile of CCS24, Buffalo Beach. Field surveys were taken 23rd December 2018, 2nd April 2019, 20th May 2019, 13th July 2019, 28th August 2019, 3rd November 2019 and 23rd December 2019.
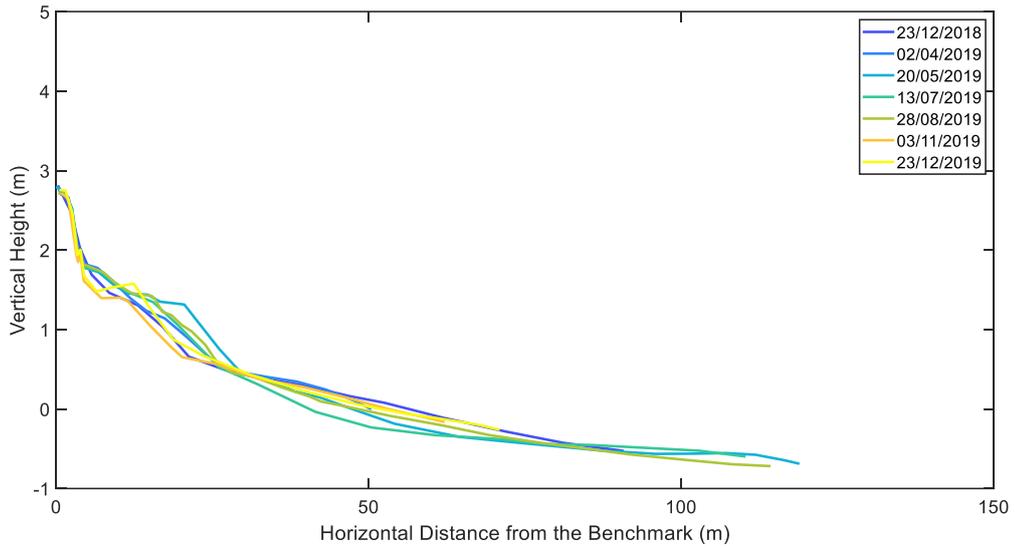
Figure 3.10. Beach profile of CCS25, Buffalo Beach. Field surveys were taken 23rd December 2018, 2nd April 2019, 20th May 2019, 13th July 2019, 28th August 2019, 3rd November 2019 and 23rd December 2019.
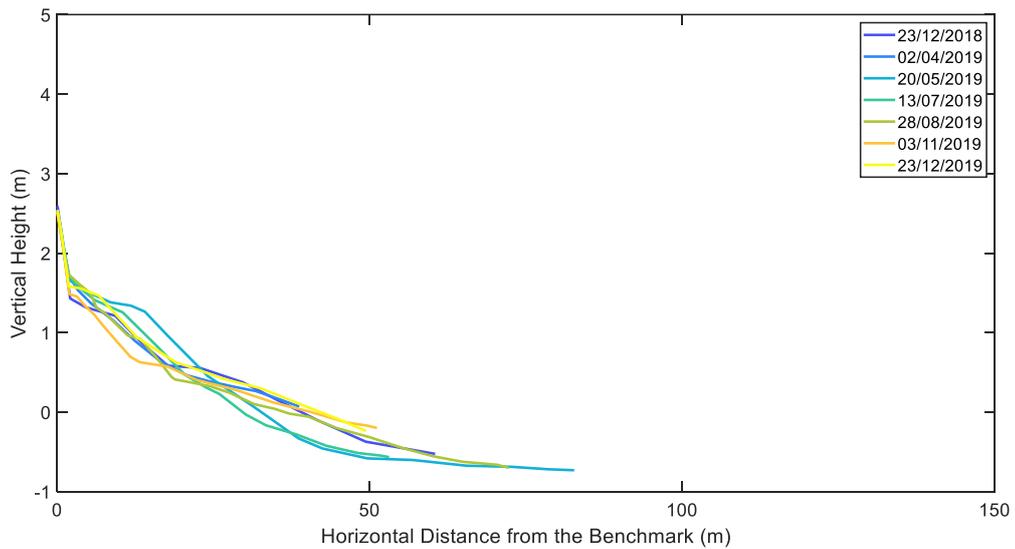
Figure 3.11. Beach profile of CCS25-2, Buffalo Beach. Field surveys were taken 23rd December 2018, 2nd April 2019, 20th May 2019, 13th July 2019, 28th August 2019, 3rd November 2019 and 23rd December 2019.
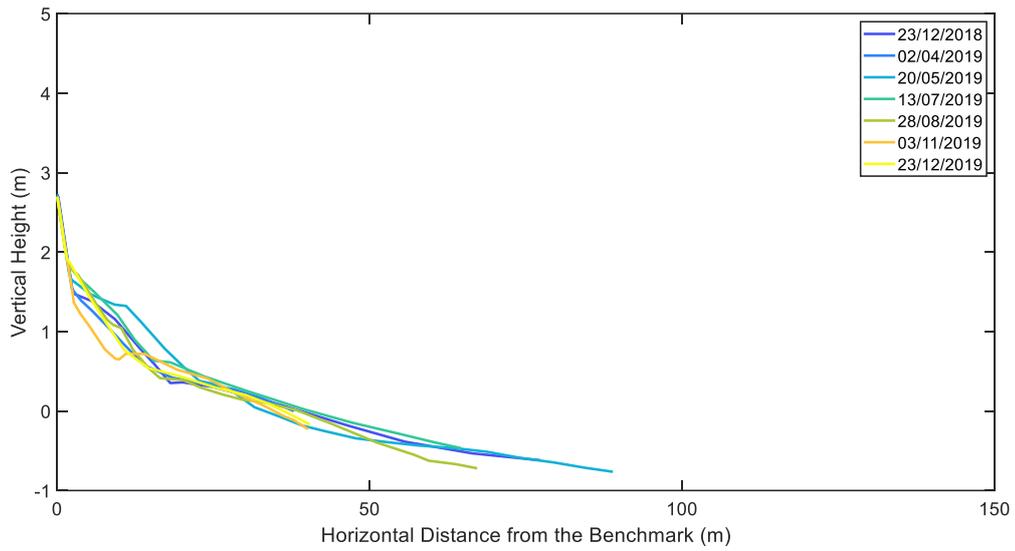
Figure 3.12. Beach profile of CCS25-3, Buffalo Beach. Field surveys were taken 23rd December 2018, 2nd April 2019, 20th May 2019, 13th July 2019, 28th August 2019, 3rd November 2019 and 23rd December 2019.
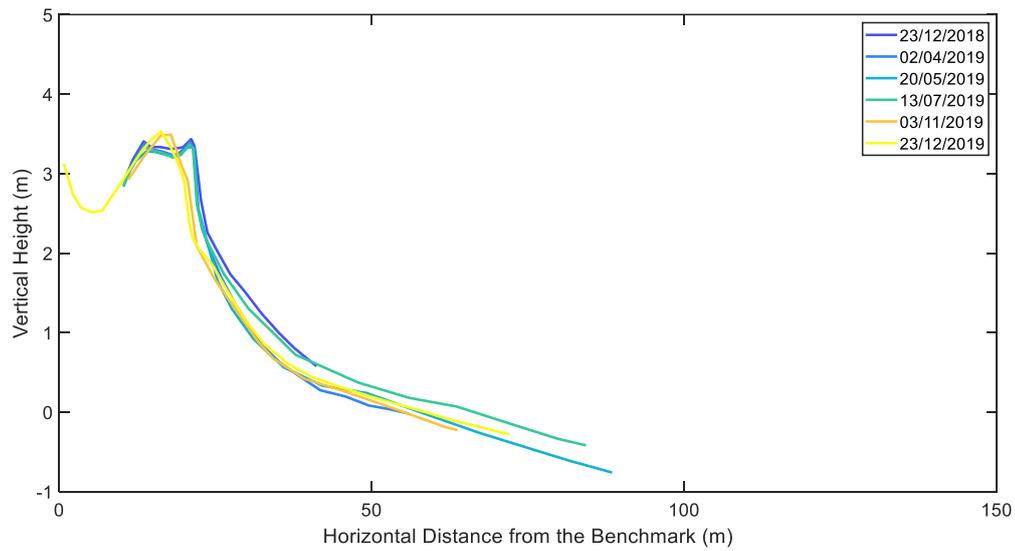
Figure 3.13. Beach profile of CCS25/1, Buffalo Beach. Field surveys were taken 23rd December 2018, 2nd April 2019, 20th May 2019, 13th July 2019, 3rd November 2019 and 23rd December 2019.

South of Buffalo Beach

Throughout the survey period there was no movement above the dune toe at CCS26/1, CCS27, CCS27/10, CCS27/8, CCS27/6, CCS27/2, CCS27/3 and CCS27/4 (Figure 3.15, 3.16, 3.17, 3.18, 3.19, 3.20, 3.21 & 3.22). However, at CCS26 there was slight accretion from May to December 2019, and at CCS27/5 there was erosion that occurred between December 2018 and early April 2019 and accretion that occurred between April and May (Figure 3.14 & 3.23).

During the time period between December and early April, the dune toe accreted at CCS26/1, CCS27/3, whilst the dune toe eroded at CCS27, CCS27/10, CCS27/8, CCS27/6, CCS27/2, CCS27/5, where especially large erosion occurred at CCS27/6 and CCS27/2. Further seaward along the beach, at CCS26/1, CCS27/10, CCS27/3 and CCS27/5 there was accretion on the upper beach face and erosion on the lower beach face and intertidal area, where at CCS27/5 a prominent berm was formed. At CCS27 there was a small amount of accretion at the upper beach face, erosion at the lower beach face and accretion in the intertidal area, as show (Figure 3.16). At CCS27/8, CCS27/6, CCS27/2 there was erosion that occurred across the beach face and the intertidal area (Figure 3.18, 3.19 & 3.20).

Between early April to mid-May, the dune toe was eroded at CCS26, the dune toe was stable at CCS26/1, CCS27, CCS27/8, CCS27/3 and CCS27/5, and the dune toe accreted at CCS27/10, CCS27/6 and CCS27/2. At CCS27/4 the dune toe has accreted between December and May. Further down the beach there was accretion at CCS26, CCS26/1, CCS27, CCS27/10, CCS27/8, CCS27/6, CCS27/2, where a small berm formed at CCS26 and CCS27/6. At CCS27/3 and CCS27/5 there was accretion on the upper beach face and erosion on the lower beach face, where at CCS27/5 the berm became slightly less pronounced. At CCS27/4 between December and May there was accretion on the upper beach face and erosion on the lower beach face (Figure 3.22).

During the time period from May to July, the dune toe eroded at all of the beach profile locations except for CCS26, where there was slight accretion. Further down the beach, there was accretion at CCS26 and CCS27 across the beach face and intertidal area. At CCS26/1 and CCS27/8, there was erosion on the upper beach

face and accretion on the lower beach face and intertidal area. At CCS27/10, CCS27/6, CCS27/3, CCS27/4 and CCS27/5 there was erosion on the upper beach face and intertidal zone, whilst accretion occurred on the lower beach face, with especially large amounts of erosion on the beach face of CCS27/4. There was erosion across the beach face and intertidal area for CCS27/2 (Figure 3.20).

From July to the end of August, there was accretion of the dune toe at all of the beach profile locations, except for CCS27/10 where the dune toe was eroded. Further down the beach, at CCS26, CCS27 and CCS27/8, there was accretion that occurred on the upper beach face and erosion on the lower beach face. Two berms formed at the locations of CCS26 and CCS27 on the upper and lower beach face, and one berm formed at CCS27/8 on the upper beach face. At CCS26/1 there was accretion on the upper beach face and a berm formed within the intertidal area with a runnel on the landward side of the berm and erosion lower in the intertidal area (Figure 3.15). At CCS27/6, CCS27/2, CCS27/3 and CCS27/4 there was accretion across the beach face and erosion on the intertidal area, where the berm present at CCS27/6 stayed in the same position and a new berm was formed in the intertidal area at CCS27/2 and on the beach face at CCS27/4. There was accretion across the beach face and intertidal area at CCS27/5, where the berm stayed in the same position.

From August to early November, there was erosion at the dune toe at the locations of CCS26, CCS27/10, CCS27/8, CCS27/3, CCS27/4, and accretion of the dune toe at CCS26/1, CCS27, CCS27/6, CCS27/2 and CCS27/5. Further down the beach, there was erosion at CCS26, CCS27, CCS27/10, CCS27/8 and CCS27/6 across the beach face and intertidal area, where one of the berms present at CCS26 and CCS27 disappeared and the berm present at CCS27/6 disappeared. At CCS26/1 there was erosion on the upper beach face and accretion occurred lower on the beach face where the runnel present was filled with sand, whilst erosion occurred where the berm previously was present. There was accretion across the beach face at the location of CCS27/2 and erosion in the intertidal area. At the south of the beach, at CCS27/3 and CCS27/4, there was erosion that occurred on the beach face and accretion that occurred in the intertidal area, where a berm formed in the intertidal area (Figure 3.21 & 3.22). At CCS27/5, there was accretion on the upper

beach face and in the intertidal area and erosion on the lower beach face, where the prominent berm disappeared. Large amounts of erosion occurred during this time period and reached the lowest elevation of the beach face throughout the survey period at the locations of CCS27/10, CCS27/8, CCS27/3 and CCS27/4.

From the early November to December, there was accretion of the dune toe at CCS26, CCS27, CCS27/10, CCS27/8, CCS27/2, CCS27/3, CCS27/4 and CCS27/5, the dune toe was stable at CCS26/1 and eroded at CCS27/6. Further down the beach, at CCS26 and CCS27/5 erosion occurred on the upper beach face and accretion on the lower beach face and intertidal area (Figure 3.14 & 3.23). CCS26/1 did not change much throughout the time period, with a small amount of accretion across the beach face and erosion in the intertidal area. At CCS27, the upper beach face is stable, whilst there was accretion on the lower beach face and erosion in the intertidal area. At CCS27/10 and CCS27/8 there was a large amount of accretion that occurred (Figure 3.17 & 3.18). At CCS27/2, CCS27/3 and CCS27/4 accretion occurred across the beach face and erosion in the intertidal area, where the berm in the intertidal area at the location of CCS27/4 disappeared. At CCS27/6 there was erosion across the beach face and intertidal area.
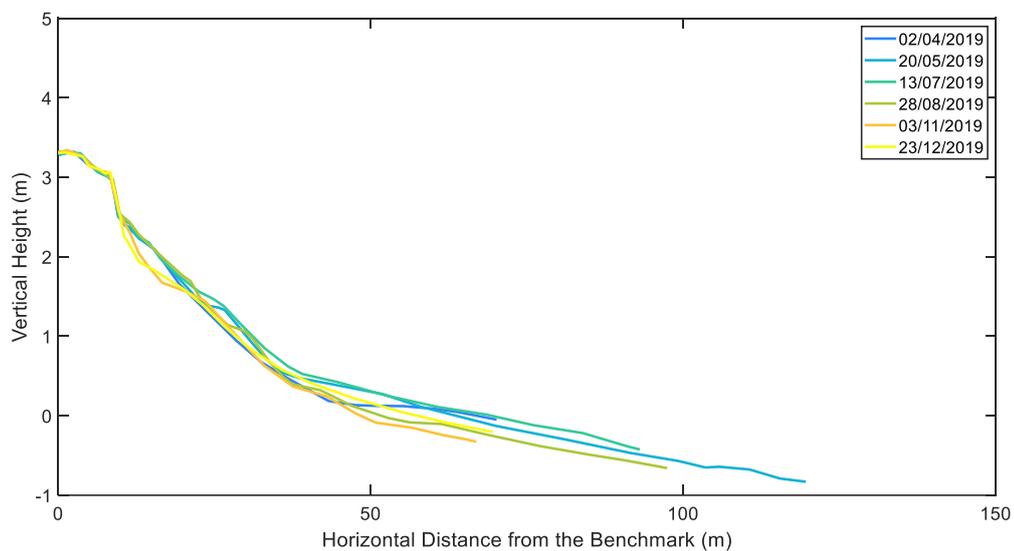
Figure 3.14. Beach profile of CCS26, Buffalo Beach. Field surveys were taken 2nd April 2019, 20th May 2019, 13th July 2019, 28th August 2019, 3rd November 2019 and 23rd December 2019.
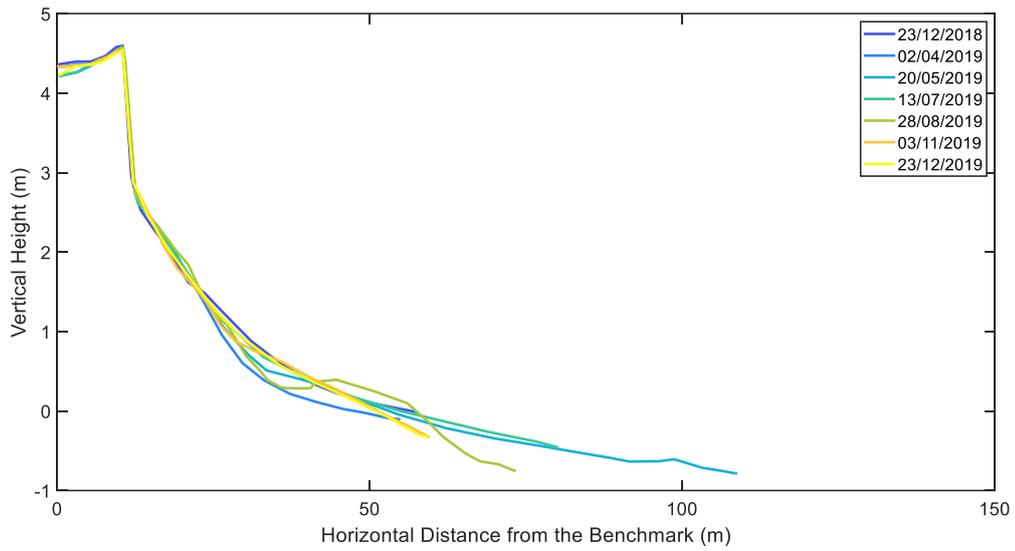
Figure 3.15. Beach profile of CCS26/1, Buffalo Beach. Field surveys were taken 23rd December 2018, 2nd April 2019, 20th May 2019, 13th July 2019, 28th August 2019, 3rd November 2019 and 23rd December 2019.
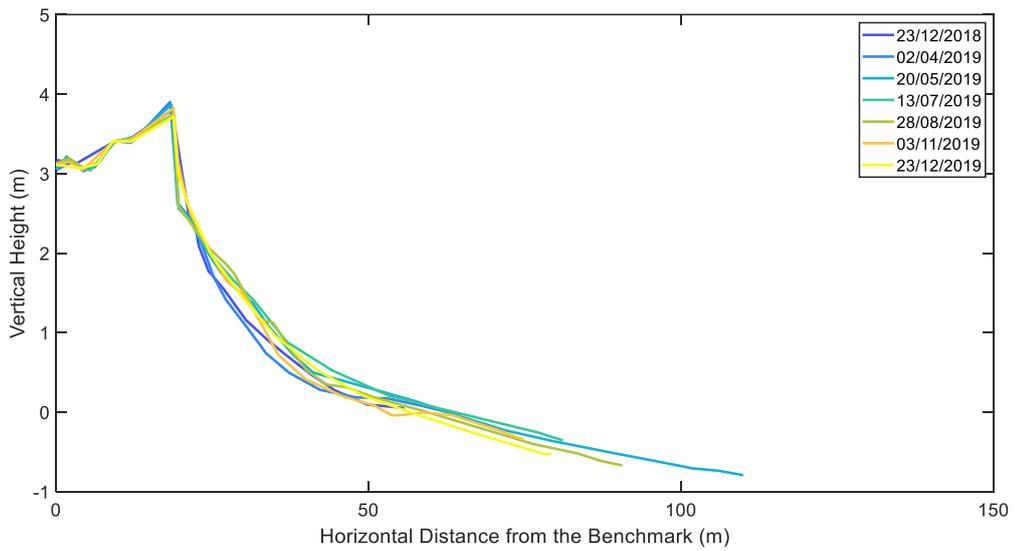
Figure 3.16. Beach profile of CCS27, Buffalo Beach. Field surveys were taken 23rd December 2018, 2nd April 2019, 20th May 2019, 13th July 2019, 28th August 2019, 3rd November 2019 and 23rd December 2019.
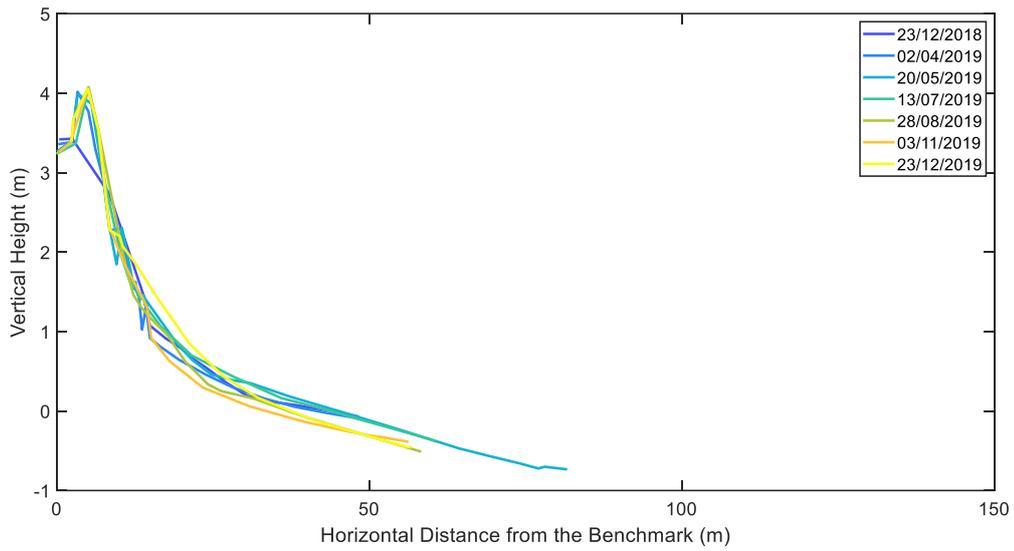
Figure 3.17. Beach profile of CCS27/10, Buffalo Beach. Field surveys were taken 23rd December 2018, 2nd April 2019, 20th May 2019, 13th July 2019, 28th August 2019, 3rd November 2019 and 23rd December 2019.
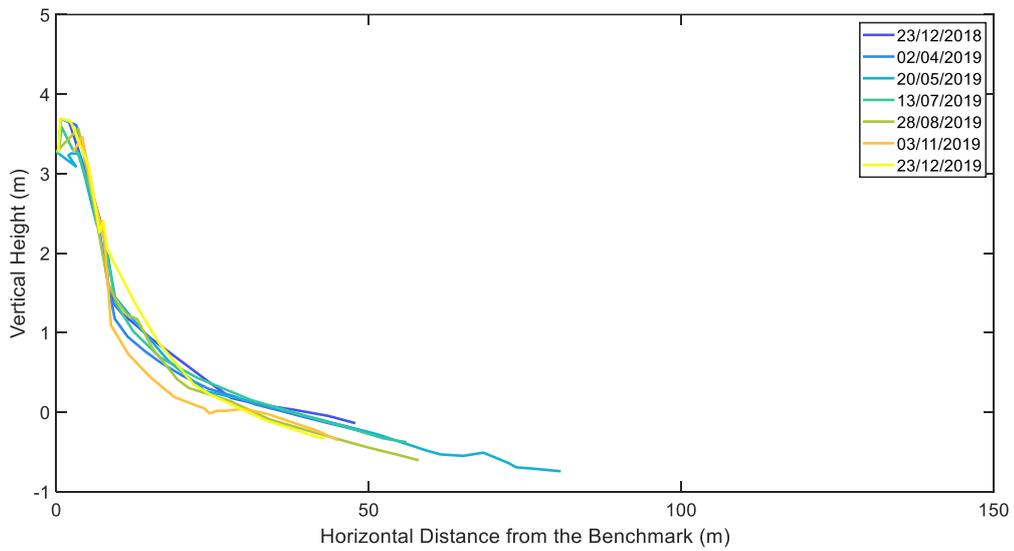
Figure 3.18. Beach profile of CCS27/8, Buffalo Beach. Field surveys were taken 23rd December 2018, 2nd April 2019, 20th May 2019, 13th July 2019, 28th August 2019, 3rd November 2019 and 23rd December 2019.
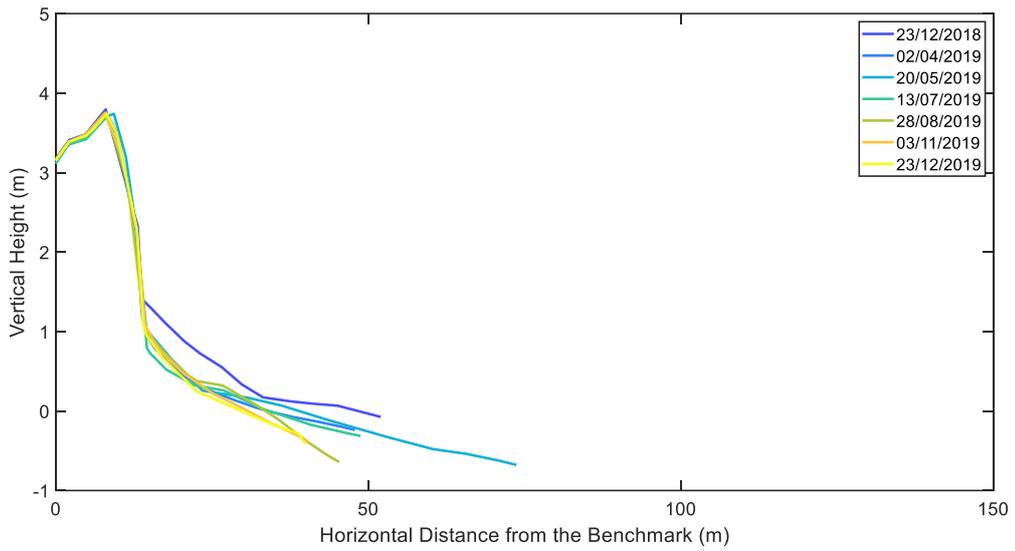
Figure 3.19. Beach profile of CCS27/6, Buffalo Beach. Field surveys were taken 23rd December 2018, 2nd April 2019, 20th May 2019, 13th July 2019, 28th August 2019, 3rd November 2019 and 23rd December 2019.
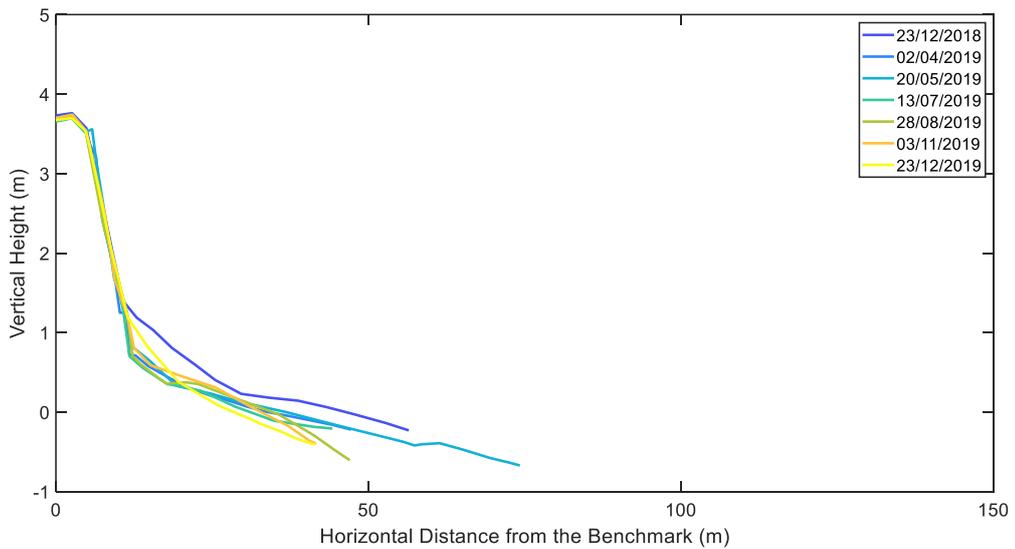
Figure 3.20. Beach profile of CCS27/2, Buffalo Beach. Field surveys were taken 23rd December 2018, 2nd April 2019, 20th May 2019, 13th July 2019, 28th August 2019, 3rd November 2019 and 23rd December 2019.
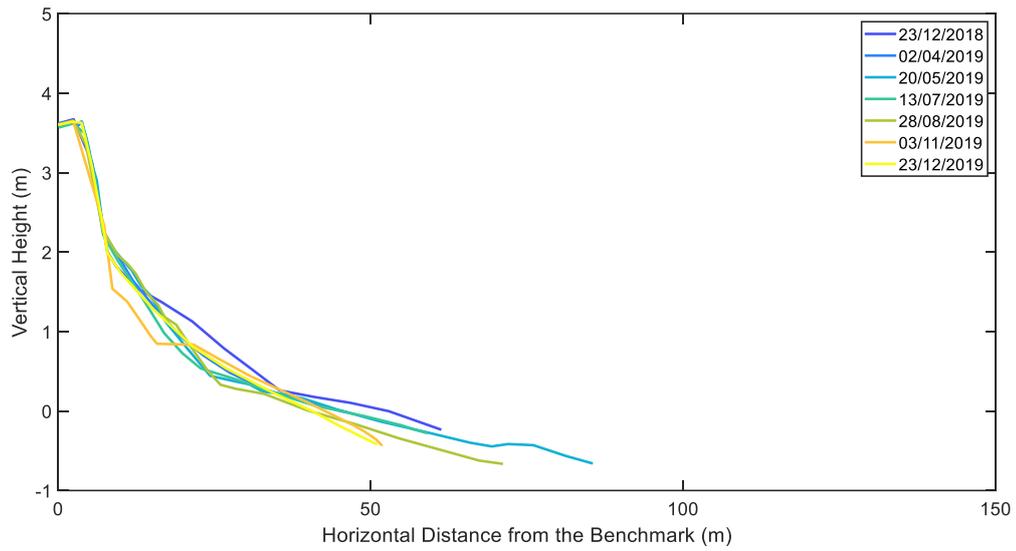
Figure 3.21. Beach profile of CCS27/3, Buffalo Beach. Field surveys were taken 23rd December 2018, 2nd April 2019, 20th May 2019, 13th July 2019, 28th August 2019, 3rd November 2019 and 23rd December 2019.
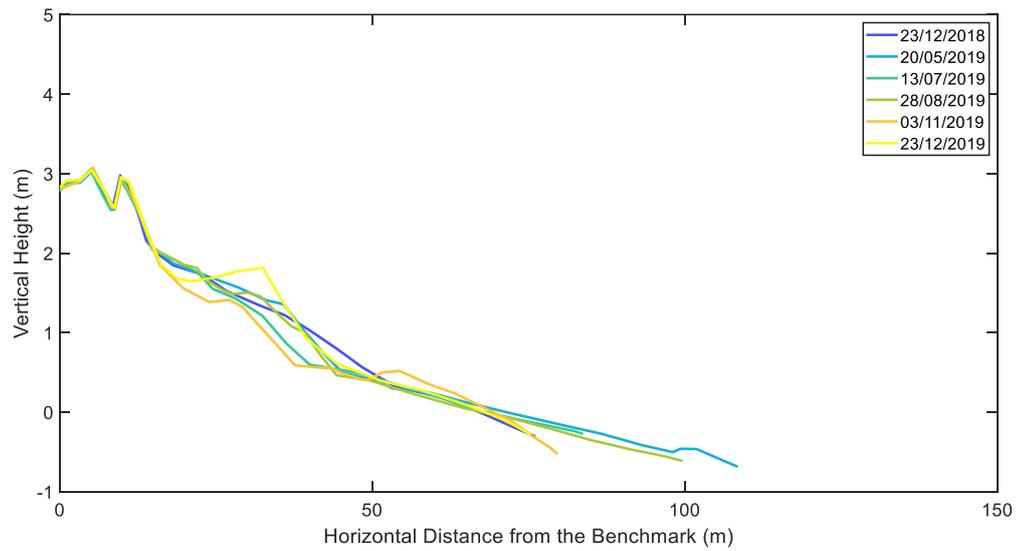
Figure 3.22. Beach profile of CCS27/4, Buffalo Beach. Field surveys were taken 23rd December 2018, 20th May 2019, 13th July 2019, 28th August 2019, 3rd November 2019 and 23rd December 2019.
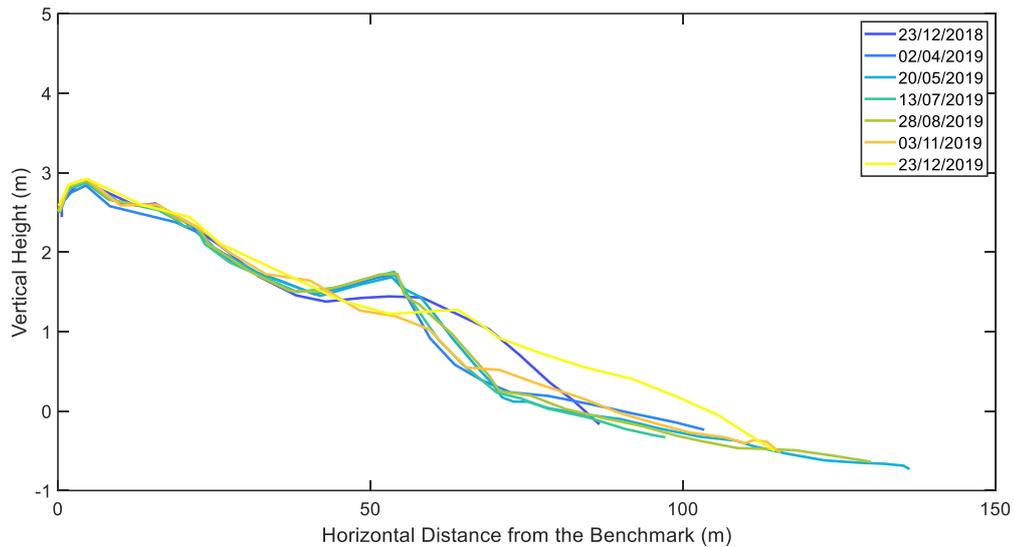
Figure 3.23. Beach profile of CCS27/5, Buffalo Beach. Field surveys were taken 23rd December 2018, 2nd April 2019, 20th May 2019, 13th July 2019, 28th August 2019, 3rd November 2019 and 23rd December 2019.

3.4.1.4 Hot Water Beach

Throughout the survey period there has been a small amount of morphological change above the dune toe at all three of the beach profile locations of CCS34, CCS35 and CSS35-1 (Figure 3.24, 3.25 & 3.26). Erosion occurred at profile CCS34 between December 2018 and April 2019, accretion between April and May, erosion during August and October and accretion again during October to December 2019, between the dune crest and dune toe. At CCS35, there was erosion of the frontal sand dune between May and July and accretion between July and August, before erosion occurred between August and October. At CCS35-1 at the north of the beach, there was a small amount of erosion between April and May 2019, accretion between July and August and erosion between August and October of the frontal sand dune below the dune crest.

During the time period of between December and early April, there was erosion at the dune toe at CCS34 and a small amount of accretion at the dune toe at CCS35 and CCS35-1. Further down the beach, at CCS34 and CCS35 there was small amount of accretion on the upper beach face to the berm and there was erosion below the berm in the intertidal area, where the berm at the location of CCS34 became more pronounced. At CCS35-1, the upper beach face was stable, and

erosion occurred at the lower beach face, where the berm that was present in December disappeared (Figure 3.26).

Between early April and the end of May, the dune toe accreted at CCS34 and eroded slightly at the dune toe at CCS35 and CCS35-1. Further down the beach, the upper beach face was stable and there was accretion across the beach face and intertidal area at all three beach profile locations. At CCS34, the berm that was previously present moved higher up the beach face and a second berm has formed further down the beach face (Figure 3.24). A berm has also formed on the lower beach face at CCS35 and CCS35-1.

Between May and July, there was a small amount of accretion at the dune toe at the profile CCS34 and erosion of the dune toe at CCS35 and CCS35-1. Further down the beach, all three beach profile locations had stable upper beach faces. At CCS34, there was a small amount of accretion across the beach face and intertidal area, apart from a small area of erosion where the second berm has disappeared. At CCS35, there has been accretion across the beach face and intertidal area, where a second larger berm formed lower on the beach face, except for erosion between the two berms present (Figure 3.25). At CCS35-1, there was erosion on the upper beach face, where the berm moved lower on the beach face and there was accretion below the berm on the lower beach face.

From July to end of August, dune toe accreted at CCS34, CCS35 and CCS35-1. The upper beach face was stable at CCS34, and there was a small amount of accretion at CCS35 and CCS35-1. At CCS34, there was erosion across the lower beach face and intertidal area apart from a second berm that has formed in the lower beach face area. At CCS35, there was a small amount of accretion above the higher berm and erosion across the lower beach face and intertidal area, where the second berm disappeared. At CCS35-1 there was accretion on the lower beach face and intertidal area, where the berm moved down the beach face.

From August to October, there was erosion of the dune toe at CCS34, CCS35 and accretion at CCS35-1. At CCS34, a large amount of erosion occurred above across the middle of the beach face at all three beach profile locations, where the berms present at CCS34 and CCS35-1 moved landward, and a new berm formed in the

same location at CCS35. There was erosion in the intertidal area at CCS34 and CCS35-1 and accretion at CCS35.

From October to December, the dune toe accreted at CCS34 and CCS35-1 and eroded at CCS35. There was accretion of the upper beach face and erosion of the lower beach face at CCS34 and CCS35, where the berms present at each location moved further up the beach face. At CCS35-1, there was accretion across the upper beach face causing the berm to disappear.
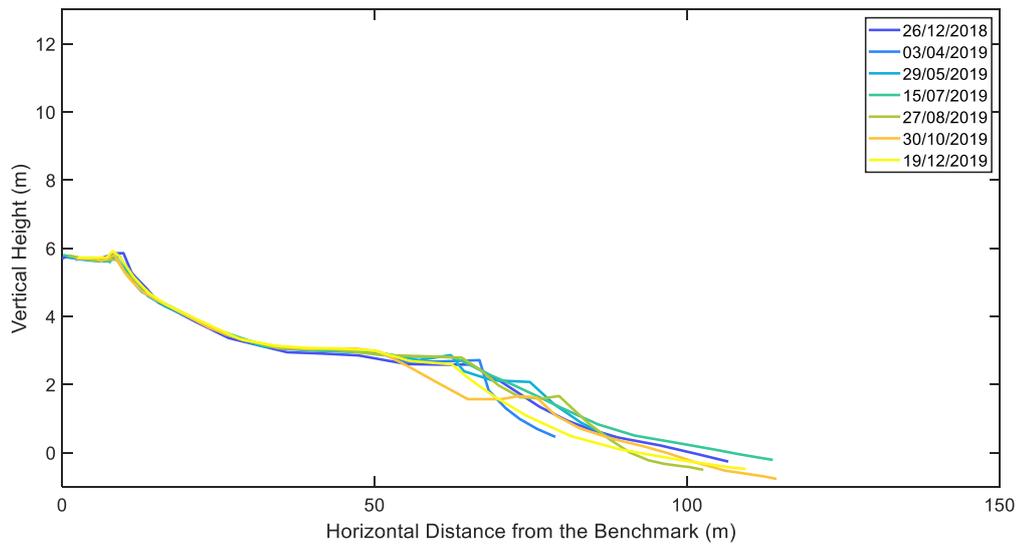
Figure 3.24. Beach profile of CCS34, Hot Water Beach. Field surveys were taken 26th December 2018, 3rd April 2019, 29th May 2019, 15th July 2019, 27th August 2019, 30th October 2019 and 19th December 2019.
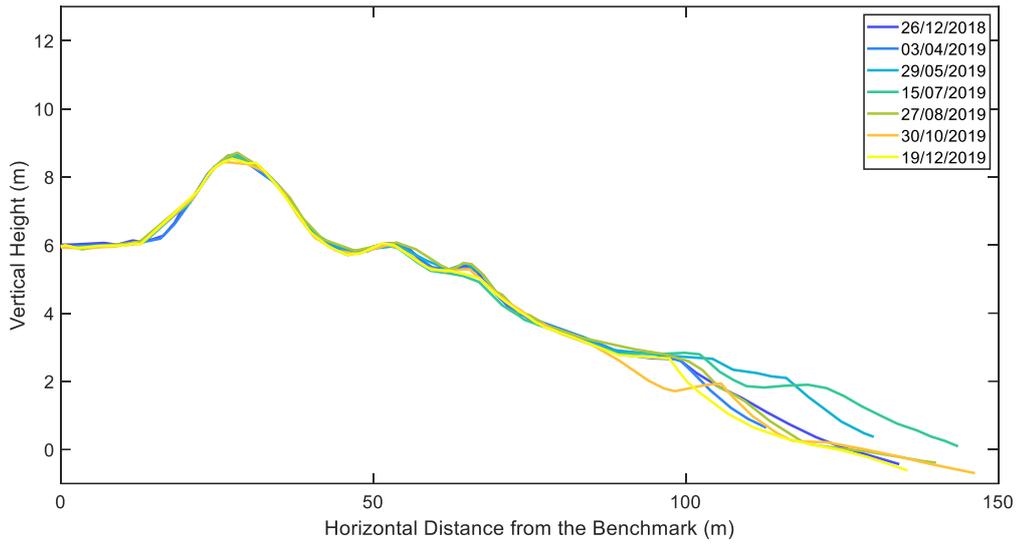
Figure 3.25. Beach profile of CCS35, Hot Water Beach. Field surveys were taken 26th December 2018, 3rd April 2019, 29th May 2019, 15th July 2019, 27th August 2019, 30th October 2019 and 19th December 2019.
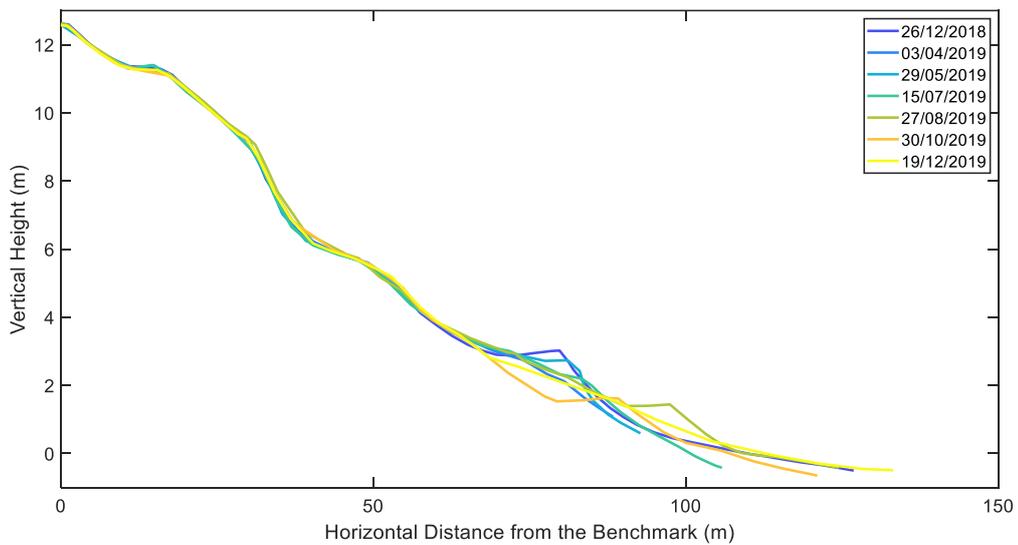
Figure 3.26. Beach profile of CCS35-1, Hot Water Beach. Field surveys were taken 26th December 2018, 3rd April 2019, 29th May 2019, 15th July 2019, 27th August 2019, 30th October 2019 and 19th December 2019.

3.4.1.5 Tairua Beach

Throughout the survey period there was little to no movement above the dune toe at CCS36, CCS36/2 and CCS37 profiles (Figure 3.27, 3.28 and 3.30). At CCS36/1 there was erosion of the foredune from March to July and a small amount of accretion from July to August, and erosion of the dune crest between May and July before accreting from July to August (Figure 3.29).

During the time period of December to the end of March, the dune toe was stable at CCS36, eroded at CCS37 and CCS361 and the dune toe accreted at CCS36/2, where a mound of sand formed at the dune toe. At CCS36 and CCS36/2, there was accretion of the upper beach face and intertidal area, and erosion of the lower beach face, where the berm present at both locations disappeared. At CCS37 and CCS36/1, erosion occurred on the upper beach face above the berm and accretion occurred on the lower beach face below the berm, at CCS37 the berm became less pronounced and at CCS36/1 the berm became more pronounced.

From March to May, the dune toe eroded at profiles CCS36, CCS36/2, CCS36/1 and accreted at profile CCS37. Further seaward along beach face, at CCS36, there was large amounts of accretion across the beach face and intertidal area of all four beach profile locations, where berms formed at CCS36 and CCS36/2, and large berms formed at CCS37 and CCS36/1.

Between May and July, the dune toe was stable at CCS36, CCS36/2 and erosion at CCS37 and CCS36/1. At CCS36 and CCS36/2 the upper beach face eroded and the lower beach face and intertidal area accreted, where the berm moved further down the beach, as shown in Figure 3.27 and 3.28. At CCS37 and CCS36/1, the upper beach face accreted and the lower beach face and intertidal area eroded, where the berm moved landward, as shown in Figure 3.29 and 3.30.

From July to August, the dune toe was stable at CCS36 and CCS36/2, the dune toe eroded at CCS37, and the dune toe accreted at CCS36/1. Further down the beach, at all four of the beach profile locations there was accretion at the upper beach face and erosion on the lower beach face and intertidal area, where the berm became more pronounced at all four locations and moved up the beach face at CCS36/1.

From August to early November, the dune toe accreted at CCS36, CCS36/2 and CCS37, and was stable at CCS36/1. Further seaward along beach face, at CCS36 there was accretion at the upper beach face and intertidal area and accretion on the lower beach face where a large berm was formed (Figure 3.27). At CCS37 the beach face and intertidal area eroded, and at CCS36/1 the upper beach face eroded and the lower beach face intertidal area accreted. Large berms formed at CCS37 and CCS36/1 (Figure 3.30 and 3.29).

From early November to December, the dune toe was stable at CCS36, CCS36/2 and CCS37, and the dune toe had accreted at CCS36/1. Further down the beach, at all four beach profile locations the upper beach face and intertidal area accreted, and the lower beach face eroded. At all of the four beach profile locations the berms that were present in November disappeared between November 2019 and December 2019.
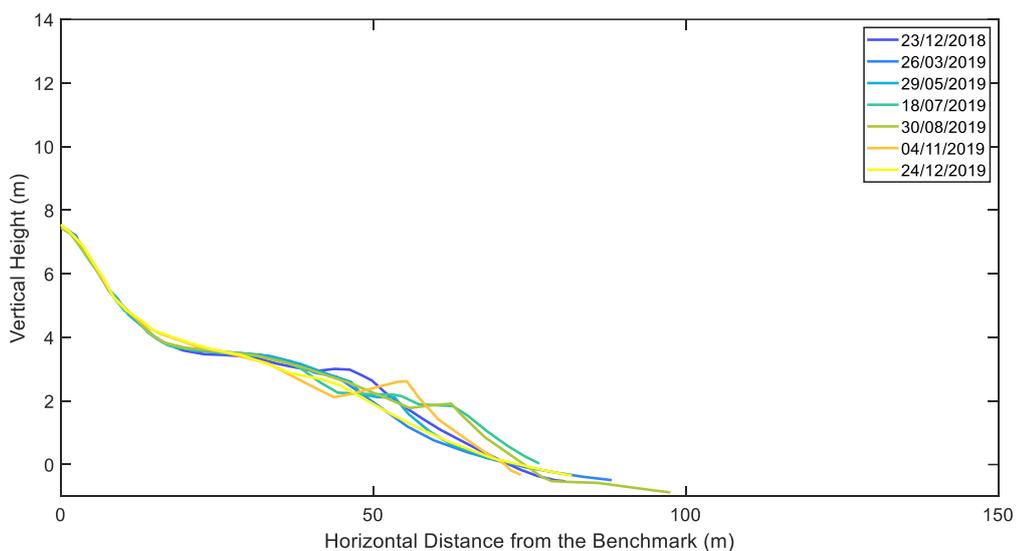
Figure 3.27. Beach profile of CCS36, Tairua Beach. Field surveys were taken 23rd December 2018, 26th March 2019, 29th May 2019, 18th July 2019, 30th August 2019, 4th November 2019 and 24th December 2019.
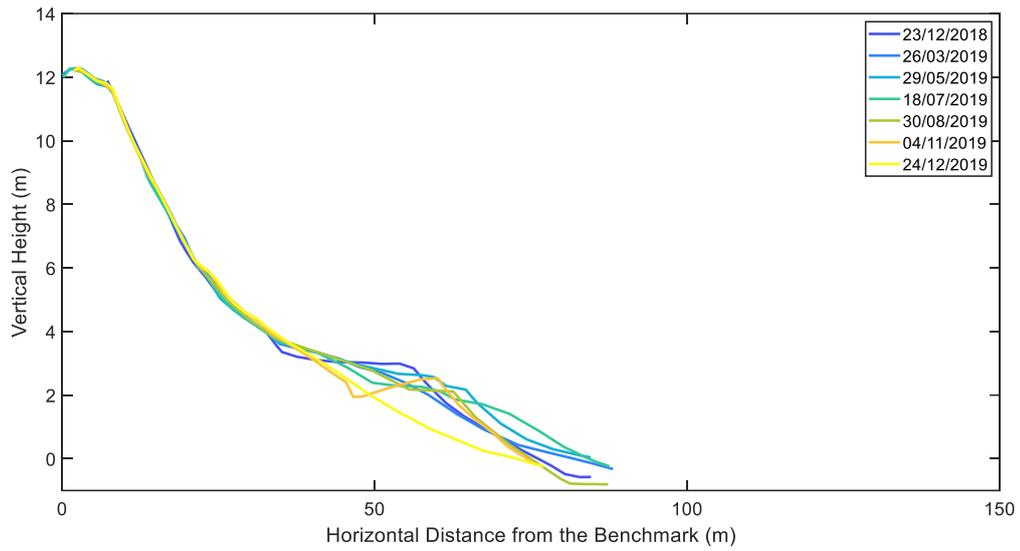
Figure 3.28. Beach profile of CCS36/2, Tairua Beach. Field surveys were taken 23rd December 2018, 26th March 2019, 29th May 2019, 18th July 2019, 30th August 2019, 4th November 2019 and 24th December 2019.
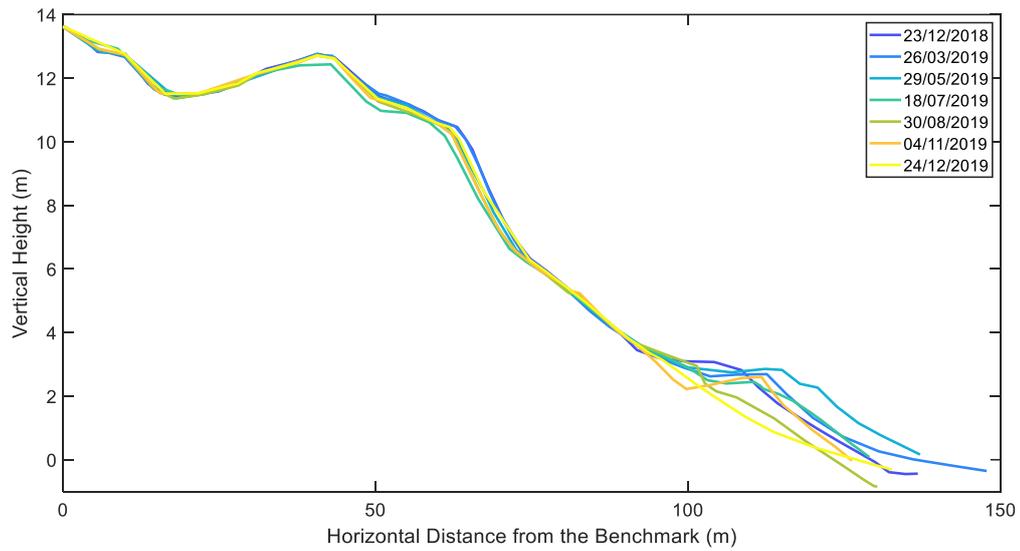
Figure 3.29. Beach profile of CCS36/1, Tairua Beach. Field surveys were taken 23rd December 2018, 26th March 2019, 29th May 2019, 18th July 2019, 30th August 2019, 4th November 2019 and 24th December 2019.
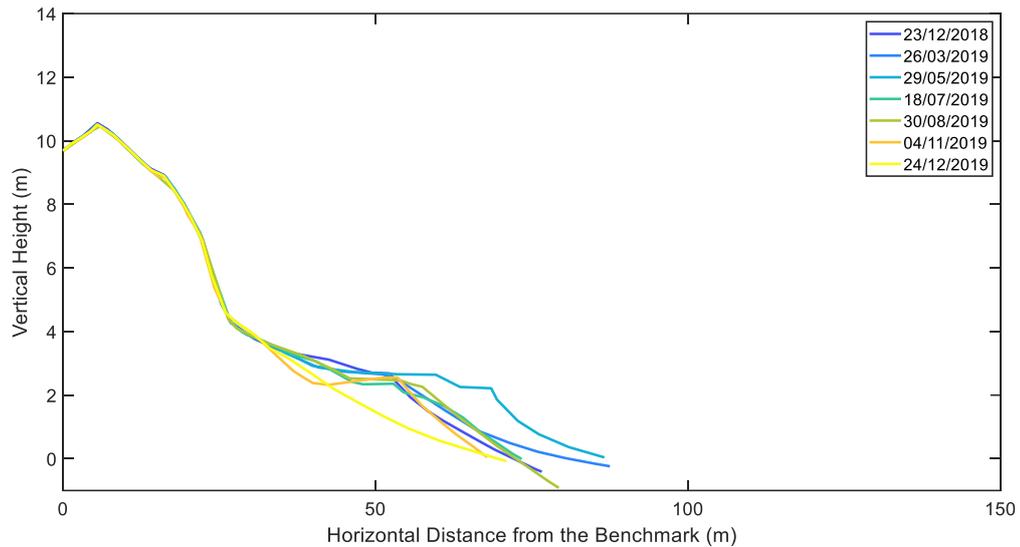
Figure 3.30. Beach profile of CCS37, Tairua Beach. Field surveys were taken 23rd December 2018, 26th March 2019, 29th May 2019, 18th July 2019, 30th August 2019, 4th November 2019 and 24th December 2019.

3.4.1.6 Ngarunui Beach (Raglan)

Between December 2018 and December 2019 there was little or no morphological change above the dune toe at the locations of RGN5 and RGNKS, (Figure 3.35 & 3.36). The dune toe eroded at RGN1 between July and December (Figure 3.31). The dune crest accreted at RGN2 between December 2018 and March 2019 (Figure 3.32). At RGN3, the back sand dunes and below the foredunes eroded and the dune crest accreted between December 2018 and March 2019, the foredunes then accreted between July and August and eroded between October and December 2019 (Figure 3.33). There was erosion from December 2018 to May 2019 at RGN4, accretion from July to August and erosion from October to December 2019 (Figure 3.34).

Between December and March, the dune toe accreted at profiles RGN1, RGN2, RGN3, RGN4 and RGNKS, and the dune toe eroded at RGN5. At RGN1 and RGN2 there was accretion of the upper beach face and erosion of the lower beach face and intertidal area. At RGN3, RGN4 and RGNKS there was accretion across the beach face and intertidal area, where accretion was especially large at RGNKS across the lower beach face and intertidal area. At RGN5 there was erosion on the

43

upper beach face and accretion across the lower beach face and intertidal area (Figure 3.35).

Between March and May, the dune toe was stable at RGN1, RGN4 and RGNKS, accreted at RGN2 and RGN3, and eroded at RGN5. Further down the beach, at RGN1 there was erosion across the beach face and intertidal area, and there was erosion across the lower beach face and intertidal area at RGN5. At RGN2, the upper beach face was stable, with a small area of accretion on the lower beach face and erosion across the intertidal area (Figure 3.32). At RGN3 and RGN4 there was accretion across the beach face and erosion across the intertidal area, where there was especially large accretion at RGN4. At RGNKS the upper beach face was stable, there was a small amount of accretion on the upper beach face, a large amount of erosion across the lower beach face and small amount of accretion at the lower intertidal area (Figure 3.36).

Between May and the end of June, the dune toe accreted at RGN1, RGN2, RGN3 and RGN5, and was stable at RGN4 and RGNKS. A ridge formed in front of the dune toe at RGN2 and RGNKS. At RGN1, RGN2, RGN4 and RGN5 there was erosion across the beach face and intertidal area. At RGN3 the upper beach face was stable and there was erosion across the lower beach face and intertidal area (Figure 3.33). At RGNKS there was accretion at the upper beach face and intertidal area, and erosion at the lower beach face, where the berm disappeared.

From the end of June to August, there was a large amount of erosion of the dune toe at RGN1 and smaller amount of erosion at RGN4 (Figure 3.31 & 3.34). The dune toe was stable at RGN2 and RGN5, whilst there was accretion at the dune toe at RGN3 and RGN5. Further down the beach, there was erosion across the beach face and intertidal area at RGN1, RGN2 and RGN3. There was accretion across the beach face and intertidal area at RGN4, RGN5 and RGNKS.

From the end of August to October, the dune toe eroded at RGN1, RGN2 and RGN5, and the dune toe accreted at RGN3, RGN4 and RGNKS. Further seaward along the beach face, there was erosion across the beach face and intertidal area at RGN1. At RGN2 and RGNKS there was accretion across the beach face and intertidal area. At RGN3 there was erosion on the upper beach face and accretion

across the lower beach face and intertidal area. At RGN4, the upper beach face was stable and there was erosion across the lower beach face and intertidal area. Whilst at RGN5 there was accretion on the upper beach face and quite a large amount of erosion on the lower beach face and on the intertidal area.

From October to December, the dune toe was eroded at RGN1, and stable at RGN2 and RGN3. The dune toe accreted at RGN4, RGN5 and RGNKS, where mounds of sand formed in front of the dune toe at RGN4 and RGN5. Further down the beach, at RGN1, RGN3, RGN4 there was accretion across the beach face and intertidal area. At RGN2 there was accretion across beach face and erosion in intertidal area. At RGN5 there was erosion on the upper beach face and accretion on the lower beach face and intertidal area. A RGNKS there was accretion on the upper beach face and erosion across the lower beach face and intertidal area.
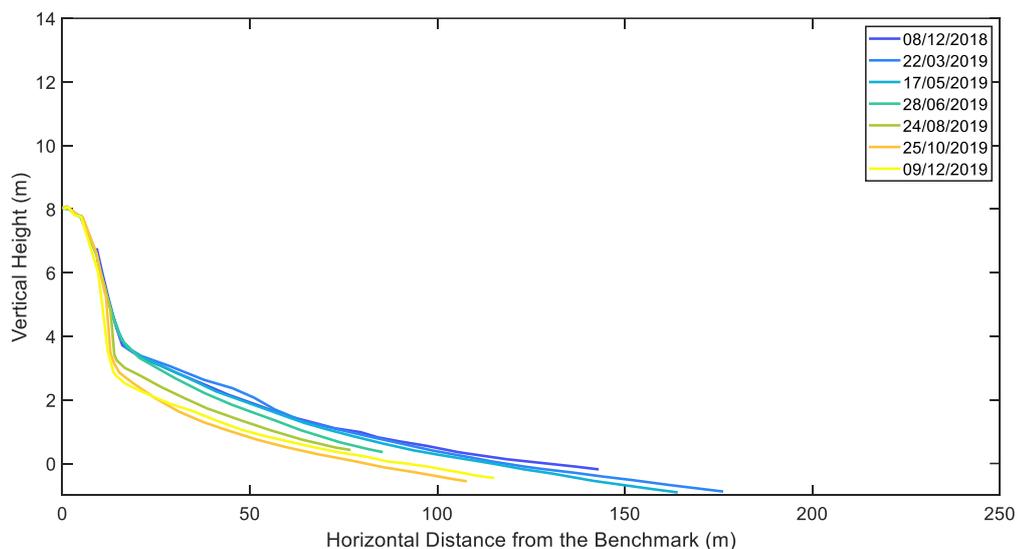
Figure 3.31. Beach profile RGN1, Ngarunui Beach, Raglan. Field surveys were taken 8th December 2018, 22nd March 2019, 17th May 2019, 28th June 2019, 24th August 2019, 25th October 2019 and 9th December 2019.
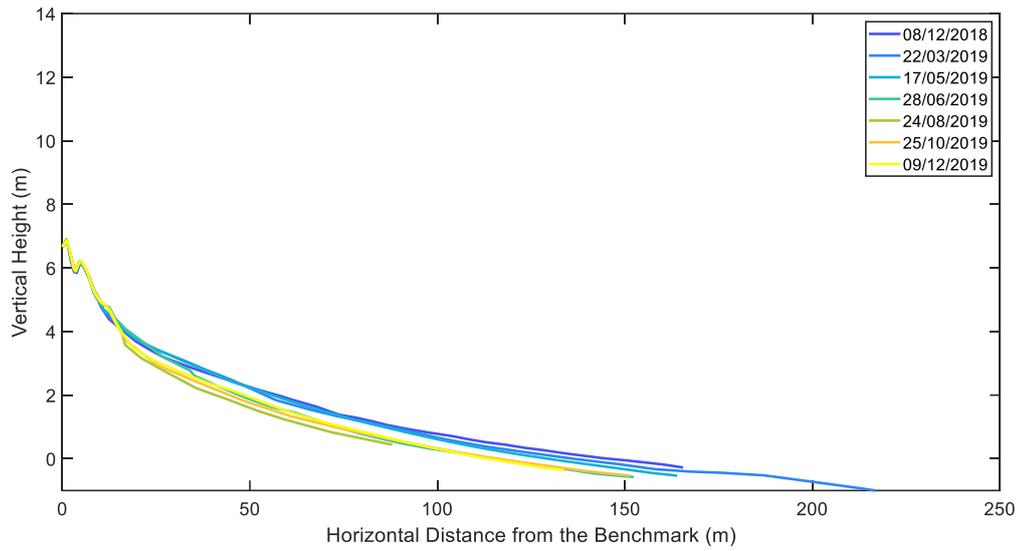
Figure 3.32. Beach profile RGN2, Ngarunui Beach, Raglan. Field surveys were taken 8th December 2018, 22nd March 2019, 17th May 2019, 28th June 2019, 24th August 2019, 25th October 2019 and 9th December 2019.
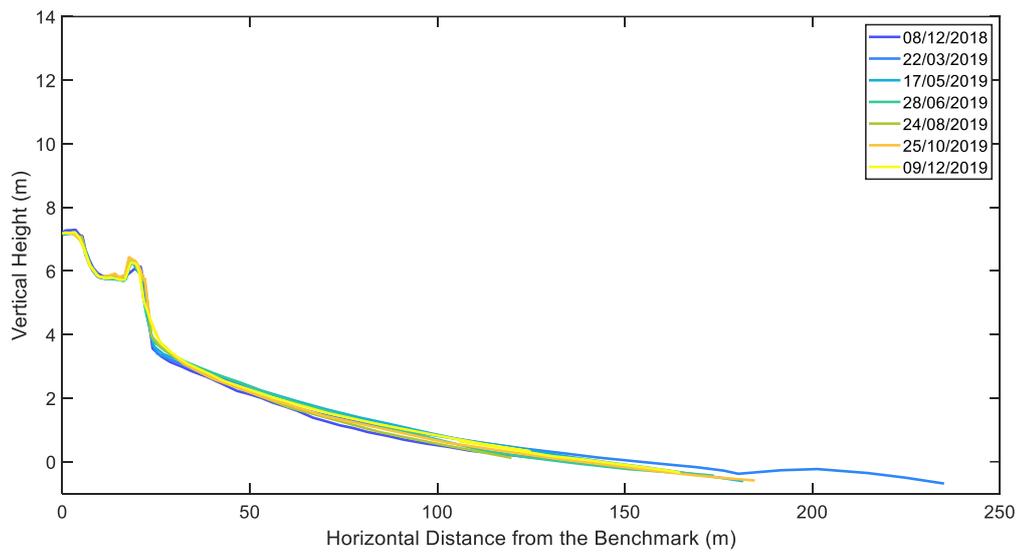
Figure 3.33. Beach profile RGN3, Ngarunui Beach, Raglan. Field surveys were taken 8th December 2018, 22nd March 2019, 17th May 2019, 28th June 2019, 24th August 2019, 25th October 2019 and 9th December 2019.
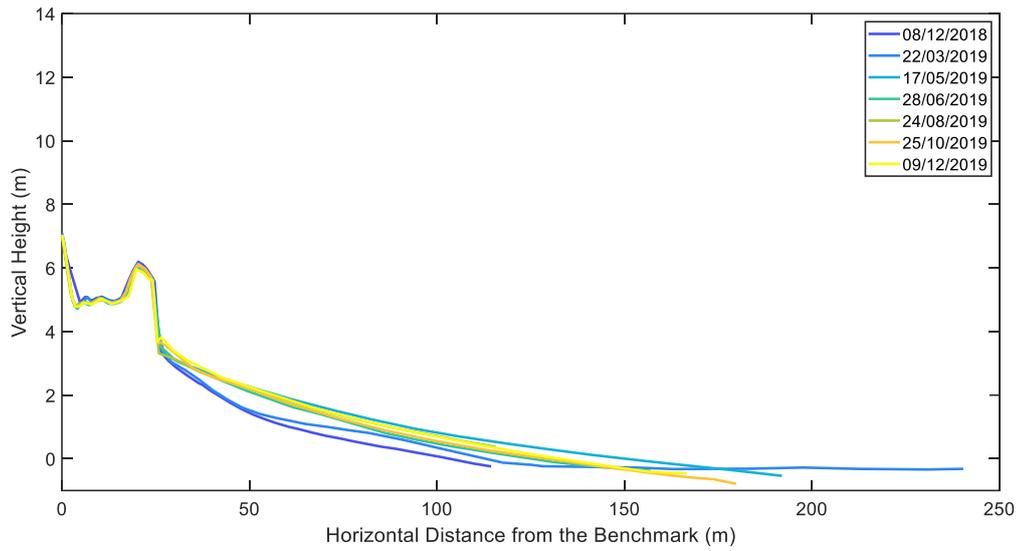
Figure 3.34. Beach profile RGN4, Ngarunui Beach, Raglan. Field surveys were taken 8th December 2018, 22nd March 2019, 17th May 2019, 28th June 2019, 24th August 2019, 25th October 2019 and 9th December 2019.
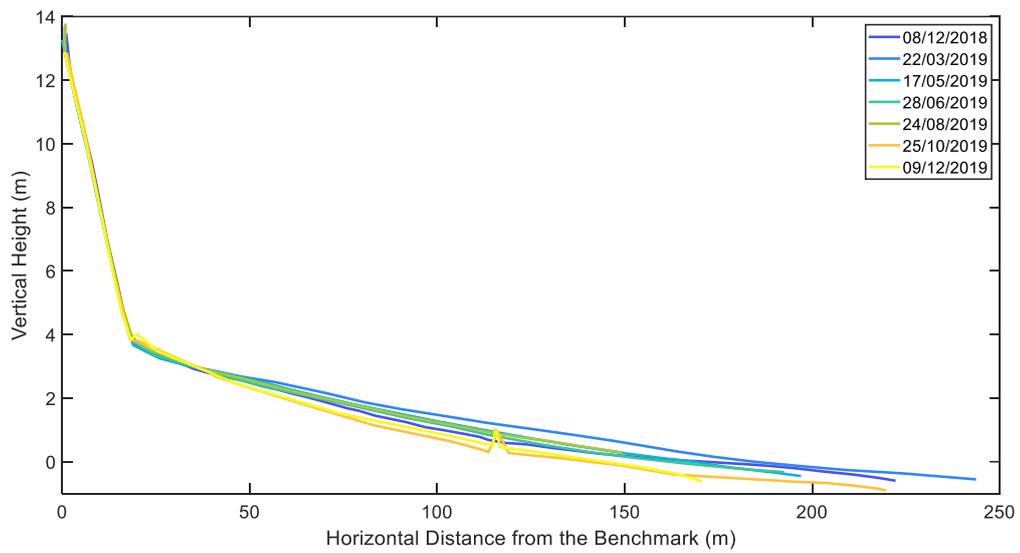
Figure 3.35. Beach profile RGN5, Ngarunui Beach, Raglan. Field surveys were taken 8th December 2018, 22nd March 2019, 17th May 2019, 28th June 2019, 24th August 2019, 25th October 2019 and 9th December 2019.
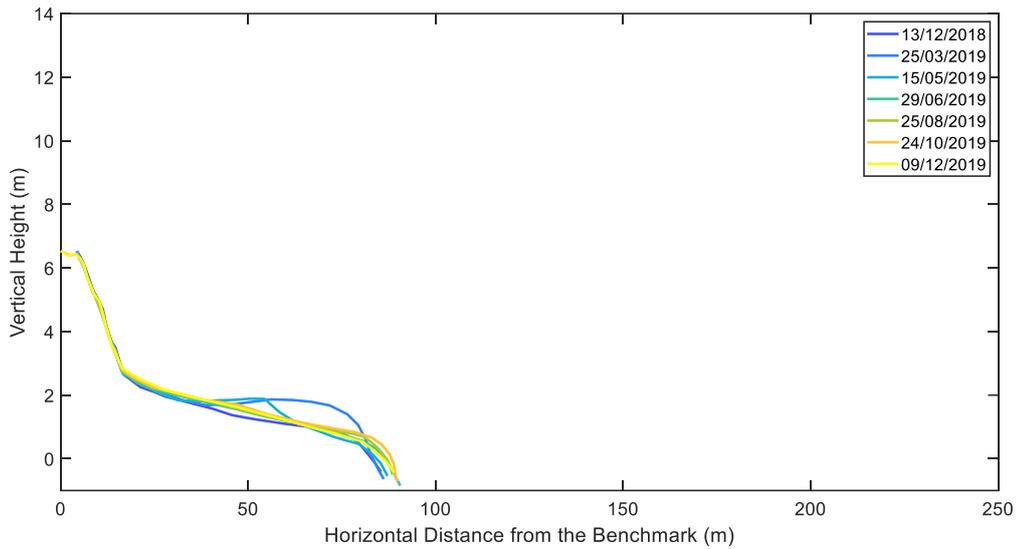
Figure 3.36. Beach profile RGNKS, Ngarunui Beach, Raglan. Field surveys were taken 13th December 2018, 25th March 2019, 15th May 2019, 29th June 2019, 25th August 2019, 24th October 2019 and 9th December 2019.

3.4.2 **Historic Beach Profile Dataset**

At Matarangi Beach CCS14, the dune toe position went through slow seaward movement followed by large sudden landward movement of the dune toe and frontal sand dune area on multiple occasions throughout the survey time period from 1979 to 2019 (Figure 3.37).
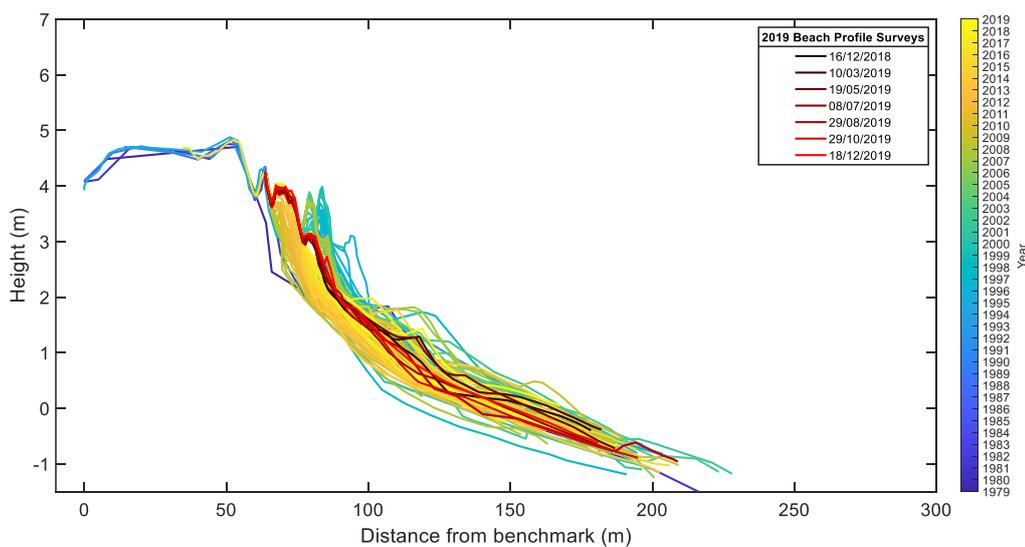
Figure 3.37. Historic Beach Profiles at CCS14, Matarangi Beach. Beach profiles from 1979 to 2019. The 2019 field survey beach profiles are shown in red.

The inflection point of the dune toe where the steep slope of the sand dune meet the lower angled beach was also shown in the historic beach profiles (Figure 3.38). How the dune toe moved with the lower beach face was shown, where changes in the lower beach face cause changes to the dune toe but to a lower magnitude, where at CCS12 (Figure 3.39), the dune toe moved landward and then seaward again.
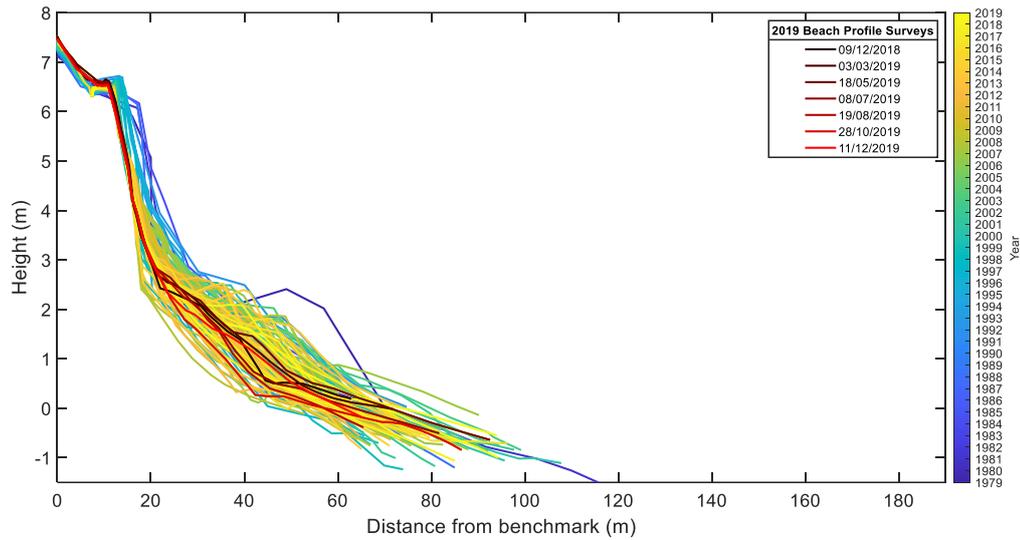
Figure 3.38. Historic beach profiles at CCS11, Whangapoua Beach. Beach profiles from 1979 to 2019. The 2019 field survey beach profiles are shown in red.
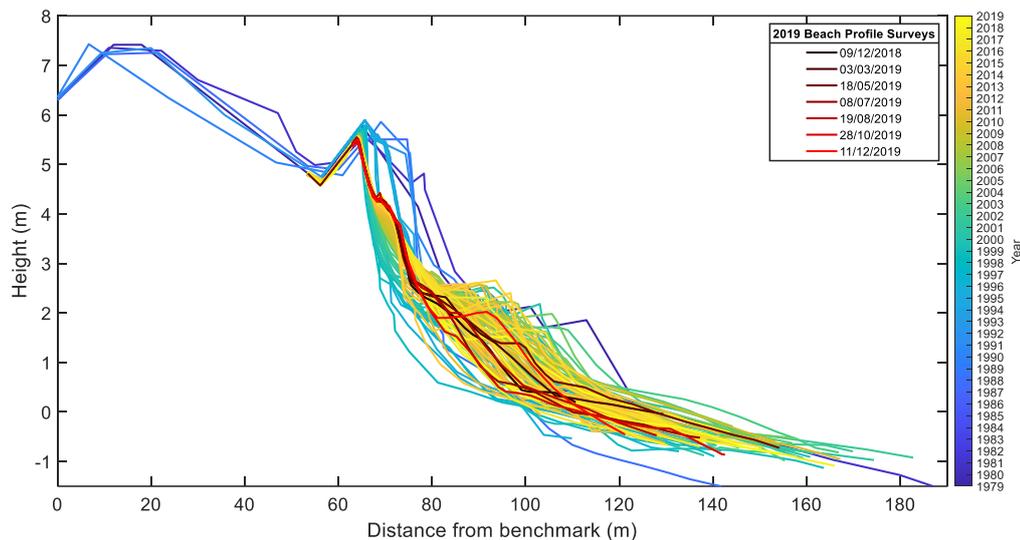
Figure 3.39. Historic beach profiles at CCS12, Whangapoua Beach. Beach profiles from 1979 to 2019. The 2019 field survey beach profiles are shown in red.

3.5 Discussion

3.5.1 Variability Across the Beach Face

The field survey beach profiles across all of the profile sites showed that the sand dunes and dune toe did not change often and when changes in elevation and beach morphology did occur the magnitude of change was small. The beach face and intertidal area changed often throughout the time period, where magnitude of change was large and, the beach morphology changed further down and across the intertidal area towards the sea. This is likely due to the influence of water on the beach area. The regions that are exposed to higher water less often such as the sand dune and dune toe, the variability of the beach morphology was low. Where the water reaches often such as the lower beach face and intertidal area, the variability of the beach morphology was high. Larson & Kraus (1993) which was a study about the temporal and spatial changes along the entire cross-section of beach profiles. This study also found that there was low variability at high elevations of beach profiles at the sand dune and dune toe area and high variability at lower elevations of the beach profiles across the beach face and intertidal area. Larson & Kraus (1993) found that the standard deviation of the change in position along the cross-sectional beach profile mostly decreased as the elevation increased.

3.5.2 Alongshore Morphological Change

The field survey beach profiles also showed that at some of the beaches surveyed, the beach morphological changes occurred along the beach at all the profile sites, whilst at other beaches surveyed the beach morphological changes and beach states were different along the beach. At Whangapoua Beach the beach morphology along the beach was very similar throughout the year for all three profile sites of CCS12, CCS11 and CCS11-1, at the profile locations of CCS12 at the north of the beach and CCS11 in the middle of the beach were especially similar. These profiles showed that there was accretion that occurred at Whangapoua beach over the summer period of both 2018-2019 and December 2019, and two erosion events over the winter period between May and July, and August and October. The beach face reached the lowest elevation during October at the end

of winter. The changes of beach morphology along the beach were also similar for Matarangi Beach. For the profile locations of CCS13, CCS14, CCS15 and CCS16 which were located along the open beach from the south of the beach to the north of the beach, all had a similar change occur throughout the year. There was accretion during the summer period with a berm present along the beach length from May to July. Throughout winter there were erosion events, between July and August and between August and October, where the beach face reached the lowest elevation recorded during October at the end of winter. The changes at CCS17 were different to the other profile site locations however, this is likely due to the location of the profile was at the harbour entrance and influenced by different hydrodynamics, than the open beach.

The morphological changes that occurred at Hot Water Beach were less similar than some of the other beaches along the length of the beach. However, there were some similarities including a berm present high on the beach face at all three profile locations of CCS34, CCS35, and CCS35-1 from December 2018 to April 2019, and the erosion between August and October 2019, where there was erosion of the upper beach face and a berm present on the lower beach face. The changes that occurred between May and August along Hot Water Beach were different along the beach where at CCS35 in the middle of the beach there was large accretion during autumn and the start of winter, where at each end of the beach at CCS34 and CCS35-1, the berm moved further down the beach face during winter. The morphological changes that occurred at Tairua Beach were also less similar than some of the other beach along the length of the beach. However, there were some similarities including the berm present high on the beach at all four profile locations of CCS36, CCS36/2, CCS37 and CCS36/1 from December 2018 to March 2019. During early November this berm returned high on the beach face with more erosion of the upper beach face behind the berm, and by December the berm disappeared and the beach was in the most eroded state throughout the year. During autumn and winter, there was differences along the beach where the north of the beach was more accreted at profile locations of CCS37 and CCS36/1 between March and May which may indicate beach rotation occurring at Tairua Beach. During winter there was also a berm present lower on the beach face at

the south end of beach at profile locations at CCS36/2 and CCS36, that is present on the north of the beach but much less pronounced.

The morphological changes that occurred at Buffalo Beach were different along the beach length, with some similarities for certain sections of the beach during certain time periods. The difference in morphological changes is likely due to the human modification of the beach face and sand dune area, in the form of sand banks, rock seawalls, beach nourishment and sand recontouring for planting. The profiles of CCS25, CCS25-2 and CCS25-3 at the north of the beach all show large amounts of accretion of the beach face between April and March, along with erosion and stable periods from May to November, and accretion once again from November to December. The beach face had the lowest elevation during November at the end of winter. At the locations of CCS25-2 and CCS25-3, there was a seawall present and CCS25 is just north of the seawall which may explain why the beach profiles of these locations were similar along with the position and angle that this area of the beach was facing. The morphological changes of landward movement of the dune and upper beach face at CCS25/1 south of the seawall were due to human modification of sand recontouring of the beach and dune area, and dune planting that occurred 24th August 2019. There were also similarities in the morphological changes at the south end of the seawall located at the south end of the beach at the profile locations of CCS27/6, CCS27/2 and CCS27/3. During December 2018, the elevation of the beach face compared to the seawall was high at all three profile locations. There was erosion between December 2018 and April 2019 and the sand face was stable throughout winter to December 2019, with higher erosion at CCS25/3 between August and November and small amount of accretion at CCS27/2 coming into the summer period. The profile locations of CCS27/4 and CCS27/5 also showed some similarities as well, where erosion occurred between August and November at the both profiles and large accretion from November to December 2019.

Houser (2013) showed that there can be considerable variation in beach morphology along the beach length. This alongshore variation would explain why each survey profile along each beach is not the same, however the time at which changes occur throughout the year are the same due to the forcing mechanisms

the beach is exposed to such as longer exposure time of higher water elevations during winter storms and wind during summer resulting in higher accretion (Castelle et al., 2015).

The beach in which showed different changes in beach morphology along the beach length was at Buffalo Beach. This in part may be due to the angle in which the beach faces changes from North to South of the Beach, however, is most likely due to the human modification of the beach and dune area along the beach. A two seawalls and a sand bank has been put in place at Buffalo Beach due to ongoing erosion and to protect existing infrastructure behind the beach, leaving many parts of the beach and sand dune area highly modified. The beach face at the location of the seawalls were flatter compared with beach profile locations at other areas of the beach which is likely caused by berms not able to form in front of seawalls due to wave reflection, increased sediment suspension and higher beach water table (Kraus & McDougal, 1996). There is also end effects of erosion occurring at each end of the seawall. This effect was evident at Buffalo Beach were erosion was noticeable at CCS27 that was situated just north of the seawall at the South of Buffalo Beach, and beach nourishment of moving sand up the beach face occurs at the south end of the seawall at profile CCS27/4 which would indicated that erosion occurs due to end effects at the south of the sea wall as well (Kraus &McDougal, 1996).

There was evidence of potential beach rotation at Tairua Beach where during Autumn erosion has occurred at the Southern end of the beach and accretion at the Northern end of the beach. Beach rotation is a coastal process in which erosion and accretion moves from one end of the beach to the other in a cyclic manner (Bracs et al., 2016). Beach rotation is likely to occur at small embayed beaches surrounded by headlands, which is characteristic of many Coromandel Beaches including Tairua Beach (Bracs et al., 2016). However, to determine whether beach rotation has occurred beach profiles collected over a longer time period need to be analysed.

3.5.3 Seasonal Patterns

There was some evidence of seasonal patterns for a number of the beaches where field surveys of beach profiles were conducted. These seasonal patterns were identified at beaches where the beach face of the summer and autumn profiles of December 2018, March/April 2019, May 2019 and December 2019, where in a more seaward and high elevation state. The beach face of the winter profiles of July, August and especially October/November 2019, were of a more landward and lower elevation state. Whangapoua Beach had these characteristics at all three beach profile locations, where the beach was most eroded in October 2019. The open beach at Matarangi Beach, where the profile site of CCS17 is excluded, had these characteristics as well with less pronounced erosion during winter compared with Whangapoua. A number of profile locations had the characteristics for seasonal patterns, such as at the north of the beach at CCS25, CCS25-2, CCS25-3, CCS27/10, CCS27/8, CCS27/6, CCS27/2, CCS27/3, CCS27/4 and CCS27/5. Beach profile locations that did not follow seasonal patterns were CCS24 and CCS27 which accreted throughout the year, CCS26 where there was no accretion during summer, CCS26/1 which was roughly stable throughout the year (with a small amount of erosion in August) and CCS25/1 due to human modification of dune reshaping and planting. Hot Water Beach also showed seasonal patterns where the berms were higher on the beach face during summer of both December 2018 and December 2019, and erosion where berms lower were down the beach in winter, especially late in winter at the end of October. Tairua beach also showed seasonal pattern characteristics, where there were small amounts of erosion during winter and berms lowering down the beach face. Until the second summer period where the berm disappeared, and erosion occurred.

At a large number of the profile sites across all of the beaches surveyed, the December 2018 beach state was similar to that of December 2019, one year later. This further showed a cyclic seasonal pattern at these beaches.

Changes that occur across the sand dunes and beach face are caused by the forcing mechanisms of wind and water (Masselink & Pattiaratchi, 2001; Davis & Fox, 1972; Hayes & Boothroyd, 1969). The influence of water is greater during winter where longer exposure times of high-water elevations from storms events, which mean

higher wave heights and wave runup. The influence of wind is greater during summer when incremental accretion of the beach face and dune area occurs in the fair-weather conditions (Masselink & Pattiaratchi, 2001; Davis & Fox, 1972; Hayes & Boothroyd, 1969). This was evident at the majority of the Coromandel Beaches where surveys were taken and aligns with what was expected to occur at these beaches, confirming theory of seasonal patterns and variation of how beach morphology is expected to change throughout each year.

3.5.4 Historic Beach Profile Dataset

There were a number of beach profiles within the historic dataset that showed the expected behaviour of the dune toe with sudden landward movement and slow seaward accretion of the dune toe. The inflection point of the dune toe was also clear across many of the profiles where the sand dunes had a steeper slope which meet the lower sloped beach at the dune toe. The profiles where the sand dunes were less steep, rolling frontal sand dunes where accretion and vegetation growth was likely to occur, the inflection point of the sand dune was less obvious (Ruz & Meur-Ferec, 2004; Splinter & Palmsten, 2012).

There were potentially some errors in the historic beach profile dataset, that likely occurred when matching the field survey profiles with the historic beach profiles. The BPAT processing of the historic beach profiles is unknown therefore there may have some unknown errors within the historic beach profile dataset.

3.5.5 Errors and Future Research

There are a number of errors that could have affected the accuracy and precision of the beach profile data. The GPS unit was mounted onto a backpack instead of mounted to a survey pole, therefore the error of the survey was increased. However, care was taken to decrease this error as much as possible by standing upright in a similar position each time a point was taken for the survey. The NRTK unit was used instead of setting up a base station at a nearby reference point to the beach. The NRT unit relies on a fixed receiver that is some distance from the beach which means that the receiver may be exposed to different atmospheric conditions than if a base station at the beach was set up for the survey, which increases the error. The distance or baseline from the station is also larger which

also introduces error. However, using the NRTK did have advantages including the time in which surveys were completed, therefore the amount of field surveys possible to complete and the amount of beaches that were able to be surveyed.

There were some of the beach profiles not included in the dataset for the surveyed beach profiles. The profile of CCS25/1 taken 28th August 2019 at Buffalo beach was not included, as the wrong benchmark was used and therefore the data was invalid. The profile of CCS26 taken 23rd December 2018 was not included due to not being able to locate the benchmark and therefore not able to survey the profile. The profile CCS27/4 taken 2nd April 2019, was not able to be taken due to beach nourishment taking place at the time and was not safe to conduct the profile survey.

Whist completing the surveys the advantage of using GPS to measure the profiles compared with the Emery method, meant that if the first point of the survey was not exactly on the benchmark but still in close vicinity, the coordinates could be related back to a more precise location of the benchmark, meaning the data of the surveyed profiles were more accurate and precise. This was advantageous as the benchmarks were sometimes hard to find the exact location of especially completing the first field survey, and some of the benchmarks that were not marked by any recognising feature, such as concrete plot, wooden post or painted mark. However, all of the field survey beach profiles were taken in the very close vicinity of the benchmark, even when not found, and were taken on the approximately the same perpendicular line with the beach length.

There was also one or two cases during early field surveys where the weather deteriorated to the point where the survey could not be completed, care was taken to avoid such weather days in future surveys and some surveys were redone in order for the data to be coherent across the entire beach where all the profiles were surveyed within one or two hours of one another. All surveys were completed within two hours of low tide which meant that as much of the intertidal area was surveyed as possible within reason of completing the fieldwork for the whole beach within the same tidal cycle.

The field survey beach profiles were added to the historic dataset using offsets provided by Waikato Regional Council which were used in the BPAT processing of the historic beach profiles. Using some of the offsets meant that the survey beach profile obviously did not match the historic beach profiles so manual editing was needed so that the survey beach profiles were matched effectively with the historic beach profiles. Some editing was also done to the historic beach profiles to remove the vertical lines within the beach profiles which were present from the BPAT processing of the data.

3.6 **Conclusions/Summary**

In Conclusion, the beach profile dataset showed the variability of the dune toe, upper beach face, lower beach face and intertidal are for the field survey profile sites. The results show that there was low variability of the dune toe and upper beach face throughout the one-year survey period. This result was expected and consolidates theory that the morphology of the upper beach and dune toe moves less often than lower on the beach face, which is inundated with water more often. At some of the surveyed beaches there was similarities found between morphological changes that occurred along the beach at different profile sites, however the result showed that there was variation alongshore in changes to the beach morphology. There was some evidence of seasonal patterns found where more erosion occurred during winter, likely due to transport of sand to offshore bars and more accretion during summer when berms were present, throughout the one-year survey period. It was also indicated through the field survey and beach profiles, that the movement of dune toe was influenced by changes that occurred further seaward of the beach, where when there was erosion, the dune toe generally moved landward and when there was accretion the dune toe generally moved seaward.

Chapter Four

Frequency and Magnitude of Changes to the Alongshore Dune Toe and Vegetation Line

4.1 Introduction

Beach morphology has been traditionally measured using beach profiles, which measure the entire cross section of the beach face from the sand dunes to the intertidal area, at one or several locations along the beach length (Cooper et al., 2000). However, there are a number of new methods that are currently being explored which may be more cost effective, use less time or provide more information than traditional beach profiles. These new methods include the use of drones, vehicle mounted RTK-GPS, satellite imagery, aerial images and video analysis (Aarninkhof et al., 2003). Where the use of drones, satellite imagery and video analysis can provide information of the entire beach face along the length of the beach, and vehicle mounted RTK-GPS and aerial images can provide information of certain features and areas of the beach face for the along the entire length of the beach (Pianca et al., 2015). Another new method being explored is to measure the dune toe of the frontal sand dunes and the vegetation line of the frontal sand dunes. Measuring the vegetation line and dune toe of the frontal sand dune could provide information along the entire beach length and may be a more viable method to measure beach morphology compared with traditional beach profiles and other new techniques, due to a potentially being lower in cost and less time consuming depending on the approach taken, when used for beach monitoring. Due to the high importance of risk management along coastal beaches and areas, including the setback distances for coastal developments along beaches and the potential risk of coastal flooding, measuring the vegetation line and dune toe of sand dunes could provide more useful information for determining the risks within the coastal beach environment and making risk management decisions (Splinter & Palmsten, 2012). Having the ability to be able to accurately determine the range in which the frontal sand dunes may move landward within the future

could mean less future damage to property and potential loss of life (Martinez & Psuty, 2004).

The vegetation line and dune toe of frontal sand dunes are distinct features of the beach face and can be easily identified. For this chapter, the vegetation line is considered to be the seaward edge of the vegetation line along the frontal sand dunes of the beach face. The dune toe is considered to be the inflection point of the frontal sand dune where the sand dune meets the beach when there is an escarpment present and the vegetation line when there is no escarpment present (Splinter & Palmsten, 2012).

The aim of this chapter was to determine the variation in the dune toe position along the length of the beach and the frequency and magnitude of change in both the horizontal and vertical position of the dune toe throughout time. A detailed analysis of the alongshore variation of the dune toe and the magnitude of change in both the horizontal and vertical position of the dune toe was undertaken using field surveys for the field survey sites of six Coromandel beaches and Ngarunui Beach, Raglan. The field surveys were conducted throughout the year long time period of December 2018 to December 2019. An analysis of the vegetation line and dune toe from the historic dataset was undertaken in order to show changes over a longer time period of 30 years (1990 – 2020). The differences between using the vegetation line and the dune toe for measuring the frontal dune toe will be compared using the historic dataset, and the distribution of the vegetation line and dune toe measured will be compared.

4.2   Expected Outcomes

There is high variability lower on the beach where water reaches more often, with each tidal cycle, compared with higher up on the face near the sand dunes which may only be reached by water during large storm events. Therefore, on the upper beach face and sand dunes the beach morphology undergoes a lower magnitude and frequency of changes (Larson & Kraus, 1993). It is therefore expected that the dune toe would move less often than beach morphology of the lower area of the beach face and intertidal area. The vegetation line and dune toe move landward during storm events and moves seaward during fair weather conditions

(Dissanayake et al., 2015; Castelle et al., 2015; Winant et al., 1975). Therefore it is expected that the historical data set and field survey dataset of the vegetation line and dune toe will show that the vegetation line and dune toe would have had sudden landward movements during storm events, particularly during winter, and slow seaward movement during fair weather conditions, particularly over summer periods (Castelle et al., 2015). It is also expected that the historic and field survey dataset will show that the dune toe does not move often and with a lower magnitude than other areas of the beach face (Larson & Kraus, 1993). The field survey dataset should show that the dune toe position varies along the beach length in cross-shore position and in height. It is expected that the historic dataset comparing the vegetation line and dune toe will show that the dune toe has a lower range and distribution of horizontal and vertical position through the measured time period, compared with the horizontal and vertical position of the vegetation line (Splinter & Palmsten, 2012).

4.3 Methods

4.3.1 Field Survey of the Dune Toe

The field surveys of the alongshore dune toe was undertaken concurrently with the beach profile surveys. For the technical methods of using the RTK GPS unit refer to Chapter 3. The dune toe was measured either directly before or after the beach profiles were surveyed. The surveyed involved walking the length of the beach along the dune toe where survey points were taken either every 0.5 m roughly or where there was a notable change in the elevation or horizontal position of the dune toe. When there was an escarpment present the inflection point along the bottom of the escarpment was considered to be the dune toe, when there was no escarpment present the vegetation line along the frontal sand dune was considered to be the dune toe (Splinter & Palmsten, 2012). The location of the dune toe was on occasion somewhat subjective, but care was taken to be consistent and survey the location of the dune toe to the best of the operators ability in order for the data gathered to be as accurate and precise as possible. Where there were seawalls and a sand bag wall present at the Buffalo Beach the dune toe was considered to be where the edge of the rocks of the seawall meet

the beach. Each beach was surveyed in the same direction where surveys were started at the South end of each beach and finished at the north end of each beach. The error of surveying the dune toe was measured by surveying Tairua Beach from South to North of the beach and then North to South of the Beach on one occasion to determine the potential error of each survey in determining the dune toe.
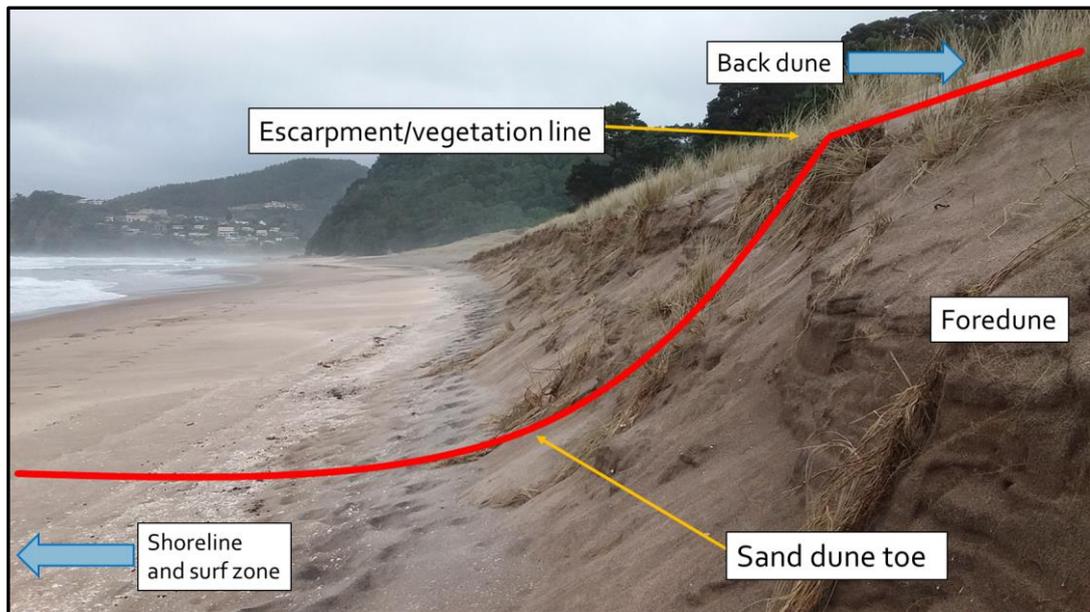
Figure 4.1. A diagram showing what is defined as the dune toe and vegetation line when there is an escarpment present.

Figure 4.2. A diagram showing what is defined as the dune toe or vegetation line when there is no escarpment present.

4.3.2 Data Analysis

The dune toe field surveys were checked for outliers and processed for data analysis using Matlab software. Buffalo Beach was split into North Buffalo Beach and South Buffalo beach for the data analysis in order to enable the data to be analysed in a meaningful way. The coordinate positions of the dune toe were plotted for all of the field surveys for each beach, where for beaches where there were gaps along the beach length, where there were areas that could not be surveyed due to river mouths or rocks outcrops. The coordinates of the alongshore dune toe was then rotated in order to determine a cross-shore and alongshore distance for each beach, which were interpolated and then plotted. The height of the dune toe alongshore was also plotted using the alongshore distance along the beach length. A psuedocolor plot was also used to represent the horizontal position and height of the dune toe, along with the difference in distance from the mean horizontal position of the dune toe and the difference in height from the mean height of the dune toe.

The vegetation line and dune toe were extracted from the historic dataset of the beach profiles. The vegetation line and dune toe were extracted from comments associated with the beach profiles from the historic dataset. The beach profiles were analysed from a text file and the previously processed in BPAT. The comments that indicated either the vegetation line or the dune toe were extracted from the beach profile dataset and a smaller vegetation line/dune toe dataset was formed. This dataset was then further split into a vegetation line dataset and a dune toe dataset, resulting in one viable vegetation line and one viable dune toe position for each date, where double ups were removed. The dune toe from the field surveys of between December 2018 and December 2019 where then added to the datasets of the vegetation line and dune toe, for field survey beaches. The vegetation line and dune toe were plotted against one another for each profile site.

The comments varied throughout the dataset, where comments indicating the present vegetation line or dune toe varied for each profile surveyed. The comments varied with the people that conducted the surveys, where there has been numerous people conducting the surveys throughout the historic dataset.

The comments that were considered to be the vegetation line were Edge of Vegetation (EV), EV pingao, EV spinifex, EV iceplant, top of dune (scarp) and top of scarp. The comments that were considered to be the dune toe were dune toe, bottom of scarp and beach, which refers to the survey has moved from on the sand dunes to the beach, which implies the position of the dune toe. There were various other comments that also indicated to be the dune toe or vegetation that were used when considered appropriate. Across the beach profiles surveys of Whangapoua Beach to Buffalo Beach, there was large variation in comments used, and the dune toe was identified regularly. Across the beach profile surveys of Maramaratotara Beach to Whiritoa Beach, only the EV was recorded regularly. The vegetation line was manually extracted from the vegetation line/dune toe dataset so that there was only one vegetation line for each date for each profile site, making sure double ups were taken out. For the dune toe to be determined, the vegetation line/dune toe dataset, was put through an individual threshold filter for each profile site (Figure 4.3). The threshold filter encompassed the inflection point of all the beach profiles for an individual profile site. Once the dataset was put through the threshold filter, the data was manually checked for any double ups of dates so that there was one dune toe position for each date for a profile site. The relative distance and relative height were plotted against time for both the vegetation line and dune toe, where the earlier position of the vegetation line or dune toe was used as the reference distance and height for each profile site. The earliest position of the vegetation line or dune toe for each profile site are shown in Table 4.1.
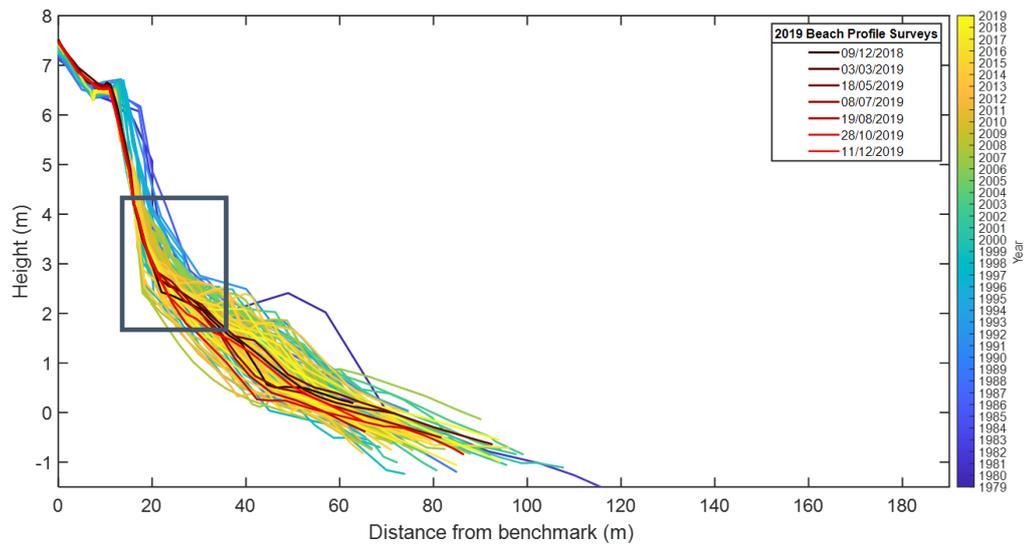
Figure 4.3. Threshold filter (grey box) used for determining the dune toe from beach profile sites. Beach Profiles for profile site CCS11, Whangapoua Beach.

Table 4.1. Reference distance (m) and height (m) for the relative distance and height of dune toe and vegetation line throughout time.

Profile Site	Date of survey	Distance (m)	Height (m)
Whangapoua			
CCS11	4th December 1991	15.90	5.47
CCS11-1	24th August 1995	87.25	4.21
CCS12	15th March 1995	76.35	3.06
Matarangi			
CCS13	4th July 1990	118.30	3.83
CCS14	8th December 1996	93.80	2.24
CCS15	10th August 1996	85.50	3.71
CCS16	23rd March 1997	142.05	3.35
CCS17	21st October 2015	8.90	3.40
Buffalo			
CCS24	4th July 1990	44.30	1.97
CCS25	24th July 1994	55.35	1.84
CCS25-2	30th September 2001	19.78	2.17
CCS25-3	4th February 2001	11.00	2.18
CCS25-1	22nd November 1992	9.10	3.41
CCS26	4th July 1992	108.90	2.57
CCS26/1	18th August 2015	11.00	4.51
CCS27	10th August 1996	6.90	4.11
CCS27/10	25th June 2014	4.00	3.71
CCS27/8	26th February 2013	2.20	3.32
CCS27/6	30th January 2007	8.70	3.76
CCS27/2	26th March 1998	3.60	3.49
CCS27/3	26th March 1998	2.35	3.44
CCS27/4	29th January 1999	2.55	3.19
CCS27/5	7th September 1998	8.00	2.16
Hot Water Beach			
CCS34	5th December 1999	18.00	4.39
CCS35	29th July 1996	61.90	3.62
CCS35-1	29th July 1996	57.40	3.84
Tairua			
CCS36	12th October 1997	79.20	7.64
CCS36-2	5th December 2003	58.60	4.23
CCS36-1	10th August 1996	88.20	4.52
CCS37	20th December 1998	147.75	5.28

4.4 Results

Within the results section there were six figures presented for the six field survey beaches for Coromandel Peninsula of Whangapoua Beach, Matarangi Beach, Buffalo Beach (which was split into North Buffalo, Middle Buffalo and South Buffalo for the figures including the alongshore dune toe horizontal position and height), Hot Water Beach and Tairua Beach, and along with Nagrunui Beach, Raglan. The horizontal position of the vegetation line and dune toe throughout time was shown in Figure 4.4, the graph showed the change in horizontal distance relative to the earliest vegetation line or dune toe position from the dataset of each profile, where the y-axis represented the change in relative horizontal distance and the x-axis represented time. The height of the vegetation line and dune toe throughout time was shown in Figure 4.5, the graph showed the change in height relative to the earliest vegetation line or dune toe position from the dataset of each profile, where the y-axis represented the change in relative height and the x-axis represented time. The distribution of the horizontal position of the vegetation line and the dune toe line was shown in Figure 4.6, where the x-axis of the histogram represented the range and distribution of the vegetation line and dune toe, and the y-axis represented the frequency of the horizontal position of the vegetation line and dune toe.

The coordinate position of the dune toe along the length of the beach throughout the survey period was shown in Figure 4.7, where the y-axis represented the latitude of the dune toe position and the x-axis represented the longitude of the dune toe position. The cross-shore distance of the dune toe along the length of the beach was shown in Figure 4.8.A, where the y-axis represented the cross-shore distance of the dune toe and x-axis represented the alongshore distance of the dune toe. The height of the dune toe was shown in Figure 4.8.B, where the y-axis represented the height of the dune to and the x-axis represented the alongshore distance along the length of the beach. The horizontal position of the dune toe was shown in Figure 4.9.A, where each bar represented the dune toe along the length of the beach at a certain point in time and the colour represented the cross-shore distance of the horizontal position of the dune toe. The difference in cross-shore distance of the dune toe from the mean horizontal position of dune toe

66

was shown in Figure 4.9.B, where each bar represented the dune toe along the length of the beach at a certain point in time and the colour represented the difference in cross-shore distance of the dune toe from the mean horizontal position of the dune toe.

4.4.1 Whangapoua Beach

There was movement of the vegetation line and the dune toe throughout the measured time period at all three profiles (Figure 4.4). There was a slow landward retreat of the vegetation line and dune toe at CCS11 (A) between 1996 and 1996, where the vegetation line retreated and there were sudden back and forth movements of the vegetation line during 2001 and 2003. The dune toe became more seaward of the vegetation line from 1996 to 2004 at the site of CCS11 and from 1997 to 2004 at the site of CCS11-1 (B). During 2004 there was a sudden seaward movement of the vegetation line at CCS11, and the vegetation line and dune toe were in the same position between 2004 and 2008, at both CCS11 and CCS11-1. During 2008, there was a sudden landward movement of the vegetation line and dune toe at CCS11 and CCS11-1. The dune toe slowly moved seaward from 2008 to 2011 and moved landward in 2012. The vegetation line and dune toe were in the same position and has stayed stable for between 2012 to 2018, with slight seaward movement of the dune toe during 2018 and 2019 at CCS11. At CCS11-1 there was large seaward movement of the dune toe during 2008 and retreat during 2011. There was large retreat of the vegetation line during 2014 at CCS11-1 and a slow seaward movement to 2019, whilst the dune toe was seaward of the vegetation line until 2019. At site CCS12 (C), at the north end of Whangapoua Beach, there was a sudden landward movement of the vegetation line during 1997 and a slow landward movement of the vegetation line through to 2019, with two large back and forth movements during 2006 and 2007 and smaller back and forth movements throughout the time period. At site CCS12 the dune toe was seaward of the vegetation line between 1997 and 2012 there was much larger back and forth movement than the vegetation line. The vegetation line and dune toe were in the same position between 2012 and 2019. There was a much larger distribution in the relative distance of the vegetation line compared with the dune toe (Figure 4.6) for all three sites of CCS11 (A), CCS11-1 (B) and CCS12 (C).
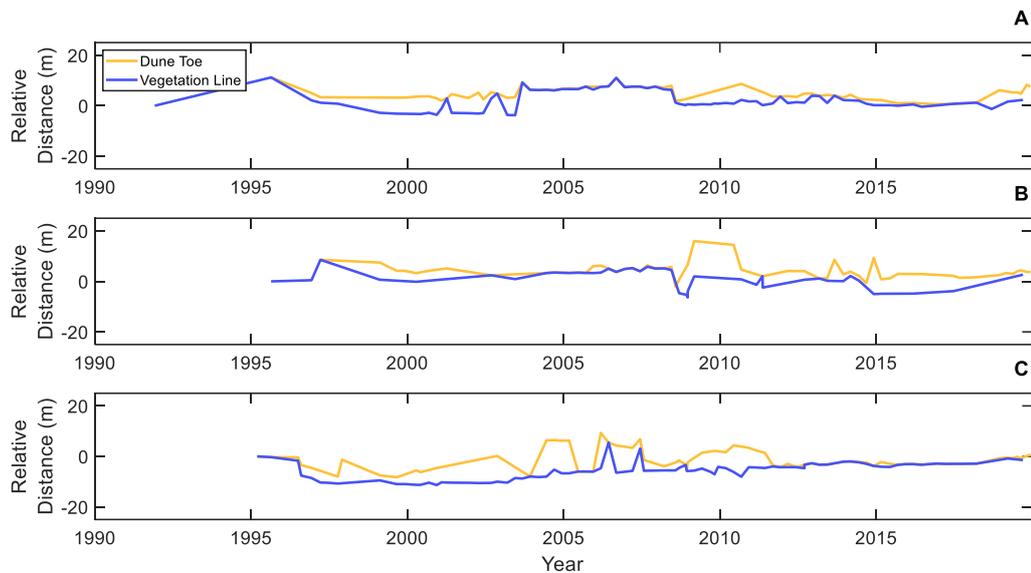
Figure 4.4. The change in relative horizontal distance of the vegetation line and dune toe, Whangapoua Beach. The vegetation line (purple line) and dune toe (orange line) for at the beach profile sites of CCS11 (A), CCS11-1 (B) and CCS12 (C).

There has also been change in the relative height of the vegetation line and dune toe throughout the measured time period (Figure 4.5). During the late 1990's to early 2000's when the dune toe was seaward of the dune toe, the height of the vegetation line was higher than the height of the dune toe, for CCS11 (A), CCS11-1 (B) and CCS12 (C). Between 2003 and 2007 the vegetation line and dune toe were the same height and horizontal position for all three sites. Between 2014 and 2019 at site CC11, the vegetation line and dune toe were in the same horizontal position but differed in height. There was a much larger variation in height of the vegetation line compared with dune toe for all three sites of CCS11, CCS11-1 and CCS12 (Appendix C.1).
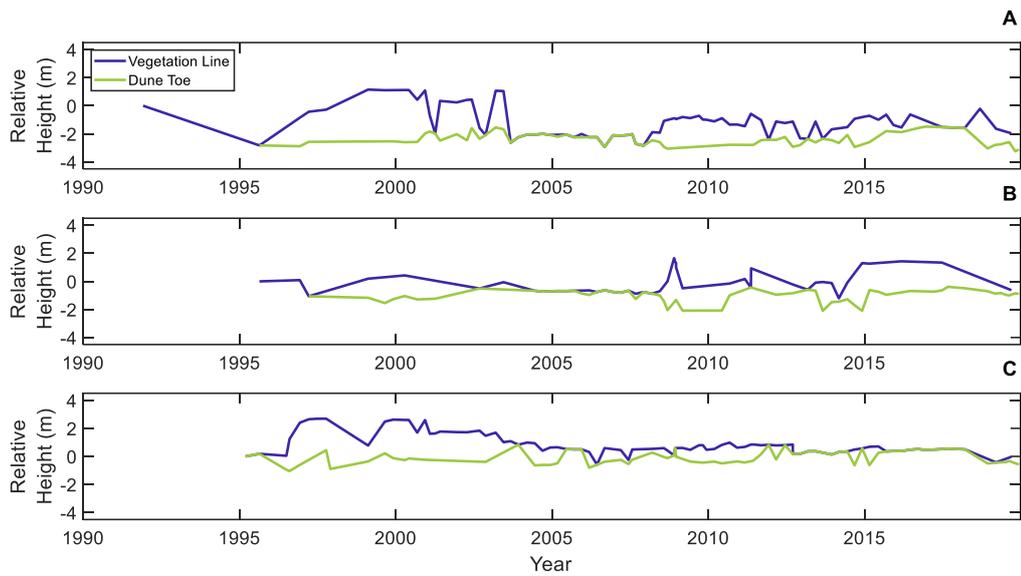
Figure 4.5. The change in relative height of the vegetation line and dune toe, Whangapoua Beach. The vegetation line (blue line) and dune toe (green line) for at the beach profile sites of CCS11 (A), CCS11-1 (B) and CCS12 (C).
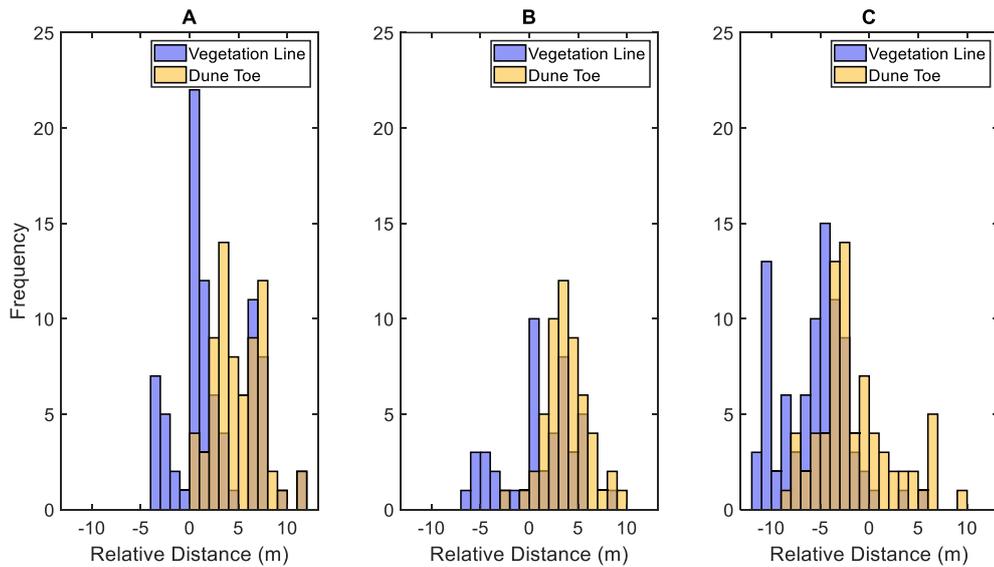
Figure 4.6. The distribution of relative horizontal distance position of the vegetation line and dune toe, Whangapoua Beach. The vegetation line (purple line) and dune toe (orange line) for at the beach profile sites of CCS11 (A), CCS11-1 (B) and CCS12 (C).

There was a small amount of change in the dune toe position along the length of Whangapoua Beach from December 2018 to December to 2019 (Figure 4.7). There was a small amount of variation of the dune toe along the beach where the dune position moved back and forth along the beach length (Figure 4.8.A). There was a

69

small amount of movement of the dune toe throughout the time period of December 2018 and December 2019 (Figure 4.8.A), where there was seaward movement of the dune toe at the south end of the beach, between the alongshore distance of -100 to 750 and at the north end of the beach between the alongshore distance of -600 and -750. There was little to no change between the alongshore distance of -300 to -600.

There was change in the height of the dune toe alongshore with large spikes in height along the beach length (Figure 4.8.B). At the south end of the beach between the alongshore distance of 200 to 750, there was a decrease in height of the dune toe and the north of the beach there was an increase in height between the alongshore distance of -150 to -800. Between the alongshore distance of -50 to -150, there was a large decrease in dune toe height (Figure 4.8.A) and increase in cross-shore distance (Figure 4.8.B).

Figure 4.9 shows that there was generally small back and forth movements of the dune toe throughout the time period of the surveys between December 2018 and December 2019 (Figure 4.9.B). The general trend of slight landward movement throughout the year at the south of the beach, between the alongshore distance of 0 to 700 is highlighted (Figure 4.9.B), along with some areas of landward movement during winter period of May 2019 to August 2019, and seaward movement during the summer period of November 2019 to December 2019 (Figure 4.9.B).
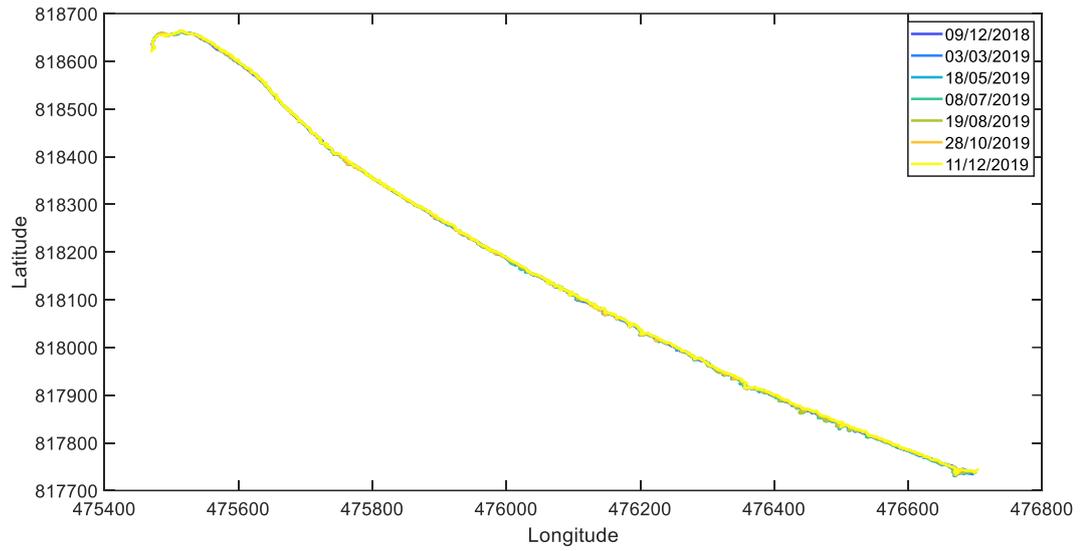
Figure 4.7. The coordinate position of the alongshore dune toe, Whangapoua Beach. Field surveys were taken 9th December 2018, 3rd March 2019, 18th May 2019, 8th July 2019, 19th August 2019, 28th October 2019 and 11th December 2019.
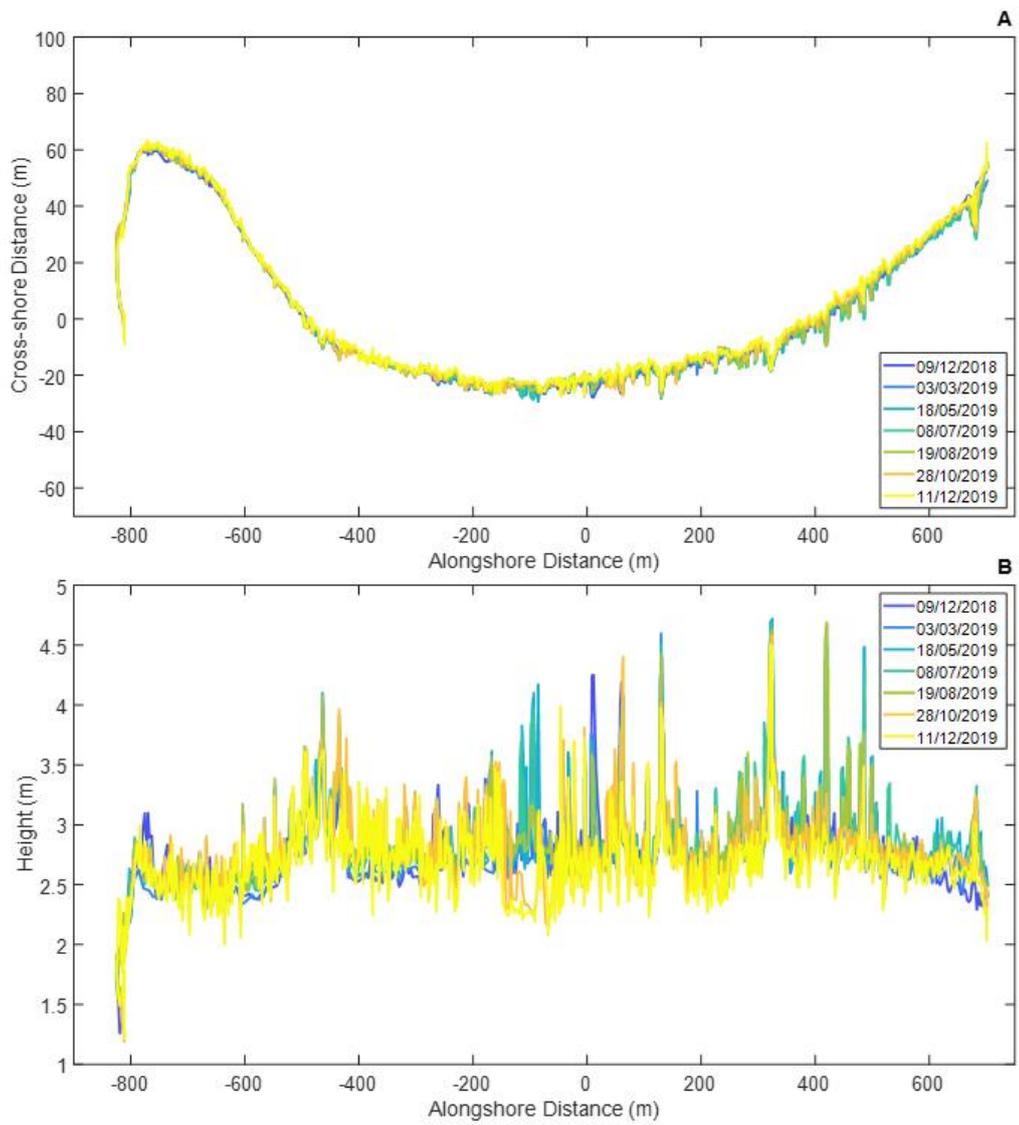
Figure 4.8. The cross-shore distance of the dune toe (A) and the height of the dune toe (B), Whangapoua Beach. Field surveys were taken 9th December 2018, 3rd March 2019, 18th May 2019, 8th July 2019, 19th August 2019, 28th October 2019 and 11th December 2019.
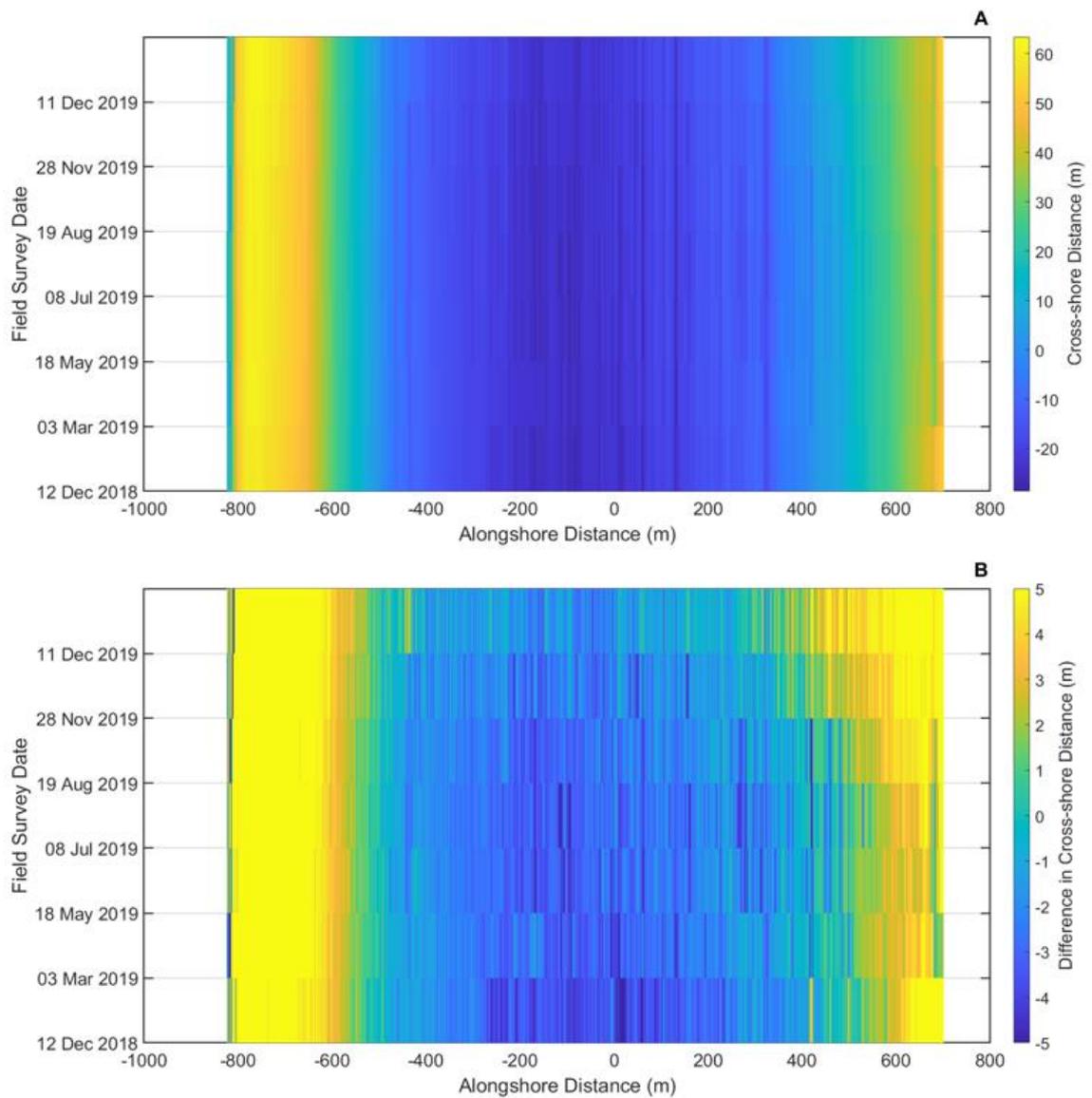
Figure 4.9. The horizontal position of the dune toe (A) and the difference of cross-shore distance of the dune toe from the mean horizontal position of the dune toe (B), Whangapoua Beach. Each bar represents a field survey of the dune toe and the colour of each bar represents the cross-shore position of the horizontal dune toe (A) and the difference of cross-shore distance from the mean horizontal dune toe position. Field surveys were taken 9th December 2018, 3rd March 2019, 18th May 2019, 8th July 2019, 19th August 2019, 28th October 2019 and 11th December 2019.

4.4.2 Matarangi Beach

There was movement of the vegetation line and dune toe throughout the measured time period at all five profile sites of CCS13 (A), CCS14 (B), CCS15 (C), CCS16 (D) and CCS17 (E) (Figure 4.10). There was a large sudden movement landward of the vegetation line and dune toe at all of the profile sites during 2008, except the dune toe of CCS16 (D) and for the site CCS17 (E) which was not measured at the time. At CCS13, the vegetation line moved back and froth in distance between 1997 to 2000, whilst the dune toe stayed in the same position. There was landward retreat of the vegetation line and dune toe at CCS14 and CC15 between 1997 and 2003, where the dune toe retreated much less than the vegetation line at CCS14. There was slow seaward movement of the vegetation line and dune toe at all three sites of CCS14, CCS15 and CCS16 between 2003 and 2005. At CCS13, during the 2002 to 2019 the vegetation line and dune toe were in the same position, except for a small landward movement on the dune toe during 2008 and large movement forward between 2014 and 2017. The vegetation line and dune toe were stable during 2008 and 2013 and moved slowly seaward between 2013 and 2019. At CCS15, the vegetation line and dune toe were also in the same position between 2008 and 2011 and then slowly moved seaward until 2019, the vegetation line was much more varied with large back forth movements during this time period. The vegetation line was much more varied in horizontal position than the dune toe between 2012 to 2019 at all four sites of CCS13, CCS14, CCS15 and CCS16, and during the late 1990's for CCS13, where there was numerous movements back and forth of the vegetation line. The larger variation in the relative distance of the vegetation line compared with the dune toe was also shown in the distribution of the relative distance for the profile sites at Matarangi Beach (Figure 4.12), except for CCS17 (E) where only a small amount of data has been collected. The distribution of the dune toe was more seaward than the vegetation line at CCS14 (B), CCS16 (D) and CCS17 (E), and slightly more seaward at CCS15 (C) (Figure 4.12).

The relative height of the vegetation line was higher than the dune toe for the majority of the measured time period (Figure 4.11), apart from between 2002 and 2005 for CCS13 (A), between 2004 to 2008 at CCS14 (B) and between 2001 and

2005 at CCS16 (D). There was a much larger variation in the height of the vegetation line compared with the dune toe, with much larger back and forth movements of higher to lower height of the vegetation line compared with the dune toe across all of the profile sites. The dune toe height was more stable at the sites of CCS14, CCS15 and CCS16 compared with CCS13 (Figure 4.11).
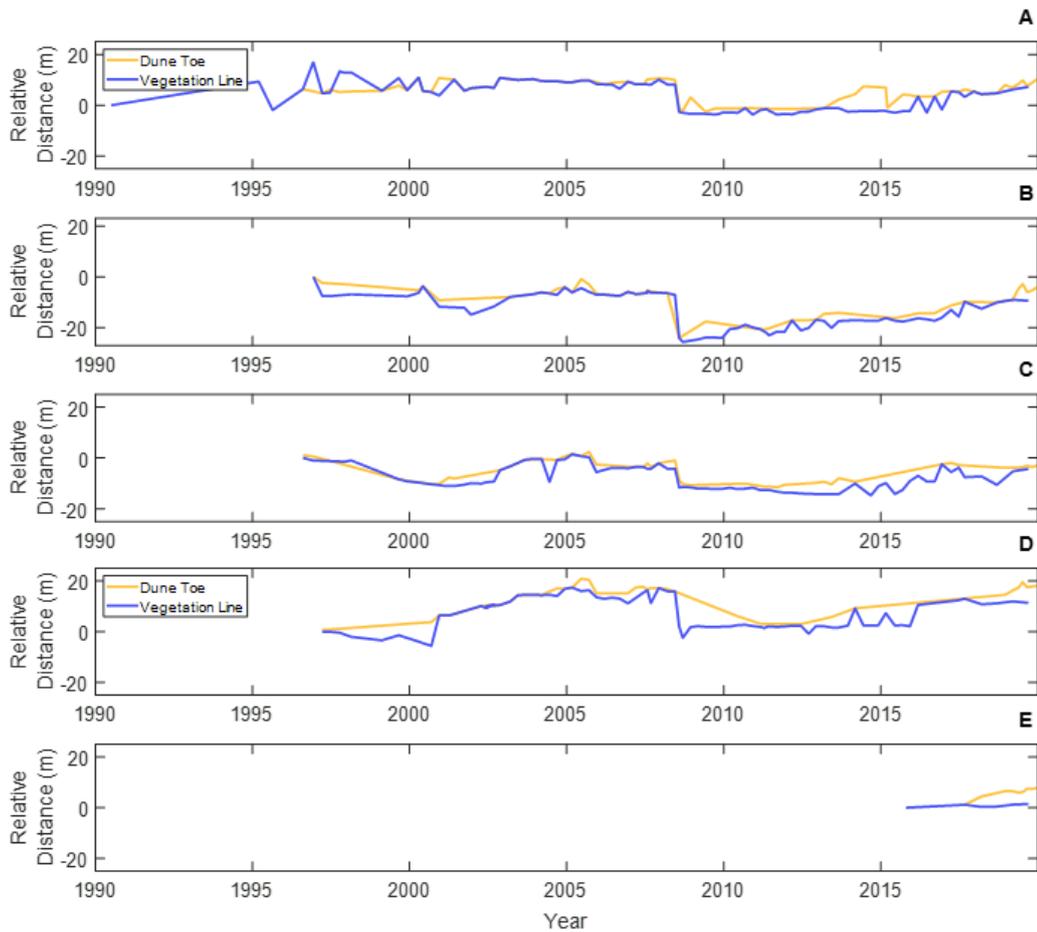
Figure 4.10. The change in relative horizontal distance of the vegetation line and dune toe, Matarangi Beach. The vegetation line (purple line) and dune toe (orange line) for at the beach profile sites of CCS13 (A), CCS14 (B), CCS15 (C), CCS16 (D) and CCS17 (E). Note the y-axis is shifted in panel B.
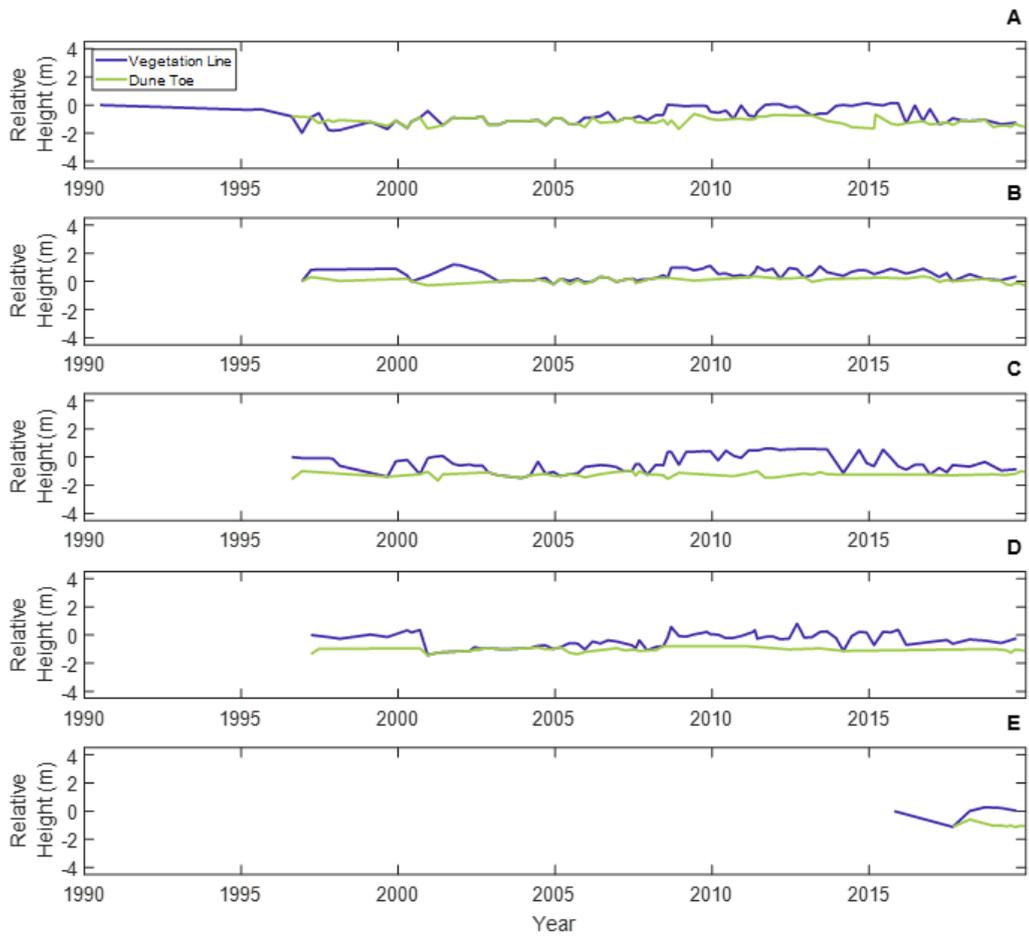
Figure 4.11. The change in relative height of the vegetation line and dune toe, Matarangi Beach. The vegetation line (blue line) and dune toe (green line) for at the beach profile sites of CCS13 (A), CCS14 (B), CCS15 (C), CCS16 (D) and CCS17 (E).
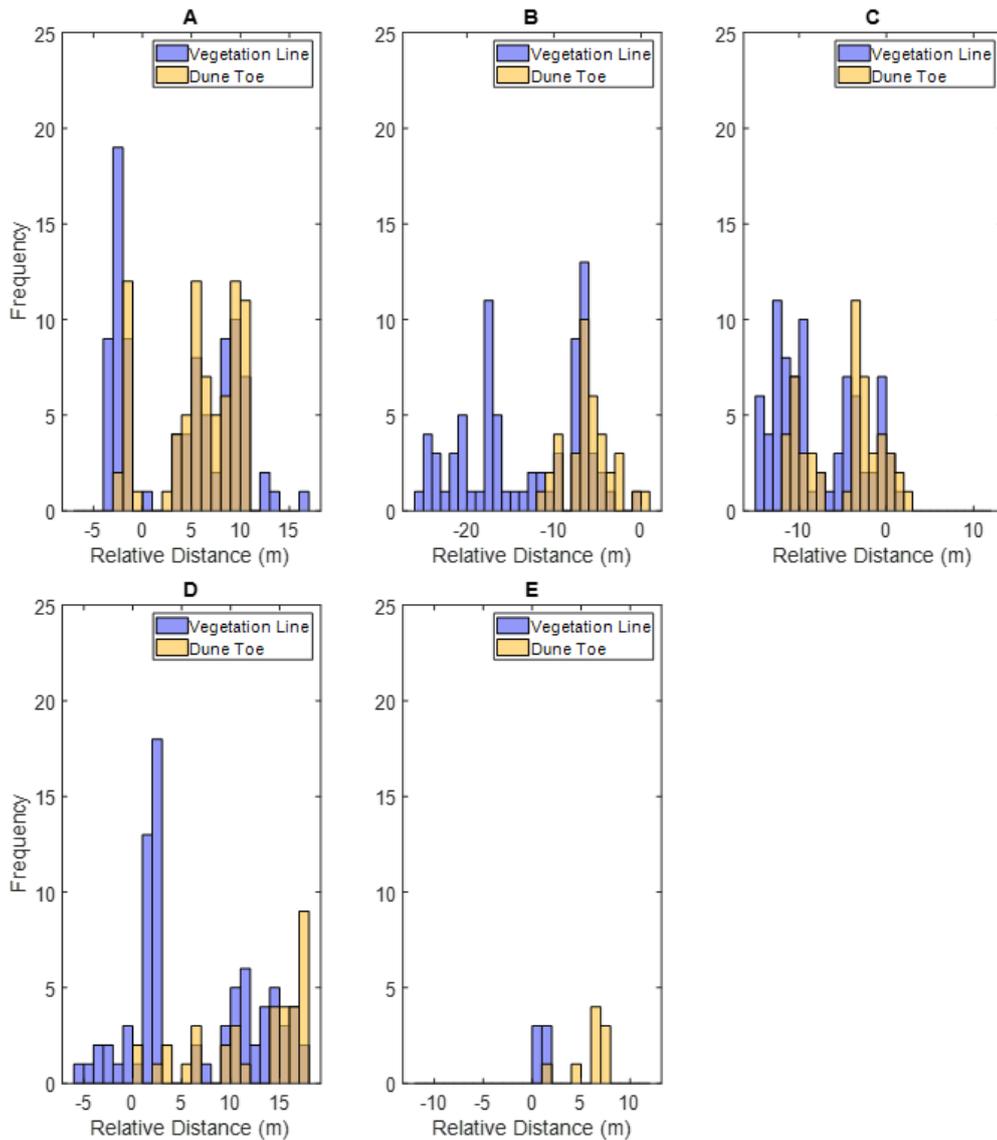
Figure 4.12. The distribution of relative horizontal distance position of the vegetation line and dune toe, Matarangi Beach. The vegetation line (purple line) and dune toe (orange line) for at the beach profile sites of CCS13 (A), CCS14 (B), CCS15 (C), CCS16 (D) and CCS17 (E). Note the shifted x-axis in panel A, B, C and D, and the different scale x-axis in panel B.

There was a small amount of change in the dune toe position along the length of Matarangi Beach from December 2018 to December to 2019 (Figure 4.13), except for at the north of the beach near the harbour entrance where much large changes occurred. There was seaward movement along the Matarangi Beach between the alongshore distance of -1400 and 1750 (Figure 4.14.A). There was a large amount of landward movement, at the north of the beach between the alongshore

distance of -1900 and -1400. The was seaward movement further south into the harbour entrance, between the alongshore distance of -1900 and -2100.

There was change in the height of the dune toe alongshore with large spikes in height along the beach length (Figure 4.14.B). At the south of the beach between the alongshore distance of 250 to 1750, there was an increase in height between December 2018 and March 2019, and then a decrease in dune toe height from March 2019 to December 2019. At the north of the beach between the alongshore distance of -1400 to 150, there was a decrease in height of the dune toe throughout the time period of December 2018 and December 2019. There was a larger decrease in height of the dune toe between the alongshore distance of -2000 to -1400 between August 2019 and October 2019 (Figure 4.14.B).

Figure 4.15 showed that there was generally small back and forth movements of the dune toe throughout the time period of December 2018 and December 2019 (Figure 4.15). There was a general trend of seaward movement throughout the year at Matarangi Beach (Figure 4.15.B), between the alongshore distance of -1500 to -1750. There were larger changes of the dune toe between the alongshore distance of -2250 to -1500, where the variability of change was higher, than along the rest of the beach length. The landward movement between -2000 and -1750 between August 2019 and October 2019 is also shown (Figure 4.15.B).
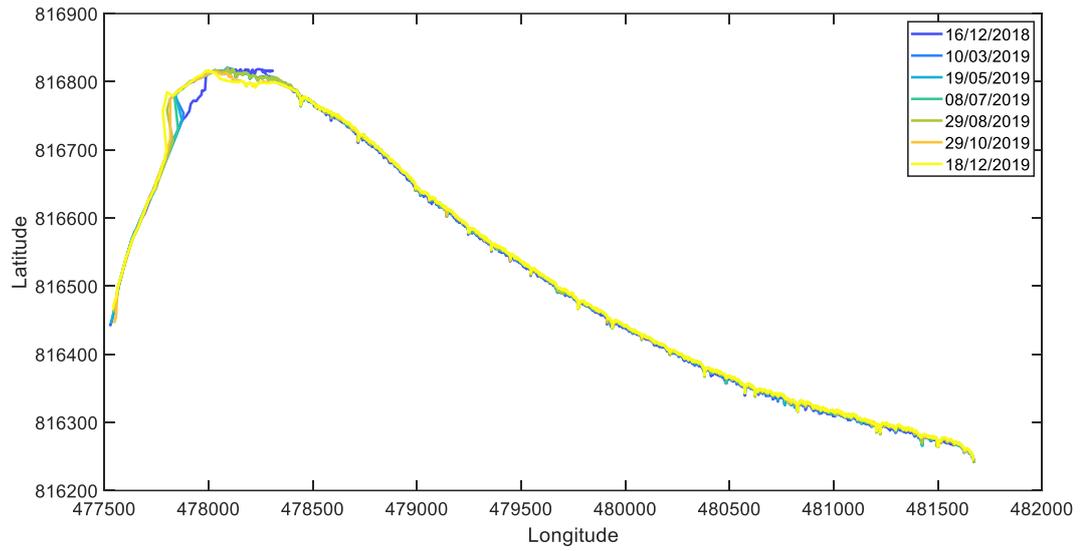
Figure 4.13. The coordinate position of the alongshore dune toe, Matarangi Beach. Field surveys were taken 16th December 2018, 10th March 2019, 19th May 2019, 8th July 2019, 29th August 2019, 29th October 2019 and 18th December 2019.
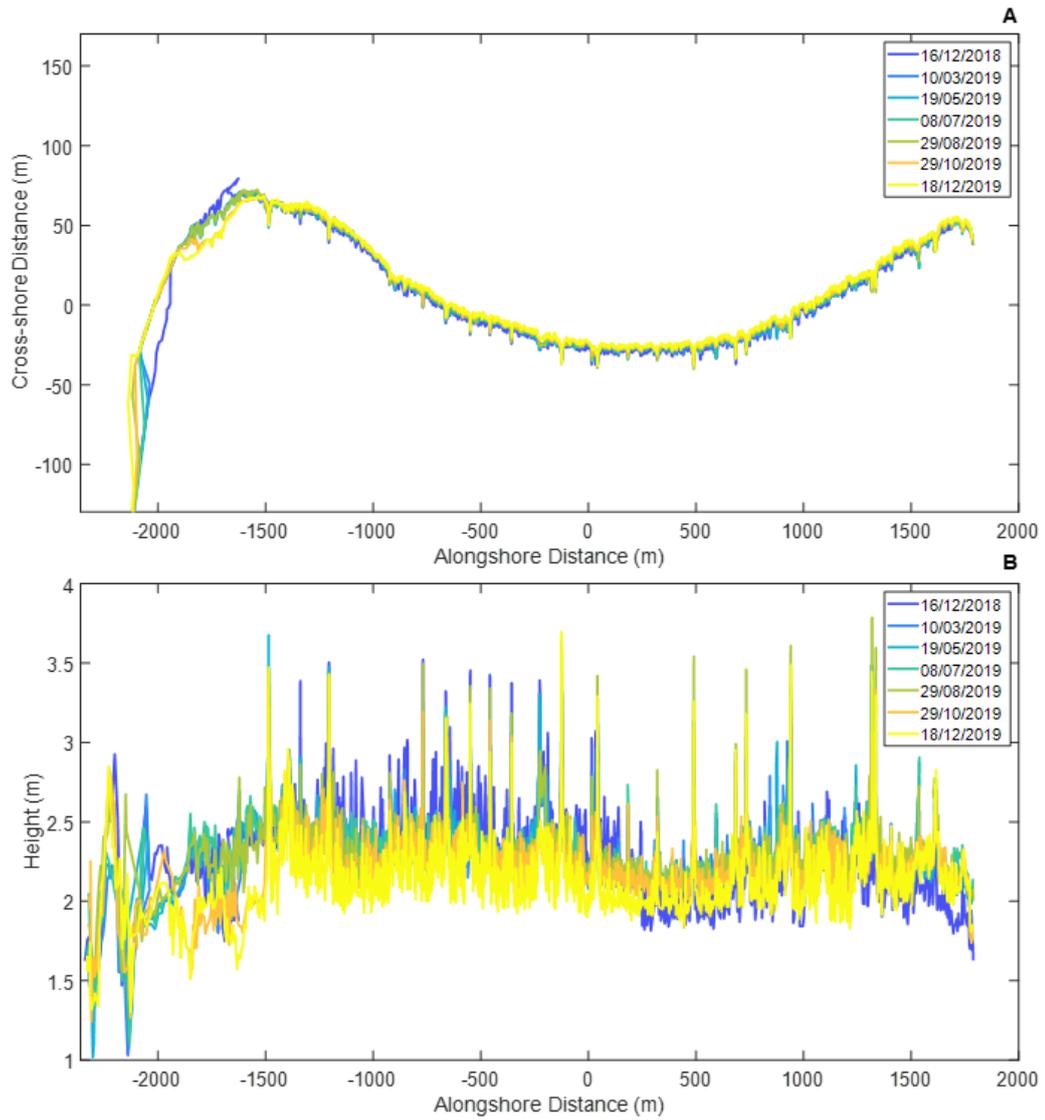
Figure 4.14. The cross-shore distance of the dune toe (A) and the height of the dune toe (B), Matarangi Beach. Field surveys were taken 16th December 2018, 10th March 2019, 19th May 2019, 8th July 2019, 29th August 2019, 29th October 2019 and 18th December 2019.
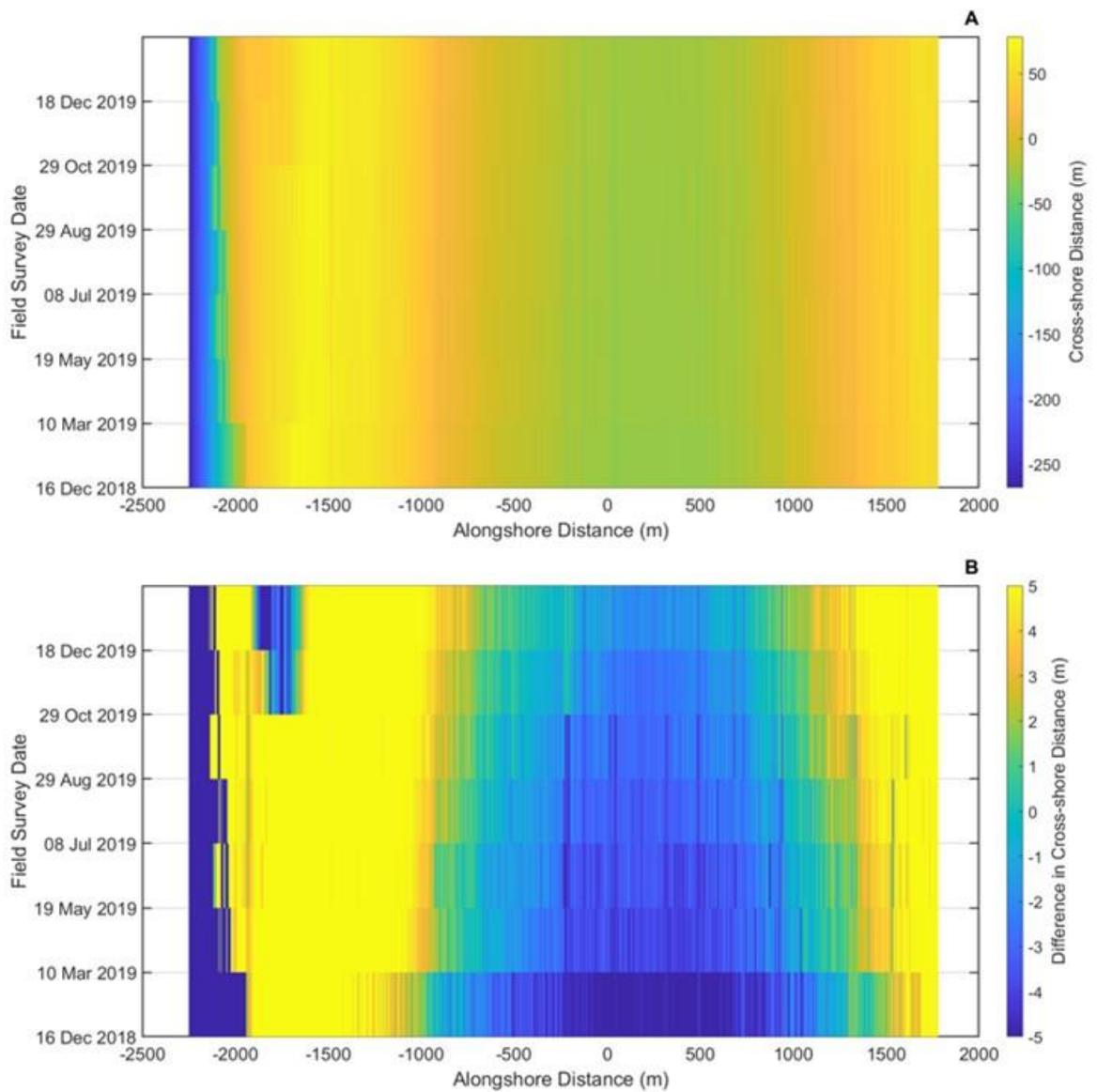
Figure 4.15. The horizontal position of the dune toe (A) and the difference of cross-shore distance of the dune toe from the mean horizontal position of the dune toe (B), MatarangiBeach. Each bar represents a field survey of the dune toe and the colour of each bar represents the cross-shore position of the horizontal dune toe (A) and the difference of cross-shore distance from the mean horizontal dune toe position. Field surveys were taken 16th December 2018, 10th March 2019, 19th May 2019, 8th July 2019, 29th August 2019, 29th October 2019 and 18th December 2019.

4.4.3 Buffalo Beach

Buffalo Beach been divided into North, Middle and South Buffalo for the horizontal position of the dune, height of the dune toe and the pseudocolour plot of the horizontal position of the dune toe, due to the wide angle that the beach was facing. The historic dataset at the beach profile sites of Buffalo Beach, consisting of the horizontal position of the vegetation line and dune toe were analysed.

There was movement of the vegetation line and dune toe throughout the measured time period at all of the fifteen profile sites of CCS24 (A), CCS25 (B), CCS25-2 (C), CCS25-3 (D), CCS25-1 (E), CCS26 (F), CCS26/1 (G), CCS27 (H), CCS27/10 (I), CCS27/8 (J), CCS27/6 (K), CCS27/2 (L), CCS27/3 (M), CCS27/4 (N) and CCS27/5 (O) (Figure 4.16). There was a sudden landward movement of the vegetation line and dune toe during 1997 at the profile sites of CCS24, CCS25, CCS25-1, CCS26 that were measured at the time. The magnitude of the change varied between the sites, with the largest change occurring at CCS26.

At the profile site of CCS24, there was a general trend of landward movement, with some small seaward movement of the vegetation line and dune toe between 2006 and 2007 and seaward movement of the dune toe during 1999 and 2014 (Figure 4.16). The dune toe was seaward of the vegetation line throughout the measured time period. The dune toe and vegetation line were stable from 2017, which is likely due human modification of a geotextile sand-bag wall that was added at the profile site in 2015. At CCS25 there was landward movement of the vegetation line and dune toe from 1994 to 2001 and both the vegetation line and dune toe were stable from 2001 to 2019, with some landward movements of the vegetation line during 2012 and 2015. The dune toe was seaward of the vegetation line for the majority of the measured time period (Figure 4.16). At the profile sites of CCS25, CCS25-2 and CCS25-3, there was a large seaward movement of the dune toe during 2005 (Figure 4.16). At the profile sites of CCS25-2 and CCS25-3, the vegetation line and dune toe were stable throughout the time, apart from the seaward movement of the dune toe in 2005. The dune toe was slightly seaward of the 'vegetation line' at both CCS25-2 and CCS25-3, however in this case the vegetation line represents the top of the seawall that is present at the both of the profile site. There were two sudden landward movements of the vegetation and

dune toe at CCS25-1 during the measured time period from 1992 and 2019 (Figure 4.16). The sudden landward movements occurred during 1997 and 2014, in between these sudden changes there was small amounts of slow landward movement and the vegetation line and dune toe was in a stable state between 2014 and 2019. At CCS26, there was a sudden landward movement of vegetation line and dune toe during 1997 and a sudden seaward movement during 2005 (Figure 4.16). The vegetation line was stable between 1997 and 2005 and the dune toe greatly varied in horizontal position. The vegetation line and dune toe were in the same position and slowly moved seaward from 2005 to 2017 before becoming stable from 2017 to 2019.

The vegetation line and dune toe were stable at the profile sites of CCS26/1 (G), CCS27 (H) and CCS27/8 (J), with some small variation of the dune toe at the profile site of CCS27 during 2005 and 2008 (Figure 4.17). At the profile sites CCS27/10 (I), CCS27/8 (J) and CCS27/6 (K), the dune toe was seaward of the vegetation line and was stable throughout the measured period, with some small variations, and seaward movement of the dune toe at the profile site of CCS27/10. At the profile sites of CCS27/2 (L), CCS7/3 (M) and CCS27/4 (N), the 'vegetation line' and dune toe were stable between 1998 and 2007, where the 'vegetation line' represented the top of the seawall present at all three of the profile sites (Figure 4.17 & Figure 4.18). The dune toe moved seaward between 2007 and 2015 and the 'vegetation line' was stable. At CCS27/2 and CCS27/3, the dune toe was stable between 2015 and 2019, whilst at CCS27/4 the dune toe moved seaward between 2015 and 2019. At the profile site of CCS27/5 (O) there was two sudden seaward movements of the vegetation line and dune toe during 2010 and 2018, with some back and forth variation of the dune toe and vegetation line during 2011 and 2015 (Figure 4.18).

The distribution of the horizontal position of the dune toe was smaller than the distribution of the vegetation line at the profile sites of CCS24 (A), CCS25 (B), CCS25-1 (E), CCS26 (F) CCS26/1 (G) and CCS27/5 (O) (Figure 4.22 & 4.24). The distribution of the horizontal position of the dune toe is larger than the distribution of the dune toe for the profile sites of CCS25-2 (C), CCS25-3 (D), CCS27 (H), CCS27/10 (I), CCS27/8 (J), CCS27/6 (K), CCS27/2 (L), CCS27/3 (M) and CCS27/4

(N). The vegetation line and the dune toe were the same distribution for CCS25-2 (D). The dune toe was more seaward than the vegetation line at the profile sites of CCS25-2, CCS27/10, CCS27/8, CCS27/6, CCS27/2, CCS27/3 and CCS27/4.

The relative height of the vegetation line was higher than the dune toe for the profile sites at Buffalo Beach of except for CCS26 (F) and CCS27/5 (O) where the vegetation line and dune toe was the same height, and at CCS27 (H) where the vegetation line was lower than the dune toe height (Figure 4.20).
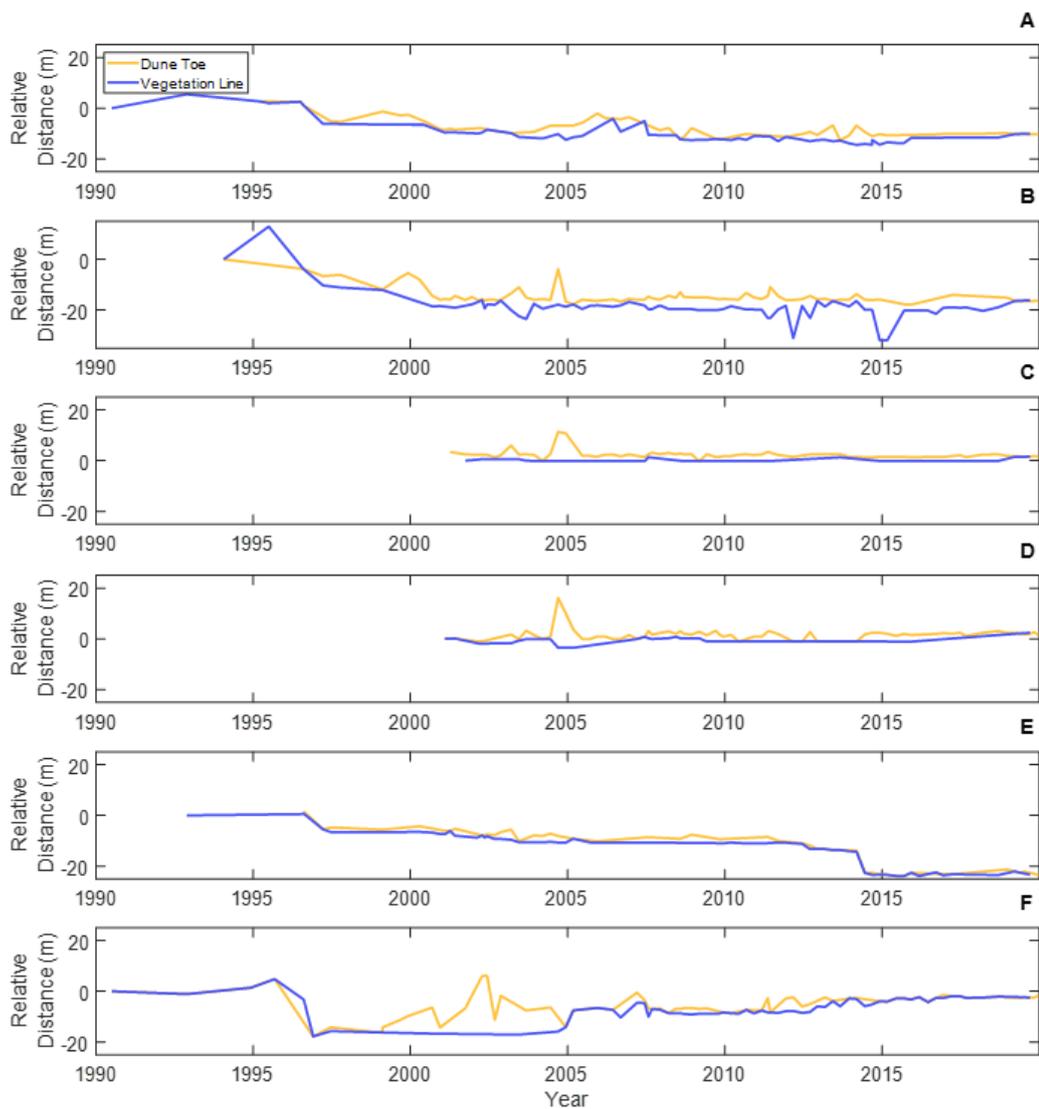
Figure 4.16. The change in relative horizontal distance of the vegetation line and dune toe, Buffalo Beach. The vegetation line (purple line) and dune toe (orange line) for at the beach profile sites of CCS24 (A), CCS25 (B), CCS25-2 (C), CCS25-3 (D), CCS25-1 (E) and CCS26 (F). Note the shifted x-axis in panel B.
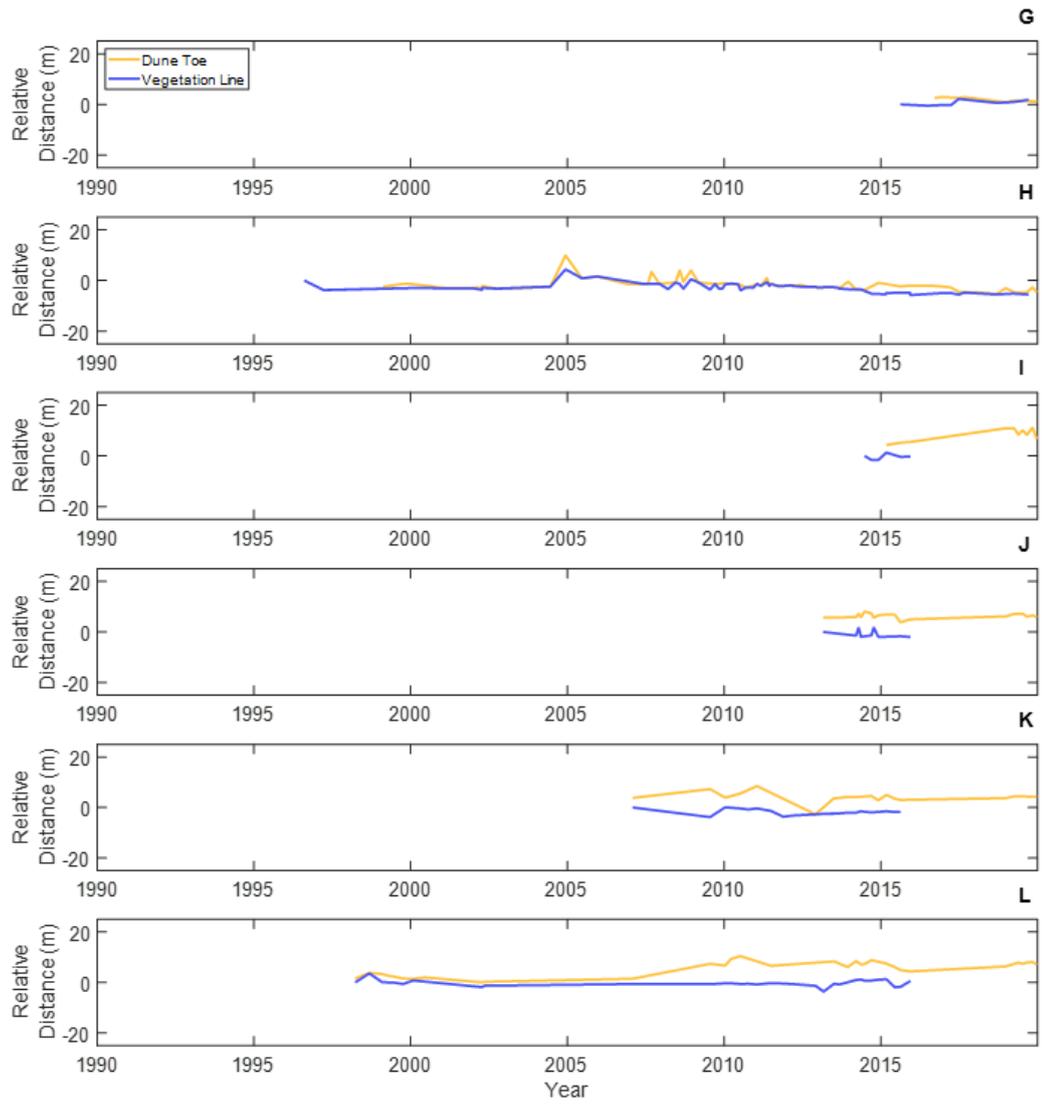
Figure 4.17. The change in relative horizontal distance of the vegetation line and dune toe, Buffalo Beach. The vegetation line (purple line) and dune toe (orange line) for at the beach profile sites of CCS26/1 (G), CCS27 (H), CCS27/10 (I), CCS27/8 (J), CCS27/6 (K) and CCS27/2 (L).
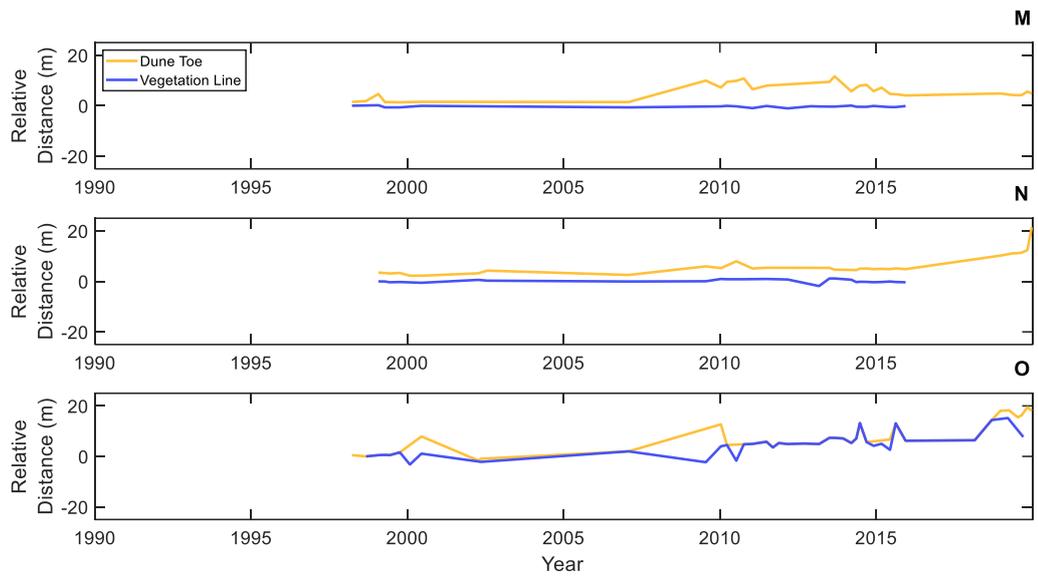
Figure 4.18. The change in relative horizontal distance of the vegetation line and dune toe, Buffalo Beach. The vegetation line (purple line) and dune toe (orange line) for at the beach profile sites of CCS27/3 (M), CCS27/4 (N), CCS27/5 (O).
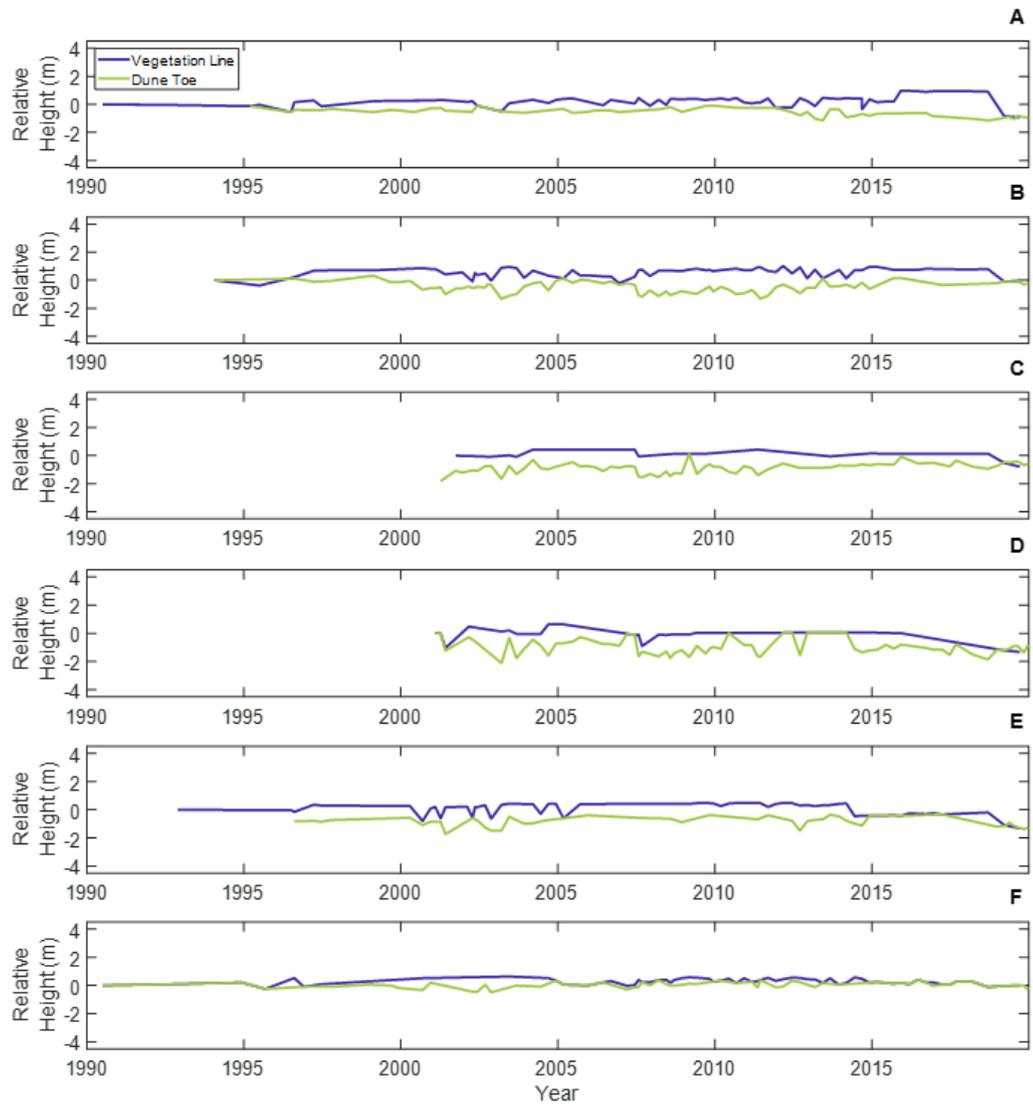
Figure 4.19. The change in relative height of the vegetation line and dune toe, Buffalo Beach. The vegetation line (blue line) and dune toe (green line) for at the beach profile sites of CCS24 (A), CCS25 (B), CCS25-2 (C), CCS25-3 (D), CCS25-1 (E) and CCS26 (F).
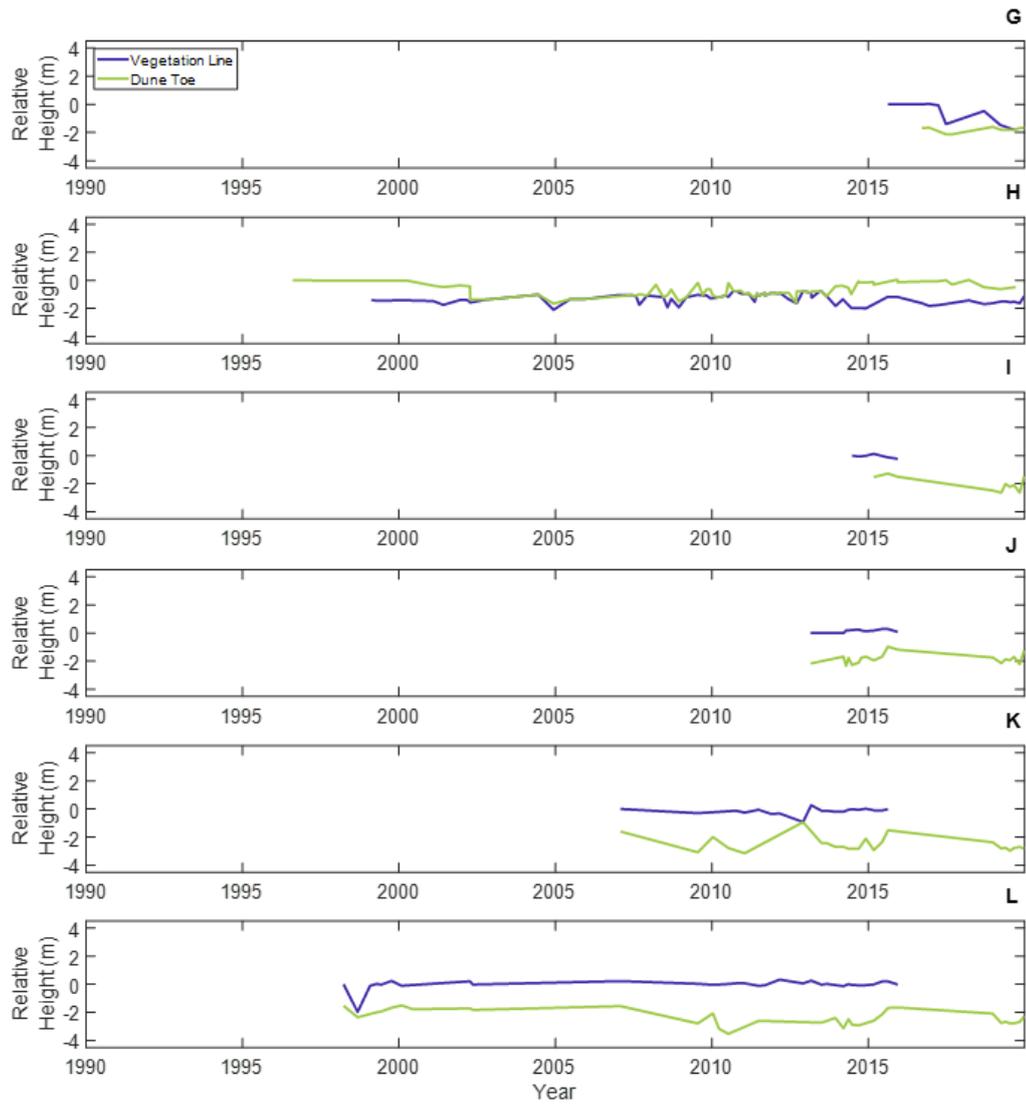
Figure 4.20. The change in relative height of the vegetation line and dune toe, Buffalo Beach. The vegetation line (blue line) and dune toe (green line) for at the beach profile sites of CCS26/1 (G), CCS27 (H), CCS27/10 (I), CCS27/8 (J), CCS27/6 (K) and CCS27/2 (L).
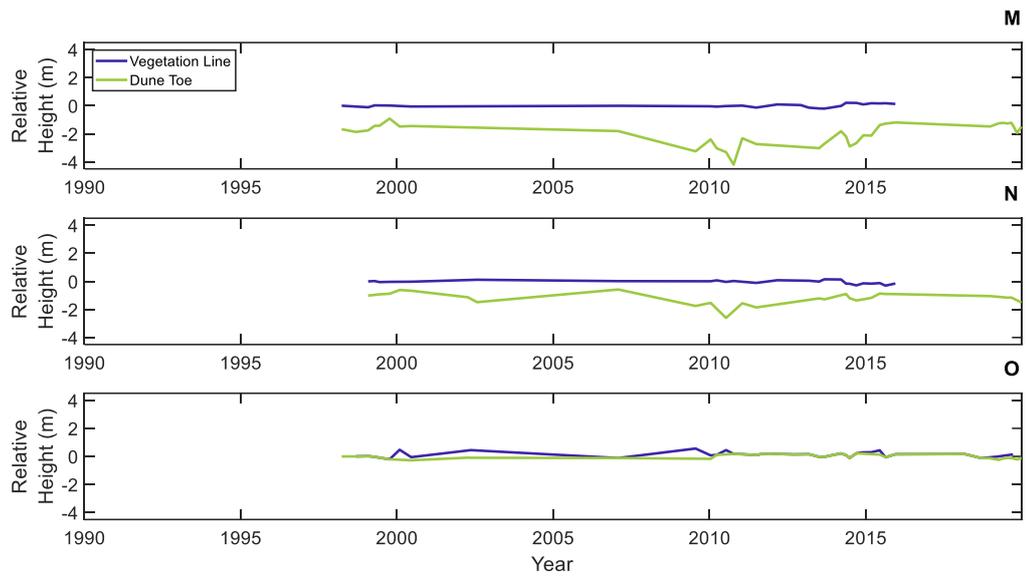
Figure 4.21. The change in relative height of the vegetation line and dune toe, Buffalo Beach. The vegetation line (blue line) and dune toe (green line) for at the beach profile sites of CCS27/3 (M), CCS27/4 (N), CCS27/5 (O).
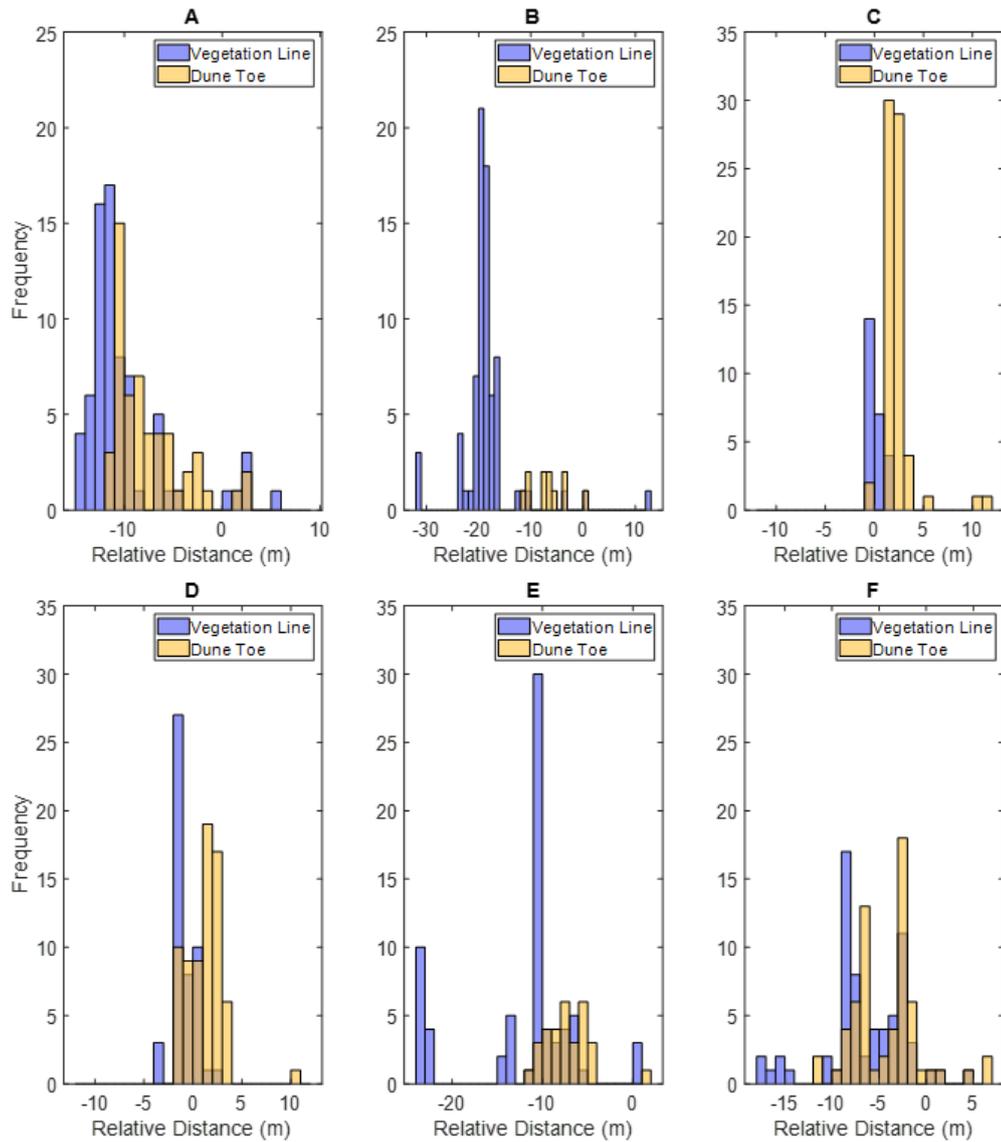
Figure 4.22. The distribution of relative horizontal distance position of the vegetation line and dune toe, Buffalo Beach. The vegetation line (purple line) and dune toe (orange line) for at the beach profile sites of CCS24 (A), CCS25 (B), CCS25-2 (C), CCS25-3 (D), CCS25-1 (E) and CCS26 (F). Not the x-axis is shifted in panel A, B, C, D, E and F, and the x-axis scale is different in panel B, E and F.
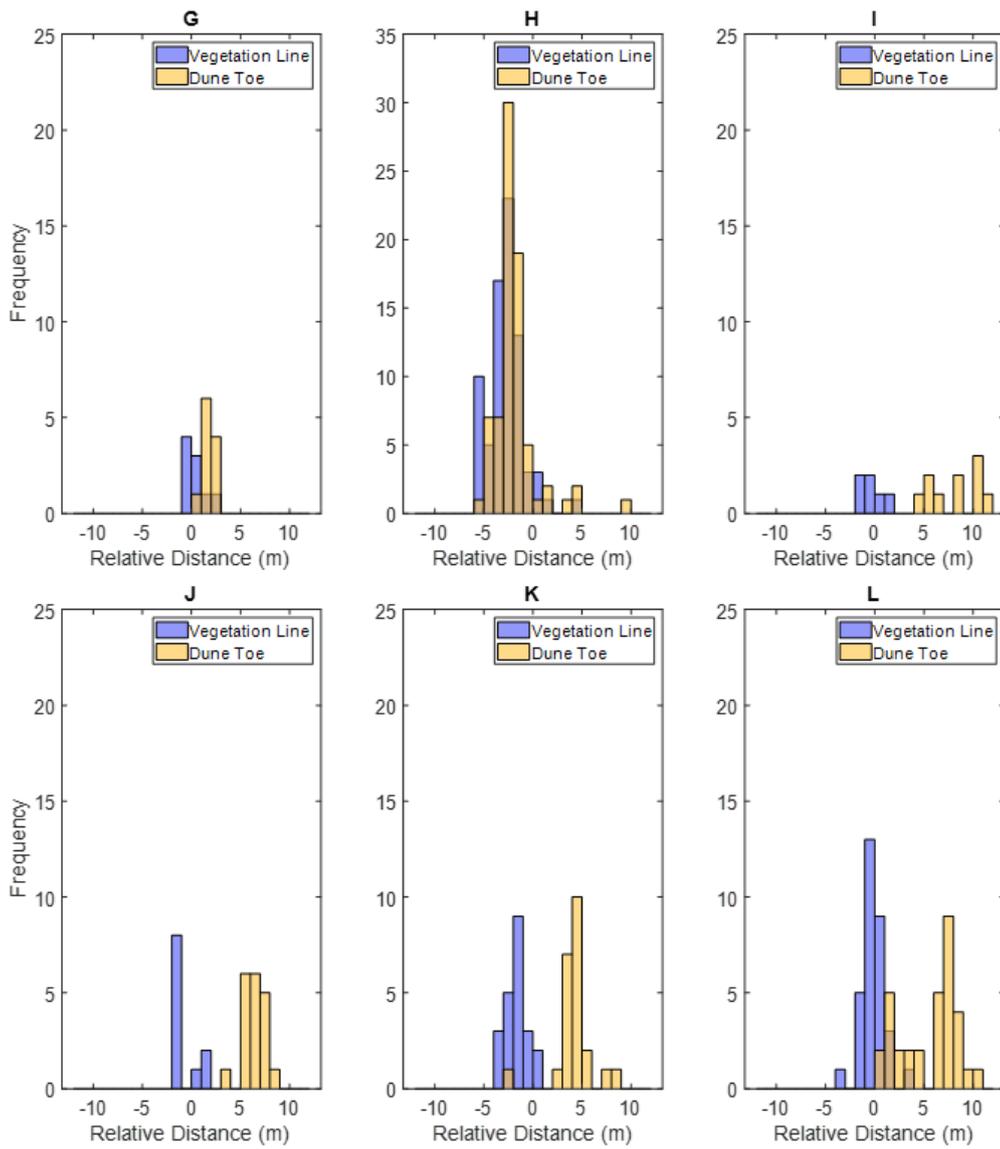
Figure 4.23. The distribution of relative horizontal distance position of the vegetation line and dune toe, Buffalo Beach. The vegetation line (purple line) and dune toe (orange line) for at the beach profile sites of CCS26/1 (G), CCS27 (H), CCS27/10 (I), CCS27/8 (J), CCS27/6 (K) and CCS27/2 (L). Note the x-axis is shifted in panel H.
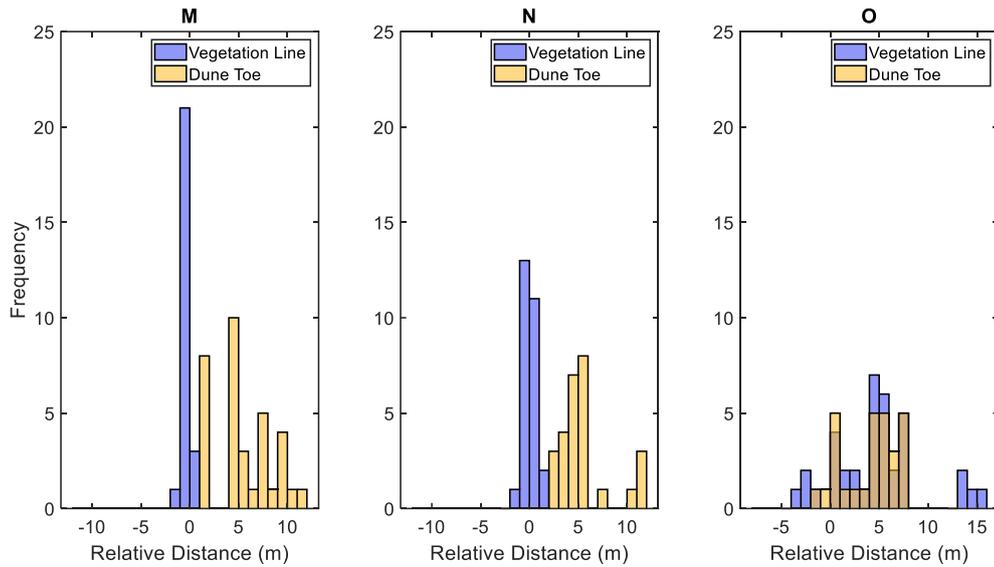
Figure 4.24. The distribution of relative horizontal distance position of the vegetation line and dune toe, Buffalo Beach. The vegetation line (purple line) and dune toe (orange line) for at the beach profile sites of CCS27/3 (M), CCS27/4 (N), CCS27/5 (O). Note the x-axis is shifted in panel O.

Northern Buffalo Beach was considered to be between the northern river mouth and the north of the beach to the east of the river mouth. Middle Buffalo Beach was considered to be between the North river mouth and the river mouth in the middle of the Buffalo Beach. South Buffalo Beach is considered to be the section of beach between the middle river mouth and the south end of Buffalo Beach (Figure 4.25). There was a small amount of change in the dune toe position along the length of Buffalo Beach from December 2018 to December to 2019 (Figure 4.25).
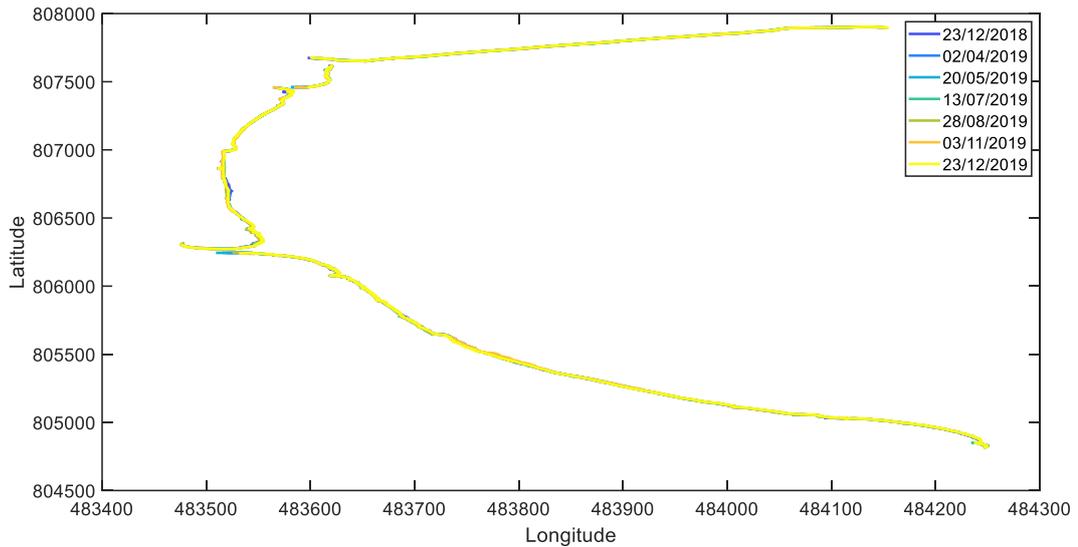
Figure 4.25. The coordinate position of the alongshore dune toe, Buffalo Beach. Field surveys were taken 23rd December 2018, 2nd April 2019, 20th May 2019, 13th July 2019, 28th August 2019, 3rd November 2019 and 23rd December 2019.

4.4.3.1 North Buffalo Beach

The dune toe moved seaward in along sections of the northern beach, between the northern river mouth and the north of the beach, during the time period of December 2018 and December 2019 (Figure 4.26.A), at the alongshore distance of between 90 to 120, -90 to 90 and -250 to -100. The dune toe moved seaward during December 2018 to November 2019 and moved back before December 2019, except for at the alongshore distance of 120 to 160. There was a geotextile sandbag wall present along the length of the northern section of the beach throughout the survey period, and the dune toe was measured along the edge of the sand-bag present at the bottom of the sand-bag wall.

There has also been change in the relative height of the vegetation line and dune toe throughout the measured time period (Figure 4.26). The dune toe was lowest in height during December 2018 to July 2019 at the alongshore distance of -80 to 260. The dune toe height increased between August 2019 to November 2019, and largely decreased between August 2019 to December 2019 between the alongshore distance between 50 to 190. The dune toe was low in height during December 2019, and the dune toe height increased to a higher dune toe height between April 2019 and August 2019. The dune toe decreased in height between

93

August 2019 and November 2019 and the dune toe increased in height between November 2019 and December 2019.

Figure 4.27.B also showed that horizontal position of the dune toe moved landward between December 2018 and April 2019 along some sections of the beach and seaward again between April 2019 and July 2019. There was landward movement of the dune toe between July and August 2019 at the alongshore distance of 0 to 400 and seaward movement at the alongshore distance or -400 to 0 (Figure 4.27).
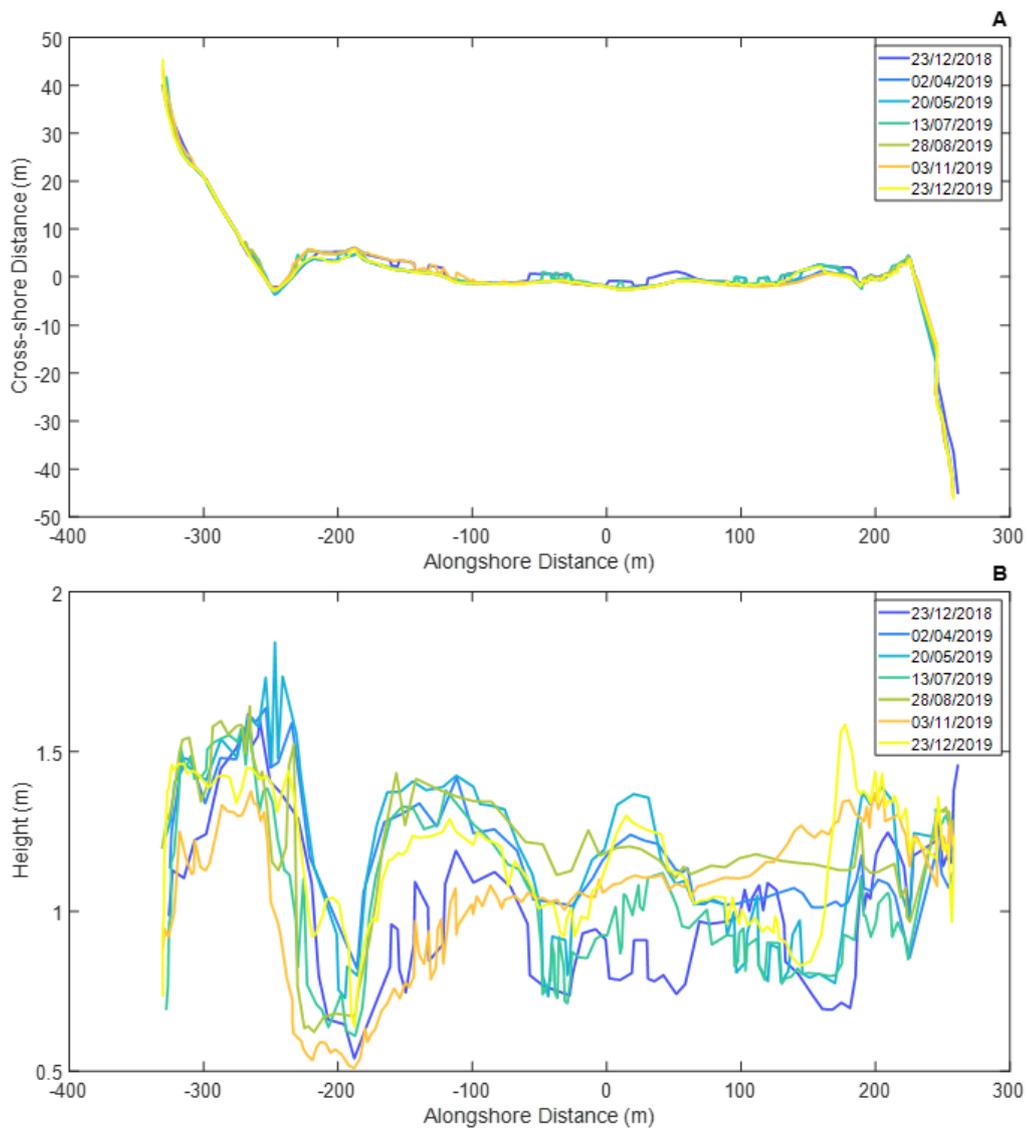
Figure 4.26. The cross-shore distance of the dune toe (A) and the height of the dune toe (B), Buffalo Beach. Field surveys were taken 23rd December 2018, 2nd April 2019, 20th May 2019, 13th July 2019, 28th August 2019, 3rd November 2019 and 23rd December 2019.
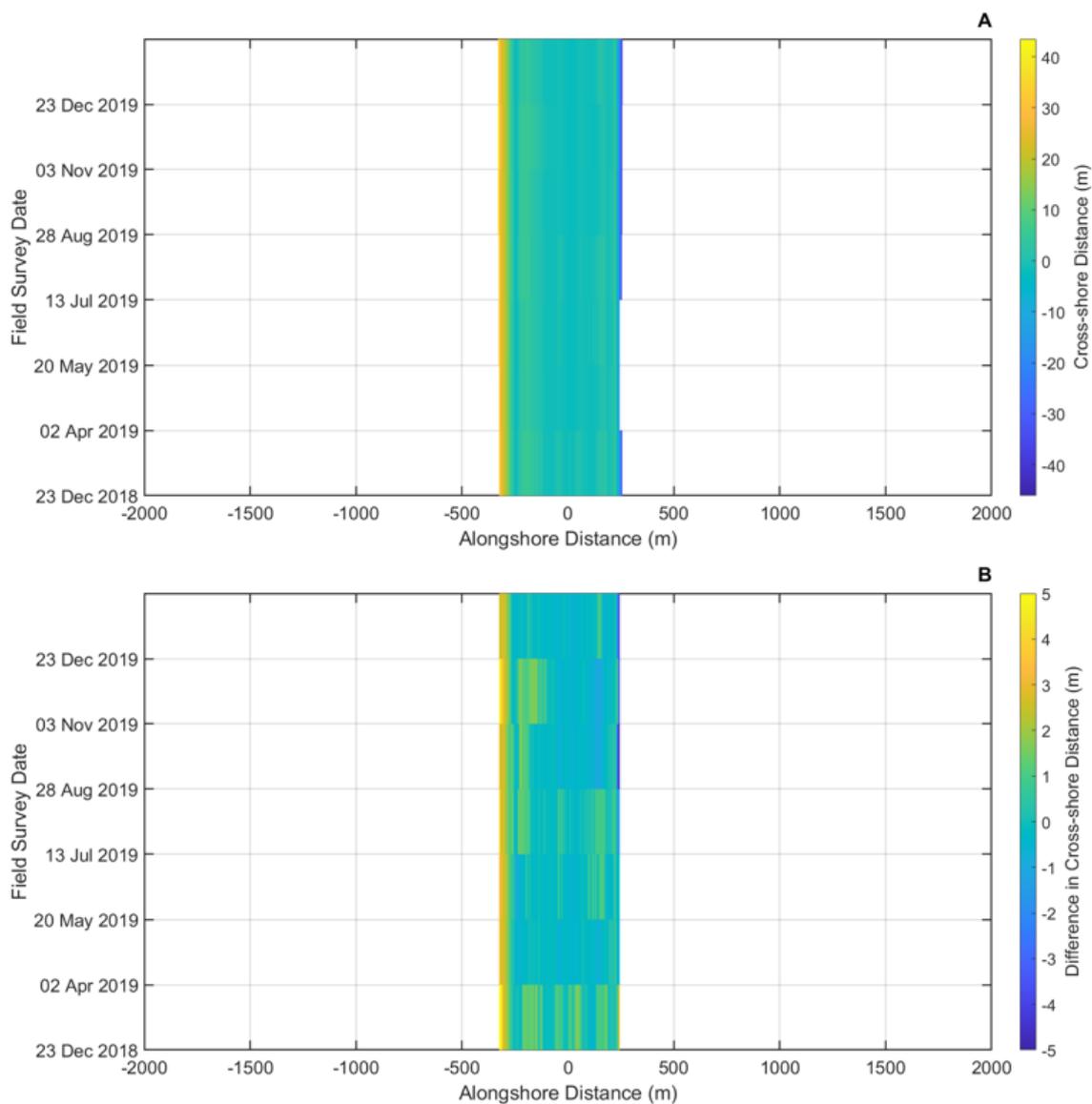
Figure 4.27. The horizontal position of the dune toe (A) and the difference of cross-shore distance of the dune toe from the mean horizontal position of the dune toe (B), Buffalo Beach. Each bar represents a field survey of the dune toe and the colour of each bar represents the cross-shore position of the horizontal dune toe (A) and the difference of cross-shore distance from the mean horizontal dune toe position. Field surveys were taken 23rd December 2018, 2nd April 2019, 20th May 2019, 13th July 2019, 28th August 2019, 3rd November 2019 and 23rd December 2019.

4.4.3.2 Mid Buffalo Beach

Along the middle of Buffalo Beach between the river mouth at the north of the beach and the river mouth at the middle of the beach, there was little change in the dune toe along the beach, where the largest changes were at the south, just north of the river mouth between the alongshore distance of 550 to 700, where seaward movement occurred (Figure 4.28.A). There was also landward movement that occurred between December 2018 to April 2019 at the alongshore distance of 190 to 400 (Figure 4.28.A).

The dune toe varied in height along the beach and from a higher dune toe height at the shore distance of 0 to 600 and a lower dune toe height at the alongshore distance of 0 to -610 (Figure 4.28.B). There was a large increase in dune toe height between December 2018 to April 2019 and a decrease in dune toe height between August 2019 to November 2019, for alongshore distance of 150 to 320. Between the alongshore distance of 320 and 490, there was a decrease in dune toe height from December 2018 to April 2019 and slowly increased in dune toe height from April 2019 to December 2019. Further North, between the alongshore distance of -400 to 0 the dune toe height increased between December 2018 to August 2019, the dune toe height decreased from August 2019 to November 2019 and increased again between November 2019 to December 2019.

The horizontal position of the dune toe went through small back and forth changes through the year of December 2018 and December 2019 (Figure 4.29.B). The dune toe of the horizontal position of the dune toe moved landward between December 2018 and April 2019, was stable between April 2019 and August 2019. There was landward movement of the dune toe at the alongshore distance of 250 during August 2019 and the alongshore distance of 0 to 150 during November 2019, before seaward movement before December 2019.
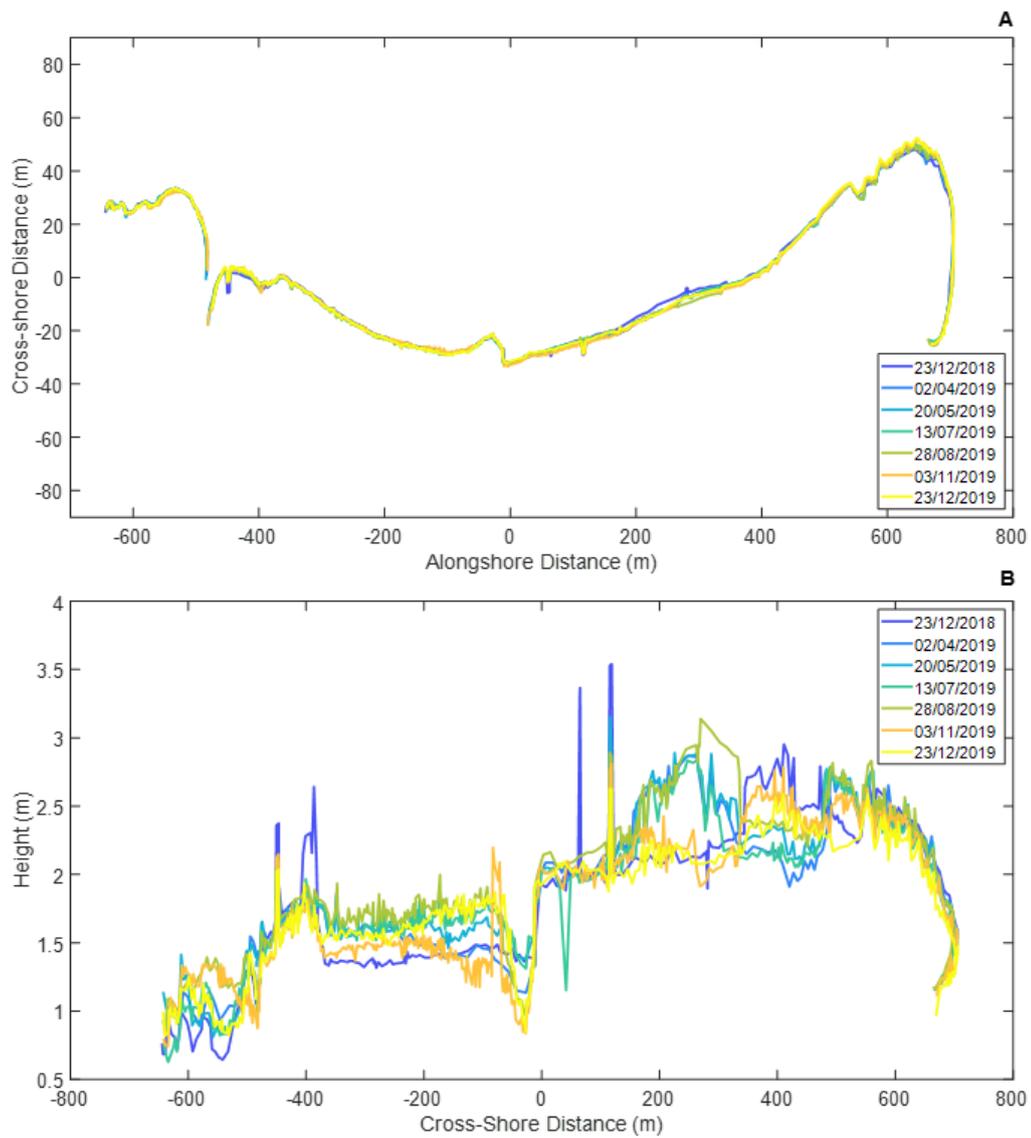
Figure 4.28. The cross-shore distance of the dune toe (A) and the height of the dune toe (B), Buffalo Beach. Field surveys were taken 23rd December 2018, 2nd April 2019, 20th May 2019, 13th July 2019, 28th August 2019, 3rd November 2019 and 23rd December 2019.
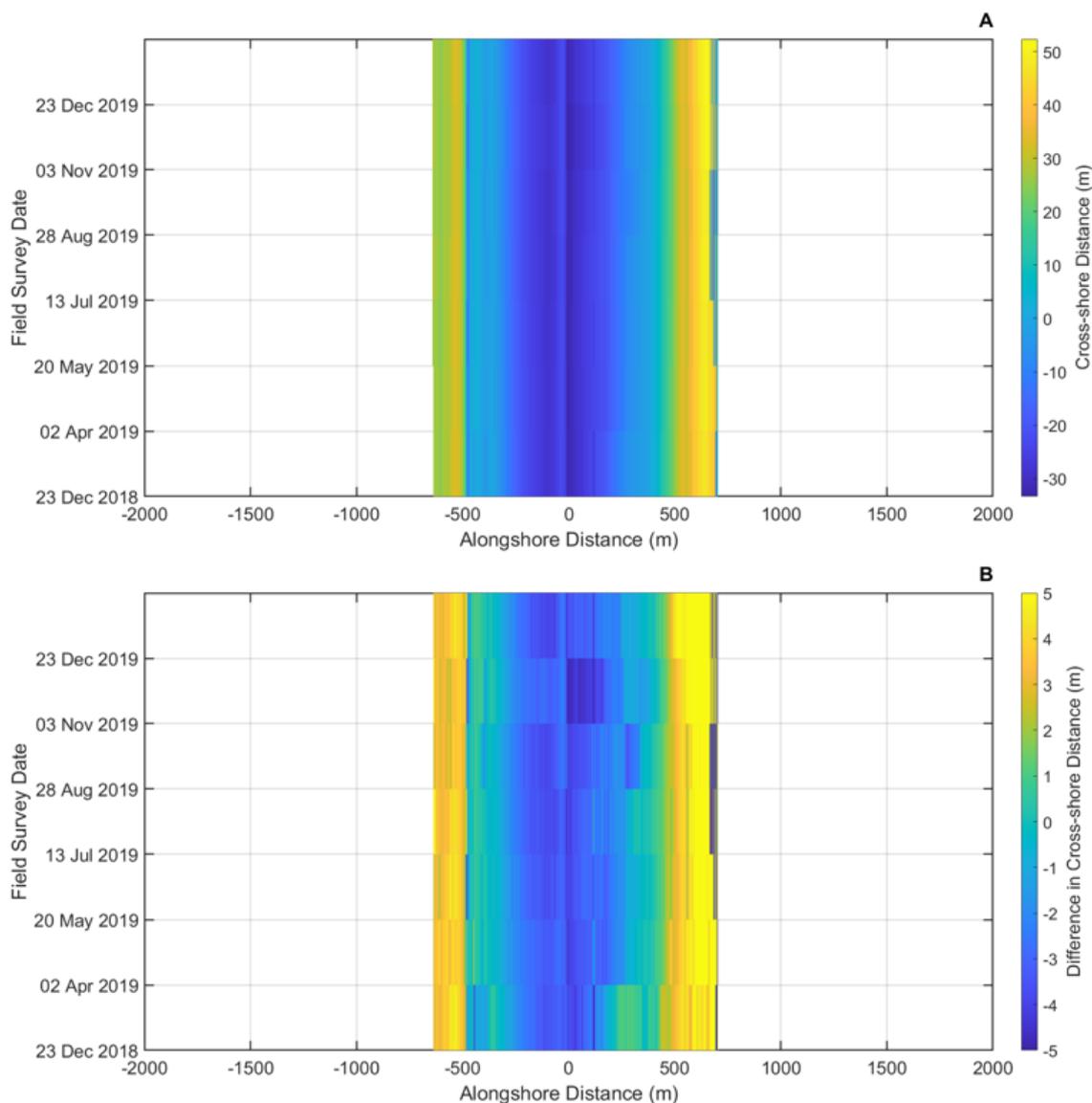
Figure 4.29. The horizontal position of the dune toe (A) and the difference of cross-shore distance of the dune toe from the mean horizontal position of the dune toe (B), Buffalo Beach. Each bar represents a field survey of the dune toe and the colour of each bar represents the cross-shore position of the horizontal dune toe (A) and the difference of cross-shore distance from the mean horizontal dune toe position. Field surveys were taken 23rd December 2018, 2nd April 2019, 20th May 2019, 13th July 2019, 28th August 2019, 3rd November 2019 and 23rd December 2019.

4.4.3.3 South Buffalo Beach

There was a small amount of change of the dune toe position along the south of Buffalo Beach during the December 2018 and December 2019 (Figure 4.30.A). There was a small amount of seaward movement at the alongshore distance of 400 to 800. There was a large amount of seaward movement between the alongshore distance of 0 to 190 between August 2019 and November 2019, before the seaward movement between November 2019 to December 2019.

There was a change in the dune toe height along the south of Buffalo Beach (Figure 4.30.B). Between the alongshore distance of -750 and -180 the dune toe decreased in height between December 2018 and December 2019, except for an increase in dune toe height between December 2018 and April 2019. Between the alongshore distance of -180 to 390, where there was a seawall present throughout the survey period, the dune toe height was more varied and larger changes occurred through the survey period. There was a decrease in dune toe height between December 2018 and April 2019, before a further decrease of the dune toe height during November 2019 and increased before December 2019. Between the alongshore distance of 400 to 600 there was a slight decrease in dune toe height throughout the survey period, and at the alongshore distance of 600 to 850 there was a slight increase in dune toe height.

The change in horizontal position of the dune toe is highlighted in Figure 4.31.A and Figure 4.31.B, where seaward change is shown between alongshore distance of 400 to 600 between December 2018 and April 2019, and the smaller seaward change at the alongshore distance of 0 between August 2019 and November 2019.
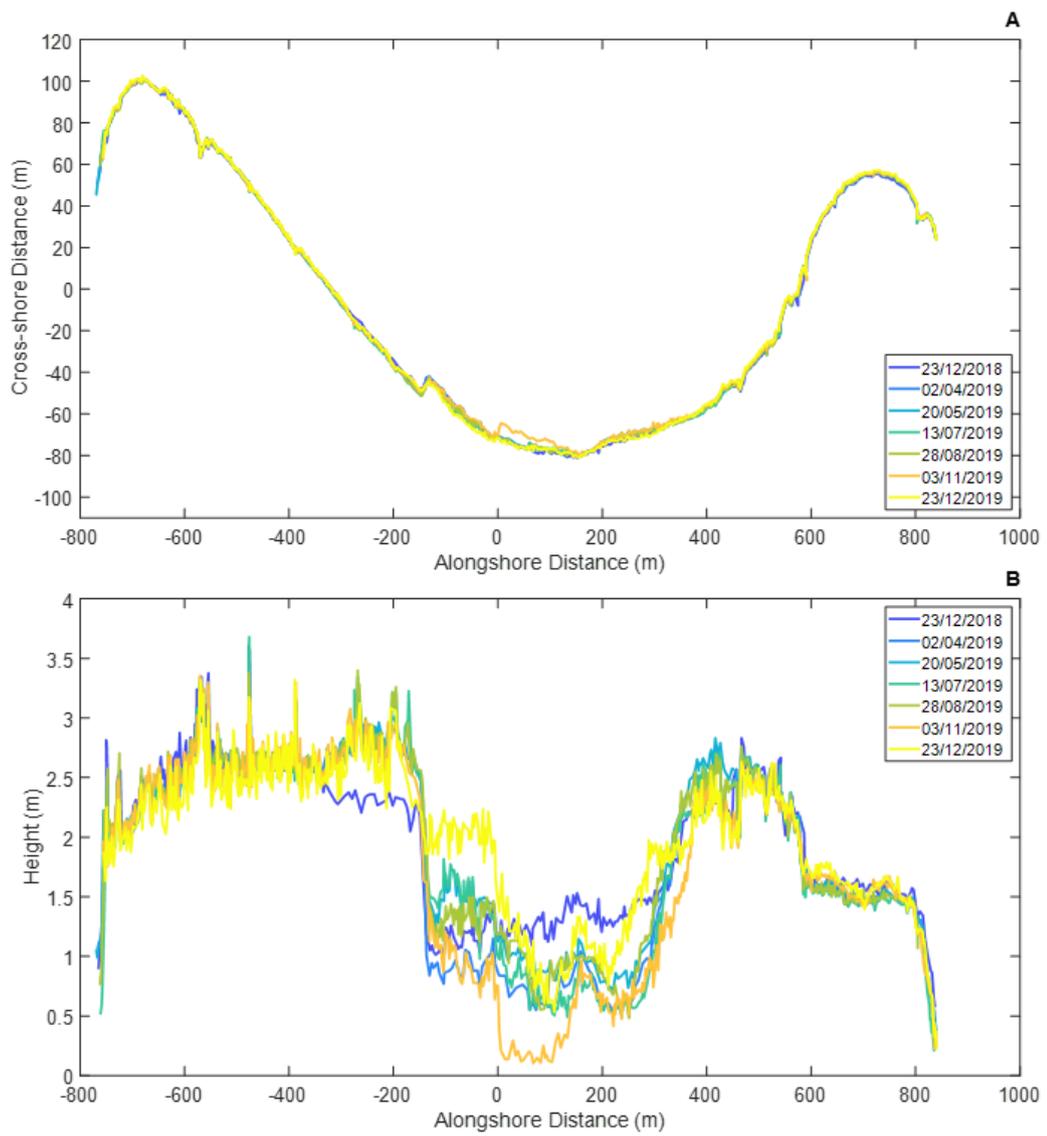
Figure 4.30. The cross-shore distance of the dune toe (A) and the height of the dune toe (B), Buffalo Beach. Field surveys were taken 23rd December 2018, 2nd April 2019, 20th May 2019, 13th July 2019, 28th August 2019, 3rd November 2019 and 23rd December 2019.
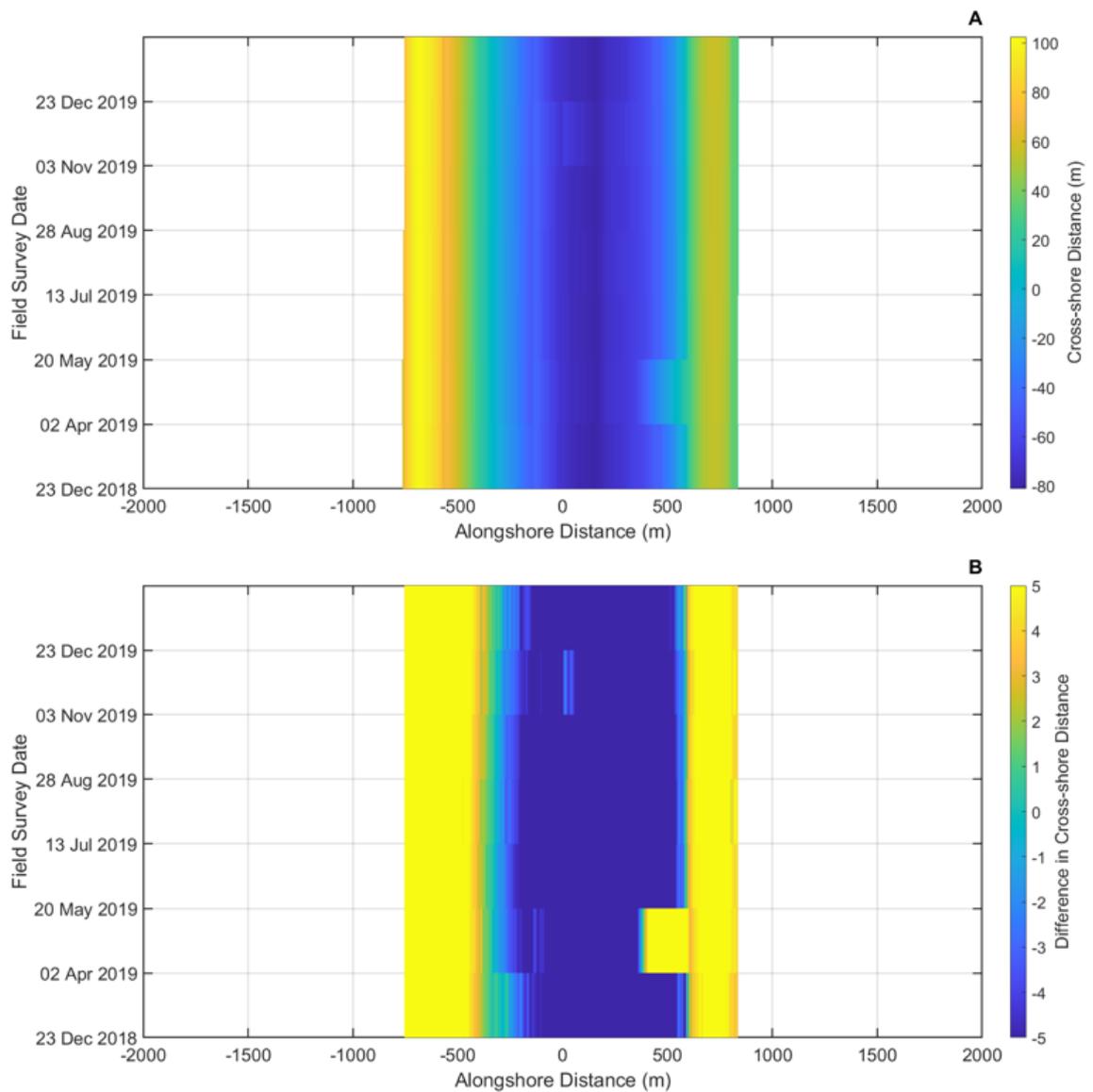
Figure 4.31. The horizontal position of the dune toe (A) and the difference of cross-shore distance of the dune toe from the mean horizontal position of the dune toe (B), Buffalo Beach. Each bar represents a field survey of the dune toe and the colour of each bar represents the cross-shore position of the horizontal dune toe (A) and the difference of cross-shore distance from the mean horizontal dune toe position. Field surveys were taken 23rd December 2018, 2nd April 2019, 20th May 2019, 13th July 2019, 28th August 2019, 3rd November 2019 and 23rd December 2019.

4.4.4 Hot Water Beach

There was movement of the vegetation line and the dune toe throughout the measured time period of CCS34 (A), CCS35 (B) and CCS35-1 (C) (Figure 4.32). The vegetation line and dune toe were in the same position throughout the measured time period for CCS34 (A), CCS35 (B) and CCS35-1 (C), except for between 1997 and 2002 for CCS35-1 (B). At CCS34, the vegetation line and dune toe slowly moved seaward between 2000 and 2003, before a sudden land ward retreat during 2003 and a second small landward retreat during 2016. The vegetation line and dune toe were stable between 2003 and 2016, and between 2016 and 2019. At CCS35, the vegetation line and dune toe were stable from 1997 and 2005, and between 2005 and 2019 there was a slow seaward movement of the vegetation line and dune toe. The distribution of the horizontal position of the vegetation line and dune toe were the similar for each profile site of CCS34 (A), CCS35 (B) (Figure 4.34). At CCS35-1, the vegetation line had a larger distribution of horizontal dune toe position compared with the distribution of the dune toe.
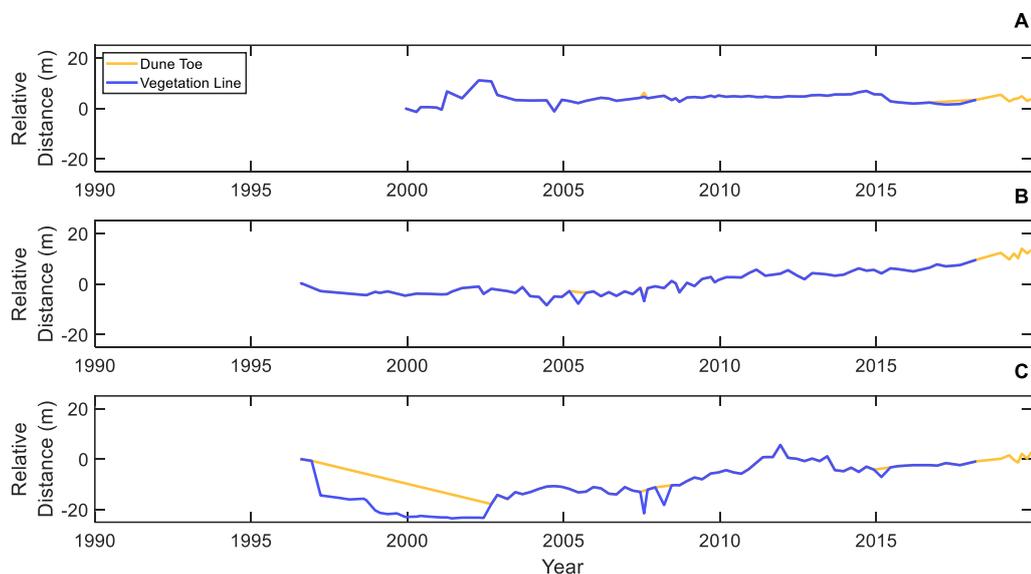
Figure 4.32. The change in relative horizontal distance of the vegetation line and dune toe, Hot Water Beach. The vegetation line (purple line) and dune toe (orange line) for at the beach profile sites of CCS34 (A), CCS35 (B) and CCS35-1 (C).
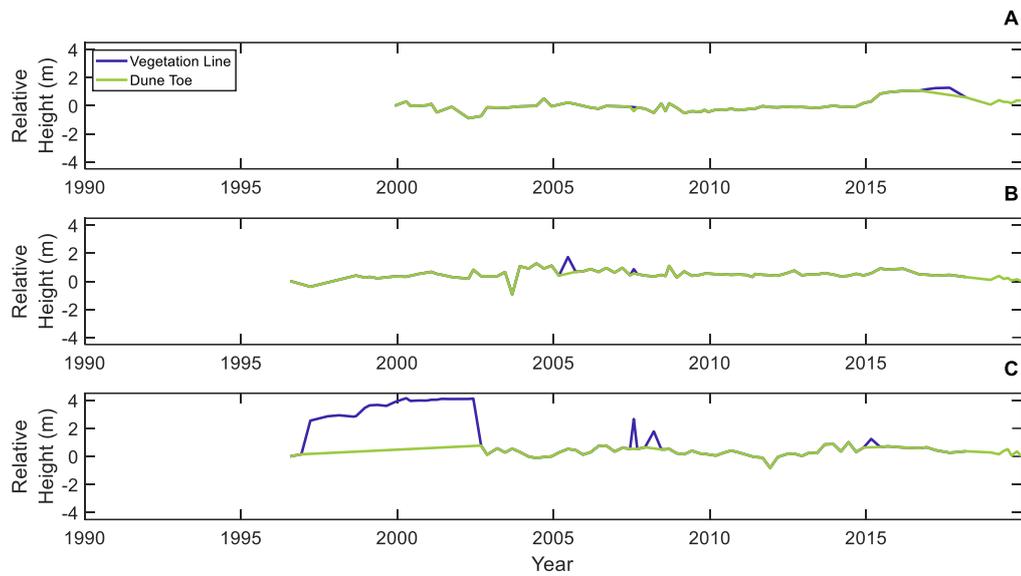
Figure 4.33. The change in relative height of the vegetation line and dune toe, Hot Water Beach. The vegetation line (blue line) and dune toe (green line) for at the beach profile sites of CCS34 (A), CCS35 (B) and CCS35-1 (C).
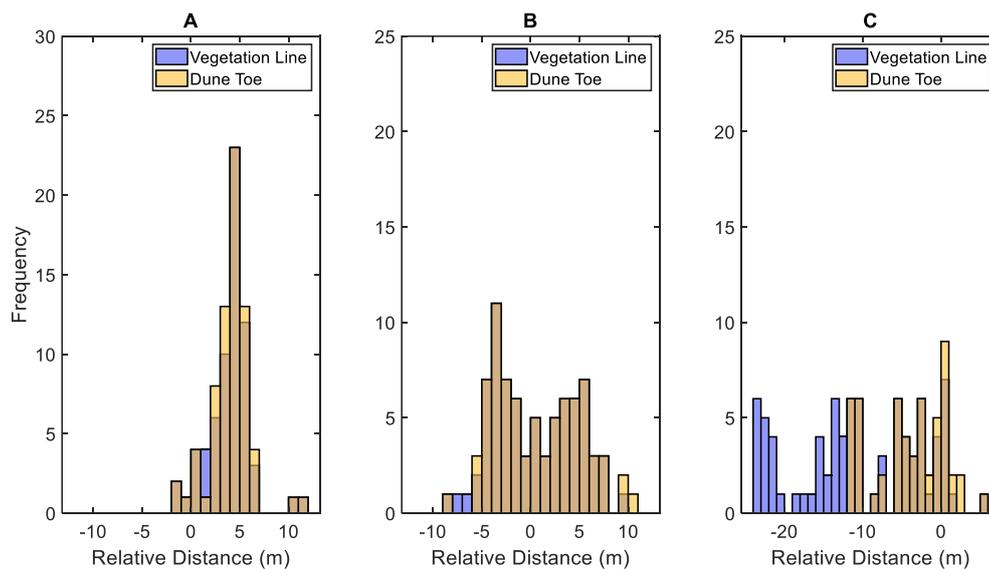
Figure 4.34. The distribution of relative horizontal distance position of the vegetation line and dune toe, Hot Water Beach. The vegetation line (purple line) and dune toe (orange line) for at the beach profile sites of CCS34 (A), CCS35 (B) and CCS35-1 (C). Note the x-axis is shifted in panel A and C, and the x-axis scale is different in panel C.

There was a small amount of change in the position of the dune toe along the beach length of Hot Water Beach during the survey period of December 2018 and December 2019 (Figure 4.35). There was a small seaward change in the dune toe position at the south of Hot Water Beach (Figure 4.36.A), between the alongshore distance of 700 and 950. At the north end of Hot Water Beach, at the alongshore

distance of between -950 and -400, there was a large seaward movement throughout the survey period. There was a smaller seaward movement of the dune toe at the alongshore distance of -400 and 480.

There was change in the height of the dune toe along the beach length of Hot Water Beach (Figure 4.36.B). The south of the beach between the alongshore distance of 800 to 950 the dune toe height remained stable throughout the survey period of December 2018 to December 2019. The dune toe height decreased throughout the survey period between the alongshore distance of 200 to 500 and 700 to 800. The dune toe height was low during December 2018, at the alongshore distance of -400 to -180 and -50 to 180, and the dune height increased between December 2018 and April 2019. The dune toe height at the alongshore distance of -50 to 180 then further increased between August 2019 and October 2019. The dune toe height at the alongshore distance of -180 to -50, decreased between August 2019 and October 2019. The dune toe height between -400 and -180 remained stable between April 2019 and December 2019. At the north end of Hot Water Beach, between the alongshore distance of -1000 to -400, there was a large decrease in dune toe height throughout the survey period.

The horizontal position of the dune toe moved seaward at the south of the beach at the alongshore position of 840 (Figure 4.37.A) and there was a general trend of seaward movement throughout the survey period, especially from August 2019 to December 2019 (Figure 4.37.B).
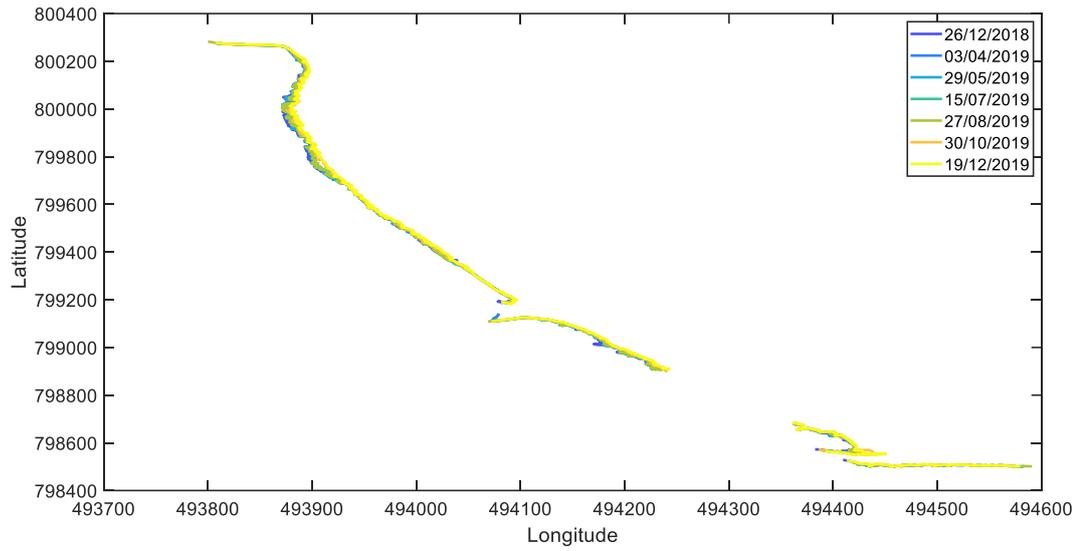
Figure 4.35. The coordinate position of the alongshore dune toe, Hot Water Beach. Field surveys were taken 16th December 2018, 3rd April 2019, 29th May 2019, 15th July 2019, 27th August 2019, 30th October 2019 and 19th December 2019.
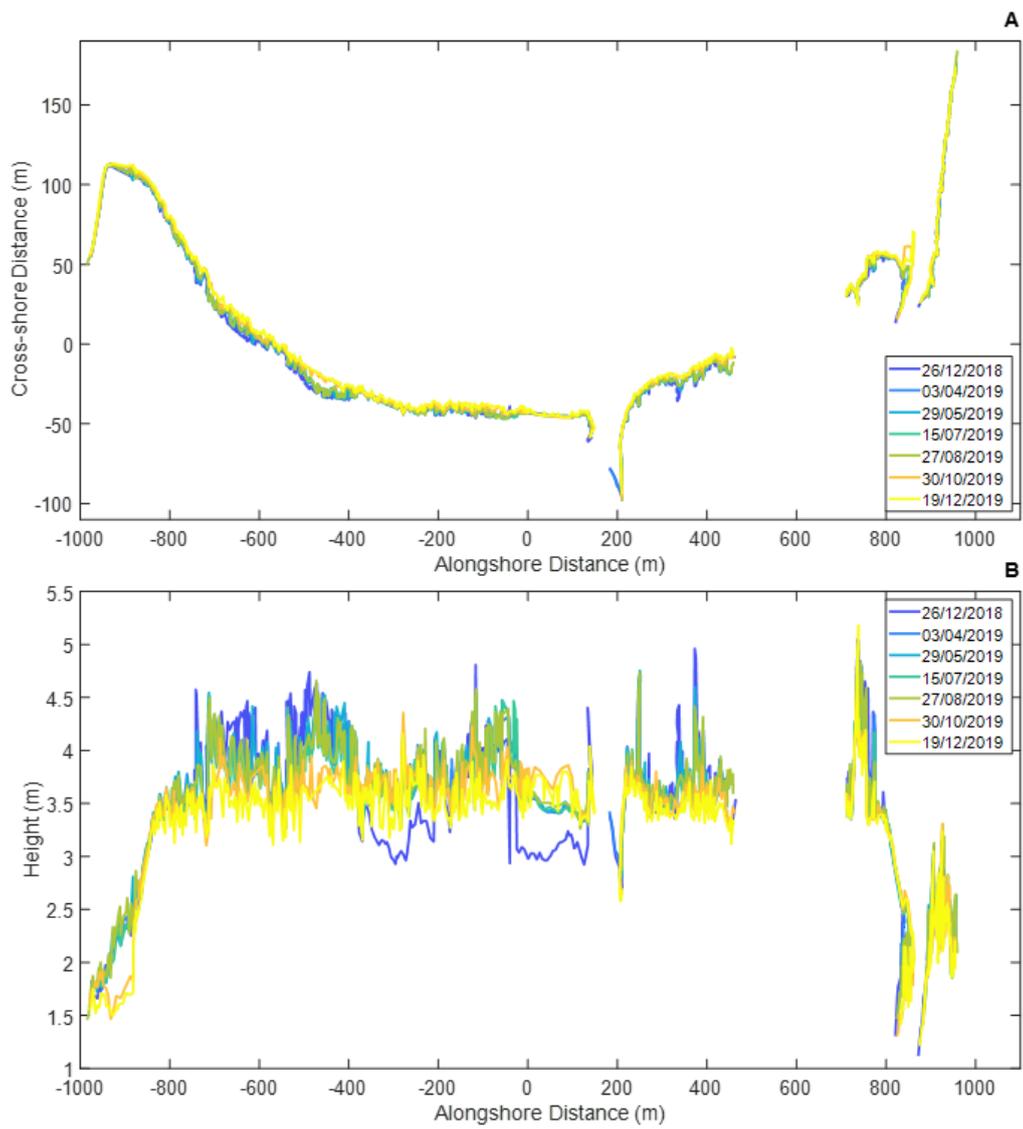
Figure 4.36. The cross-shore distance of the dune toe (A) and the height of the dune toe (B), Hot Water Beach. Field surveys were taken 16th December 2018, 3rd April 2019, 29th May 2019, 15th July 2019, 27th August 2019, 30th October 2019 and 19th December 2019.
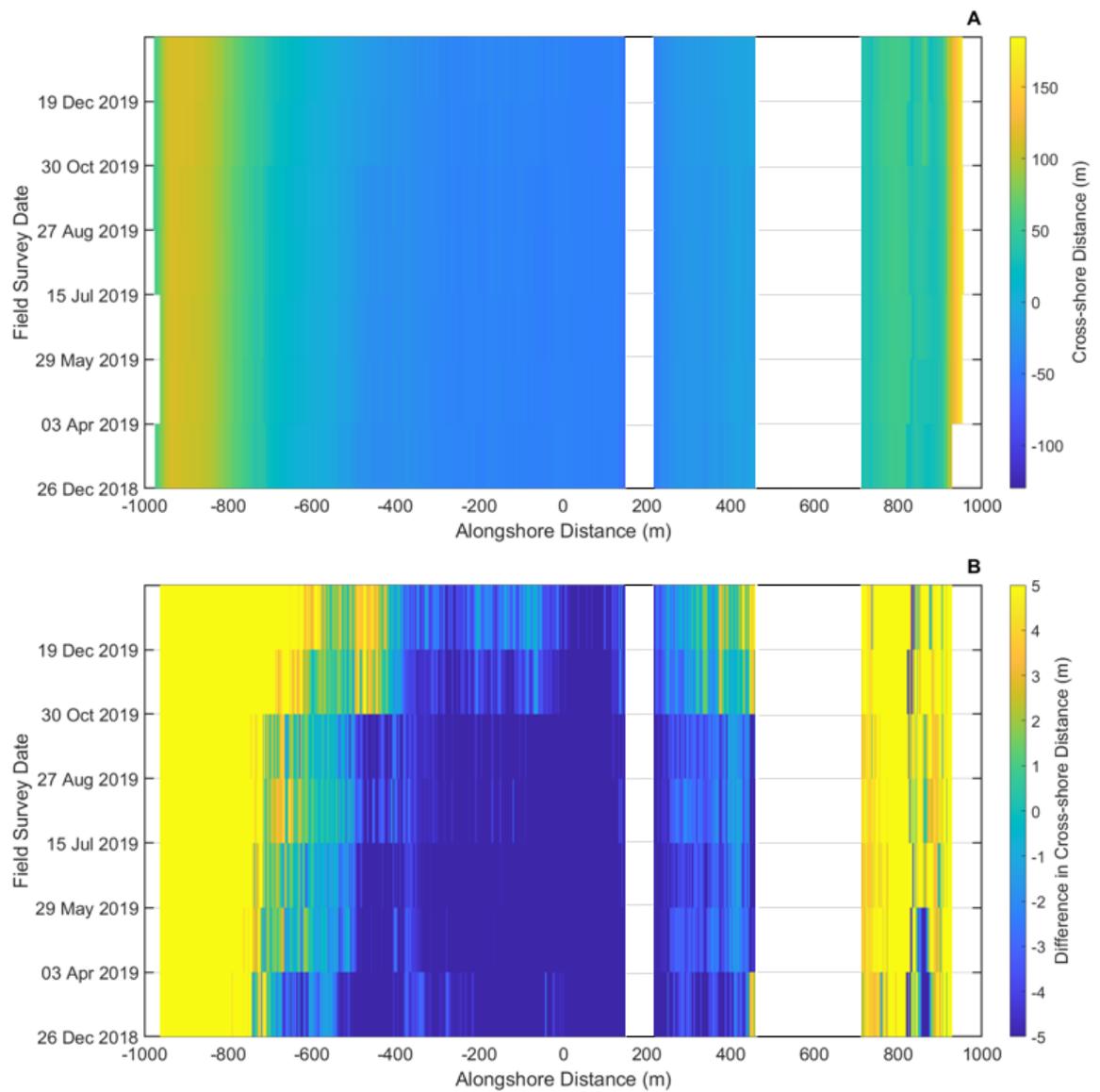
Figure 4.37. The horizontal position of the dune toe (A) and the difference of cross-shore distance of the dune toe from the mean horizontal position of the dune toe (B), Hot Water Beach. Each bar represents a field survey of the dune toe and the colour of each bar represents the cross-shore position of the horizontal dune toe (A) and the difference of cross-shore distance from the mean horizontal dune toe position. Field surveys were taken 16th December 2018, 3rd April 2019, 29th May 2019, 15th July 2019, 27th August 2019, 30th October 2019 and 19th December 2019.

4.4.5 Tairua Beach

There was movement of the vegetation line and the dune toe throughout the measured time period of CCS36 (A), CCS36-2 (B), CCS36-1 (C) and CCS37 (D) (Figure 4.38). The vegetation line and dune toe were in the same position throughout the majority of the survey period for all four of the profile sites except for from 2017 to 2019, and between 2003 and 2008 for CCS36 (A). At CCS36, there was a sudden seaward movement of the vegetation line and dune toe during 1997. The vegetation line was stable between 1997 and 2004 before the vegetation line moved landward during 2004 and was stable until a seaward movement in 2007. The vegetation line and dune toe remained stable until 2017. The dune toe then moved seaward until 2019. At CCS36-2, the vegetation line and dune toe remained stable throughout the measured time period, except for 2019, where the dune toe moved seaward. At CCS36-1, there was landward movement of the vegetation line and dune toe between 1997 to 2000 before slow seaward movement until 2007, with small back and forth movements. The vegetation line and dune toe remained stable between 2007 to 2018. At CCS37, the vegetation line and dune toe slowly moved seaward between 1998 and 2011. There was a large sudden landward movement during 2011 and small landward movement during 2016. The distribution of the horizontal position of the vegetation line was the same for CCS36-2 (B), CCS36-1 (C) and CCS37 (D) (Figure 4.40). The distribution of the horizontal position of the vegetation line was large than the dune toe for the profile site of CCS36 (A).
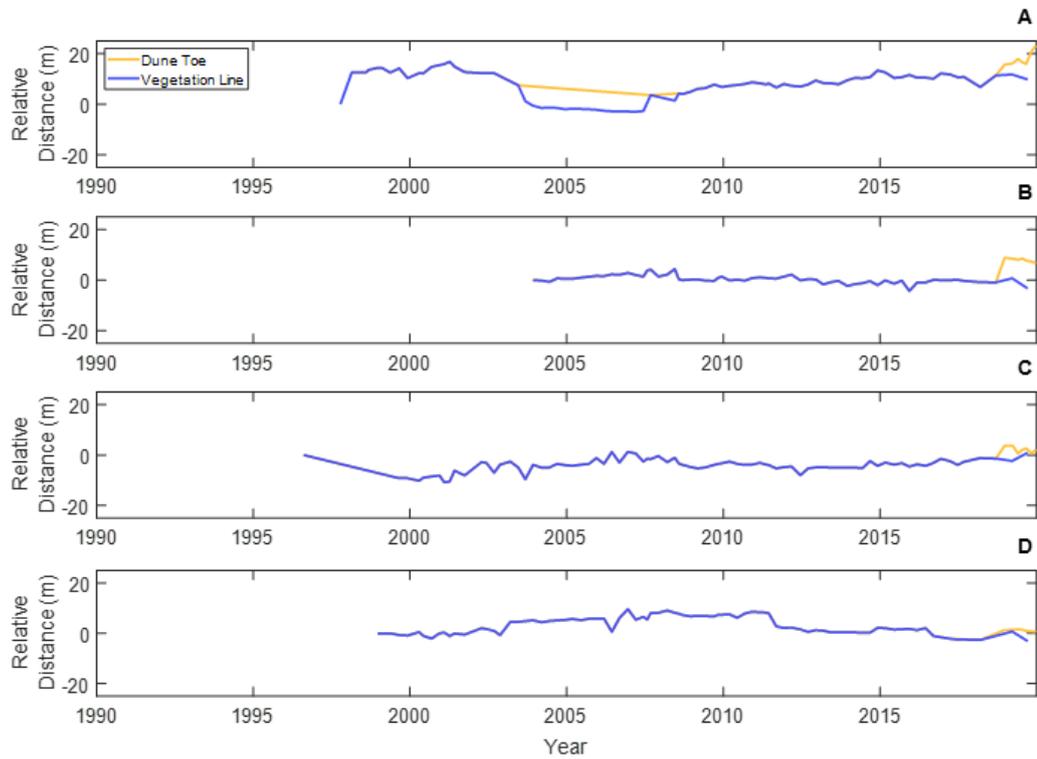
Figure 4.38. The change in relative horizontal distance of the vegetation line and dune toe, Tairua Beach. The vegetation line (purple line) and dune toe (orange line) for at the beach profile sites of CCS36 (A), CCS36-2 (B), CCS36-1 (C) and CCS37 (D).
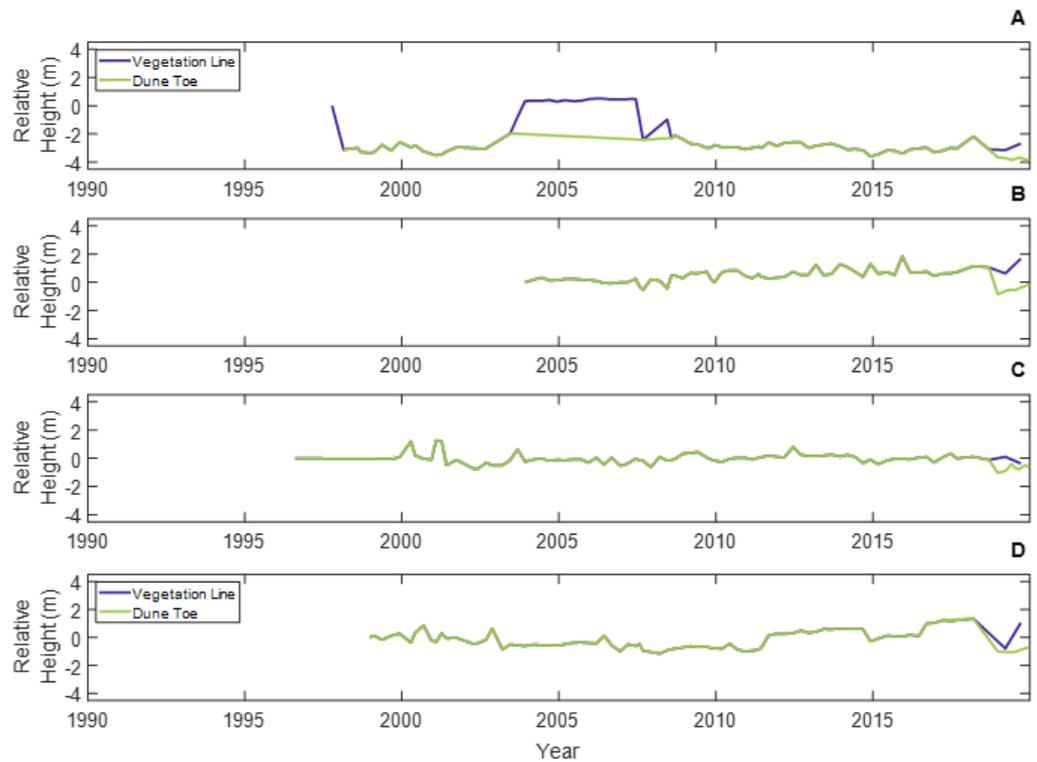
Figure 4.39. The change in relative height of the vegetation line and dune toe, Tairua Beach. The vegetation line (blue line) and dune toe (green line) for at the beach profile sites of CCS36 (A), CCS36-2 (B), CCS36-1 (C) and CCS37 (D).
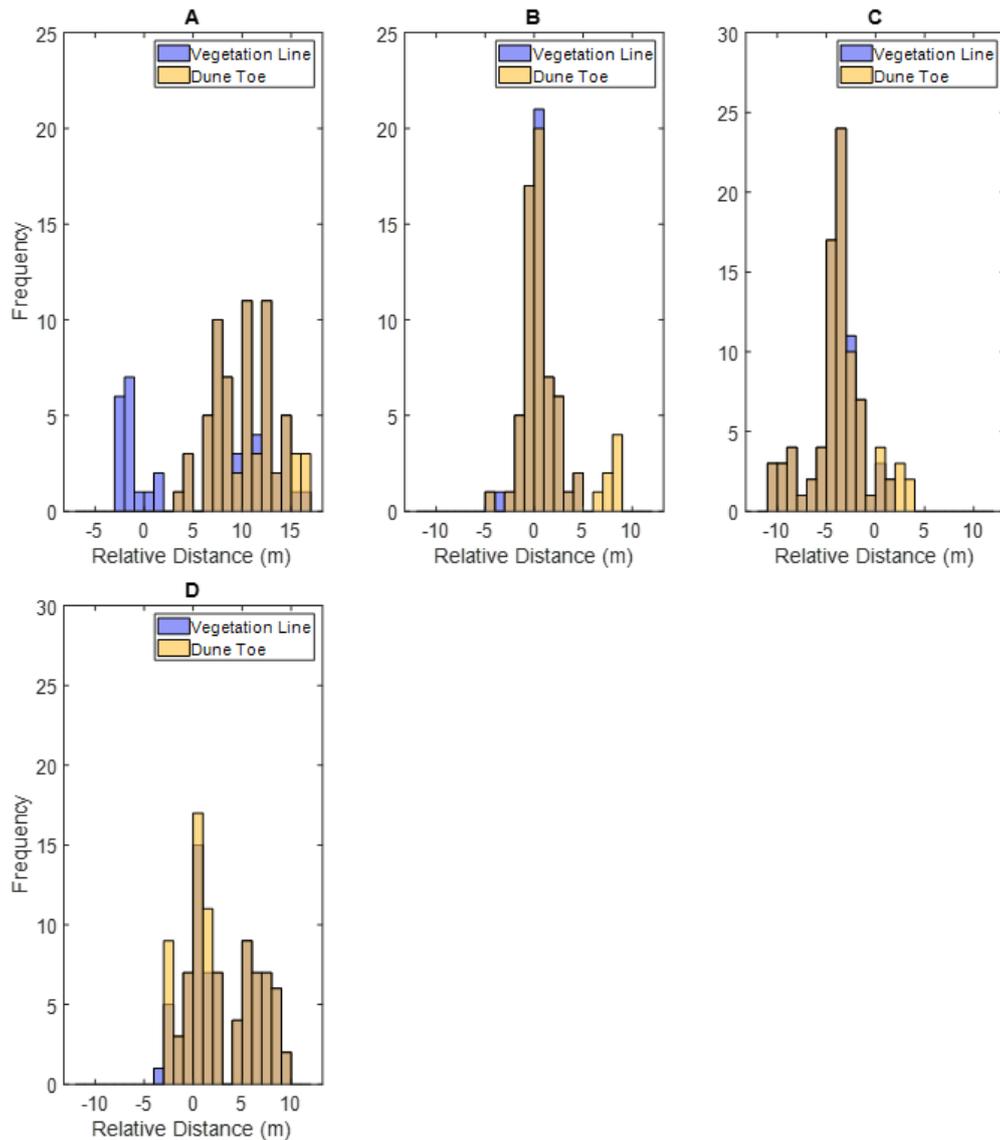
Figure 4.40. The distribution of relative horizontal distance position of the vegetation line and dune toe, Tairua Beach. The vegetation line (purple line) and dune toe (orange line) for at the beach profile sites of CCS36 (A), CCS36-2 (B), CCS36-1 (C) and CCS37 (D). Note the x-axis is shifted in panel A and C.

There was a small amount of change in the position of the dune toe along the beach length of Tairua Beach during the survey period of December 2018 and December 2019 (Figure 4.41). There was a seaward movement of the dune toe throughout the survey period along the length of the beach except for between the alongshore distance of -500 and -300 between December 2018 and March 2019 (Figure 4.42.A). There was particularly large seaward movement at the alongshore distance of between 100 and 400.

There was change in the height of the dune toe along the beach length of Tairua between December 2018 and December 2019 (Figure 4.42.B). At the north end of the beach, between the alongshore distance between -680 to -430, the height of the dune toe was stable throughout the survey time period. The height of the dune toe decreased along the beach from the alongshore distance of -430 to 500, except for between the alongshore distance of -500 to -300 where the dune toe increased between December 2018 and March 2019.

Figure 4.43 highlighted the seaward movement of the dune toe throughout the survey period along the beach length of Tairua Beach especially between August 2019 and December 2019 (Figure 4.43.A & Figure 4.43.B). The small back and forth changes to the horizontal position of the dune toe area also highlighted in Figure 4.43.B.
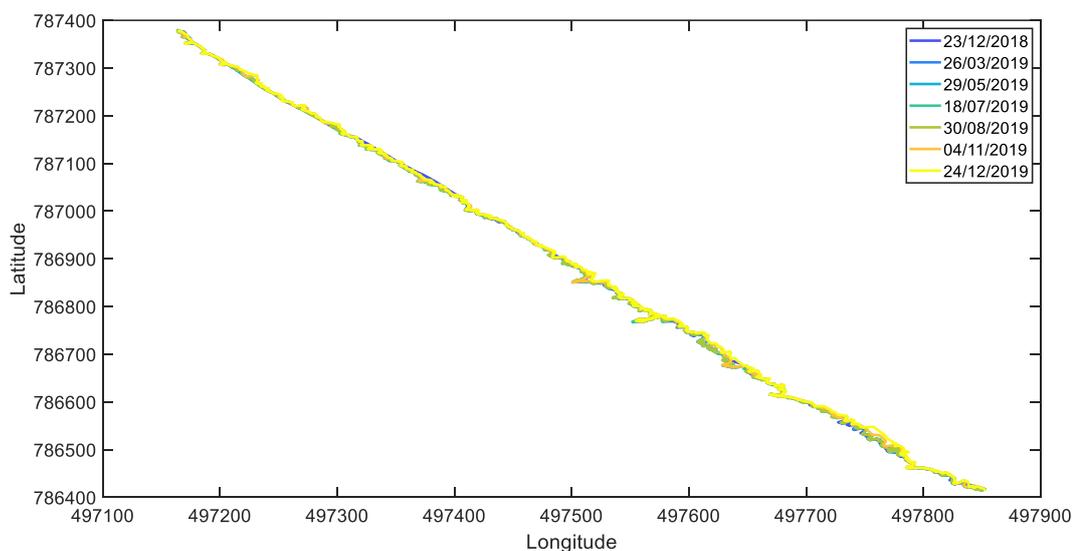
Figure 4.41. The coordinate position of the alongshore dune toe, Tairua Beach. Field surveys were taken 23rd December 2018, 26th March 2019, 29th May 2019, 18th July 2019, 30th August 2019, 4th November 2019 and 24th December 2019.
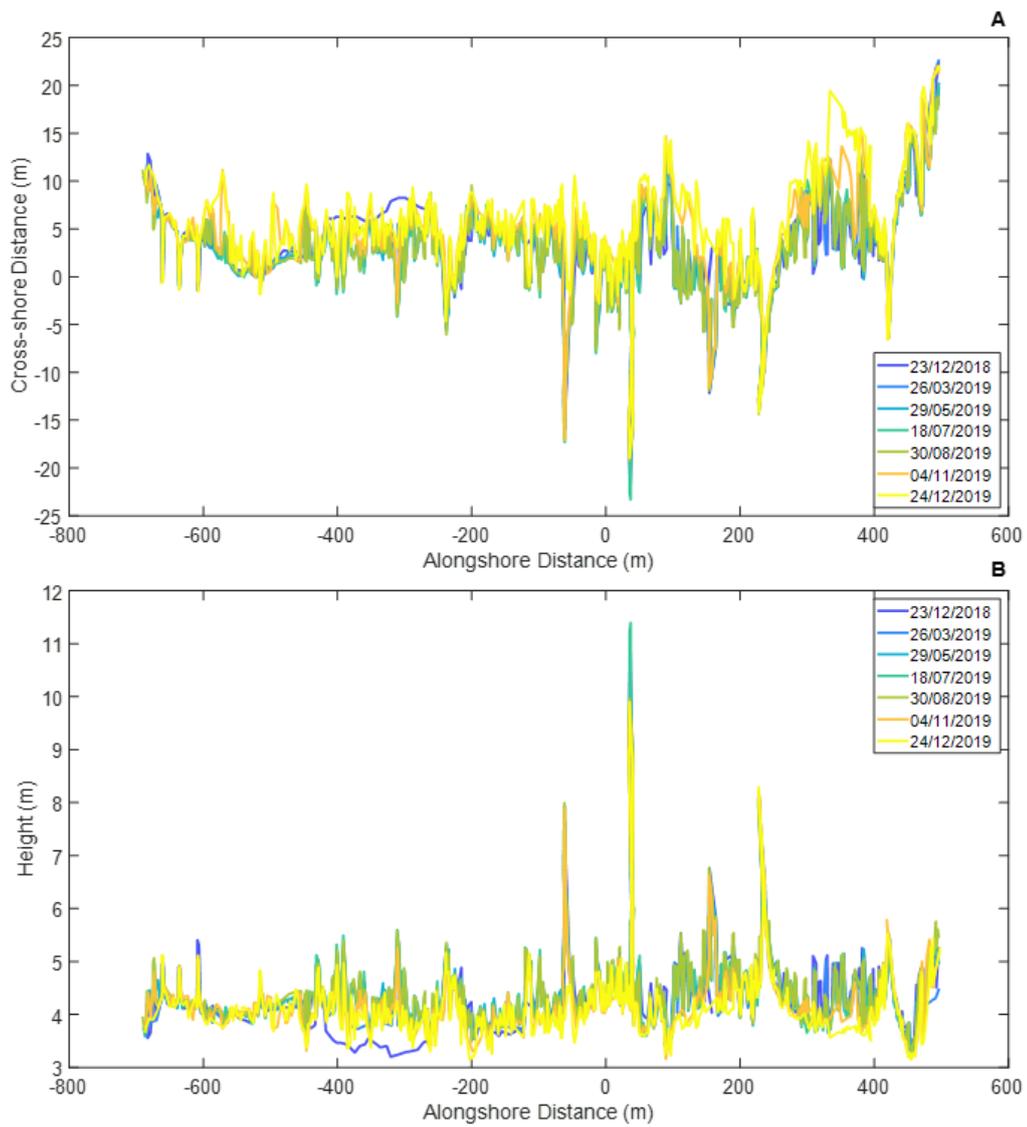
Figure 4.42. The cross-shore distance of the dune toe (A) and the height of the dune toe (B), Tairua Beach. Field surveys were taken 23rd December 2018, 26th March 2019, 29th May 2019, 18th July 2019, 30th August 2019, 4th November 2019 and 24th December 2019.
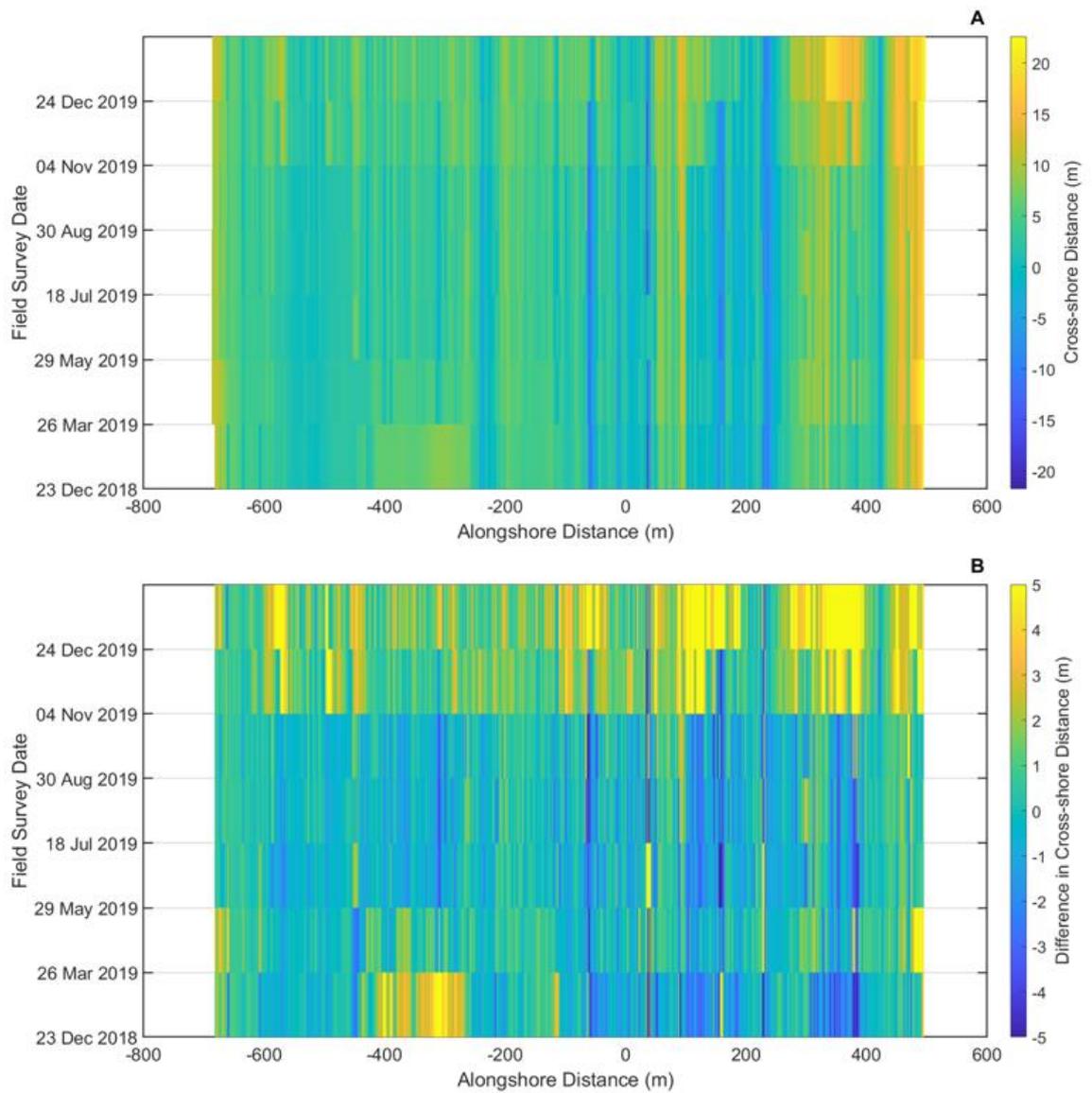
Figure 4.43. The horizontal position of the dune toe (A) and the difference of cross-shore distance of the dune toe from the mean horizontal position of the dune toe (B), Tairua Beach. Each bar represents a field survey of the dune toe and the colour of each bar represents the cross-shore position of the horizontal dune toe (A) and the difference of cross-shore distance from the mean horizontal dune toe position. Field surveys were taken 23rd December 2018, 26th March 2019, 29th May 2019, 18th July 2019, 30th August 2019, 4th November 2019 and 24th December 2019.

4.5   Discussion

4.1.1   Changes in the Horizontal Position of the Vegetation Line and Dune Toe

It was expected that there would be a sudden landward movement of the vegetation line and dune toe during storm events and slow seaward movement during fair weather conditions. There were two profile sites of CCS11 and CCS11-1 at Whangapoua Beach where sudden landward movement occurred during 2008, and at CCS12 there was a sudden landward that occurred in 1997. There was a sudden landward movement for all four of the profile sites of CCS13, CCS14, CCS15 and CCS16 at Matarangi Beach during 2008, which showed that this change was likely due to a single storm event that caused erosion of the dune toe and landward movement of the vegetation line along the majority of the beach. The expected pattern of the sudden change in the landward movement of the dune toe, followed by long of stable or accreted dune toe was shown well at the profile site CCS25-1 at Buffalo Beach, which showed two large sudden landward movements, with stable dune toe position between the large sudden changes. There were also multiple smaller sudden changes in the dune toe position at CCS37 at Tairua Beach. The sudden landward changes that occurred at the various profiles site could be explained by individual storm events or a series of storm events. Where the water has reached the dune toe and erosion has occurred, over a period of hours or days, therefore causing a sudden change (Suanez et al., 2012; Thornton et al., 2007).

There was also slow seaward movement and accretion present at a number of different profile sites throughout the measured time periods. There was slow seaward movement of the vegetation line at the profile site of CCS12 at Whangapoua Beach, where the vegetation line moved seaward for a period of 12 years, with the exceptions of a few back and forth spikes in the vegetation line. Accretion of the dune toe occurred at profile sites of CCS13, CCS14, CCS15 and CCS16 at Matarangi Beach between 2008 to 2019, with some back and forth movement during this time period. The was also slow seaward movement of the vegetation line and dune toe at the profile site of CCS35, throughout the measured

114

period, with some small back and forth movements throughout the time period. The slow seaward changes that has occurred at the various profile sites could be explained by long periods of fair weather conditions causing slow accretion to occur, whilst water has not reached the dune toe during storm events that have occurred during the time period (Castelle et al., 2015; Ruz & Meur-Ferec, 2004; Quartel et al., 2008).

The vegetation line and dune toe were fairly stable at a number of profile sites as well which was expected to occur. The dune toe was stable between 2008 and 2019 at the profile site of CCS11 and between 1997 to 2008 at CCS11-1. At Buffalo Beach the vegetation line and dune toe were stable at the profile sites of CCS25, CCS25-2, CCS25-3, CCS26/1, CCS27, CCS27/2 and CCS27/4 at Buffalo Beach. The vegetation line and dune toe were mostly stable for CCS34 of Hot Water Beach and at the profile sites of CCS36-2 and CCS36-1, at Tairua Beach. The stable vegetation line and dune toe that occurred throughout the time period at the various profile sites is likely due to water not reaching the dune toe during storm events that occurred throughout the time period and no large accretion or rapid growth of vegetation within the area, causing the dune toe to remain stable (Splinter et al., 2018).

The vegetation line and dune toe were much more varied than expected at a number of the profile sites. The dune toe at the profile sites of CCS11-1 and CCS12, at Whangapoua Beach, had large back and forth changes of the dune toe but not the vegetation line, which was unexpected. At the profile site of CCS26, Buffalo Beach, there was also large sudden seaward changes to the dune toe but not the vegetation line, which cannot be explained by slow accretion of sand during fair weather conditions. The large variations of vegetation line and dune toe can be explained by either large storm events, transport of sand from other areas of the beach, rapid vegetation growth or inconsistencies of the data within the dataset (Pye & Blott, 2008; Quartel et al, 2008).

There was also a number of sudden seaward movement at a number of profile sites, which was unexpected. During 2004 there was a sudden large seaward movement of the vegetation line and a smaller sudden seaward change of the

dune toe, at the profile site of CCS11, Whangapoua Beach. There was also sudden seaward change of the vegetation line at CCS16 at Matarangi Beach during 2001. Due to the sudden nature of the changes for these sites, the seaward change could not have been due to fair weather conditions causing slow accretion, but from transport of sand from another area of the beach or nearshore zone, including propagating bores and swash, or rapid growth of vegetation within the area (Quartel et al, 2008).

4.1.2 Distribution of the Horizontal Position of the Vegetation Line and Dune Toe

The range in distribution of the horizontal position of the vegetation line was larger than the range of distribution for the horizontal position of the dune toe for the majority of the profile sites along all of the surveyed beaches, except for CCS17 at Matarangi Beach, CCS227, CCS27/6, CCS27/2, CCS27/3 and CCS27/4 at Buffalo Beach, and CCS36-2 and CCS36-1 at Tairua Beach. The larger distribution of the vegetation line compared with dune toe showed that the dune toe was a more defined measure of the frontal sand dune as a feature of the beach and may mean that the dune toe would be a better measure to use for beach monitoring than the vegetation line alone (Splinter et al., 2018; Splinter & Palmsten, 2012).

The horizontal position of the dune toe was more seaward than the horizontal position of the vegetation line for the majority of the profile sites along all of the surveyed beaches, except for CCS13 at Matarangi Beach, CCS34 and CCS35 at Hot Water Beach, and CCS36-2, CCS36-1 and CCS37 at Tairua Beach, which were in the relatively the same position. The more seaward position of the dune toe compared with the vegetation line, showed that the dune toe and the vegetation line were not generally in the same location. The vegetation line and dune toe are sometimes assumed to be in the same location due to the similarity of the features being at the front of the frontal sand dune toe. These differences in location should be taken into account when using the vegetation line and the dune toe as a beach monitoring measure (Splinter & Palmsten, 2012).

4.1.3 Changes in the Vertical Position and Distribution of the Vegetation Line and Dune Toe

The height of the dune toe was generally lower than the height of the vegetation line for the majority of profile sites for along all of the surveyed beaches. This confirmed that the vegetation line sometimes represented the top of an escarpment, whilst the sand dune toe represented the bottom of the escarpment where the steep frontal sand dune meets the lower angled beach. The distribution in height of the vegetation line and dune toe (roughly ±4 m for most profiles sites) is generally much lower than the distribution of the horizontal position of the vegetation line and dune toe (roughly ±12 m for most profiles sites). This would suggest that the change in height of the vegetation line and dune toe is generally lower than the change in the horizontal position of the vegetation line and dune toe (Splinter et al., 2018).

4.1.4 Changes in Alongshore Dune Toe

There were small amounts of the change in dune toe along the length of each of the survey beaches, throughout the survey time period between December 2018 and December 2019. The small amount of change in the dune toe throughout the year was expected, due to the lower influence of water, only during storm events, on the upper beach face compared with the lower beach face that is influenced by water during every tidal cycle (Splinter et al., 2018; Thornton et al., 2007). Therefore, lower variability and small changes of the dune toe position was expected (Larson & Kraus, 1993). There was some section of the survey beaches where the change in the alongshore dune toe was larger than the rest of the beach. This occurred at the South of Whangapoua Beach, the North of Matarangi Beach near the harbour entrance, in front of the sandbag wall at the north end of Buffalo Beach, near the middle river mouth and in front of the seawall at the south of at Buffalo Beach, along the North end of Hot Water Beach and the south end of Tairua Beach. There was general trend of seaward movement or accretion of the dune toe throughout the year at Whangapoua Beach, Matarangi Beach, Hot Water Beach and Tairua Beach, along with landward (erosion) and seaward (accretion) movement of the dune toe along Buffalo Beach.

There was alongshore variation in the dune toe, shown within the cross-shore position of the dune toe along the length of the beach for all the survey beaches, where the cross-shore position moved back and forth along the length of the beach, this was shown in the small spikes of the dune toe along the shore. It was expected for there to be alongshore variation in the position of the dune toe where beach morphodynamics are likely to be varied along the beach length, where nearshore dynamics and transport of sand along beach influence the upper beach face and dune toe, along with differences in sand dune formation and accretion patterns during fair weather conditions (Larson & Kraus, 1993; Splinter et al, 2018).

There was changes in the dune height at all of the survey beaches, along the length of each beach. There was a decrease in dune toe height at the south end of Whangapoua Beach, and along the entire beach length of Matarangi Beach, Hot Water Beach and Tairua Beach. There was both an increased and decrease of the dune toe height along various sections of Buffalo Beach. The decrease in the dune toe height was expected due to the seaward movement of the horizontal position of the dune toe, where the dune toe was expected to move along the angle of the beach slope (Larson et al., 2004; Splinter & Palmsten, 2012). The downwards angle of the dune toe movement was likely due to the growth of vegetation line down the sand dune face towards the beach and the accumulation of sand along the front sand dune (Quartel et al., 2008). The largest spikes of the height of the dune toe can be explained due to the presence of accessways onto the beach which were surveyed.

The psuedocolor plots of the horizontal position of the dune toe highlighted the small back and forth changes that occured of the dune toe at all of the beaches, throughout the surveyed time period of December 2018 to December 2019, and the alongshore variation of the horizontal position of the dune toe. The plots highlighted the accretion of the dune toe that occurred at Matarangi Beach throughout the year and the seasonal patterns of erosion during winter and accretion during summer at Hot Water Beach and the accretion during summer at Tairua Beach. During winter there are storm events more often which was likely to have caused the small amount of erosion at the dune toe and the fair weather

conditions usually result in the accretion of the upper beach face and sand dunes, which would have caused the accretion of the dune toe during the summer period (Castelle et al., 2015; Pye & Blott, 2008).

Buffalo Beach was the only field survey beach that had sections of the beach that was human modified, in the form of seawalls at the middle and south section of Buffalo Beach, a sand bag wall at the north section of buffalo beach and beach renourishment on the south section of buffalo beach, south of the seawall. The seawalls and sandbag wall caused the horizontal position of the dune toe to stay in a similar position, except for when erosion occurred at the dune toe and lower rocks were exposed that were also further seaward. The horizontal position of the dune toe was shown by the historical vegetation line and dune toe at the beach profile sites and the alongshore dune toe surveyed throughout the year between December 2018 and December 2019. The change in the height of the dune toe increased, along the seawall and sandbag wall throughout the year, between December 2018 and December 2019. The seawall at the south of Buffalo showed the change in the dune height, where the dune height along the sea wall was at a lower height than the dune toe and the changes in height were greater at the seawall, especially during winter where erosion caused to dune toe height to lower dramatically along a small section of the beach. The greater changes in height of the dune toe along sections of the beach with seawalls may be due to wave energy reflecting off the seawall causing different erosion patterns (Kraus & McDougal, 1996).

4.1.5 Errors and Future Research

The vegetation line and dune toe data that was taken from the comments made from the beach profiles of an historic dataset between 1990 and 2019. These comments varied greatly between each profile surveyed and there were inconsistencies in the indication of the vegetation line and dune toe between beach profile surveys at the same location and across different beach profile sites. The majority of the beach profile surveys of Whangapoua Beach to Buffalo Beach, (including the field survey beaches of Whangapoua Beach, Matarangi Beach and Buffalo Beach) were completed by one field operator and the beach profile surveys of Maramaratotara Beach to Whiritoa Beach (including the field survey

beaches of Hot Water Beach and Tairua Beach) were taken by a different field operator. There was an obvious difference in the comments made by both operators, where one operator provided a large amount of detailed comments, where sometimes it was not clear where the vegetation line or the dune toe was located as multiple locations were indicated, and one exact location was decided upon from the multiple indicated for the vegetation line and dune toe dataset. The other operator was clear where the edge of the vegetation line was where one location was indicated, however the dune toe was rarely indicated. These differences in the comments associated with the beach profiles may have caused differences in the results found between the beaches of Whangapoua Beach, Matarangi Beach and Buffalo Beach compared with the beaches of Hot Water Beach and Tairua Beach. The difference in comments also highlighted the subjectivity of identifying the features of the vegetation line and dune toe. This subjectivity could affect the identified changes in dune toe from historic datasets already present and for future datasets that include the vegetation line and dune toe feature. The use of standardised definitions of the vegetation line and dune toe would be useful for future beach monitoring, and the analysis of past datasets that include the vegetation line and dune toe. The dune toe was also only taken from the comments left from past beach profile surveys. Due to time restrictions individual dune toe from each beach profile taken was not able to be identified. Therefore, the historic changes of the dune toe found and a more accurate and precise representation of the changes in dune toe encompassing the whole dataset (where there was no comment) could have been completed if time allowed. This also may have affected the results found for the changes in the dune toe. Future research of the changes of the dune toe using the historic dataset could include identifying the dune toe using the inflection point between the sand dune and beach to encompass the whole dataset. The changes in dune toe could also be compared with storm events that occurred during the time period in order to explain why the changes in horizontal position of the dune toe occurred.

There was also a small amount of subjectivity present when surveying the alongshore dune toe along the field survey beaches, where the two definitions of where the dune toe was located when an escarpment was present and no

escarpment present, was followed (Splinter & Palmsten, 2012). However, if a different person was to conduct the same survey, the results may have been different. The sue of the backpack instead of a pole to mount the RTK-GPS receiver onto, also introduced another source of error.

For beach monitoring of the dune toe, a standardised definition of the dune toe needs to be agreed upon and used throughout the surveys, so that surveys are consistent and coherent (Splinter et al., 2018). The optimum frequency of the survey needs to also be determined, where it has been shown here the dune toe does not move very often (the dune toe does not change much throughout a year) but goes through sudden changes. The spatial extent of monitoring of the dune toe also needs to be decided upon, where the entire beach length could be measured, certain sections of the beach could be monitored or just the dune toe position at already established beach profile sites could be monitored. The alongshore dune field surveys that were completed over the year between December 2018 and December 2019, took a similar time or slightly longer time than measuring the beach profiles at each beach. The time needed to complete the dune toe surveys would decrease if a smaller spatial extent was used compared with the entire length of the beach, decreasing time spent and the cost of each survey.

4.6 Conclusions/Summary

In Conclusion, it was found that some of the profiles behaved as expected with sudden landward movement of erosion and slow seaward movement when the sand dune toe accreted. However, there were also profiles sites in which the vegetation line and dune toe did not move in a way that was expected with sudden seaward changes and sudden large back and forth changes of the vegetation line and dune toe. The range of distribution of the vegetation line was larger than the range of the distribution of the dune toe and the dune toe was generally more seaward than the vegetation line. The height of the dune toe was generally lower than the height of the vegetation line, this was expected as the dune toe was the inflection point between the sand dune slope and the beach. It was also found that the cross-shore horizontal position of the vegetation line and dune toe changed to

a greater magnitude that vertical position of the vegetation line and dune toe. The alongshore dune toe underwent small change through the one-year survey period of between December 2018 and December 2019, of mostly accretion. There was variation in the alongshore dune toe position, which was shown with the varied cross-shore position of the dune toe along the beach length, with continuous back and forth cross-shore distances. There was also changes in the dune toe height throughout the survey time period of mostly accretion at the field survey beaches. The changes in the horizontal position and height of the dune toe were different on areas of Buffalo Beach where human modification had occurred. There were greater changes in the height of the dune toe and a smaller amount of change in the horizontal position of the dune toe due to the fixed stationary position of the seawalls. There is a degree of subjectivity that has been found when measuring and identifying the vegetation line and dune where the vegetation line is generally not in the same place as the dune toe which has strong implications for using vegetation as a measure of dune movement. For the future of beach monitoring using the dune toe a standardised definition and technique for surveying the dune toe needs to be established along with appropriate temporal and spatial extent of the beach monitoring.

Chapter Five

Video Analysis of the Horizontal Position of the Vegetation Line

5.1 Introduction

The traditional method to measure beach processes has been to use cross-beach transects commonly known as beach profiles; traditionally these are surveyed using the emery method and more recently using RTK GPS (Aarninkhof et al., 2003; Emery, 2003; Cooper et al., 2000). As shown within this thesis, there are now long-term datasets of beach profiles for many beaches in New Zealand and across the world. These long-term datasets are important for determining historical trends and for predicting future trends of morphological change. This information can used for example, to predict potential risk of human life and damage to property. Beach profile surveys have low resolution and require a high level of effort to collect. New methods and techniques include the vehicle mounted GPS, LiDAR imagery, aerial photography (including drones), satellite imagery and video analysis (Pianca et al., 2015). All of these provide a higher resolution data, and vary with cost and practicality of use, compared with traditional methods (Pianca et al., 2015; Aarninkhof et al., 2003). Video analysis is a technique that is both low cost (after the initial set up cost) and can provide large spatial and temporal datasets (Splinter et al., 2011; Balouin et al., 2014). For these reasons, video analysis may become a key method in the future for beach monitoring and assessing beach health (Pianca et al., 2015; Splinter et al., 2011; Smith & Bryan, 2007).

Video analysis involves mounting a camera to a high elevation location overlooking the coastal zone to record an aspect or feature of the beach nearshore zone or dune area (Almar et al., 2008; Smith & Bryan, 2007; Bogle et al., 2001). The camera then captures images of the area throughout each day in order to build a continuous long-term dataset. The images can then be used for analysis. Specific features within the image such as the position of different beach features (i.e berms, shoreline and offshore bars) can be identified using colour characteristics

(Almar et al., 2008) (Smith & Bryan, 2007) (Bogle et al., 2001). The colour characteristics such as the red, green and blue light ratio and light intensities, and the images are rectified from pixel coordinates to real world coordinates in order to determine the movement or change in beach features (Huisman et al., 2011) (Smith & Bryan, 2007) (Balouin et al., 2014) (Plant et al., 2007).

Video analysis has been used to measure a variety of different coastal processes and aspects of beach morphodynamics, from nearshore surf bar positions, swash characteristics, shoreline and berm positions, beach cusps occurrence and subaerial beach profiles, along with the anthropogenic effects on beaches such as beach attendance and beach user locations (Bogle et al., 2001; Gallop et al., 2011; Huisman et al., 2011; Almar et al., 2008; Beuzen et al., 2019; Smith & Bryan, 2007; Balouin et al., 2014; Cuur, 2000). These applications have established video analysis as a low-cost technique, which can provide valuable multipurpose datasets with a high temporal frequency (Splinter et al., 2011). Due to the immense amount of data that can be gathered from using video analysis over long time periods, video analysis has the potential to replace traditional methods of gathering data for coastal monitoring (Splinter et al., 2011). The position of the frontal edge of the dune is important for coastal management and yet is not a commonly mapped or studies feature of the beach environment through video analysis. Dune toe the indistinguishable light characteristics of the sand dune toe that cannot be identified through the technique of video analysis, the sand dune toe of the sand dune cannot be measured using video analysis, only the vegetation line can be identified (Splinter et al., 2011).

The movement of the vegetation line present at the frontal sand dune is a beach feature that has not yet been extensively measured using video analysis. However, due to the prominence of the vegetation line in video, there is potential that video analysis would provide important information about the horizontal variability of sand dunes. Therefore, the aim of this chapter is to successfully create a new method which determines the horizontal position of the vegetation/dune toe using video analysis techniques. The light signature of the sand dune toe is not easily detectable through video analysis, and so the vegetation line is the only measure of dune variations that can be tracked with video (Splinter et at., 2011).

5.2 **Expected Outcomes**

The new method of identifying the vegetation line on sand dunes will aid in determining the horizontal movement of the frontal sand dune toe (Splinter et al., 2011). Due to the use of this method already providing a detailed analysis of one beach, Tairua Beach, it should be possible to detect changes in the horizontal position of the sand dunes to a high level of detail. It is expected that determining the position of the vegetation line of Tairua Beach will result in a number of observations. These observations included that the vegetation line moves landward during storm events when water levels are elevated and water is hitting the dune area (Rijn, 2009; Yates et al., 2009; Palmsten & Holman, 2012). The dune toe should move seaward slowly over time during recovery periods after or between storms (Aubrey, 1979). Variation in the vegetation line along the length of the beach is also expected and the variation of the horizontal position of the vegetation line is expected to change over time (Larson & Kraus, 1993; Saye et al., 2005). Tairua Beach is known to rotate, and so that and other similar coastal processes should affect the horizontal position of the frontal sand dunes (Bracs et al., 2016). The new method used to determine the vegetation line of the sand dunes may potentially have sources of error. These errors include the accuracy and precision of the rectification process of the images used, where control points are manually picked and identified in each image (Holman et al., 1991). Using representative or assumed dune toe height, for the elevation of rectification may also cause an error in horizontal position of the vegetation line (Guimaraes et al., 2016). Video analysis has been previously used for beach features that move very quickly (i.e. relatively large distances over a short period of time) such as offshore surf bars, but not for features that move slowly or infrequently such as sand dunes, therefore the accuracy and precision of identification of the horizontal position of sand dunes within the image may need to higher than for other features, to show changes throughout time(Smith & Bryan, 2007). This analysis will attempt to quantify these levels of error and assess if the error is acceptable for measuring the position of the dune vegetation line.

5.3 Methods

A video camera located on Paku Hill at the south end of Tairua Beach was installed by WRC and NIWA in September 1997, as part of the New Zealand "CamEra" network for coastal monitoring (Almar et al., 2008). The camera has an elevation of approximately 70 m (70.48 m) above chart datum (Almar et al., 2008). The camera's field of view includes the back dunes (to the houses behind the dunes), the foredunes, the nearshore zone of Tairua Beach and part of the sea. The field of view excludes, approximately 50 meters of the south end of the beach below where the camera is situated. The camera takes 600 images (0.5 Hz) over a 15-minute time period every hour during daylight hours, and the images are averaged to produced one 'time exposure' image for each hour (Figure 5.1).

Figure 5.1. An example of one of the images that are captured, as part of the "CamEra" network, of Tairua Beach. Figure two. An example of one of the averaged 'time exposure' images for one hour at Tairua Beach.

A coloured 760 by 570 pixel image for before October 2009 or 1500 by 2020 pixel image for after October 2009 was produced every daylight hour. Assuming that the dune toe does not change over a short time scale, one image per month, from the 20-year dataset, was selected for analysis. Care was taken to avoid the use of images that were taken in foggy weather conditions, or at certain times of the day (normally at the very start and end of each day) where there was large shadowing on the beach area, or in certain light levels were avoided, so that the vegetation line could be found more easily. Images that had smudges or sea spray on the camera lenses were also avoided, along with objects present that obscured the

view of the beach/vegetation line, such as trees and a wooden frame that was present within the field of view for a few months. Changes in the position of the camera and camera distortions were corrected for using a lab-based algorithm. The images were analysed using Matlab software. A mask was set up to capture the characteristics of the pixels, of the beach and foredune area within the selected image (Figure 5.2). The first boundary of the mask was along the back of the foredune and the second boundary was along the shoreline, the entire length of the beach.
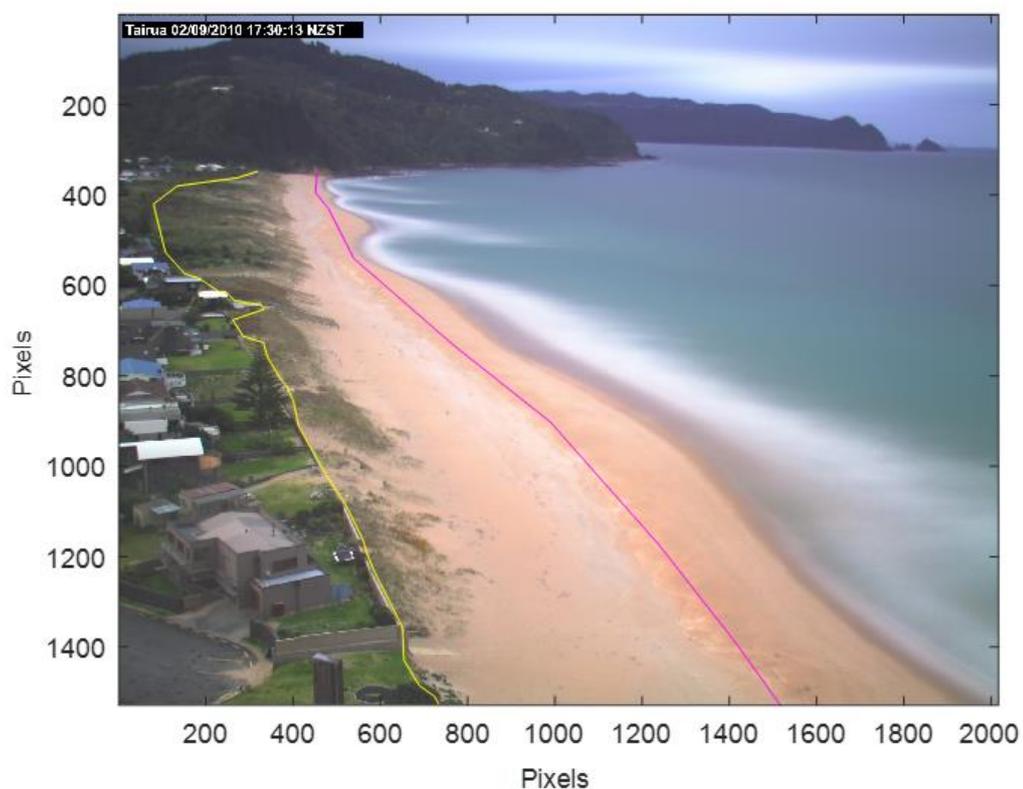
Figure 5.2. Image showing where the masked area of the dunes and beach is situated. Pixels of interest were within the horizontal transects between the first boundary (yellow line) and second boundary (pink line) shown on the image.

Within the mask area, characteristics of each pixel were identified and analysed for the entire length of the beach. Each pixel within the image had a different intensity of red, green and blue light. The ratio of between two or more of those colours of light could change throughout the image as well, and therefore these were used to identify features within the image. The characteristics that were

explored as good markers of the vegetation line were the light intensity and the ratio of green-light to red-light were investigated (Figure 5.3). There was a slight change in the ratio of green-light to red-light, from an area of vegetated dunes to an area of sand which encompasses the beach, but not enough to be distinguishable. However, the intensity of light of all three colours changed from an area of vegetated dunes to an area of sand. Therefore, a combination of the green-light to red-light ratio and the intensity of light was used to identify the vegetation line along the foredunes.
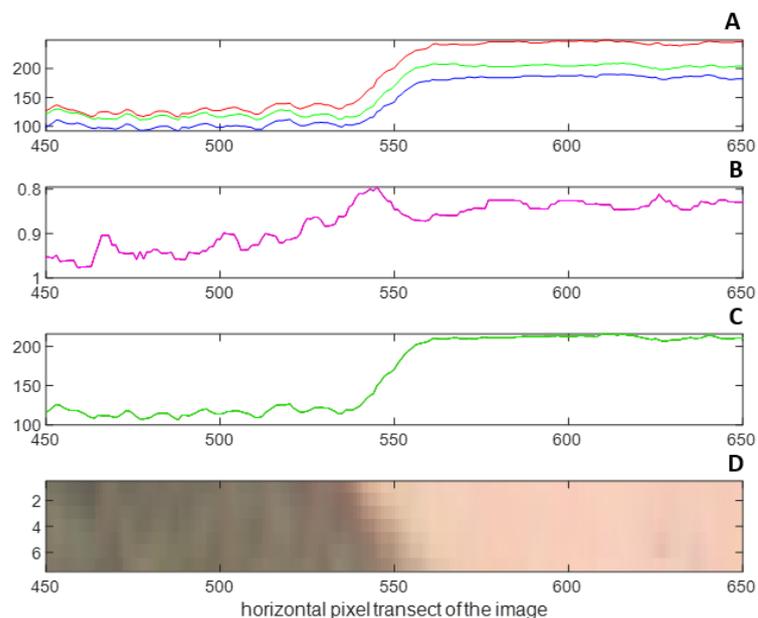
Figure 5.3. The red, green and blue light intensity (A), the red-light to green-light ratio (B), the intensity of light (C), the colour of the vegetation line (D), for part of a horizontal transect of pixels from the image.

In order to determine the detection thresholds between sand and vegetation, a sample of pixels were taken from the image of several areas of vegetated dunes, including sparsely vegetated areas, densely vegetated areas and areas of different species of dune plants (mostly spinifex and pingao could have been distinguished due to differing colours of green for spinifex and orange for pingao) (Figure 5.4). A sample of pixels were also taken of several areas of sand, including different shades of colours of sand to encompass/represent the different colours of the whole beach (Figure 5.4).
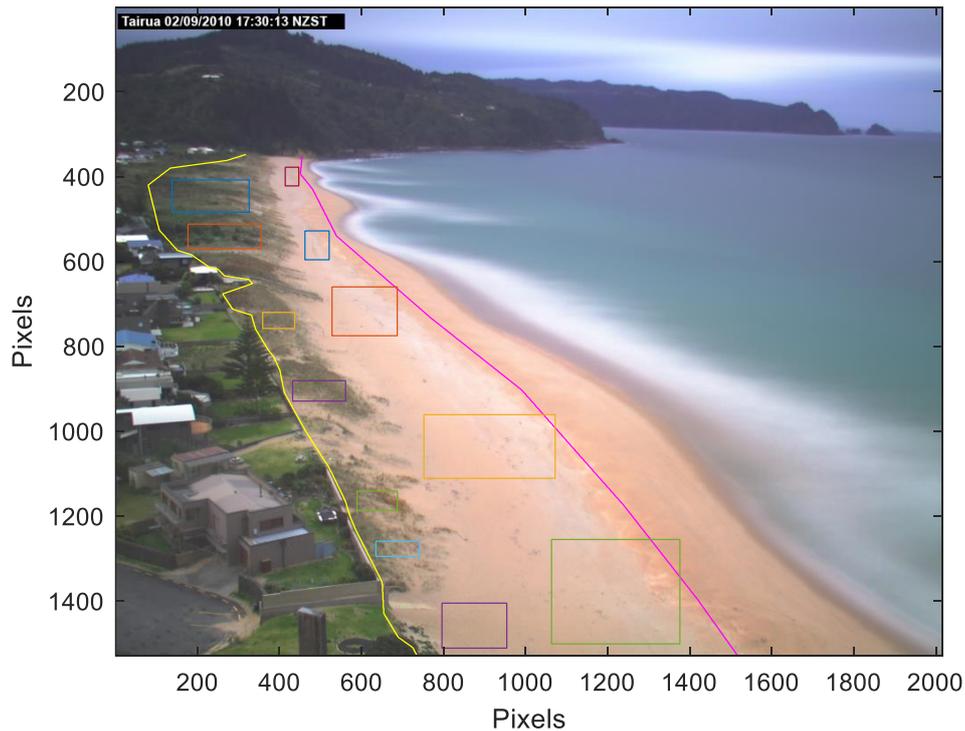
Figure 5.4. An example of samples taken from the image to determine thresholds for classification which represented the dune area and sand area (coloured squares) within the masked area (yellow and pink lines).

The ratio of green-light to red-light was plotted against the average light intensity of red, green and blue, for each pixel from the sample of pixels (Figure 5.5). The scatter plot showed that there were two distinct clusters that overlapped, which could be divided into three distinct classes, based on the differing combinations of green-light to red-light ratios and average intensity of green, red and blue light (Figure 5.5). The three classes were the 'dune' area which consists of densely vegetated sand dunes, the 'transition zone' which was the sparsely vegetated dune area (normally along the vegetation line at the front of the sand dunes) and the 'sand' area which consisted of the majority of the beach (Figure 5.6). The thresholds based on the green-light to red-light ratio and the average intensity of green, red, and blue light, for each of the classes were established from the clusters of the sample pixels.
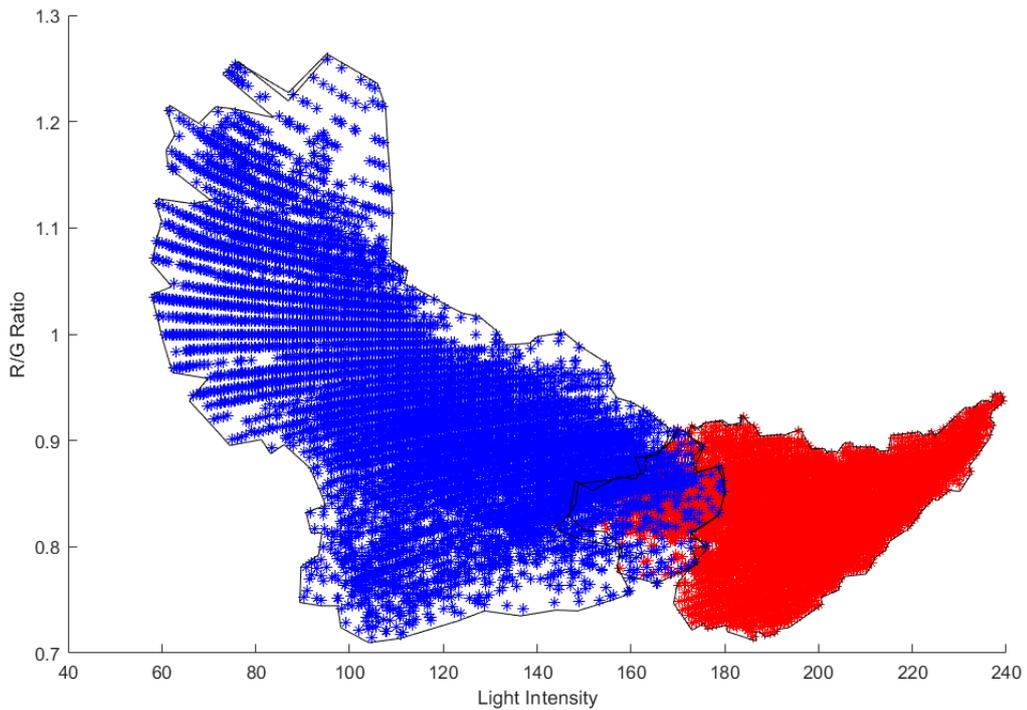
Figure 5.5. The green-light to red-light ratio against the light intensity of red, green and blue light, for the sample of pixels from the image. The blue dots represented the sample of pixels from the vegetated dune area and the red dots represented the sample of pixels from the sand area of the beach.

Dune area = densely vegetated dune area

Transition area = sparsely vegetated area, mix of vegetation and sand

Sand area = sand area of the beach, where no vegetation was present
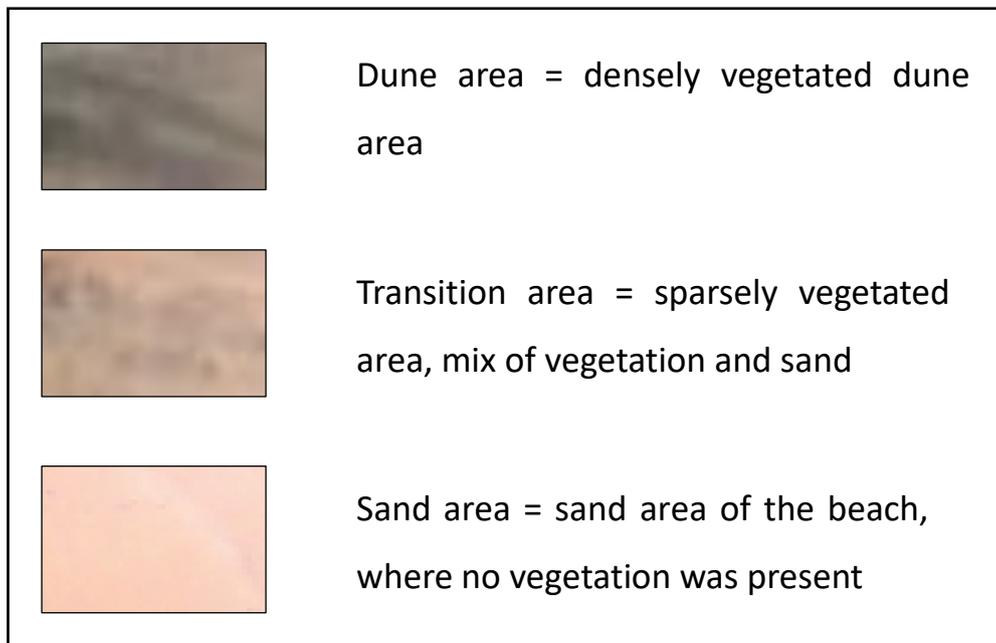
Figure 5.6. A visual example from an image which showed the three classes of 'dune' area, 'transition' area and 'sand' area.

130

Each pixel within the mask of the image was classified, by searching each horizontal line of pixels within the image for colour characteristics that matched the threshold conditions. Each class was allocated a number (dune area = 3, transition zone = 2, and sand area = 1) and each pixel within the mask, was allocated a number based on whether the thresholds for one of the three classes were meet (pixels that did not meet the thresholds for any of the classes were allocated 0). The number for each pixel was stored and plotted (Figure 5.7).
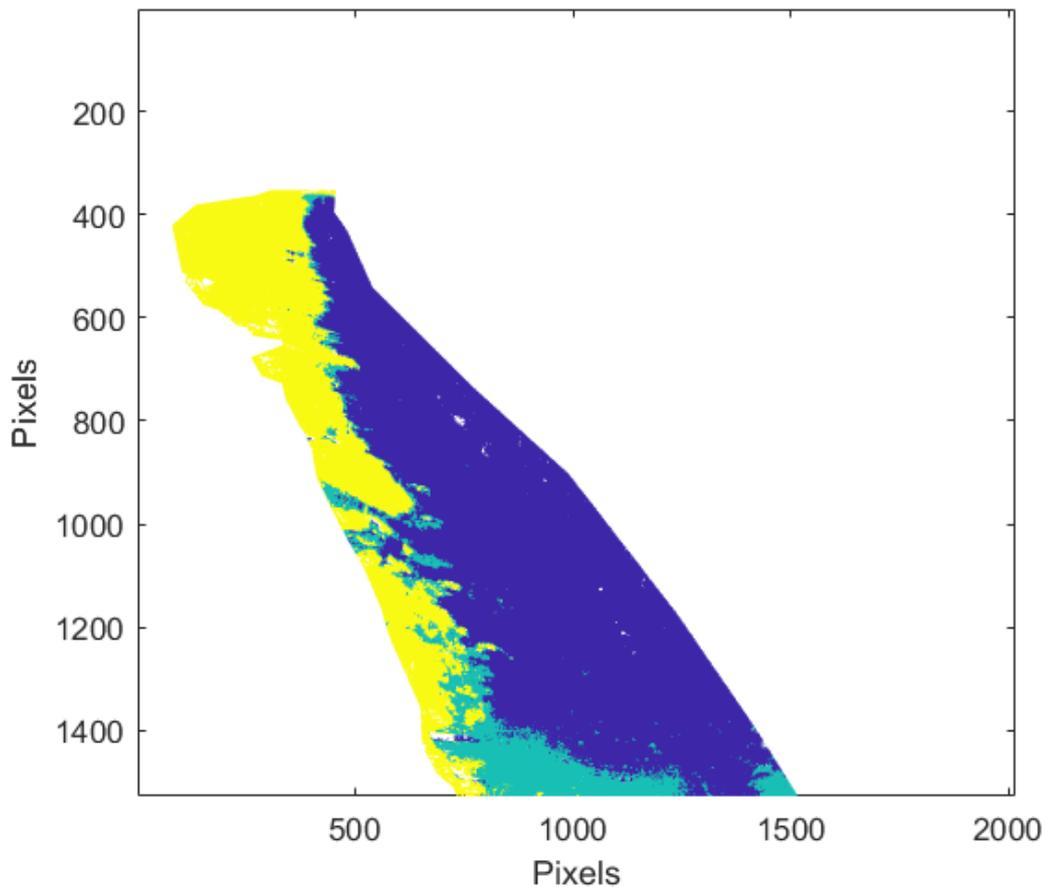
Figure 5.7. The class of pixels within the masked area of the image. The three classes were the dune area (yellow), transition area (green) and sand area (purple).

To detect the location of the vegetation line (which is often patchy) an accumulative running sum of the class number was produced along every horizontal line of pixels within the image. When the cumulative running sum of the class number went below a certain threshold (the number 11 was chosen through trial and error), the position of this pixel (potential vegetation line

position) was stored and plotted (Figure 5.8). All of the potential points of the vegetation line were plotted (Figure 5.9).
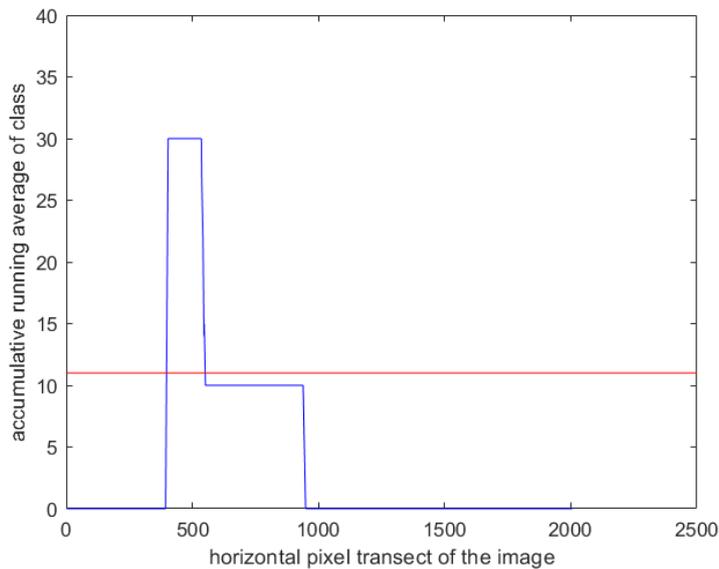
Figure 5.8. The cumulative running average of the class of pixels for one horizontal transect (blue) and the threshold (11) for the position of the vegetation line (red).

In order to smooth the resulting vegetation line, the running mode was calculated using 40 pixel lines (Figure 5.10). Finally, the nearest point to the running mode, was then found and determined to be the position of the vegetation line (Figure 5.11 & Figure 5.12). A small amount of manual editing was necessary in order to correct anomalies in the resulting vegetation line in order to improve the quality of the data.
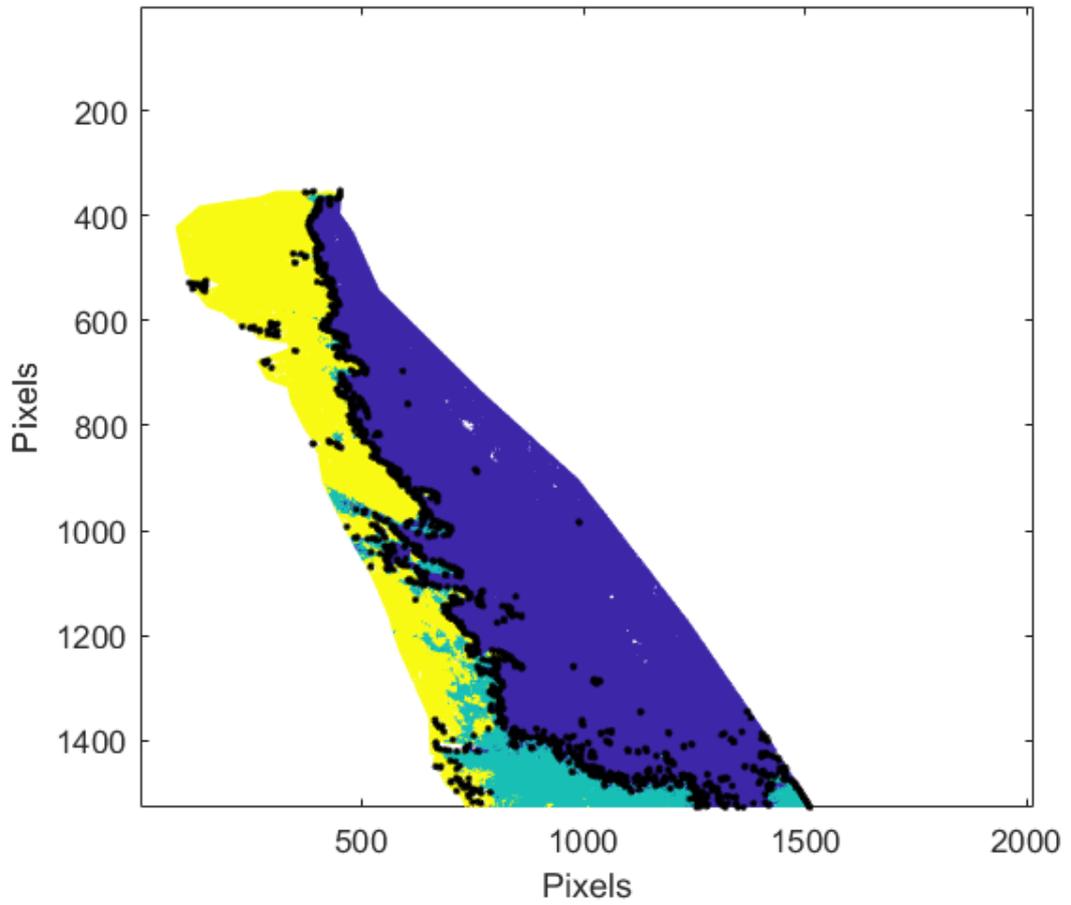
Figure 5.9. The class of pixels within the masked area of the image and the potential vegetation line position (black dots). The three classes are dune (yellow), transition (green) and sand (purple).
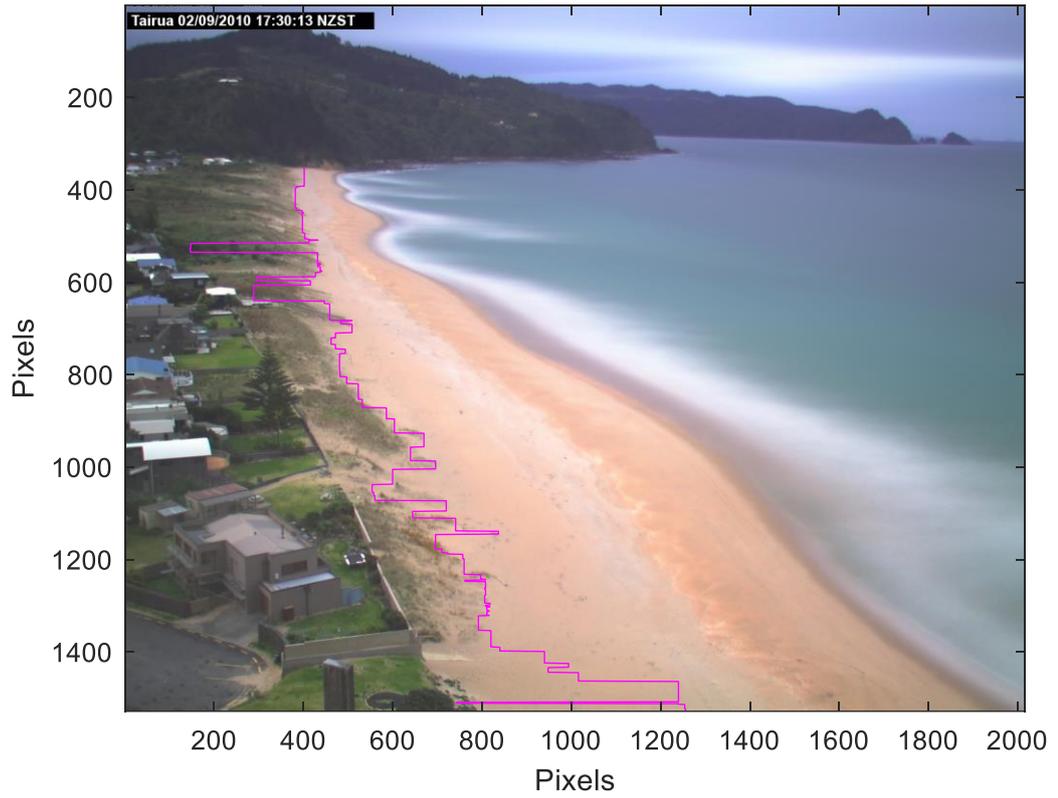
Figure 5.10. The running mode of the potential vegetation line position (magenta line).
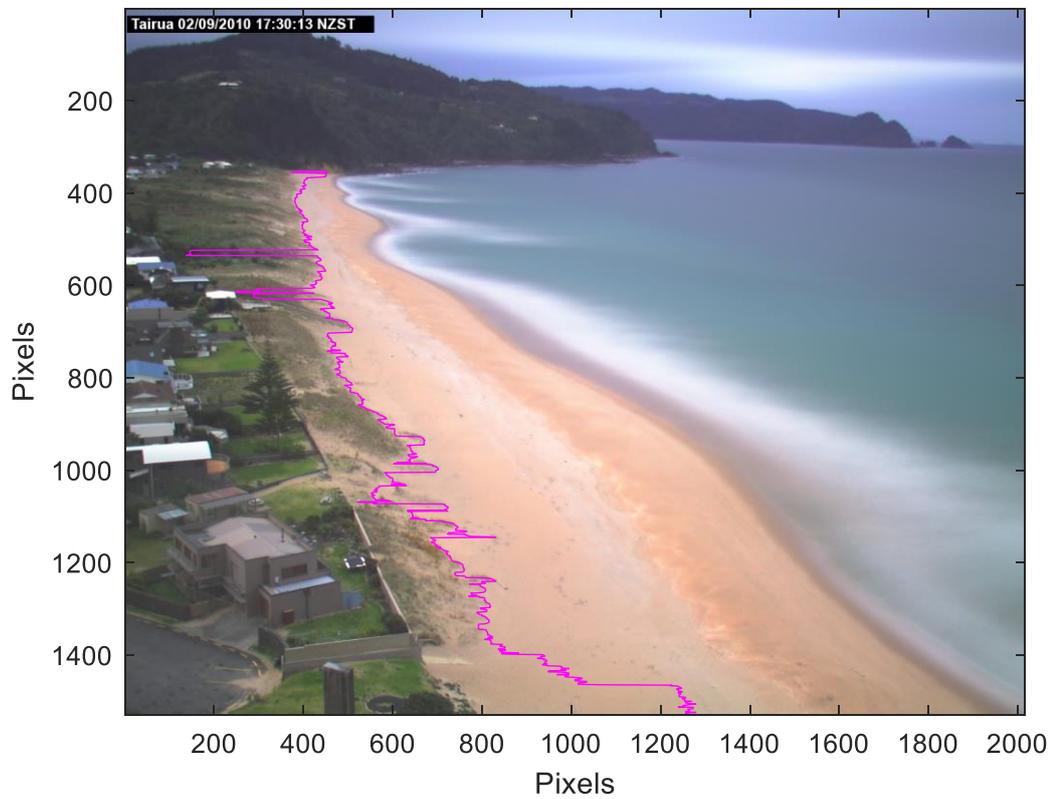
Figure 5.11. The generated vegetation line (magenta line), before manual editing.
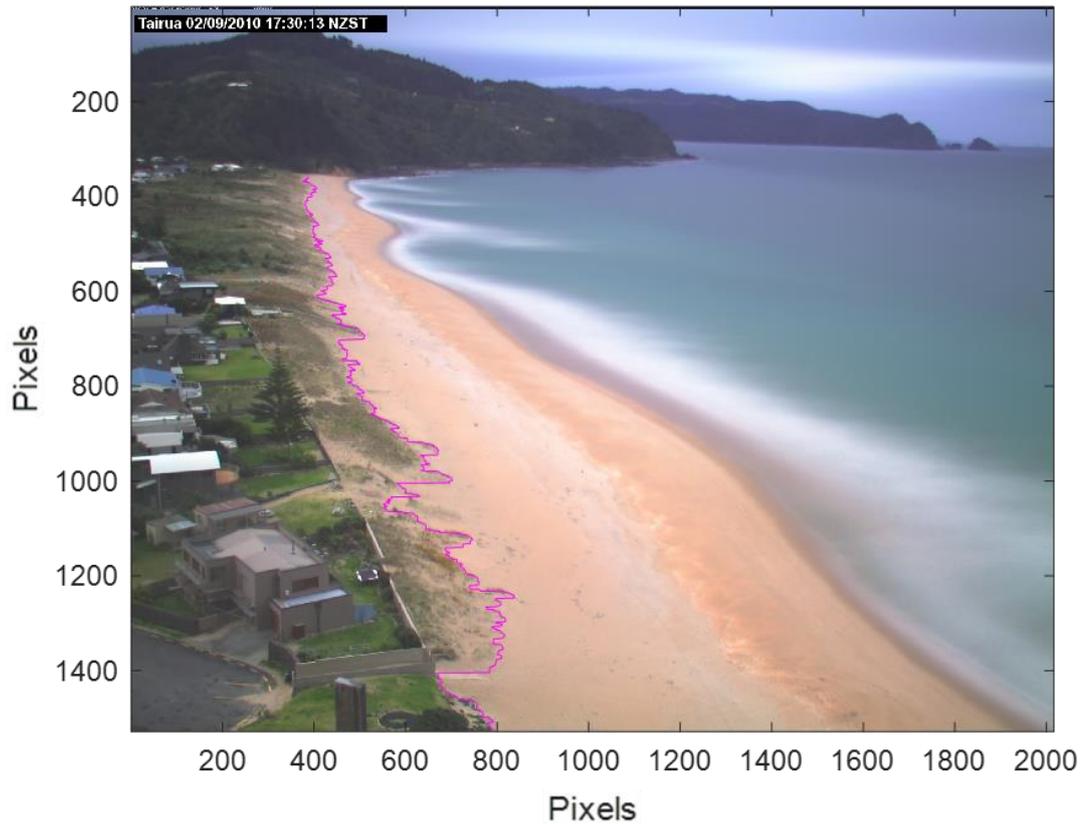
Figure 5.12. The final vegetation line (magenta line), after manual editing.

The image and the vegetation line were rectified in order to determine the horizontal change in the position of the dune toe (Figure 5.13). Rectification involved using control points within the image, such as trees, rooftops, fences, and rocky outcrops, to correct small movements of the camera. These movements can occur due to weather and tampering. A specifically designed algorithm was used to correct positions within the image, from the control points used that were ground true, were transformed from pixel coordinates into real-world coordinates (Montano et al., 2019; Almar et al., 2008). The average height of the dune toe for Tairua was 4.7 m (calculated from the surveys), and this value was used for the rectification of the vegetation line (Plant et al., 2007). Previous images, close in date to the current image, were used as reference images against which the position was corrected for the current image.

135
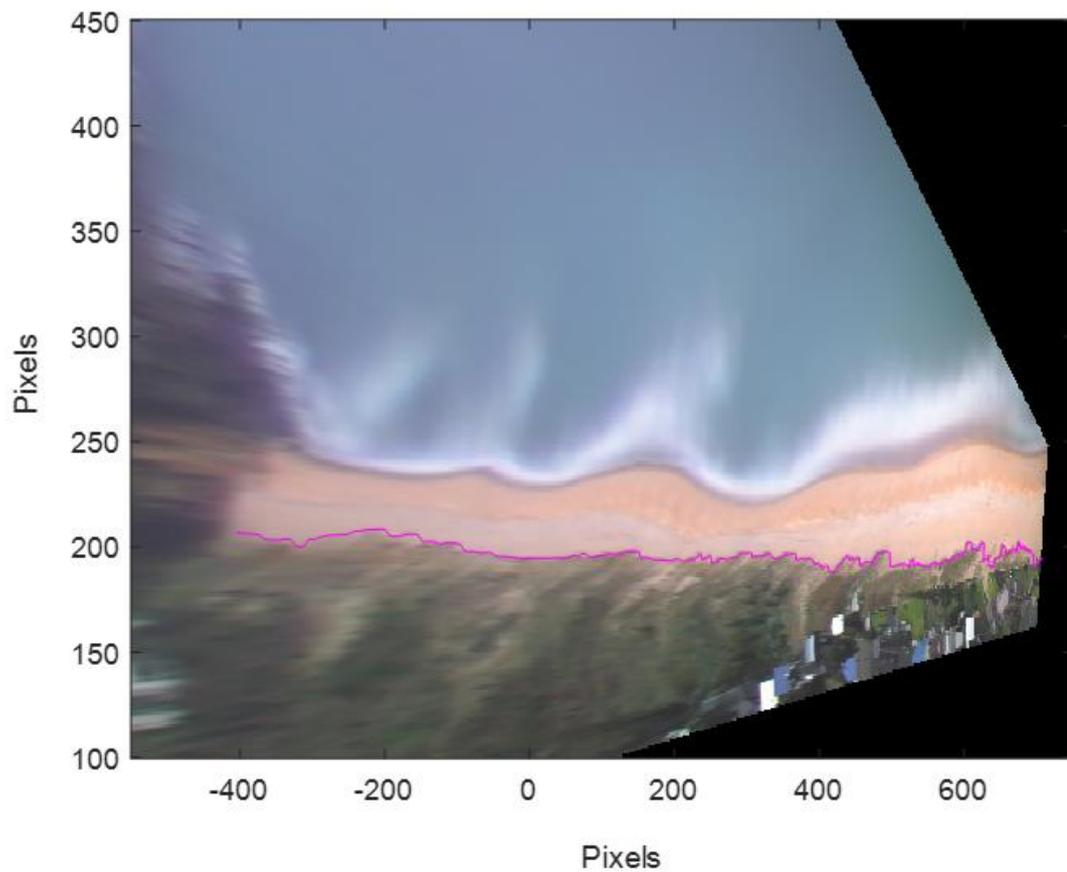
Figure 5.13. The rectified image, showing the final vegetation line (magenta line).

The horizontal position of the dune toe for the length of Tairua Beach was determined and plotted for every three months between 2002 and 2019, from the data produced using the new method of video analysis for the determining the vegetation line. The average horizontal dune toe position for every three months, from the image analysis was plotted against the detrended shoreline position and mean shoreline position for the same given time period (Figure 5.14). The linear regression for the mean shoreline position and the horizontal position of the vegetation line with a lag-period of 16 days was determined. A number of different lag-period between 1-20 days was tested, where a lag-period was found to be the optimum lag-period.

5.4 **Results**

Figure 5.14 shows the horizontal position of the vegetation along Tairua Beach, between 2002 and 2019. Each horizontal strip on the figure, shows the position of the vegetation line (showed by the colour scale) at that instant in time, where blue is more landward and yellow is more seaward. The north end of the beach is the left end of each strip and the south end of the beach is the right end of the strip.

In 2002, the horizontal position of the vegetation line at the south end of the beach was seaward. Most areas within the middle of the beach were landward, with some variation. At the north end of the beach, the vegetation line was mostly seaward, with some variation. Between 2002 and 2008, the horizontal position of the vegetation line at the south end of the beach moved greatly landward. The vegetation line at the middle of the beach stayed mostly the same and at the northern end of the beach there was some seaward movement in some places. Between 2008 and 2014 at the south end of the beach, the vegetation line moved seaward and then stabilised, there was slight seaward movement in the middle of the beach and at the north end of the beach a large amount of movement seaward. Between 2014 and 2019, at the south end of the beach there was seaward movement, but overall there was slight movement landward of the dune toe. In the middle of the beach there was period of slight landward movement and then a period of slight seaward movement. At the north end of the beach horizontal position of the vegetation line moved landward, for approximately three years and then there was movement seaward for three years and then movement landward again.
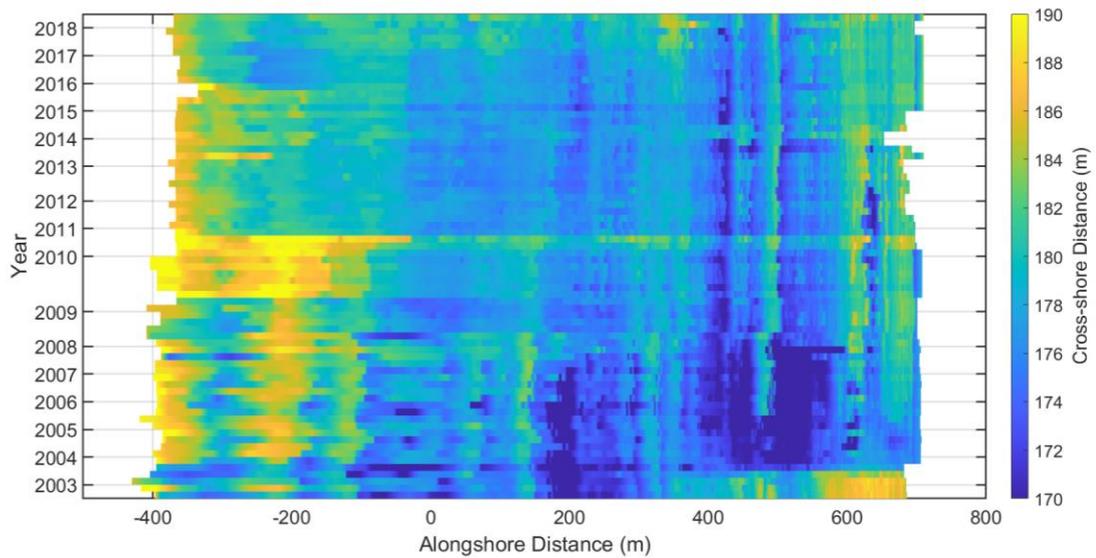
Figure 5.14. The horizontal position of the vegetation line throughout time, from 2002 to 2019, yellow shows areas that are seaward and dark blue areas are landward.

Throughout the whole time period of which the samples were taken there was a large variation of the horizontal position of the vegetation line along the beach length. Figure 5.15 shows the average horizontal position of the vegetation line for each sample throughout time, along with the detrended shoreline position and the detrended mean shoreline position. The figure shows that the shoreline position was highly variable and vegetation line was much less variable. The horizontal position of the vegetation line was shown to be somewhat correlated to the shoreline position or the mean shoreline position, when visually assessing the data, where there were periods of time where the shoreline position increased and the vegetation line increased but to a lesser degree. Good examples showing these synchronous changes can be shown for the years of 2002 to 2004 and 2006 to 2008, 2013 to 2014.
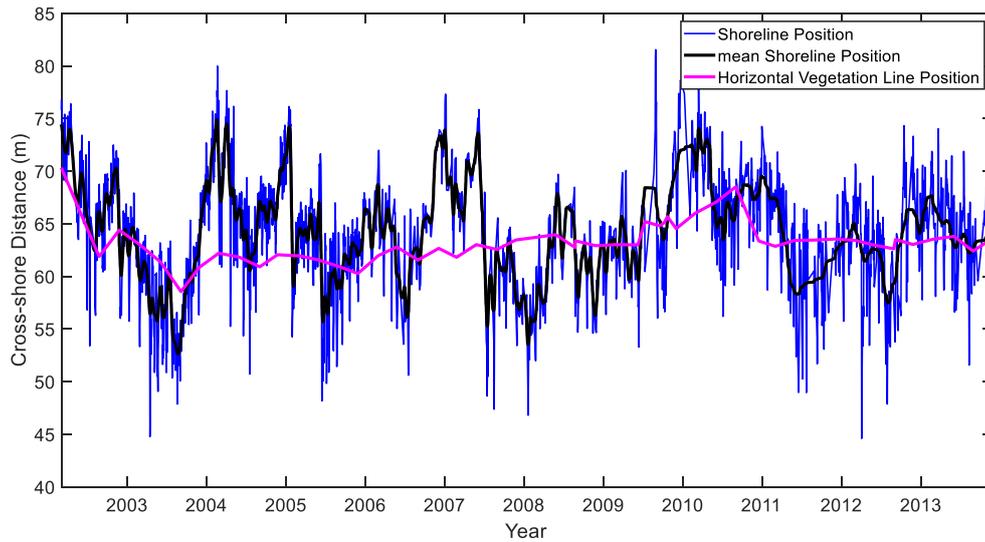
Figure 5.15. The average horizontal position of the vegetation line (magenta line), alongside the horizontal position of the shoreline (blue line) and the running mean of horizontal position of the shoreline (black line), throughout time.

Figure 5.16 showed the average horizontal position of the vegetation line and the running-mean shoreline position at the exact same time at which the average horizontal position of the vegetation line was taken. The linear regression analysis was used from this data, where a 16-day lag period was added to the horizontal vegetation line position.
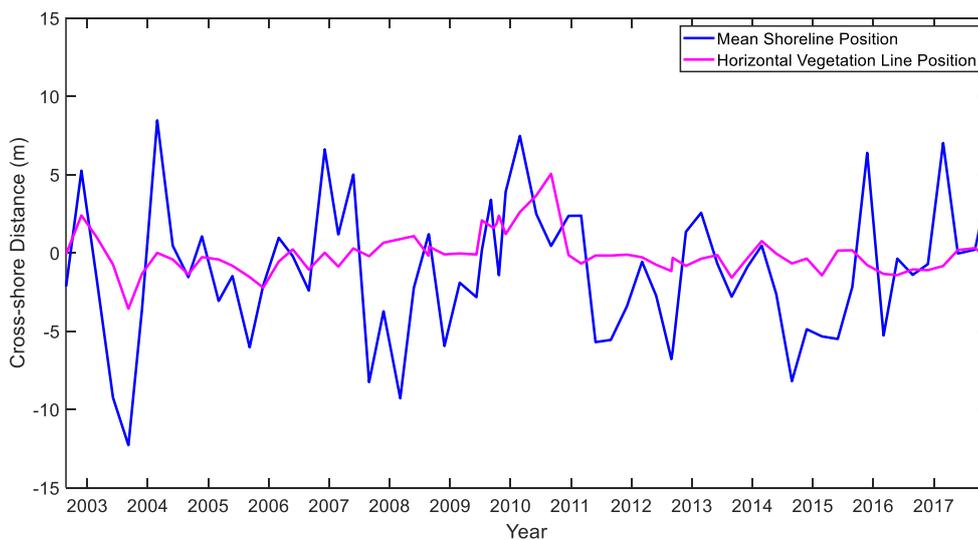
Figure 5.16. The running-mean shoreline position and the horizontal vegetation line position throughout time, with mean shoreline points matched to the vegetation line position, for Tairua Beach.

139

Figure 5.17 showed the running-mean shoreline position versus the horizontal vegetation line position. Figure 5.17 shows the variation in the horizontal vegetation line position was 6 m with an outlier at -5 m and the variation in the mean shoreline position was roughly 26 m. Therefore, the variation in the horizontal position of the vegetation line is much less than the variation in the shoreline position. A linear relationship between the mean shoreline position and the horizontal vegetation line position was evident. Least squares regression analysis produced an R-squared value of 0.0796, with a p-value of 0.0207.
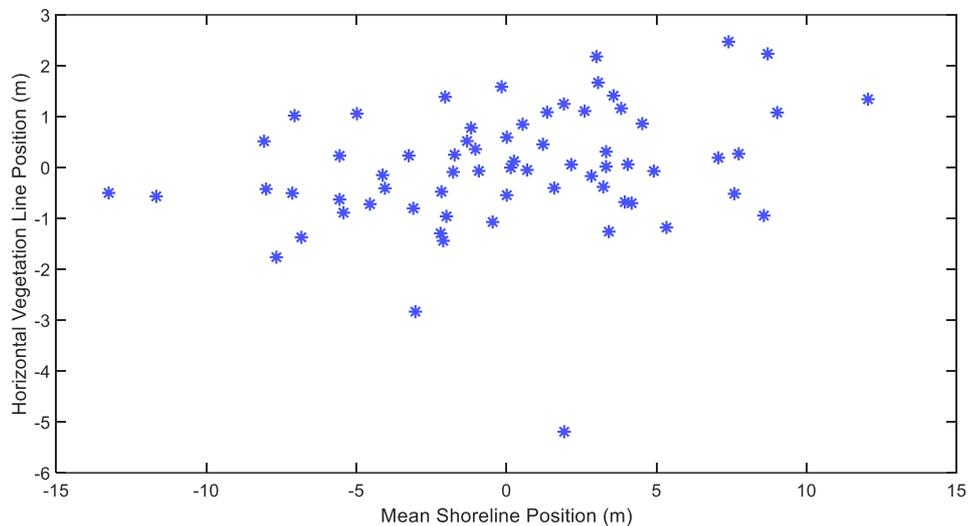
Figure 5.17. Mean shoreline position versus horizontal vegetation line position for Tairua Beach.

5.5 Discussion

Figure 5.14 showed the changes in the horizontal position of the vegetation line throughout time. This figure showed the variation in the horizontal position of the vegetation line both along the length of the beach and throughout time. Erosion events were determined by landward retreat of the horizontal position of the vegetation line and accretion was determined by seaward movement of the vegetation line. The largest erosion events that occurred were at the south end the beach during the early 2000s (2002 to 2008) and at the North end of the beach during 2009 and 2016. During these events, the vegetation line endured a sudden

move landwards follow by a prolonged period of time at which the vegetation line was stable in this new position before accretion occurred and slowly moved seaward again (Larson & Kraus, 1993) (Pye & Blott, 2008). For example, at the south end of the beach it is shown that the erosion event occurred suddenly, and the vegetation line stayed roughly in the same position for four years (2003 to 2007) before the sand dunes could recover in 2007, the vegetation line then stayed relatively stable for the rest of the time period, with some small movement (Larson & Kraus, 1993) (Pye & Blott, 2008).

There have also been many areas where accretion that has occurred on Tairua Beach during the time period. The major areas include the middle of the beach during the majority of the time period and at the North of the beach in two episodes of between 2002 to 2009 and between 2010 and 2015. The accretion events show that the vegetation slowly moves seawards over long time periods, rather than sudden movements (Ruz & Meur-Ferec, 2004).

The changes in the shoreline position occurred often and were much larger than the changes that occurred at the vegetation line position which were infrequent and smaller (Larson & Kraus, 1993). This was likely due to the frequency of water levels reaching different areas of the beach and the role that wave impact/ water levels have on beach morphodynamics (Larson & Kraus, 1993). The shoreline is positioned in the lower beach area of the intertidal zone, where inundation occurs at every tidal cycle. Whereas, the vegetation line is positioned further up the beach where water only reaches this area of the beach during storm events and during high tides, with the influence of storm surges, beach setup and wave runup (Palmsten & Holman, 2012) (Yates et al., 2009). The influence of water is reflected in the shoreline position which changes frequently and the vegetation line which stays the same for long period of time with sudden changes due to storm events (Larson & Kraus, 1993) (Saye et al., 2005).

There was a very small but significant correlation between the shoreline position and the horizontal position of the vegetation line at a lag period of 16 days. This correlation showed that the processes that occur lower down the beach face may also influence the upper beach face and within the frontal dune area.

5.5.1 Errors/Future Research

There are a number of further improvements that could be made to this new method that would increase the efficiency and time needed to analysis the data and improve the technique of the new method. These improvements include the use of machine learning for identifying the clusters from the samples of pixels when classifying the vegetation (Figure 5.6). Using machine learning would enable automatic identification of the clusters rather than having the identify the cluster manually, which would increase time efficiency. Some of the most time-consuming parts of the method used to determine the vegetation line was identifying the control points for each image so that the image rectification could be corrected for minor camera movements. There were roughly 30 control points used for each image, which was needed in order to obtain a low error in image movement and high accuracy of the rectified image (Hollman, 1991). To identify these control points and rectify each new image took roughly two hours. There was a consistent problem throughout the majority of the images during the rectification process, where in some rectified images, the positions of known features moved up to 1 m in distance at the south of the beach, where camera resolution was high and up to 3 m at the North end of the beach, where camera resolution was low. The movement in the position of features was exacerbated further away from the camera position where the camera resolution was low due to the algorithms used for rectification. Due to the using the closest image by date as the reference image for the rectification of the new image, the movement in the rectified images could accumulate with the number of images from the target image, which was ground true. Extra care and attention to detail was taken to ensure that the error shown was not an operator error and many of the images were rectified multiple times, by manually identifying the control points, in order for the error to be resolved and later minimised when resolution of the error was not possible. Therefore, this error increased the time needed for image rectification, roughly from 30 mins - 1 hour to 2 or more hours for each image. Further improvement of the rectification process within the method would be to automate the rectification process, so that manual identification of each control point is not needed.

The second most time-consuming part of the method was manually editing the potential vegetation line. Due to colour characteristics of walked upon sand and seaweed on the beach and other anomalies, sometimes the vegetation line would be in the wrong place for some rows of the pixels within the image. For the images used in the analysis, the occurrence of the vegetation line not matching the true position of the vegetation line for each row of the image was roughly 5-25%, equated to between 10 min to 1 hour of manual editing time needed for each image. Therefore, further improvements to the new method would be decrease the amount of manual editing necessary by being able to distinguish the vegetation line from anomalies more easily.

Limitations on the number of images analysed was due to the time-consuming nature of both rectification of the images and the manual editing necessary for determining the final vegetation line. Ideally image analysis for every month (or even week) within the dataset would have been completed. However, due to the limitations of the method only image analysis for every three months was achieved, and so one image per season was analysed. Further improvement to the method would be to decrease the time needed to analyse each image, in order to increase the extend of the dataset used for analysis and increase the temporal space of the dataset. Further improvement of the dataset could be made by investigating individual storm events and analysing images before and after the storm event in order to determine how much the horizontal position of the vegetation line move due to one storm or over one tidal cycle, within a period of a few hours. This high level of detail may give more insight into processes that are occurring to cause the vegetation to move horizontally.

Other improvements include the use of more than one camera installing to take images of Tairua Beach (Splinter et al., 2011). There are a number of beaches in Australia (look up the names of the beaches) that already have multiple cameras operating, which has increased the accuracy of measuring changes to beach features, as there are multiple camera views used in the analysis process (Splinter et al., 2011). However, increasing the camera views for a single beach would involve more cost and more time needed for analysis to be completed (Splinter et al., 2011). There may also be a small amount of error in using the average dune

toe from the 2018/2019 surveys as the rectification elevation, small photogrammetric errors caused by the differences in elevation to the actual elevation may have occurred within the dataset (Plant et al., 2007). In the future, different types of vegetation may also be able to be identified, not only density of vegetation (Acosta et al., 2005). The native species of Spinifex and Pingao can already be distinguished by eye within the vegetation of sand dunes by their colour characteristics of green and orange colouring. Therefore, if this colouring of vegetation present could be identified through a unique set of colour characteristics, a more detailed analysis could be conducted in future providing more information about the vegetation present in the sand dunes and how beach processes are affected by these different types of vegetation. Lastly, further development of the method and of satellite resolution could result in the use of satellite imagery to identify the vegetation line of sand dunes and the change in horizontal position of the vegetation line. Currently resolution in most areas and datasets available are of roughly 10 m resolution which is not of high enough accuracy to determine significant changes in the vegetation line of sand dunes throughout time.

5.6 Conclusions/Summary

The vegetation line was successfully determined using video analysis, however there could be some improvements made to the technique used in order to decrease the time for measuring the horizontal position of the dune toe and also increase the accuracy and precision of the measurement. The measurement of the vegetation line of sand dunes showed that the vegetation line moved far less often compared with shoreline, which is on the lower beach face, and inundated with water more frequently. Video analysis could be used in the future as potentially a new method for beach monitoring, in which high frequency and spatial distribution of data is possible.

Chapter Six

Using a Simple Model to Predict Observed Dune Toe Changes

6.1 Introduction

A numerical model can be used to predict changes in the horizontal position of the dune toe and a number of different types of models have been developed to undertake this task. When models are used in the right context and are known to have a reasonable error for a variety of situations, models for dune erosion can be useful tools for understanding coastal processes, hazard risks and changes in the beach morphology for the past, present and future (Kriebel & Dean, 1985; Splinter and Palmsten, 2012). Naturally, well established sand dunes protect the areas behind the coastline from flooding and inundation, including the human population and property (Splinter & Palmsten, 2012). The prediction of future dune erosion would be an important indicator of the protection sand dunes provide in the future and the risk of the sand dunes breaching, removing the protection from inundation, with sudden and potentially catastrophic consequences (Splinter & Palmsten, 2012). Future predictions of dune erosion may also become a useful tool for planning in the future to avoid past mistakes and improve future coastal settlement planning.

This chapter aims to use the simple, time-dependent model from Splinter and Palmsten (2012) to predict the change in volume eroded the dune and the subsequent changes to the dune toe, throughout time, using measured beach profiles at Tairua Beach as validation. Specifically, predictions of the model will be tested using the historical beach profile dataset from WRC, field surveys of beach profiles during 2018-2019 and the CamEra video analysis dataset, in order to determine whether predictions calculated are within reasonable error. A quantitative analysis using the CamEra video analysis will be used to determine the observed number of times water hits the dune toe and validate the result of the model. There are a number of important definitions and assumptions that are

used within the model. The initial dune toe position is based on the initial profile used in the model, and all subsequent changes are relative to that position. The beach slope is considered to be the mean slope of the beach between initial dune toe position and the mean sea level elevation of the initial profile. The dune slope is considered to be the mean slope between the maximum dune height and the initial dune toe position (Figure 1). It is assumed that within the model the maximum dune height does not change, as inundation over the top of the frontal dunes was assumed to not occur, the only processes modelled are the collision and overwash regime, which occur when the water elevation exceeded the dune toe position (Ausbury & Sallenger, 2000) (Splinter & Palmsten, 2012).

6.2 Expected Outcomes

There have been a small number of dune erosion models produced where both laboratory and field data has been used to test the dune erosion models. Therefore, the quality of models from the literature have improved, but there is still scope for improvement. Factors for the quality of models presently within the literature, include the amount of field data available for model testing and the diversity of this data present. The diversity of data may include different beach states, beach rotation, upper dune profiles, wave climates, and long-term climatic patterns. The diversity of data results in a large number of undetermined factors that cause uncertainty when predicting dune erosion, and presently, the need for assumptions and calibration parameters within the dune erosion model.

For the model used in Splinter et al. (2012), which has been modified for the use in this study for Tairua Beach, there are a number of assumptions made for the behaviour of dune erosion. However, these assumptions and limitations are likely to cause a potential error in the successful prediction of the volume of eroded sand and the change in dune toe position. The model assumes that the dune toe will recede along a line governed by the average slope of the beach face (Figure 1) and the angle of the receding dune front is equal to the dune slope before erosion event. These assumptions may cause the volume of sand eroded to either be lower or higher than the historic data shows, because scour may occur below the dune toe or the slope of the profile in the newly eroded are might change. If erosion

causes a different angle to the beach slope below the dune toe, there will also be implications to predicting the correct wave runup and dune exposure, appropriate for each time step within the model, leading to a higher error in the volume of eroded sand and the new position of dune toe. The beach slope is used in the runup calculation. The dune area above the dune toe may also eroded in a different way compared with the dune slope angle which may also cause an error in the volume of sand eroded above the initial dune toe and therefore the new position of the dune toe determined. The calibration coefficients used in the Splinter et al. (2012), previous papers and early versions of this model, were not disclosed. Therefore, the calibration coefficient values were assumed, using trial and error.

Even with these assumptions in place for this study, the dune erosion model is hypothesised to be able to predict dune erosion within a reasonable degree of error, over long time periods. One of the conditions for whether erosion occurs for a given time step is whether the water level reaches the initial dune toe position.

6.3 Literature Review

There are a number of models already present that attempt to successfully predict the change in dune toe. Some of which have used previous models and added or combined methods and values used to improve the results of the model. Throughout time, the dune erosion models, has increased in complexity and the decreased in the error of prediction for dune erosion. The main two approaches to models for dune erosion within the literature has been the beach equilibrium profile theory and the wave impact theory approach. Both approaches started with simple models and became more complex with each new method produced.

Vellinga (1982) and Kriebel and Dean (1985) were some of the first dune erosion models produced, where Vellinga used the 'wave impact theory' and Kriebel and Dean (1985) used the theory of the beach equilibrium profile in order to predict dune erosion (Vellinga, 1982; Kriebel & Dean, 1985). Vellinga (1982) used a number of laboratory experiments of different scales to understand how erosion occurred at the dune, where sediment concentration and orbital velocity

measurements were considered. A simple model based upon, surge water level, wave height and sediment characteristics was formed and compared with a storm surge event in Netherlands. The model confirmed the dimensionless fall velocity parameter, now known as Dean's parameter, which relates the external force acting on the dune and the sediment characteristics of the dune, with the slope of the beach. Due to the simplicity of the model, the feedback of changing morphology was not considered, and the model was not time dependent. The model from Vellinga (1982) was thought to be one of the first models for predicting dune erosion, which uses a laboratory setting, and later application to field data, to determine already known principles and incorporate these principles into a useable model (Vellinga, 1982; Kriebel & Dean, 1985).

Kriebel and Dean (1985) was the first dune erosion model to consider the theory of the equilibrium profile, where if the beach profile is exposed to a constant wave climate over a long time period, the beach profile will reach an equilibrium state (Kriebel & Dean, 1985). However, when there is an inconsistent wave climate where there are periods of low wave action and storm events, the beach profile is changed most likely due to erosion by the storm, and transported to offshore limit of sand movement of the edge of the offshore surf bar. Therefore, during the recovery period after the storm, sand will be transported back up onto the beach face, so that the beach profile returns to an equilibrium state. The Kriebel and Dean (1985) model is a more complex model compared with earlier models, due to the model being the first time-dependent model and requiring more input values. Models that are not dependent on time give the total dune erosion from a single storm event. However, time dependent models, take into account changes in morphology, wave height and water level throughout an individual storm event. Therefore, if inputs and parameters of the model are more reasonable, the prediction of the dune erosion of time dependent models should be more successful than models that do not depend upon time (Kriebel & Dean, 1985).

Overton and Fisher (1984) builds on the work of Vellinga (1982) and uses the relationship between the external force of the water level reaching the dune toe and the sediment characteristics of the model. However, Overton and Fisher (1984) is a time dependent model that considers the swash force for the external

force acting on the dune and takes into account the time that the swash is hitting the dune and exposed to the dune. The model then predicts how long it will take for the dune face to be undermined due scour at the dune toe. Therefore, increasing the success of the prediction of the volume of sand eroded from the dune. Also, the Overton and Fisher (1984) has a small amount of simple inputs compared to the model from Kriebel and Dean (1985), which makes it more practical to use in a wider range of scenarios (Overton & Fisher, 1984).

The Overton et al. (1994) model builds upon the model produced in Overton and Fisher (1984) and considers in-depth the use of swash parameters within the model. In pervious literature the further development of the model was reduced due to the limited amount of knowledge surrounding the swash parameters, such as swash height, swash velocity and swash period. These swash parameters were much harder to be determined and there was less data present, due to swash parameters being nearshore processes compared with offshore parameters such as wave height and wave period. Therefore, for the model to be progressed, there was knowledge needed for how parameters from outside of the surf zone, transformed once in the nearshore zone, due to hydrodynamics, was reached in order to for accurate swash parameters and for predictions to be made. Linear wave theory was used to determine the wave height across shore, as the wave travelled from deep water the edge of the offshore surf zone. Wave height transformation within the surf zone was calculated using the breaking wave dissipation model by Thieke and Sobey (1990), with slight modifications made to the model. Swash height is very complex and therefore was modelled from the linear relationship between the beach face slope in order for a value of swash height to be possible, the swash velocity was calculated using the swash height value and swash period was statistically modelled. The swash force was calculated from these parameters. The volume of sand eroded is the output of the model. The not so good predictions from the model were limited in accuracy by the estimation of wave run up (Overton et al. 1994).

The model from Larson et al. (2004) builds on the models produced in Overton and Fisher (1988) and Overton et al. (1994). The Larson et al. (2004) also uses the 'wave impact theory' which assumes that there is a linear relationship between

the momentum flux of the bores acting on and hitting the dunes and the weight of the sediment being eroded from the dunes. The model Larson et al. (2004) used both field data and laboratory data, including data from Vellinga (1986) to produce an equation to determine the volume of sand eroded from the dune. The sediment properties were taken into account, alongside the swash parameters and the time in which the swash is exposed to the dune, based on the work of Nishi and Kraus, (1996), which is used in the model used for this study. Also, the Larson et al. (2004) model uses analytical solutions to determine the runup height R and an empirical transport coefficient (C_s) which increases the prediction abilities of the model. Due to difficulties determining the optimum runup height for the model, a new simple runup height equation was produced using the simple to determine parameters of wave height and wavelength. The C_s equation was determined using a least-square fitting of solutions using a variety of laboratory and field data sets (Larson et al., 2004).

The Stockdon et al. (2006) paper then proposed a much more complex and improved equation to calculate runup, compared with the simple runup equation from Larson et al. (2004). This improved runup equation using the parameters of deep-water wave height, deep water wavelength and the intertidal beach slope, also attempts to improve the prediction ability of dune erosion. The advantage of this runup equation compared with previous equations used in models that the equation can be used for a variety of beach conditions and with varying beach profile states (Stockdon et al., 2006).

Wave impact models have since increased in complexity by considering the mass failure of sand dunes and taking into account the strength of dunes and how notch evolution and mass failure occurs at the dune scarp. Erikson et al. (2007) produces a model which uses the hydrodynamic forces on the dune and geotechnical parameters of the strength of the dune to determine how the dune front collapses and therefore the rate of sand eroded from the dune. Due to Erikson et al. (2007), alongside Palmsten and Holman (2011), taking into account the instability of the dunes, should therefore increase the prediction of dune erosion.

Roelvink et al. (2009), produces the XBeach model which builds on the previous work of Vellinga (1982), Overton and Fisher (1984) and Overton et al. (1994) using a physics based model of external force of swash and sediment characteristics of the dune. However, the XBeach model is more complex than previous models and takes into account the wave-group forcing of swash (surf-beat), sediment transport, alongshore variation in dune height, the rip channels present, and the four different impact storm scales (Ausbury & Sallenger, 2000). The disadvantages to models such as XBeach was that the further complexity results in more input data needed for the model to make predictions. Therefore, Models such as XBeach are only appropriate to well-known sites, where boundary conditions can be established, and a high level of detail is necessary to answer questions such accurate volumes for single storm events, and changes during extreme storm conditions (Roelvink et al., 2009).

6.4 Methods

The model used to predict the changes in the position of dune toe for this study was based from the model outlined in Splinter and Palmsten (2012). The dune toe model within Splinter and Palmsten (2012) was a combination of simpler models from Larson et al. (2004) and Palmsten and Holman (2012) which were combined and modified in order to improve the prediction of the change in the position of dune toe. The models of Larson et al. (2004) and Palmsten and Holman (2012) are based from the same principles and extends the work of Overton and Fisher (1988) and Overton et al. (1994).

The model determined the change in the position of the dune toe, by using 'wave impact theory' to determine the force exerted onto the sand dunes from the waves, which caused a movement of sediment from the sand dunes and transported elsewhere onto the beach or out to sea. The measurement of the impact of the waves, and therefore, the erosion or the volume of sand lost from the sand dune toe area was calculated and used to determine the change in the position of the dune toe (Figure 6.1).

Palmsten and Holman (2012) identified that the only time that loss of sand from the sand dune toe occurred was when the elevation of the water level was above the elevation of the dune toe position. The water elevation is made up of a number of components including, the tide, wave runup and storm surge elements, which all contribute to the overall water elevation.

When the elevation of the water level was above the elevation of the dune toe, a collision occurred where the wave impacted the sand at the position of the dune toe and above, in which loss of sand occurred. The probability of a collision occurring over a given time period is shown in the equation from Palmsten and Holman (2012), where the water elevation is greater than the dune toe elevation, in relation to the setup of the water level from swash and the standard deviation of swash about the mean water level, as shown:

$$N_c = \left[\sum p \left(Z_R + Z_{tide} + Z_{surge} > Z_b, \langle \eta \rangle, \sigma_s \right) \right] \frac{t}{T} \qquad (1)$$

Where z_R (m) is the parameterized runup, z_{tide} (m) is the measured or modeled tide, z_{surge} (m) is the surge elevation. Z_b (m) is the elevation of the dune toe, $\langle \eta \rangle$ represents the contribution of the setup or the mean water level to swash and σ_s represents standard deviation of swash about the mean water level. N_c estimates the number of collisions between the waves and the dune toe, based on an assumed Gaussian distribution of runup.

Once the time of collisions was established, the volume of sand that was lost during the time of collisions was determined. The model outlined in Splinter et al. (2012), which was based from models within Larson et al. (2004) and Palmsten and Holman (2012), calculated the volume of eroded sand per unit width alongshore, ΔV (m^3/m) of the dune toe as the dune retreats, as shown below in equation 2:

$$\Delta V = 4C_s (R - z_b)^2 \frac{t}{T} \qquad (2)$$

Where C_s is a calibration coefficient that depends on the ratio between the deep water root mean square wave height $H_{o,rms}$ (m) and the median grain diameter d_{50} (mm), which parameterizes the physics of the interaction between the

hydrodynamics that occur and the weight of the sediment present within the sand dunes. The parameterized runup is represented by R (m), z_b (m) is the elevation of the dune toe, t (s) is the duration of the exposure and T (s) is the wave period. The probability of exposure time N_c given in equation one replaced t/T to give an accurate determination of time in which collisions of waves and the dune toe occurred. In Larson et al. (2004), C_s is defined as:

$$C_s = \frac{1}{2} \frac{C_E}{C_u^2} \frac{\rho}{\rho_s} \frac{1}{1-p} \tag{3}$$

Where C_E is an empirical coefficient which describes the relationship between estimated swash force and the weight of eroded sand. C_u is an empirical coefficient describes the relationship between the bore speed and the bore height, ρ (kg/m³) is the density of water, ρ_s (kg/m³) is the density of the sediment, and p is the sediment porosity.

There are two possible runup, R, values that could be used within the model, R1 (m) from Larson et al. (2004), and R2 (m) from Palmsten and Holman (2012). In Larson et al. (2004) the parameterized runup used a simple equation, R1, shown as:

$$R1 = 0.158\sqrt{H_{o,rms}L_o} \tag{4}$$

A series of large wave flume experiments were used to determine the runup, where the best fit comparison of the measured runup from the flume experiments where compared with the deep water wave height $H_{o,rms}$ (m), and the wavelength L_o (m). Palmsten and Holman (2012) used a more complex formula to determine the runup, where R2 was defined as:

$$R2 = 1.1\left\{0.35\tan\beta(H_oL_o)^{1/2} + \frac{[H_oL_o(0.563\tan\beta^2+0.004)]^{1/2}}{2}\frac{n}{2}\right\} \tag{5}$$

Where H_o (m) is the deep-water significant wave height and n = [1,2] is number of standard deviations about the mean water level (16% and 2% exceedence level).

The first term inside the bracket represents the contribution of the setup or the mean water level, $\langle \eta \rangle$, to swash, and the second term represents the standard deviation of swash, σ_s, about the mean water level.
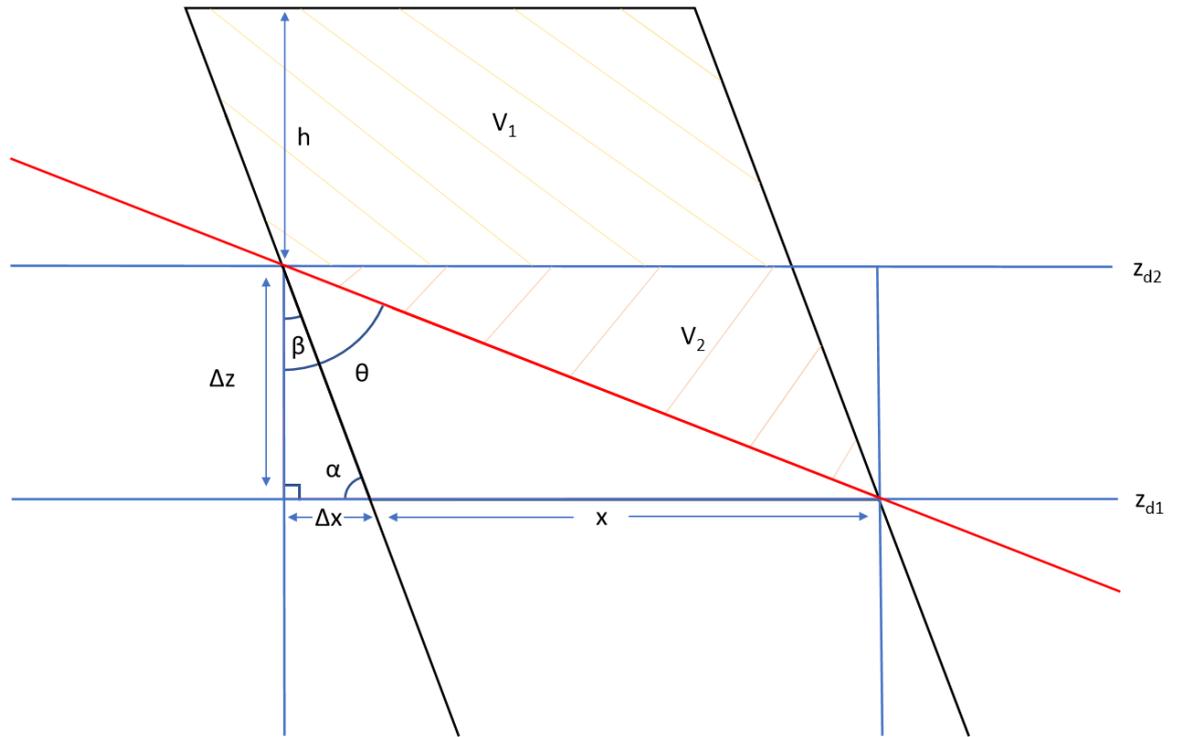
Figure 6.1. A diagram showing how to the new dune toe position was determined. The variables used are shown in equations 6 to 17.

A series of equations were used to determine the new position of the dune toe, from the calculated volume of eroded sand per unit width alongshore, ΔV (m³/m), determined in equation 2. The volume of eroded sand per unit width alongshore ΔV (m³/m) can be divided into two components of V_1 (equation 6) and V_2 (equation 7) and can be expressed as shown below:

$$V_1 = hx \tag{6}$$

$$V_2 = \frac{\Delta z x}{2} \tag{7}$$

$$V = V_1 + V_2 = x\left(\frac{\Delta z}{2} + h\right) \tag{8}$$

Where h (m) is the change in elevation between the maximum height of dune toe and elevation of the new dune toe position and Δz (m) is the change in elevation between initial dune toe position and the new dune toe position.

Two right angled triangles were determined, using the angles of the beach slope (tanβ) and the dune slope (tanθ), which was considered to be the slope of the profile between the maximum dune height and the initial dune toe. The angles can be expressed as shown in equations below:

$$tan\theta = \frac{\Delta x + x}{\Delta z} \tag{9}$$

$$tan\beta = \frac{\Delta x}{\Delta z} \tag{10}$$

Equations (9) and (10) were then used to determine the components need to calculate x(t), which was then substituted into equation (8), as shown below:

$$x(t) + \Delta x = \Delta z tan\theta \tag{11}$$

$$x(t) + (\Delta z tan\beta) = \Delta z tan\theta \tag{12}$$

$$x(t) = \Delta z (tan\theta - tan\beta) \tag{13}$$

The components of x(t) were then substituted into the equation 7, as shown below:

$$V = \Delta z (tan\theta - tan\beta)\left(\frac{\Delta z}{2} + h\right) \tag{14}$$

Which was then rearranged to:

$$0 = \left(\frac{tan\theta - tan\beta}{2}\right)(\Delta z^2 + 2\Delta z h) - V \tag{15}$$

The change in elevation between the initial dune toe and the new dune toe position, Δz, was calculated using the quadratic formula, which was then substituted into equation 12, as shown below:

$$0 = \Delta z^2 + 2\Delta z h - \alpha V$$

$$\Delta z = -2h \pm \sqrt{(4h^2 + 4V\alpha)}$$

$$\Delta z = -2h \pm 2\sqrt{(h^2 + V\alpha)}$$

$$\Delta z = -2h \pm 2\sqrt{\left(h^2 + \frac{2V}{tan\theta - tan\beta}\right)} \qquad (16)$$

In both Larson et al. (2004) and Palmsten and Holman (2012), the new position of the dune toe was determined in Equation 17, where it was assumed that the dune retreated along the same trajectory of $tan\beta_t$, as shown in Equation 17:

$$z_b(t) = \tan\beta_t(t)x(t) + z_b(0) \qquad (17)$$

Where x is the cross-shore axis.

For the within the model the beach slope and dune slopes were assumed to stay constant throughout the time of which the model was run. A range of C_e and C_u values were tested, and appropriate values were used for calibration with guidance from existing shoreline data for Tairua Beach.

6.4.1 Dune toe model production and implementation

The model was produced and run in Matlab software. The data used for the model was sourced from shoreline data from the ocean collective. This data included significant wave height, tide, storm surge and shoreline datasets (Figure 6.3 & 6.4). This data was obtained from the Shoreshop dataset (Available at https://coastalhub.science/data). The beach profile data used in the model was from the historic beach profile dataset from Waikato Regional Council and the initial beach profile used was of CCS36 at Tairua Beach 22nd February 1998 (Figure 6.5). A flow chart of how the model was run is shown in (Figure 6.2).

Dune Toe Model Flow Chart

Load wave and tide data

Load initial beach profile and dune toe position

Go through one time increment

Calculate the wave and tide associated variables

Calculate the runup

Calculate the probability that the water level is above the dune toe position, if dune is wet

If dune is wet, water level> dune toe

If dune is dry, water level < dune toe

Calculate the calibration coefficient

Calculate the volume of the eroded sand

Calculate the horizontal change in the position of the dune toe

Calculate the new position of the dune toe

Save volume of eroded sand and the new dune toe position

Replace the initial dune toe position with the new dune toe position

Save the initial dune toe as the dune toe position and save the eroded sand volume as 0 m³/m

Legend
Data Inputs
Time increment
Data Outputs

Figure 6.2. A schematic showing how the model is run for every time increment, the arrows shows the order of the equations calculated for the model. The light blue shaded boxes show the data inputs, the orange shaded box shows the time increment for each model run and the dark blue boxes show the data outputs for each time increment of the model run.

The input data of deep water significant wave height H_o (m), wave period T (s), measured tide z_{tide} (m), and time t (s) (in relation to the significant wave height, should be every 3 hours) was loaded into the model. An initial beach profile was also loaded into the model, along with the dune toe position z_b (m) of the initial beach profile. The following process was then completed for every time increment, that was set as the time for which the model ran for. The dynamic variables of root mean square of deep water wave height $H_{o,rms}$ (m), and wave length L_o (m), were calculated from deep water significant wave height H_o (m), and the wave period T (s). The two different runup values of R1 (m) and R2 (m), were calculated using equations 4 and 5. One of the runup values was added to equation to determine whether the water level reached the dune toe position for the time increment. If the water level did not reach the dune toe elevation, the initial or current dune toe position is saved and the sand volume that has been eroded was saved as 0 m^3/m. The next time increment is then run through the model. If the water level was calculated to be above elevation of the dune toe, the amount of erosion or loss of sand was calculated along with the new position of the dune toe. The calibration coefficient C_s was calculated using the static variables of density of water ρ (kg/m^3), density of sediment ρ_s (kg/m^3) and sediment porosity, and the dynamic variables of C_E and C_U. The volume of eroded sand ΔV (m^3/m) was then calculated using equation 2, using the C_s value, the runup R1 or R2 (m) value, initial or current dune toe position z_b (m), time of exposure t (s) and wave period T (s). The change in the horizontal position of the dune toe x(t) was then calculated, using equation 6 to 16. Lastly, the new position of the dune toe was determined, equation 17. The volume of eroded sand ΔV (m^3/m) and the new position of the dune toe was saved. The new position of the dune toe replaced the initial dune toe position in the model and the next time increment for the model was run. A time series graph of the volume of eroded sand and a time series graph of the horizontal position and height of the dune toe were plotted. The model was then run with a lower elevation of dune toe in order to test the model worked correctly. A quantitative analysis of the imagery during the same time period was also used in order to validate or invalidate the models results of change in horizontal position of the dune toe.
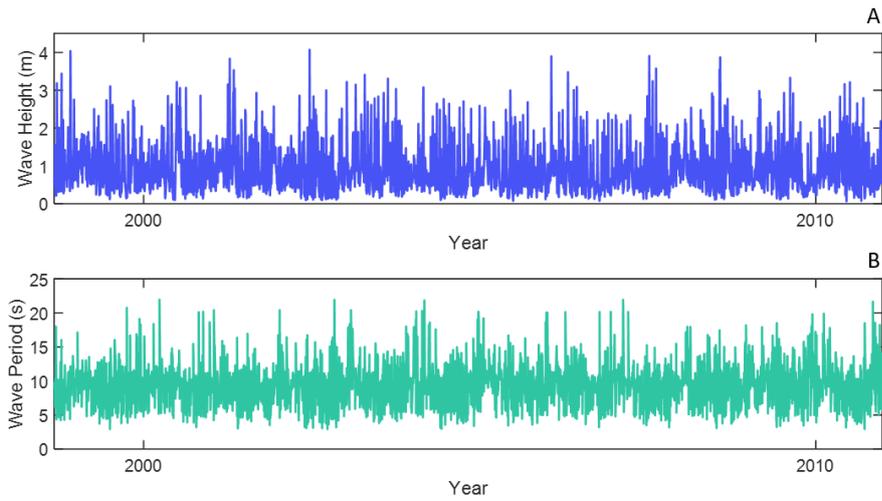
Figure 6.3. Significant wave height (m) (A) and wave period (s) (B) for Tairua beach between 1998 and 2011.
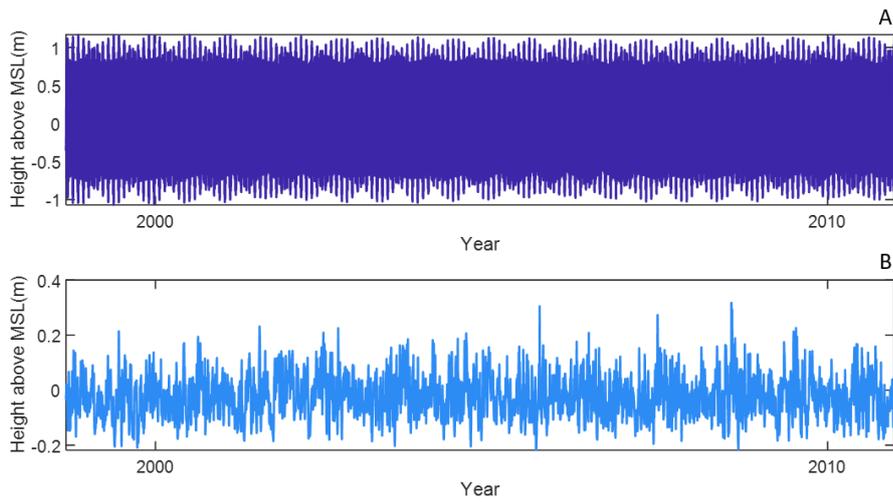
Figure 6.4. Tide height (m) (A) and storm surge height (m) (B) for Tairua Beach between 1998 and 2011.
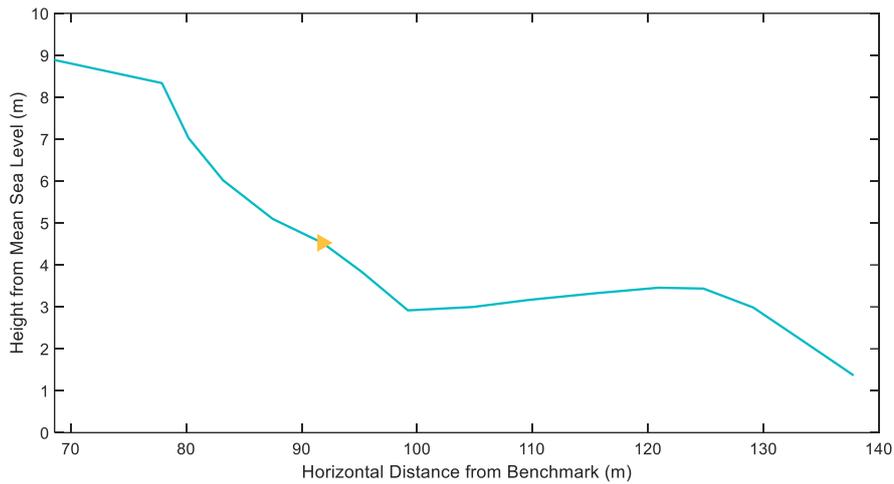
Figure 6.5. Initial Beach profile from the beach profile location of CCS36, Tairua Beach, taken 22nd February 1998.

6.5 Results

6.1.1 Model Prediction of Dune Toe

Figure 6.6 and 6.9 shows the prediction of the horizontal distance that the dune toe moved from the model, where the y-axis shows the horizontal distance of the dune toe and the x-axis shows the time period. Figure 6.7 and 6.10 shows the prediction of the change in height of the dune toe moved from the model, where the y-axis shows change in height of the dune toe and the x-axis shows the time period. Figure 6.8 and 6.11 shows the prediction of change in volume of the sand dune due to change in position of the dune toe, where the y-axis shows the change in volume of the sand dune and the x-axis shows the time period.

When the model was run for the dune toe position of the beach profile (Figure 6.5), it was found that the horizontal position and the height of the dune toe (Figure 6.6 and 6.7) did not move throughout the time period of between 1998 and 2011. There was also not change in the volume of the sand dune above the dune toe position (Figure 6.8).

160
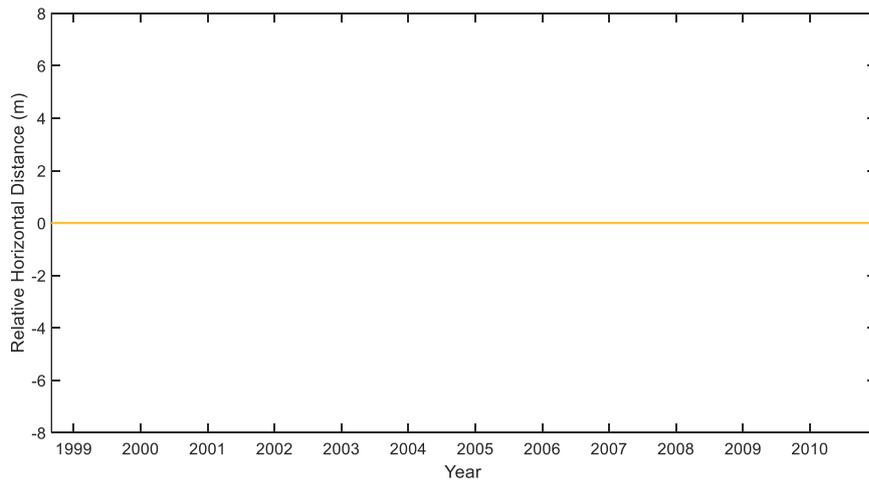
Figure 6.6. The predicted change in the horizontal position of the dune toe from the model between 1998 and 2011.
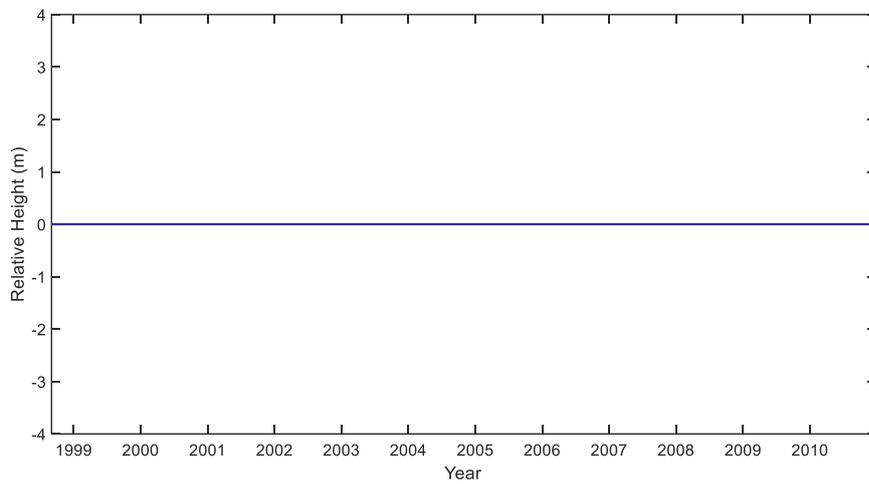
Figure 6.7. The predicted change in the relative height of the dune toe from the model between 1998 and 2011.
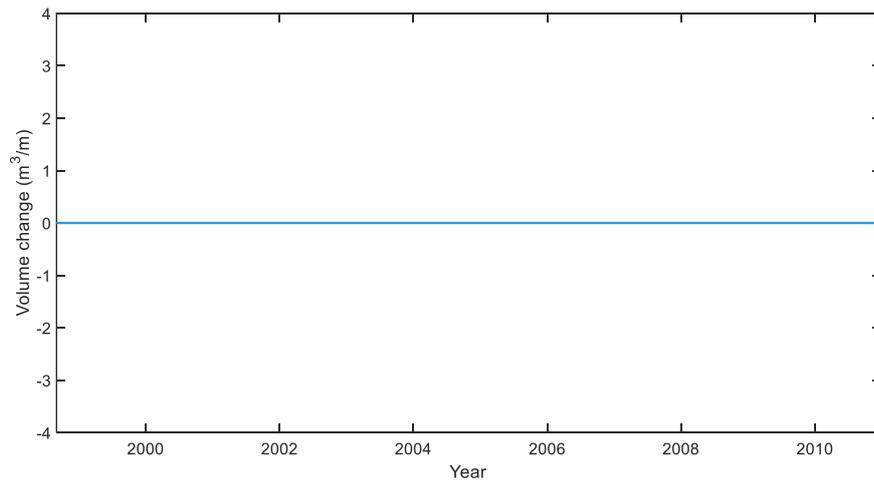
Figure 6.8. The predicted change in the volume of the dune toe from the model between 1998 and 2011.

When the model was run at a lower elevation (1.849 m above MSL) using the same beach profile the model did indicate a change in the elevation (Figure 6.9), horizontal position (Figure 6.10) of the 'dune toe' and there was a volume change of the sand dune (Figure 6.11). This validated that the model worked correctly.
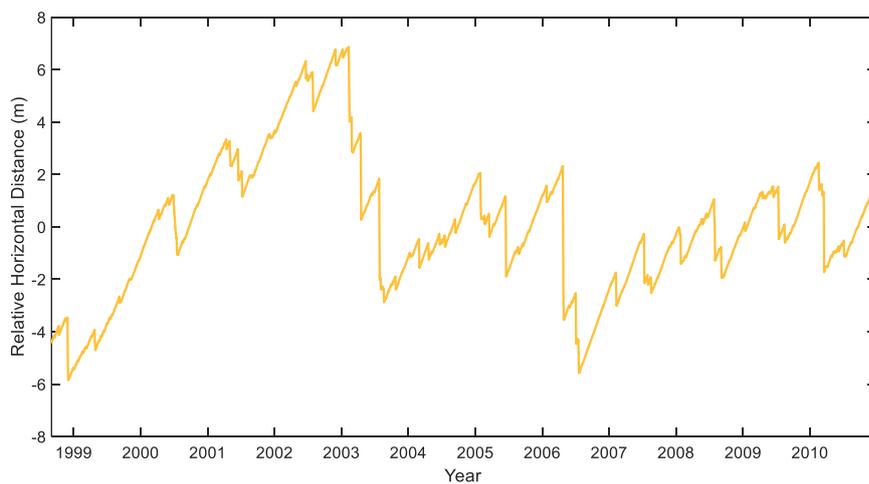
Figure 6.9. The predicted change in the horizontal position of the dune toe if the elevation was at 1.849 m, from the model between 1998 and 2011.
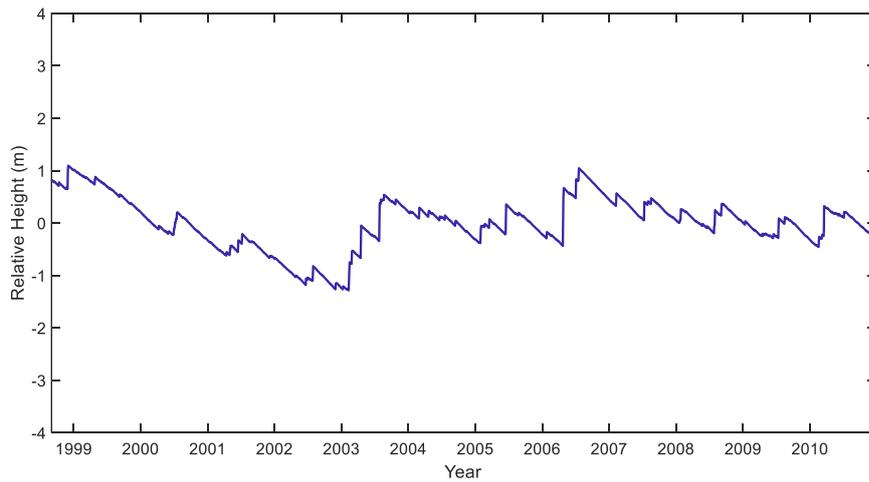
Figure 6.10. The predicted change in the horizontal position of the dune toe if the elevation was at 1.849 m, from the model between 1998 and 2011.
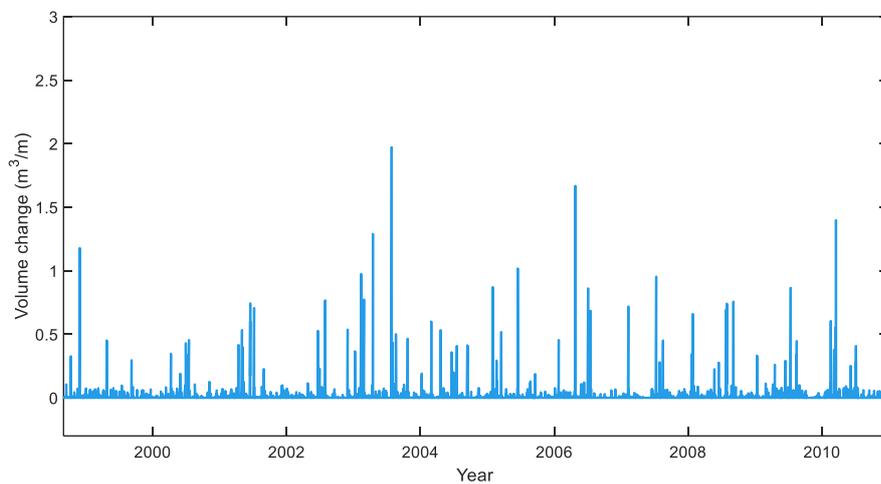
Figure 6.11. The predicted change in the horizontal position of the dune toe if the elevation was at 1.849 m, from the model between 1998 and 2011.

6.1.2 Quantitative Analysis of Water Reaching the Dune Toe

Figure 6.12 shows examples of when the water elevation reached the dune toe. Tables 6.1, 6.2 6.3 and show the date and duration in which the water reached the vegetation line and dune toe. Water reached the dune toe on a number of occasions throughout the time period of 1998 to 2011 (Table 6.1, 6.2, 6.3 and 6.4). The number of occasions in which water reached the dune toe varied throughout each year, where for some of the years within the time period, water did not reach the dune toe at all (2007 and 2010), whilst during other years (2000, 2001 and 2003), water reached the dune toe numerous times. The duration that water

163

reached the dune toe varied generally from less than one hour to 4 hours, with exception of a 9-hour duration on 29th November 1998. Water reached the dune toe at times during both summer and winter (Table 6.1, 6.2 6.3 and 6.4).

Figure 6.12. Examples of when water reached the vegetation line/dune toe at Tairua Beach. The imagery was taken 29th November 1998 (A), 16th April 2003 (B), 16th April 2003 (C) and 20th August 2003 (D).

Table 6.1. The date and duration (hours) in which water elevation reached the dune toe position between 1998 and 2000.

Date	Duration (hours)
28th November 1998	1
29th November 1998	9
29th November 1998	<1
30th November 1998	1
21st February 1999	<1
4th July 2000	<1
16th July 2000	2
16th July 2000	2
18th July 2000	1
19th July 2000	1
18th August 2000	2
19th August 2000	2
27th August 2000	2
15th December 2000	1

Table 6.2. The date and duration (hours) in which water elevation reached the dune toe position between 1998 and 2000.

Date	Duration(hours)
13th April 2001	2
2nd May 2001	1
5th May 2001	2
7th July 2001	1
8th July 2001	<1
5th September 2001	1

Table 6.3. The date and duration (hours) in which water elevation reached the dune toe position between 1998 and 2000.

Date	Duration (hours)
10th January 2003	1
27th February 2003	4
15th April 2003	<1
16th April 2003	3
16th April 2003	4
17th April 2003	1
20th May 2003	<1
16th June 2003	<1
27th July 2003	<1
30th July 2003	<1
3rd August 2003	3
4th August 2003	2
5th August 2003	1
6th August 2003	1
7th August 2003	3
13th August 2003	<1
15th August 2003	1
20th August 2003	3
30th August 2003	<1
1st September 2003	1
2nd August 2003	<1

Table 6.4. The date and duration (hours) in which water elevation reached the dune toe position between 1998 and 2000.

Date	Duration (hours)
20th April 2004	1
7th May 2004	<1
29th January 2005	2
29th January 2005	<1
30th January 2005	3
15th June 2005	2
24th January 2005	2
24 January 2006	1
26th January 2008	<1
30th July 2008	1
11th January 2009	<1
12th January 2009	<1
24th January 2011	<1
4th July 2011	<1
5th July 2011	1
6th July 2011	2

6.2 Discussion

The model predicted that the horizontal position and the height of the dune toe did not move through the time period between 1998 and 2011. The model was then checked using a lower elevation of the beach profile, in order to check whether the model worked correctly. There was a change of the horizontal position and height of the 'dune toe' when a lower initial dune toe position was used, therefore confirming that the model ran correctly. The analysis of imagery at Tairua Beach showed that water did reach the vegetation line and dune toe, on multiple occasions during the time period that the model was run. Therefore, the model was unsuccessful in the prediction of when water reached the dune toe and the position of the dune toe throughout the time period of between 1998 and

2011. There are likely numerous reasons why the model did not correctly predict the change in the dune toe position. There are a number of assumptions that are included within the model, such as the wave runup, time of exposure of the dune toe and the angle of the dune toe erosion. The model did not predict when the water reached the dune toe position correctly, therefore it is likely that there was error in the predicted water elevation of the model. The model did not predict any change in the horizontal position of the dune toe, therefore it is not known whether the model would have predicted the change in the horizontal position of the dune toe correctly if the water elevation was predicted correctly during the model run (Splinter & Palmsten, 2012). The water elevation was a combination of three variables which included storm surges, tide and wave runup. The wave run up was calculated using an equation, and therefore likely to be the source of error for the prediction of water elevation for the model (Splinter & Palmsten, 2012).

The imagery analysis of the water reaching the dune toe at Tairua Beach between 1998 and 2011 confirmed that the model was not successful. Water reached the vegetation line and dune toe multiple times during the time period. Only imagery and duration in which water reached the dune toe for daylight hours were able to be recorded, therefore water has likely reached the dune toe more often than what was recorded. The quality of the imagery varied throughout the dataset and increased water elevations often coincide with storm events and rain. Therefore, there was often poor-quality imagery during storm events when water could reach the dune toe and some occasions of water reaching the dune toe may have been missed. The water reached the dune toe on a number of occasions during summer which was a surprising result, as it was expected that the storm events, where water reached the dune toe were more likely to occur during winter (Castelle et al., 2015).

6.3 **Conclusions/Summary**

In Conclusion, the model did not predict the change in the horizontal position of the dune toe successfully. The model predicted that the water did not reach the dune toe position throughout the time period of 1998 and 2011 and therefore the dune to position did not move. However, an analysis of imagery at Tairua Beach did confirm that water did reach the vegetation line and dune toe throughout the time period between 1998 and 2011. The model did not predict any change in the horizontal position of the dune toe, therefore it is not known whether the model would have predicted the change in the horizontal position of the dune toe correctly if the water elevation and exposure of the dune toe was predicted correctly.

Chapter Seven

Conclusions and Recommendations

7.1 Introduction

This research aimed to determine the change in the horizontal position of the vegetation line and dune using numerous methods for eastern Coromandel beaches and Ngarunui Beach Raglan. There were a number of datasets used to obtain this information, the datatsets included the historic beach profile dataset consisting of 40 years of beach profile cross-sections, field surveys at five Cormandel beaches and Ngarunui Beach, and Camera Imagery, alongshore shoreline data for Tairua Beach. The conclusions in this chapter relate to expected outcomes identified within each chapter and address the research aims of the thesis identified and outlined in Section 1.2.

7.1.1 Traditional Methods of Using Beach Profiles to Measure Dune Toe and Beach Morphology

The aim of Chapter 3 was to determine the short-term changes in beach morphology and the dune toe using beach profiles, which was the traditional method for beach monitoring and is still commonly used. The analysis showed that there was high variability across the lower beach face and intertidal area and low variability across the upper beach face and in the sand dunes. This was likely due to the influence of water, where the lower beach and intertidal area was inundated with every tidal cycle, however the upper beach face and sand dunes, including the dune toe was only inundated when large tides or storm events occurred. On occasion such as at Whangapoua Beach and Matarangi Beach morphological change was similar along the length of the beach across all of the profile sites between one field survey to the next, however generally there was alongshore variation in morphological change observed across the length of each beach. The alongshore variation was especially high for Buffalo Beach which had sections of the sand dunes and dune toe that are highly modified with sandbag

wall and sea walls present. This highlighted the effect to beach morphology natural shape of the beach, caused by human modification. There was also some evidence of seasonal patterns present at some of the Coromandel beaches where more erosion occurred during the winter months and accretion during the summer months. This confirmed that water inundation of the dune toe caused by storm events, which occur more often during winter were the likely cause of erosion at the dune toe. The historic beach profile dataset highlighted that the dune toe at certain beach profiles have gone through sudden large landward changes of erosion at the dune toe, followed by slow seaward movement and accretion of the dune toe. Using beach profiles for beach monitoring highlighted the different aspects of the beach that beach profiles can measure including berms and movement of sand across different areas of the beach. The historic beach profile dataset also showed how the dune toe can be identified by the easily distinguishable inflection point of where the steeply sloped sand dunes meet the low angled beach face. Using beach profiles also highlighted the great effort and expense needed to measure beach morphology with the amount of time the surveying of profiles has taken to complete and restrictions on monitoring times during low tide periods.

7.1.2 Frequency and Magnitude of Changes to the Alongshore Dune Toe and Vegetation Line

The aim of Chapter 4 was to determine the frequency and magnitude of change of the horizontal position and vertical position of the dune toe and vegetation line. The horizontal and vertical position of the vegetation line and dune toe was determined from the historic beach profile dataset, along with the distribution of the dune toe was compared with the vegetation line. The alongshore dune toe throughout a one-year survey period of December 2018 to December 2019 was also analysed. The results showed that sudden landward movement of the dune toe did occur at some profile sites of Coromandel beaches, followed by long period of low seaward movement and accretion of the dune toe, which was likely due to storm events followed by fair weather conditions. However, there was much more

variation of the dune toe and vegetation line found at other profile sites and some unexpected seaward movement of the dune toe did occur. These seaward movements could only be explained by transport from other areas of the beach or rapid vegetation growth. The distribution of the horizontal position of the dune toe compared with the vegetation line showed that the vegetation line and dune toe were generally not at the same location as the vegetation line and that the distribution of the horizontal position of the dune toe was less varied than the horizontal position of the vegetation line, which has strong implications for using vegetation as a measure of dune movement. The alongshore dune toe surveyed through a one year-period showed that the dune toe does not move very much throughout a one-year period, therefore meaning that beach monitoring could be undertaken less frequently, reducing cost and effort needed for beach monitoring. There was also differences alongshore in the magnitude of change of the dune toe and the height of the dune toe, along the beach. The change in height of the dune toe was of an obviously greater magnitude at Buffalo Beach in areas of the beach that have been modified, where sections of the beach where the two seawalls and the sandbag wall were present. This highlighted how modification of the sand dunes and dune toe cause the horizontal position of the dune toe to be more stable throughout time by the change in height increased, where the height decreased more dramatically during storm events and more erosion occurred at these locations. All of these results can help to determine the frequency and magnitude of beach monitoring needed when using the vegetation line and dune toe as a measurement for beach monitoring.

7.1.3 Video Analysis of the Horizontal Position of the Vegetation Line

The aim of Chapter 5 was to determine whether video analysis could be used as new method in measuring the vegetation line, where CamEra Imagery taken from Tairua Beach once a month was used for the analysis from 2002 to 2019. The different light characteristics vegetation and dune toe were used to determine different classes of vegetation across the beach face and ultimately where the horizontal position of the vegetation line of the frontal sand dune occurred. The images were then rectified and changes in the horizontal position of the

vegetation line throughout time at Tairua Beach were determined. The results showed that the use of video analysis for measuring the vegetation line was successful. However, further improvements could be made to the method in order to increase the accuracy of the technique used and the time taken to determine the vegetation line for each image and therefore increase the amount of data that could analysed. Ideally each week throughout the dataset would be measured in order to observe all of the sudden in the horizontal position of the vegetation line. The results from the horizonal position of the vegetation line found throughout time highlighted the alongshore variation of the horizontal position of the vegetation line and the long term patterns of erosion and accretion that occurred along various sections of the beaches at Tairua beach between 2002 and 2019. The average horizontal position of the vegetation line was found to slightly correlated with average shoreline position of Tairua beach.

7.1.4 Using a Simple Model to Predict Observed Dune Toe Changes

The aim of Chapter 6 was to produce a simple model that predicted the erosion of the dune toe at Tairua Beach, an analysis of the CamEra imagery of water reaching the dune toe throughout the time period of 1998 and 2011 was undertaken to validate the dune erosion model. The model predicted that the water did not reach the dune toe position throughout the time period of 1998 and 2011, and therefore the dune toe did not move. However, the analysis of the imagery taken at Tairua beach did confirm that water did reach the vegetation line and dune toe throughout the time period. The model did not predict any change in the horizontal position of the dune toe, therefore it is not known whether the model would have predicted the change in horizontal position of the dune correctly if the water elevation and exposure of the dune toe was predicted correctly. Therefore, if the wave run up was calculated more reasonably for Tairua beach, the dune erosion model may have been more successful.

7.2 **Recommendations for Future Research**

Key findings within this thesis, have shown that there are a number of different methods that can be used to measure in the future to measure the vegetation line and dune toe and that these methods and results could be important for future beach monitoring and risk management decision making. However, there could be more research done within this area to increase the knowledge surrounding the changes in the vegetation line and dune toe, and also to increase the efficiency of methods within the future in order to make the methods more suitable to use as a helpful tool for consistent long term beach monitoring. Future research for understanding the what causes changes occur at the dune toe could include further focus on individual events where duration that water inundates the dune toe is recorded in more detail and focus into what happens during specific storm events. Also, what causes the dune toe to erode during one storm event, whilst no erosion occurs during the nest storm event. This could be done through using a combination of RTK-GPS surveying before and after storms along with the use of imagery to observe the duration of inundation of water at the dune toe position. Future research could also focus on testing the most appropriate time scale and spatial distribution of beach monitoring of the dune toe and vegetation line. Due to the alongshore dune toe not moving often throughout the one-year period, monitoring of the dune toe could be done less frequently to potentially once a year or less and along either the whole beach length, small sections of the overall beach length (i.e. 5 x 100 m sections for 1000 to 2000 m long beach), or just at the already established beach profiles sites, combining historic data with new data collected in the future. Due to the subjectivity surrounding identifying the dune toe and vegetation line of frontal sand dunes, a standardised definition of what the dune toe is could be made and used throughout different councils and organisations so that there is little variation in determining the dune toe from one operator to another. Further research could also go into making the video analysis technique more efficient and effective, by increasing the accuracy of the method in correctly finding the vegetation line and also decrease the amount of time need to analyse each individual image. The simple model produced to determine the erosion of dune toe could not reasonably predict the dune toe. However, the dune erosion model could be tested across different profile sites of Tairua Beach or

other Coromandel Beaches to determine whether the model could reasonably predict the change in the erosion of the dune toe under different conditions.

References

Acosta, A., Carranza, M. L., Izzi, C.F. (2005). Combining land cover mapping of coastal dunes with vegetation analysis. *Applied Vegetation Science*, 8, 133-138.

Almar, R., Coco, G., Bryan, K. R., Huntley, D. A., Short, A. D., & Senechal, N. (2008). Video observations of beach cusp morphodynamics. *Marine Geology*, 254, 216-223.

Andrade, F., & Ferreira, M. A. (2006). A simple method of measuring beach profiles. *Journal of Coastal Research*, 22(4), 995-999.

Arrninkhof, S. G. J., Ruessink, B. G., & Roelvink, J. A. (2005). Nearshore subtidal bathymetry from time-exposure video images. *Journal of Geophysical Research*, 110, 1-13.

Asbury, H., & Sallenger, Jr. (2000). Storm impact scale for barrier islands. *Journal of Coastal Research*, 16(3), 890-895.

Aubrey, D. G. (1979). Seasonal patterns of onshore/offshore sediment movement. *Journal of Geophysical Research*, 84(10), 6347-6354.

Balouin, Y., Rey-Valette, H., & Picand, P.-A. (2014). Automatic assessment and analysis of beach attendance using video images at the Lido of Sete beach, France. *Ocean & Coastal Management*, 102, 114-122.

Beuzen, T., Harley, M. D., Splinter, K. D., Turner, I. L. (2019). Controls of variability in berm and dune storm erosion. *Journal of Geophysical Research*, 124(11), 2647-2665.

Bogle, J. A., Bryan, K. R., Black, K. P., Hume, T. M., & Healy, T. R. (2001). Observations of rip formation and evolution. *Journal of Coastal Research*, 34, 117-127.

Bose, S. (1984). Beach and dune erosion during storm surges by P. Vellinga – Discussion. *Coastal Engineering*, 8, 189-192.

Bracs, M. A., Turner, I. I., Splinter, K. D., Short, A. D., & Mortlock, T. R. (2016). Synchronised patterns of erosion and deposition observed at two beaches. *Marine Geology*, 380, 196-204.

Bruun, P. (1984). Beach and dune erosion during storm surges by P. Vellinga – Discussion. *Coastal Engineering*, 8, 171-188.

Castelle, B., Marieu, V., Bujan, S., Splinter, K. D., Robinet, A., Senechal, N., & Ferreira, S. (2015). Impact of the winter 2013-2014 series of severe Western Europe storms on a double-barred sandy coast: Beach and dune erosion and megacusp embayments. *Geomorphology*, 238, 135-148.

Copper, N. J., Leggett, D. J., & Lowe, J. P. (2000). Beach-Profile measurement, theory and analysis: Practical guidance and applied case studies. *Water and Environment*, 14(2), 79-88.

Curr, R.H.F., Koh, A., Edwards, E., Williams, A.T., & Davies, P. (2000). Assessing anthropogenic impact on Mediterranean sand dunes from aerial digital photography, *Journal of Coastal Conservation*, 6, 15-22.

Davis, R. A., Fox, W. T. (1972). Coastal processes and nearshore sand bars. J. Sediment. *Petrol*, 42, 402-412.

Dissanayake, P., Brown, J., & Karunarathna, H. (2015). Impacts of storm chronology on the morphological changes of the Formby beach and dune system, UK. *National Hazards and Earth Systems Sciences*, 15, 1533-1543.

Emery, K. O. (1961). A simple method of measuring beach profiles. *Limnology and Oceanography,* 6 (1), 90-93.

Erikson, L. H., Larson, M., & Hanson, H. (2007). Laboratory investigation of beach scarp and dune recession due to notching and subsequent failure. *Marine Geology*, 245, 1-19.

Fisher, J. S., & Overton, M. F. (1984). Numerical model for dune erosion due to wave uprush. *19th International Conference on Coastal Engineering*.

Gallop, S. L., Bryan, K. R., Coco, G., Stephens, S. A. (2011). Storm-driven changes in rip channel patterns on an embayed beach. *Geomorphology*, 127, 179-188.

Gorman, R. M., Bryan, K. R., & Liang, A. K. (2003). Wave hindcast for the New Zealand region: nearshore validation and coastal wave climate. *New Zealand Journal of Marine and Freshwater Research,* 37, 567-588.

Guimaraes, P. V., Pereira, P. S., Calliari, L. J., & Ellis, J. T. (2016). Behaviour and identification of ephemeral sand dunes at the backshore zone using video images. *Anais da Academia Brasileira de Ciencias*, 88(3), 1357-1369.

Harley, M. D., Turner, I. L., Short, A. D., & Ranasinghe, R. (2011). Assessment and integration of conventional, RTK-GPS and image derived beach survey methods for daily to decadal coastal monitoring. *Coastal Engineering*, 58, 194-205.

Hayes, M. O., & Boothroyd, J. C. (1969). Storms modifying agents in the coastal environment. In: *Hayes M. O. (Ed), Coastal Environments. NE Massachusetts, Department of Geology, University of Massachusetts, Amherst*, 290-315.

Healy, T. (2002). Enhancing coastal function by sensible setback for open duned coasts. *Solutions to Coastal Disasters '02*, 794-807.

Holman, R. A., Lippmann, T. C., O'Neill, P. V., & Hathaway, K. (1991). Video estimation of subaerial beach profiles, *Marine Geology*, 97, 225-231.

Houser, C. (2013). Alongshore variation in the morphology of coastal dunes: Implications for storm response. *Geomorphology*, 199, 48-61.

Huisman, C. E., Bryan, K. R., Coco, G., & Ruessink, B. G. (2011). The use of video imagery to analyse groundwater and shoreline dynamics on a dissipative beach, *Continental Shelf Research*, 1-29.

Kraus, N. C., & McDougal, W.G. (1996). The effects of seawalls on the beach: Part I, An updated Literature Review. *Journal of Coastal Research*, 12(3), 691-701.

Kriebel, D. L., & Dean, R. G. (1985). Numerical simulation of time-dependent beach and dune erosion. *Coastal Engineering*, 9, 221-245.

Larson, M., Erikson, L., & Hanson, H. (2004). An analytical model to predict dune erosion due to wave impact. *Coastal Engineering*, 51, 675-696.

Larson, M., & Kraus, N. C. (1993). Temporal and spatial scale of beach profile change, Duck, North Carolina. *Marine Geology*, 117, 75-94.

Montano, J., Coco, G., Antolinez, J. A.A., Buezen, T., Byran, K., Cagigal, L., Castelle, B., Davidson, M., Goldstein, E., Vega, R. I., Idier, D., Ludka, B., Anari, S. M., Mendez, F., Murray, B., Plant, N., Robinet, A., Rueda, A., Senechal, N., Simmons, J., Splinter, K., Stephens, S., Townend, I., Vitousek, S., & Vos, K. (2019). Shorecasts: A blind-test of shoreline models. *Coastal Sediments*, 627-631.

Masselink, G., & Pattiaratchi, C. B. (2001). Seasonal changes in beach morphology along the sheltered coastline of Perth, Western Australia. *Marine Geology*, 172, 243-263.

Nishi, R., & Kraus, N. C. (1996). Mechanism and calculation of sand dunes erosion by storms. *25th International Conference on Coastal Engineering*. 3034-3047.

Overton, M. F., Fisher, J. S., & Hwang, K. N. (1994). Development of a dune erosion model using SUPERTANK data. *Coastal Engineering*, 2488-2502.

Palmsten, M. L., & Holman, R. A. (2012). Laboratory investigation of dune erosion using stereo video. *Coastal Engineering*, 60, 123-135.

Pianca, C., Holman, R., & Siegle, E. (2015). Shoreline variability from days to decades: results of long-term video imaging, *Journal of Geophysical Research: Oceans*, 120, 2159-2178.

Plant, N. G., Aarninkhof, S. G. J., Turner, I. L., & Kingston, K. S. (2007). The performance of shoreline detection models applied to video imagery. *Journal of Coastal Research*, 23(3), 658-670.

Pye, K., & Blott, S. J. (2008). Decadal-scale variation in dune erosion and accretion rates: An investigation of the significance of changing storm trade frequency and magnitude on the settle coast, UK. *Geomorphology*, 102(3-4), 652-666.

Quartel, S., Kroon, A., Ruesslink, B.G. (2008). Seasonal accretion and erosion patterns of a microtidal sandy beach. *Marine Geology*, 250(1-2), 19-33.

Rijn, L. C. (2009). Prediction of dune erosion due to storms. *Coastal engineering*, 56, 441-547.

Roelvink, D., Reniers, A., van Dongeren, A., van Thiel de Vries, L., McCall, R., & Lescinski, J. (2009). Modelling storm impacts on beaches, dunes and barrier islands. *Coastal Engineering*, 56, 1133-1152.

Ruz, M. H., & Meur-Ferec, C. (2004). Influence of high-water levels on aeolian sand transport: upper beach/dune evolution on a macrotidal coast, Wissant Bay, northern France. *Geomorphology*, 60(1-2), 73-87.

Saye, S. E., van der Wal, D., Pye, K., & Blott. S. J. (2005). Beach-dune morphological relationships and erosion/accretion: An investigation at five sites in England and Wales using LIDAR data. *Geomorphology*, 72, 128-155.

Simarro, G., Bryan, K. R., Guedes, R. M.C., Sancho, A., Gullien, J., & Coco, G. (2015). On the use of variance images for runup and shoreline detection. *Coastal Engineering,* 99, 136-147.

Smith, R. K., & Bryan, K. R. (2007). Monitoring beach face volume with a combination of intermittent profiling and video imagery. *Journal of Coastal Research*, 23(4), 892-898.

Splinter, K.D., Kearney, E.T., Turner, I.T. (2018). Drivers of alongshore variable dune erosion during a storm event: Observations and modelling. *Coastal Engineering*, 131, 31-41.

Splinter, K. D., Palmsten, M. L. (2012). Modeling dune response to an East Coast low. *Marine Geology*, 329-331, 46-57.

Splinter, K. D., Palmsten, M. L., Holman, R. A., & Tomlinson, R.B. (2011). Comparison of measured and modeled run-up and resulting dune erosion during a lab experiment. *The Proceedings of the Coastal Sediments 2011*, 782-795.

Splinter, K. D., Strauss, D. R., & Tomlinson, R. B. (2011). Assessment of post-storm secovery of beaches using imaging techniques: A case study at Gold Coast, Australia, *IEEE transaction on geoscience and remote sensing*, 49(12), 4704-4716.

Stockdon, H., Holman, R. A., Howd, P. A., Asbury, H., & Sallenger, Jr. (2006). Empirical parameterization of setup, swash, and runup. *Coastal Engineering*, 53, 573-588.

Suanez, S., Cariolet, J.M., Cancouet, R., Ardhuin, F., Delacourt, C. (2012). Dune recovery after storm erosion on a high-energy beach: Vougot Beach, Brittany (France). *Geomorphology*, 139-140, 16-33.

Thieke, R. J., & Sobey, R. J. (1990). Cross-shore wave transformation and mean flow circulation. *Coastal Engineering*, 14(5), 387-415.

Thornton, E.B., MacMahan, J., Sallenger Jr., A.H. (2007). Rip currents, mega-cusps, and eroding dunes. *Marine Geology*, 240(1-5),151-167.

Vellinga, P. (1982). Beach and dune erosion during storm surges. *Coastal Engineering*, 6(4), 361-387.

Winant, C. D., Douglas, L. I., & Nordstrom, C. E. (1975). Description of seasonal beach changes using empirical eigenfunctions, *Journal of Geophysical Research,* 80(15), 1979-1986.

Wood, A., Bryan, K. R., Smith, Coco, G., & Pickett, V. (2009). Indicator beaches on the Coromandel Peninsula, New Zealand. *Coasts and Ports 2009: IN a Dynamic Environment*, 224-230.

Wright, L. D., Short, A. D., & Green, M. O. (1985). Short-term changes in the morphodynamic states of beaches and surf zones: An empirical predictive model, *Marine Geology*, 62, 339-364.

Yates, M. L., Guza, R. T., & O'Riley, W. C. (2009). Equilibrium shoreline response: Observations and modelling. *Journal of Geophysical Research*, 114, 1-16.

Appendices

Appendix A: Aerial Photographs of Field Survey Profile Sites

Appendix A showed the aerial photographs of the field survey beaches, where physical features of the beach are shown alongside where the beach profile sites are located.
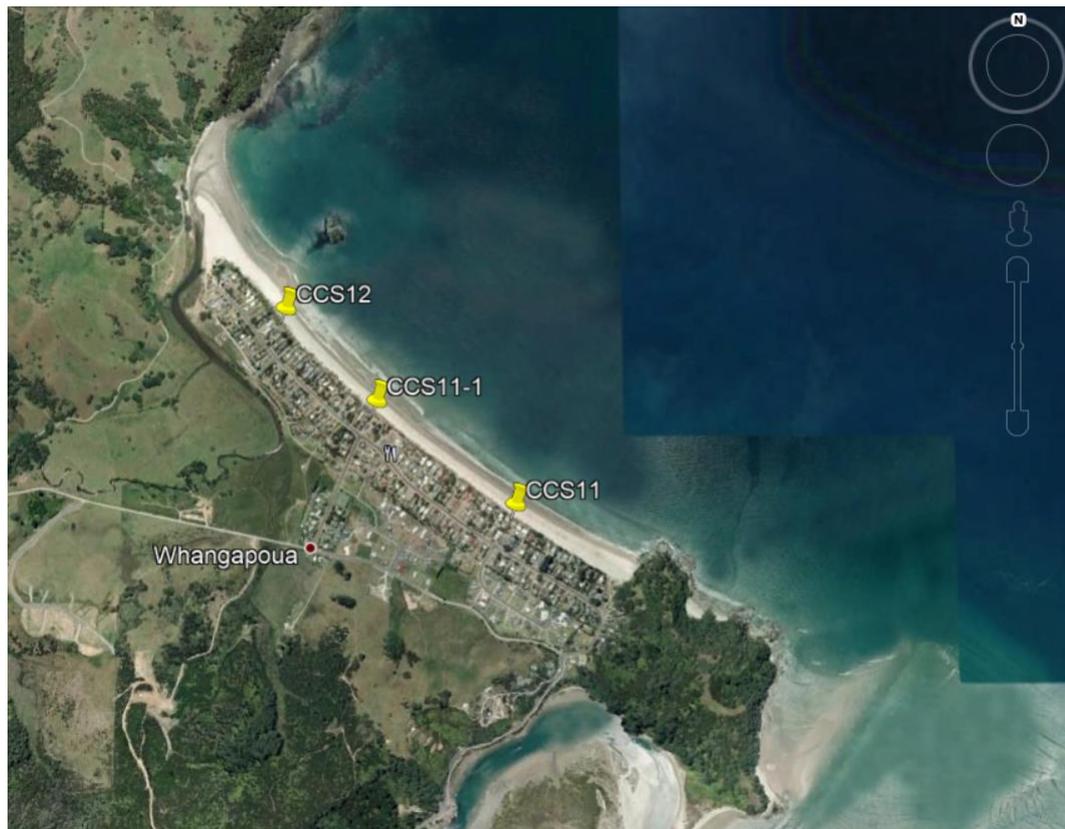
Figure A.1. Beach profile sites, Whangapoua Beach of CCS12, CCS11-1 and CCS11.

Figure A.2. Beach profile sites, Matarangi Beach of CCS13, CCS14, CCS15, CCS16 and CCS17.

Figure A.3. Beach profile sites, North Buffalo Beach of CCS24, CCS25, CCS25-2, CCS25-3 and CCS25/1.

Figure A.4. Beach profile sites, South Buffalo Beach of CCS26, CCS26/1, CCS27, CCS27/10, CCS27/8, CCS27/6, CCS27/2, CCS273, CCS27/4 and CCS27/5.

Figure A.4. Beach profile sites, Hot Water Beach of CCS34, CCS35 and CCS35-1.
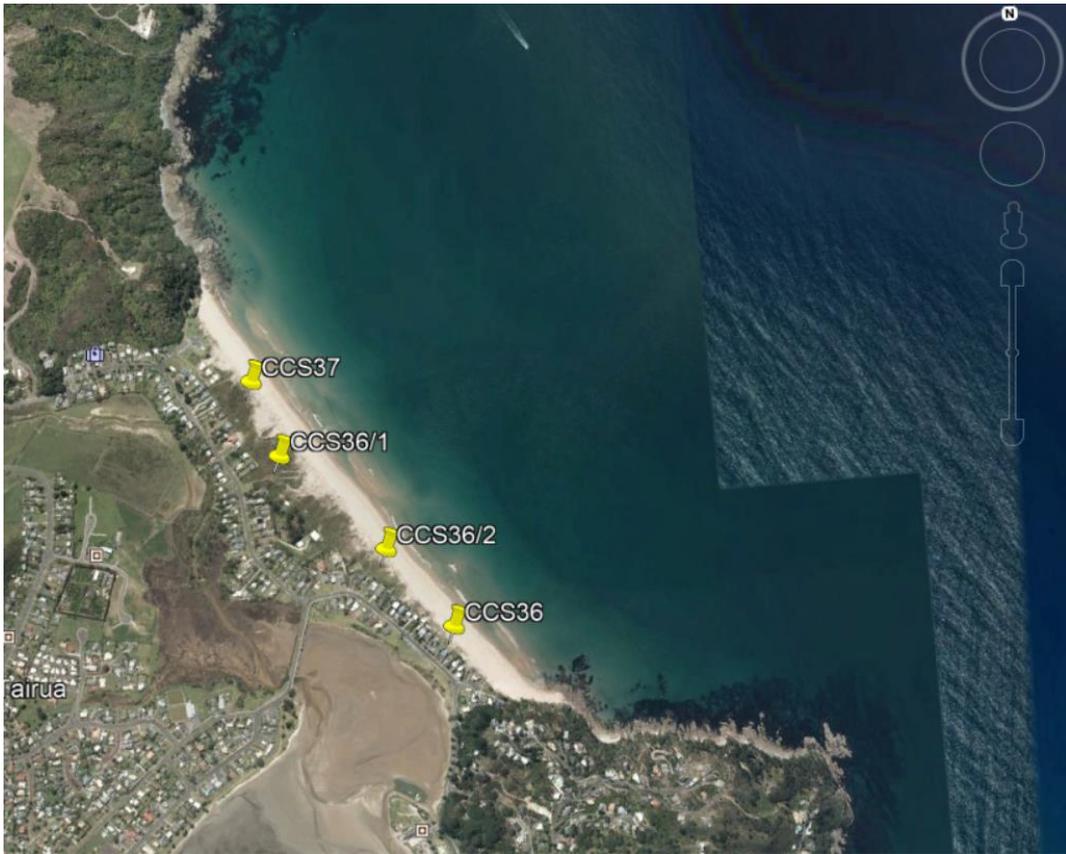
Figure A.5. Beach profile sites, Tairua Beach of CCS37, CCS36/1, CCS36/2 and CCS36.

Figure A.6. Beach profile sites, Ngarunui Beach Raglan of RGN1, RGN2, RGN3, RGN4, RGN5 and RGNKS.

Appendix B: Historic Beach profiles Dataset

Appendix B showed the historic beach profiles for all of the 20 eastern Coromandel Beaches, where the field surveys completed at 5 Coromandel Beaches and Ngarunui beach, Raglan, are marked in red on the figures.

Whangapoua Beach
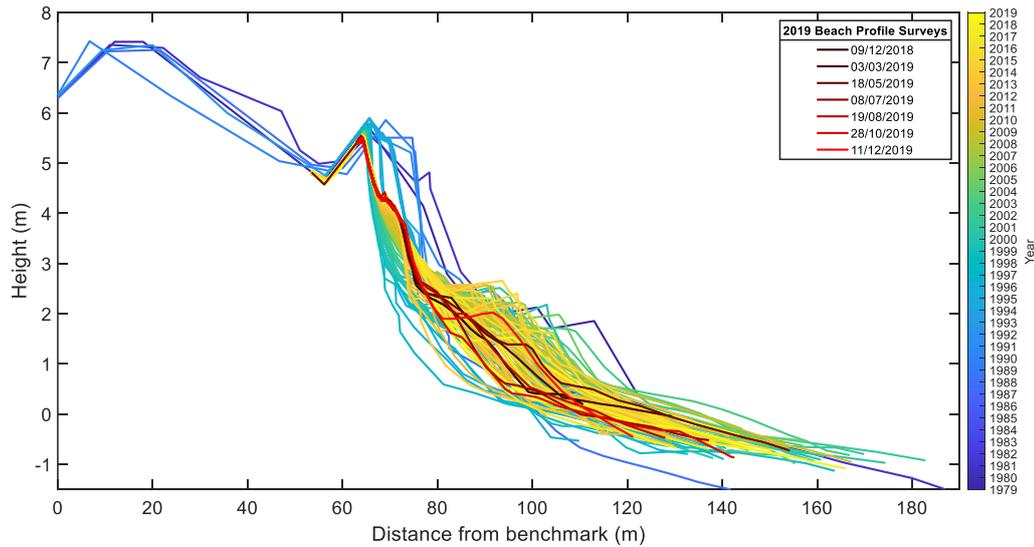
Figure B.1. Beach profile of CCS12, Whangapoua Beach. Field surveys were taken 9ᵗʰ December 2018, 3ʳᵈ March 2019, 18ᵗʰ May 2019, 8ᵗʰ July 2019, 19ᵗʰ August 2019, 28ᵗʰ October 2019 and 11ᵗʰ December 2019.
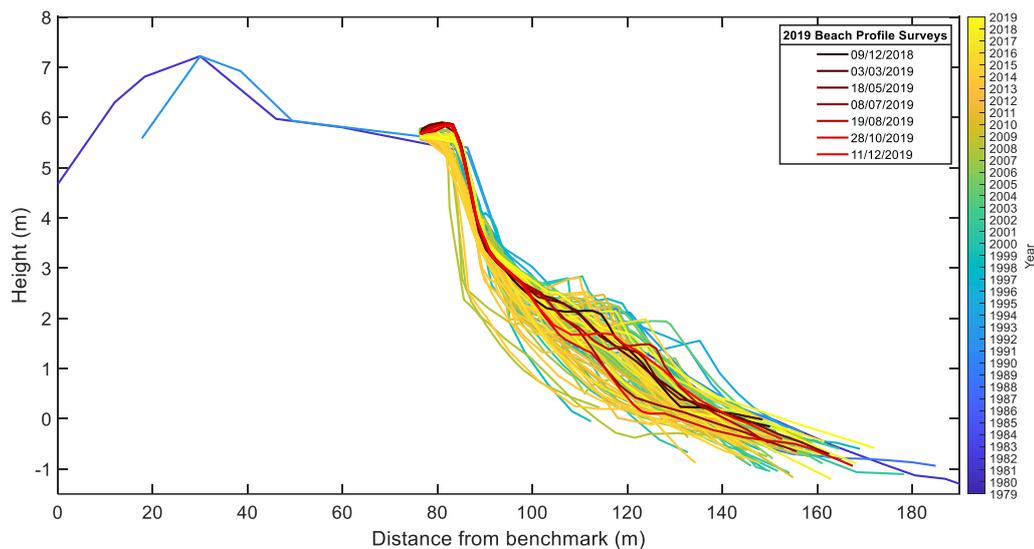
Figure B.2. Beach profile of CCS11-1, Whangapoua Beach. Field surveys were taken 9ᵗʰ December 2018, 3ʳᵈ March 2019, 18ᵗʰ May 2019, 8ᵗʰ July 2019, 19ᵗʰ August 2019, 28ᵗʰ October 2019 and 11ᵗʰ December 2019.
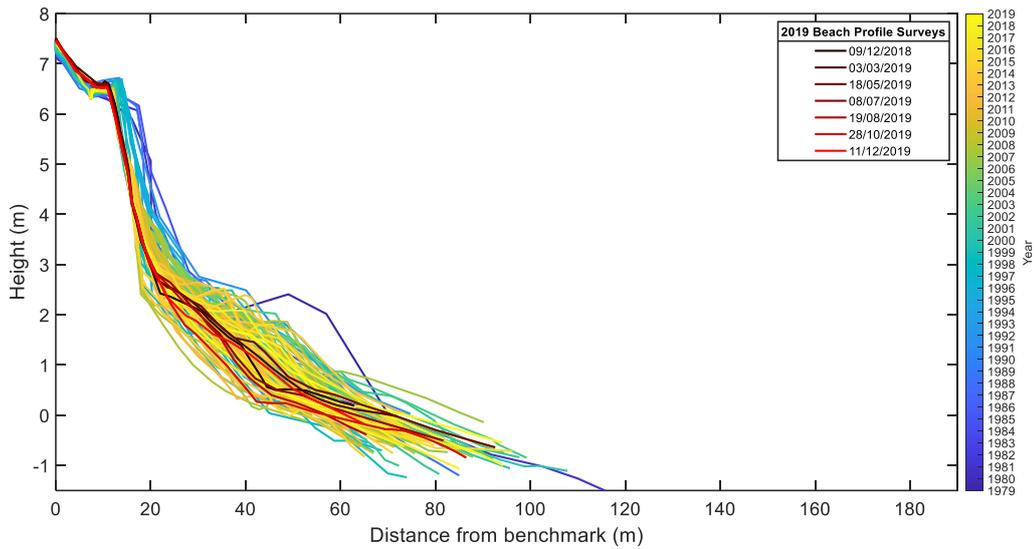
Figure B.3. Beach profile of CCS11, Whangapoua Beach. Field surveys were taken 9th December 2018, 3rd March 2019, 18th May 2019, 8th July 2019, 19th August 2019, 28th October 2019 and 11th December 2019.
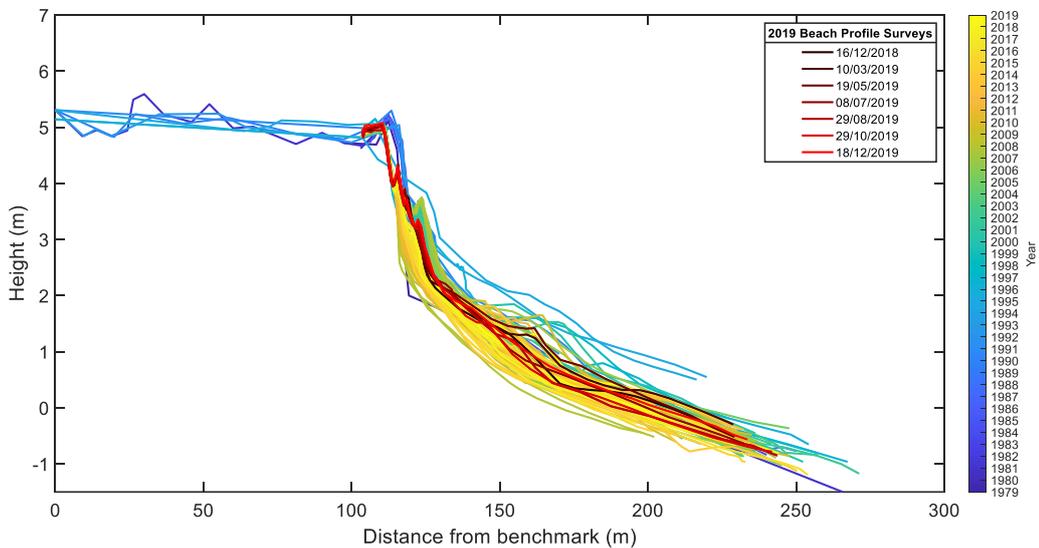
Matarangi Beach

Figure B.4. Beach profile of CCS13, Matarangi Beach. Field surveys were taken 16th December 2018, 10th March 2019, 19th May 2019, 8th July 2019, 29th August 2019, 29th October 2019 and 18th December 2019.
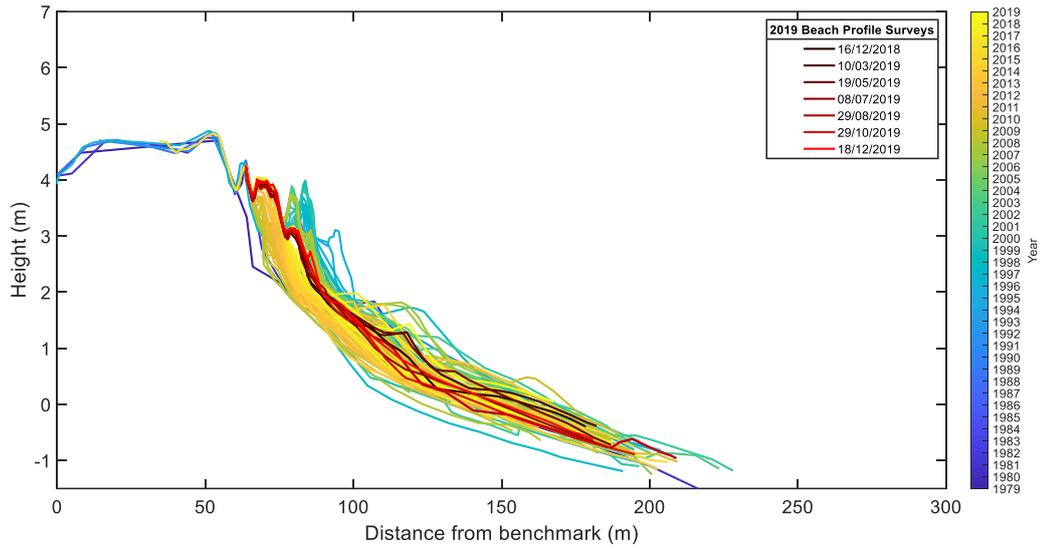
Figure B.5. Beach profile of CCS14, Matarangi Beach. Field surveys were taken 16th December 2018, 10th March 2019, 19th May 2019, 8th July 2019, 29th August 2019, 29th October 2019 and 18th December 2019.
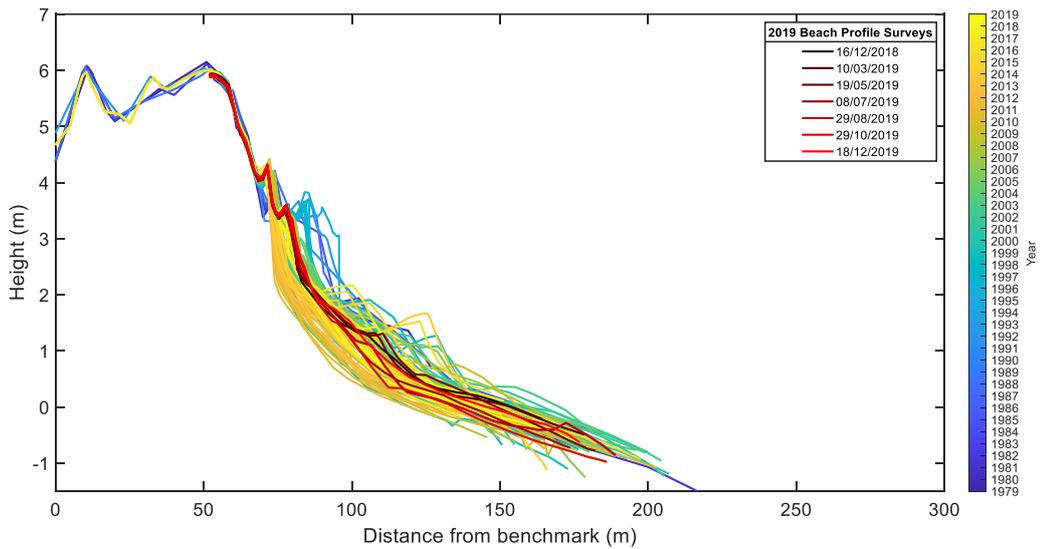
Figure B.6. Beach profile of CCS15, Matarangi Beach. Field surveys were taken 16th December 2018, 10th March 2019, 19th May 2019, 8th July 2019, 29th August 2019, 29th October 2019 and 18th December 2019.
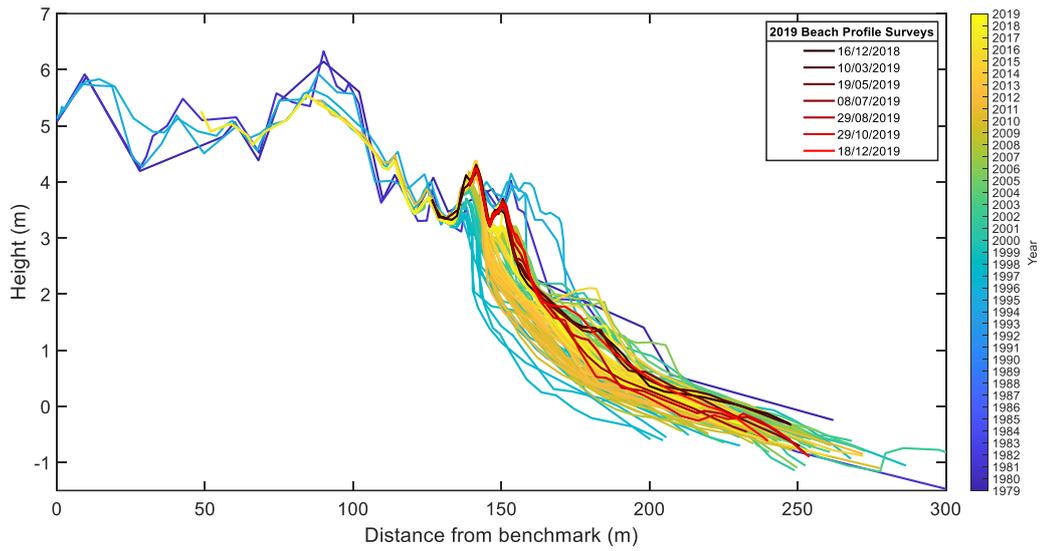
Figure B.7. Beach profile of CCS16, Matarangi Beach. Field surveys were taken 16th December 2018, 10th March 2019, 19th May 2019, 8th July 2019, 29th August 2019, 29th October 2019 and 18th December 2019.
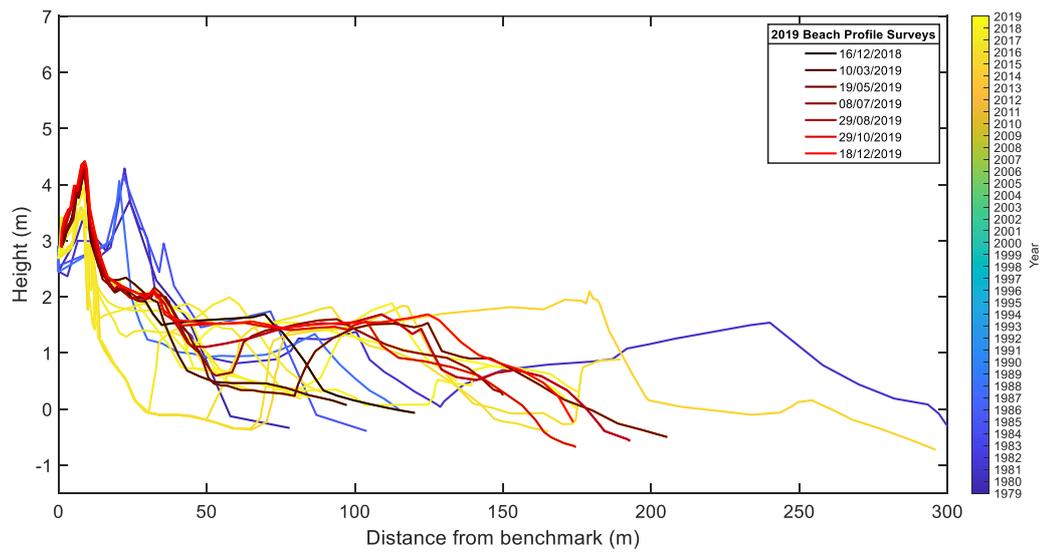
Figure B.8. Beach profile of CCS17, Matarangi Beach. Field surveys were taken 16th December 2018, 10th March 2019, 19th May 2019, 8th July 2019, 29th August 2019, 29th October 2019 and 18th December 2019.

Rings Beach
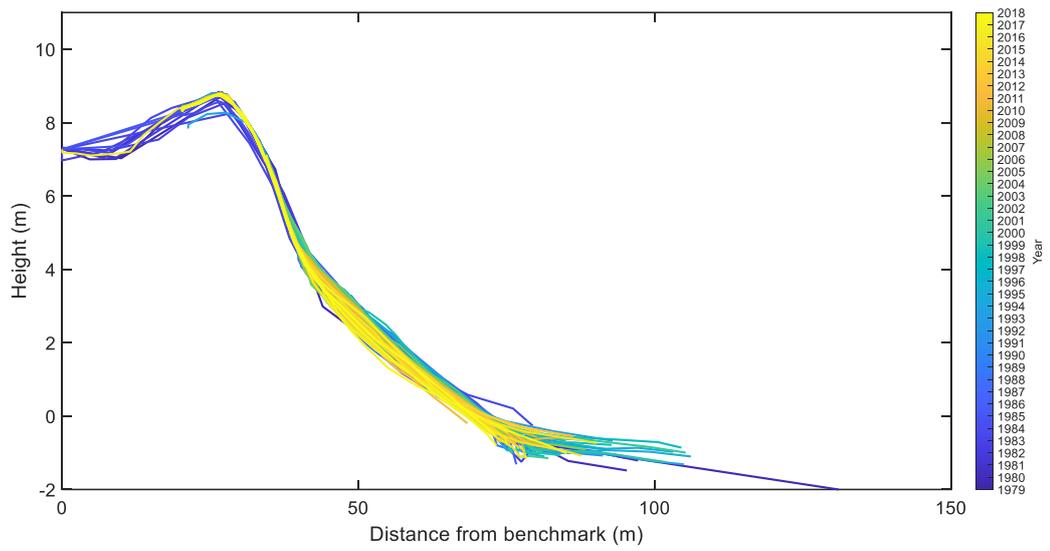
Figure B.9. Beach profile of CCS18, Rings Beach.

Kuaotunu West Beach
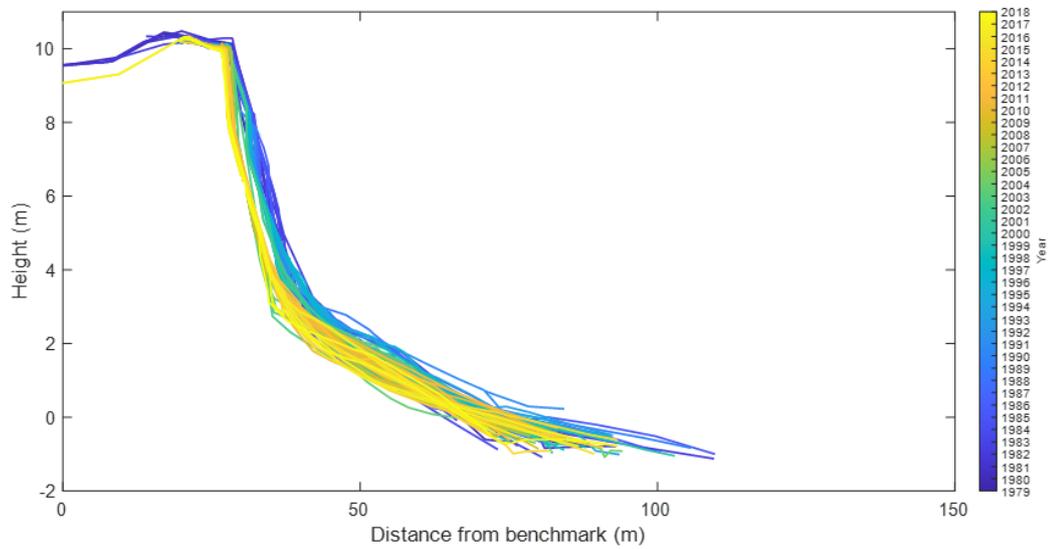
Figure B.10. Beach profile of CCS19-1, Kuaotunu West Beach.
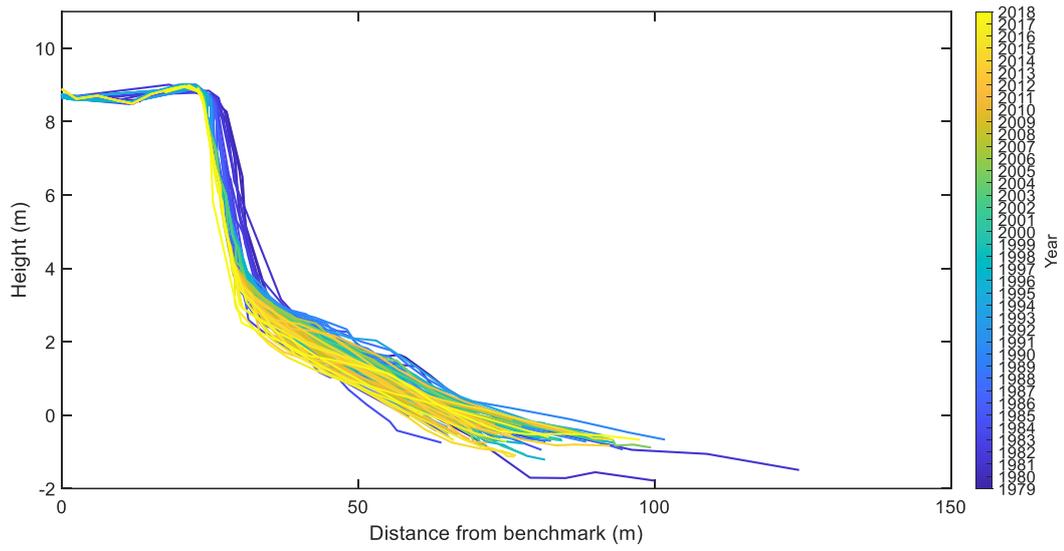
Figure B.11. Beach profile of CCS19-4, Kuaotunu West Beach.
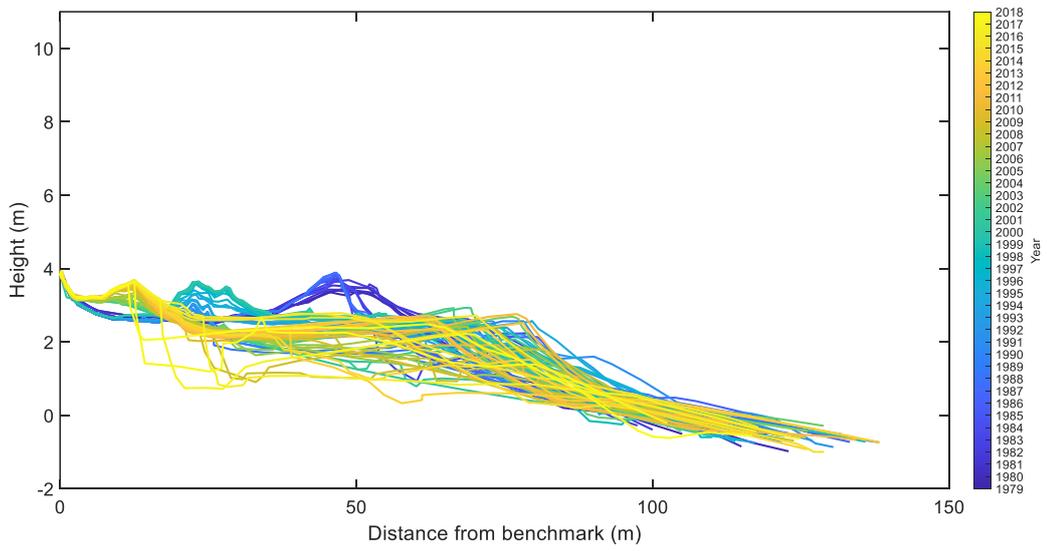
Figure B.12. Beach profile of CCS19-5, Kuaotunu West Beach.
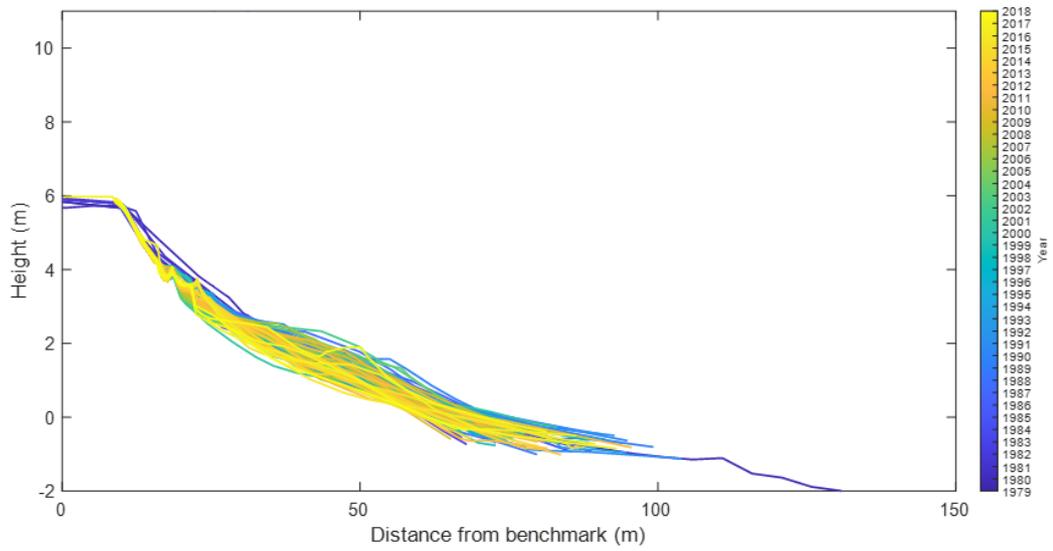
Figure B.13. Beach profile of CCS20, Kuaotunu East Beach.
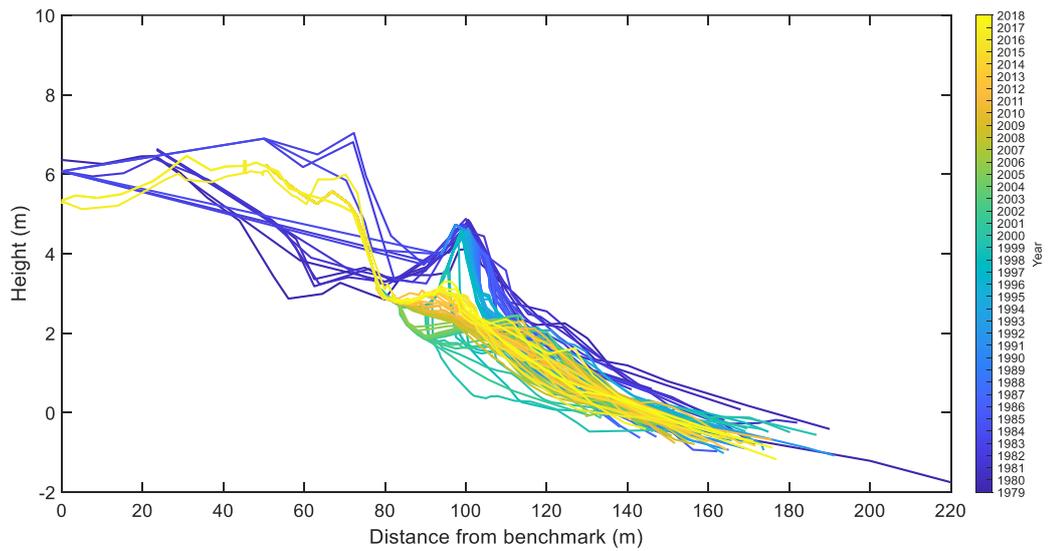
Figure B.14. Beach profile of CCS21, Kuaotunu East Beach. Note the axis scale is different.

Otama Beach
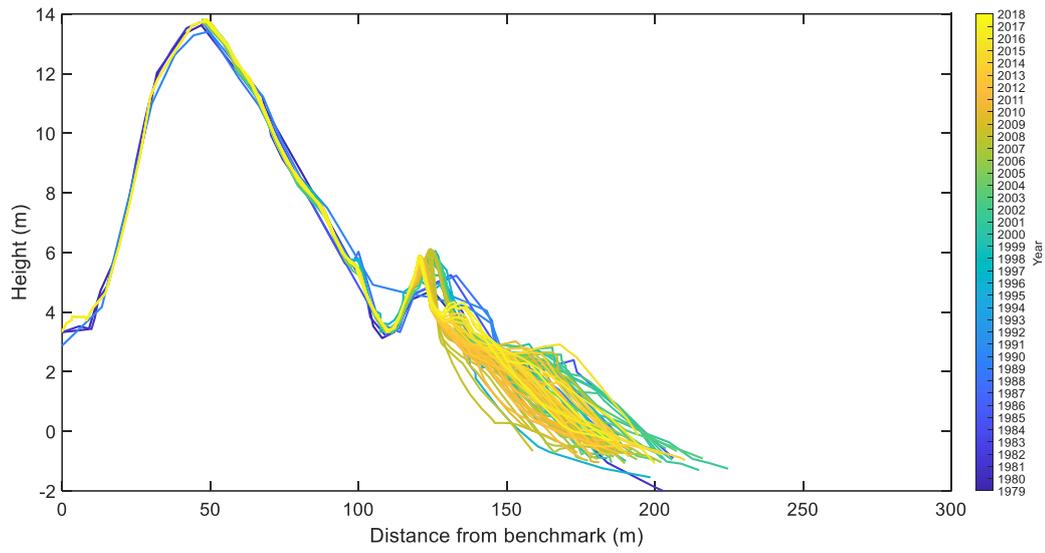
Figure B.15. Beach profile of CCS45, Otama Beach.
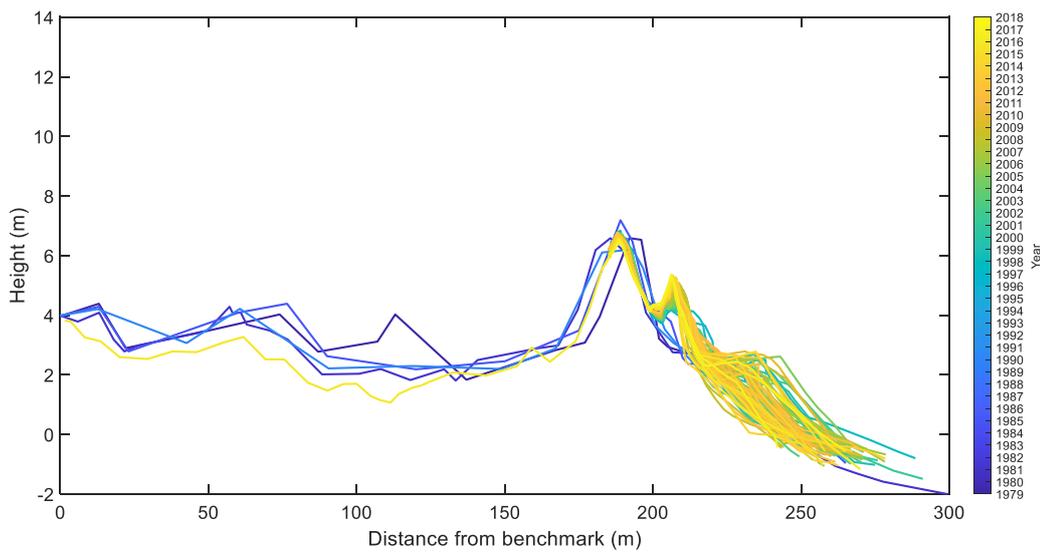
Figure B.16. Beach profile of CCS46, Otama Beach.

Opito Beach
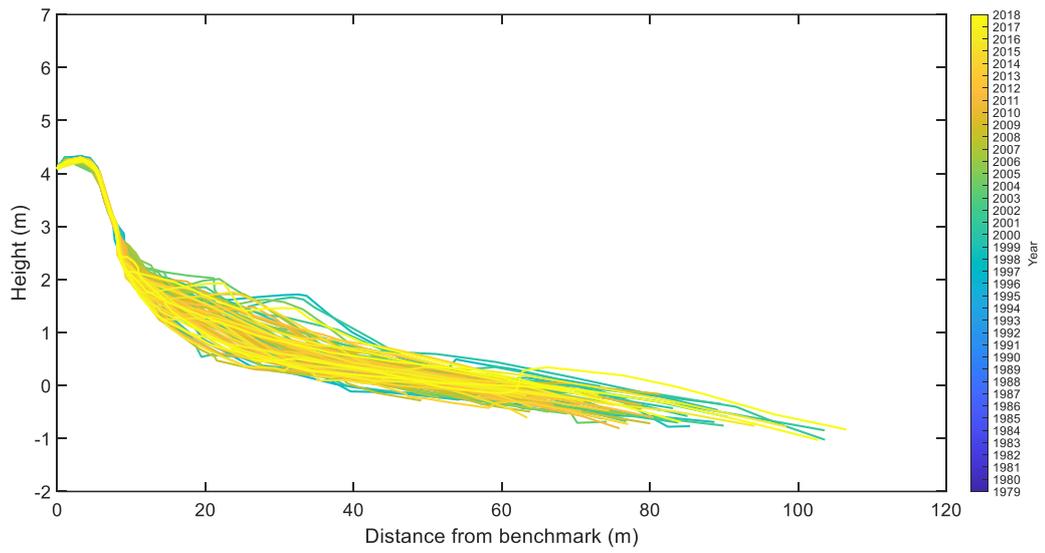
Figure B.17. Beach profile of CCS47-1, Opito Beach.
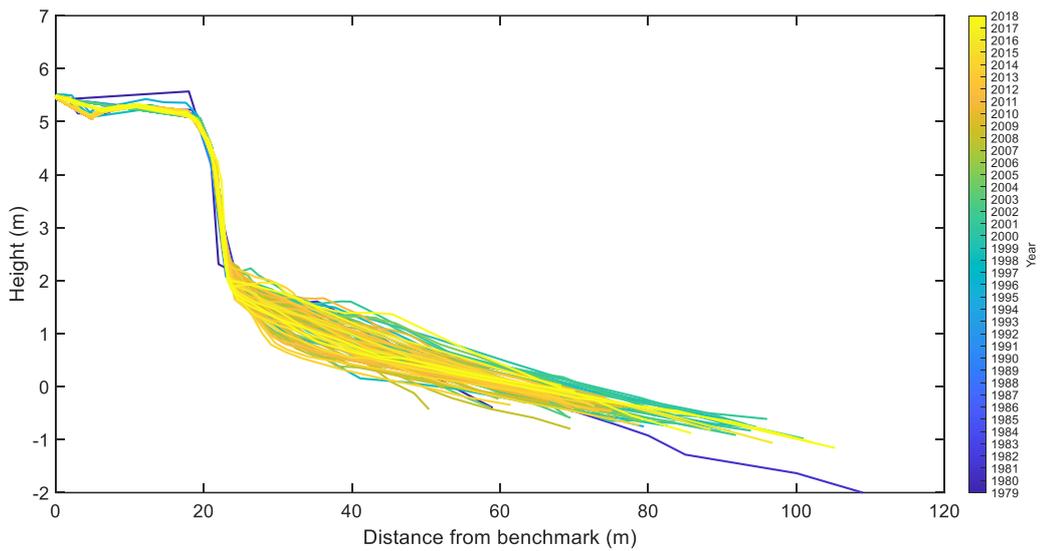
Figure B.18. Beach profile of CCS48, Opito Beach.
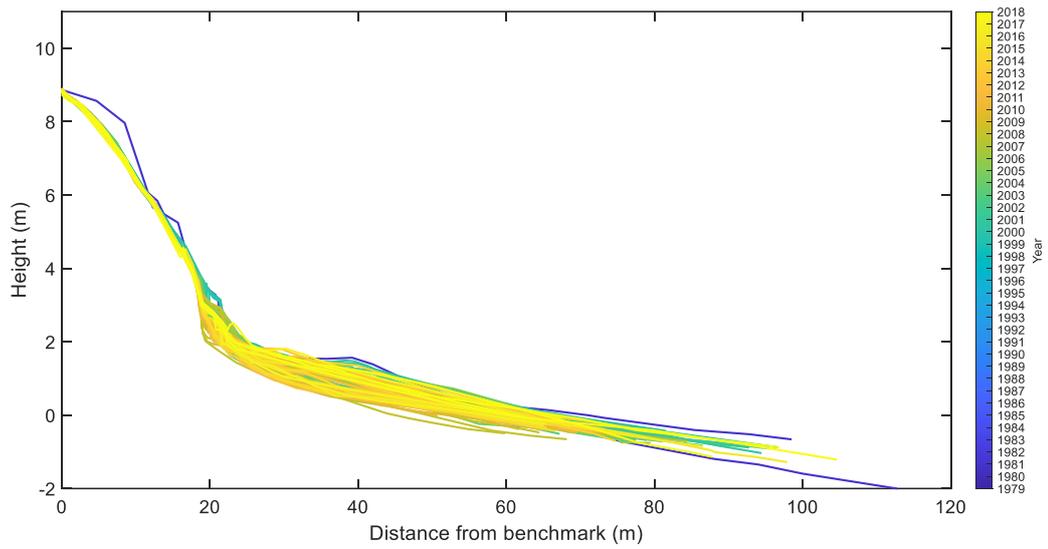
Figure B.19. Beach profile of CCS48-1, Opito Beach. Note the y-axis scale is different.
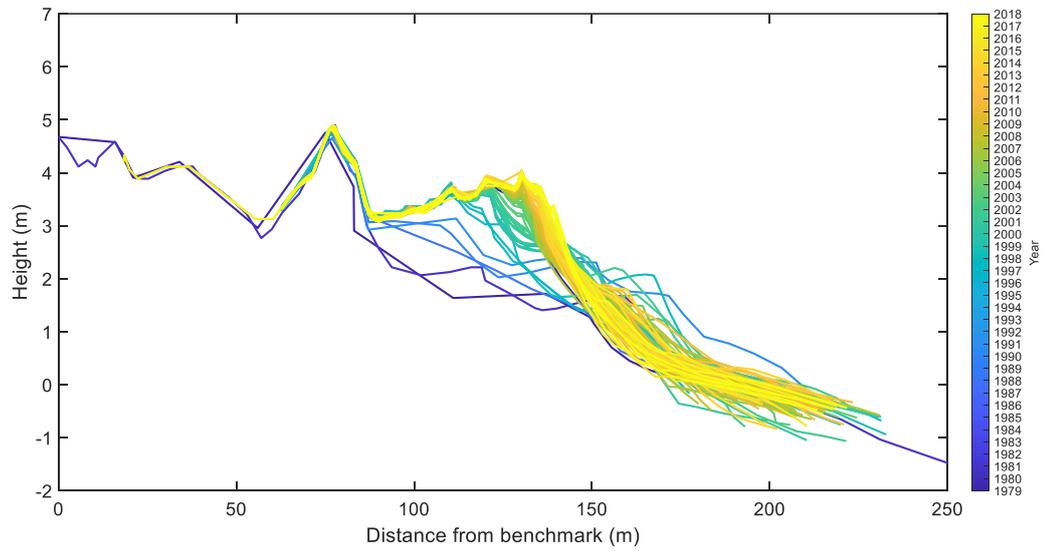
Figure B.20. Beach profile of CCS49, Opito Beach. Note the x-axis scale is different.
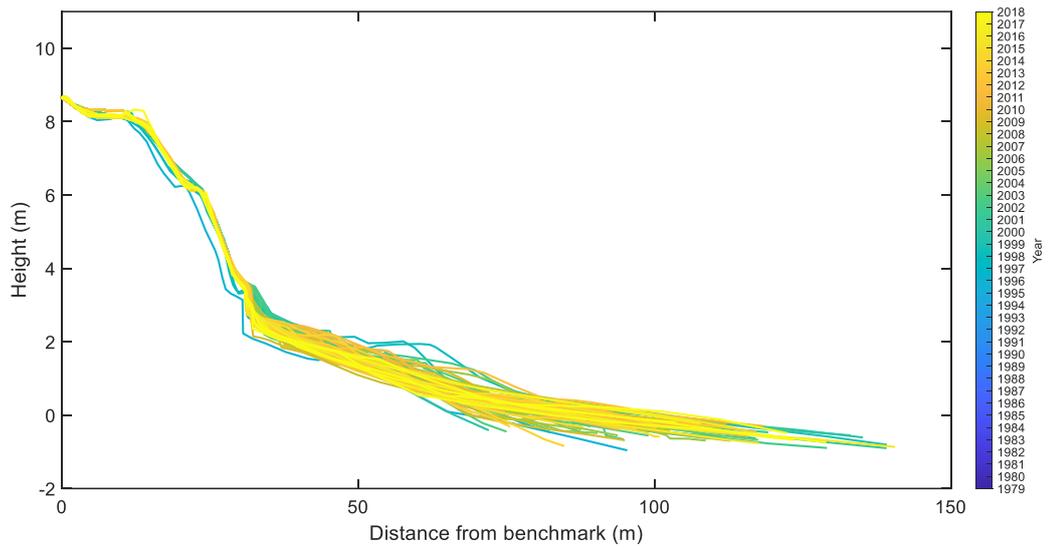
Figure B.21. Beach profile of CCS49-1, Opito Beach. Note x-axis and y-axis scale is a different.

Wharekaho Beach
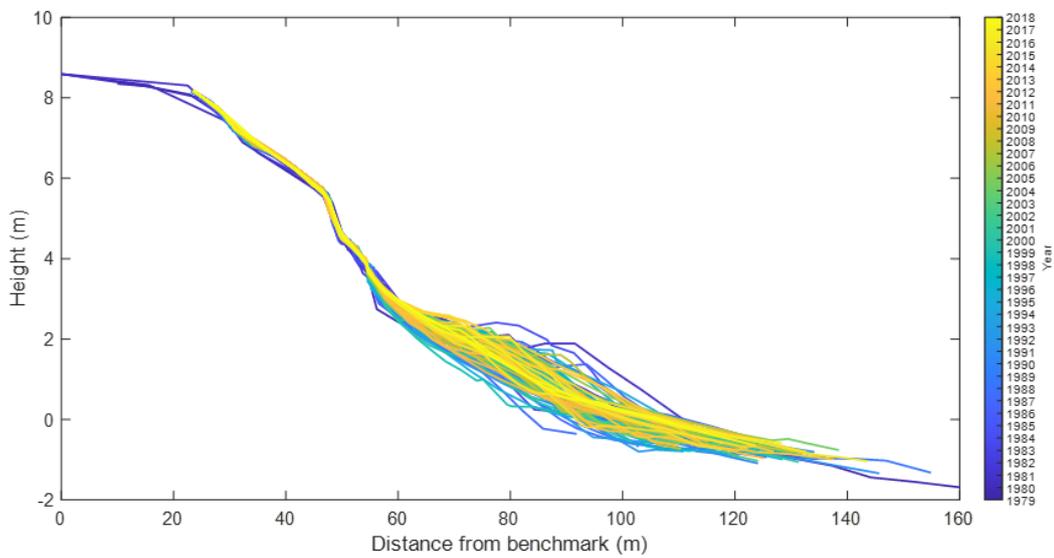
Figure B.22. Beach profile of CCS22, Wharekaho Beach.
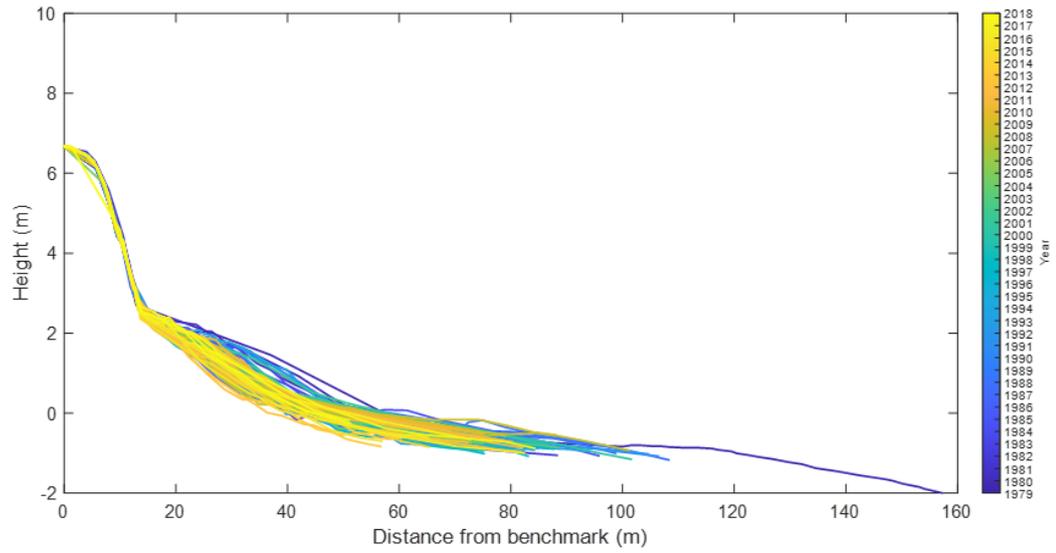
Figure B.23. Beach profile of CCS22-1, Wharekaho Beach.
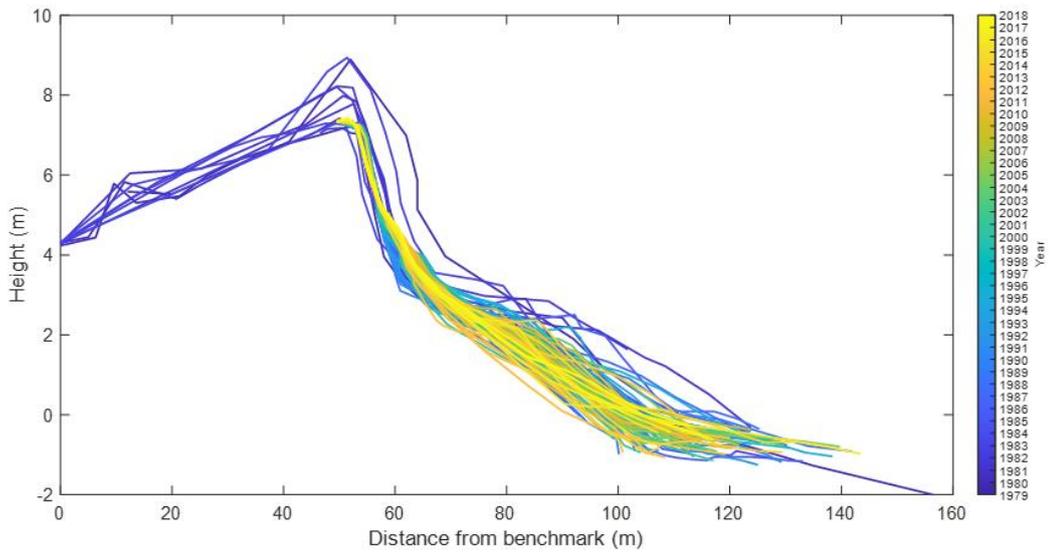
Figure B.24. Beach profile of CCS23, Wharekaho Beach.

Buffalo Beach
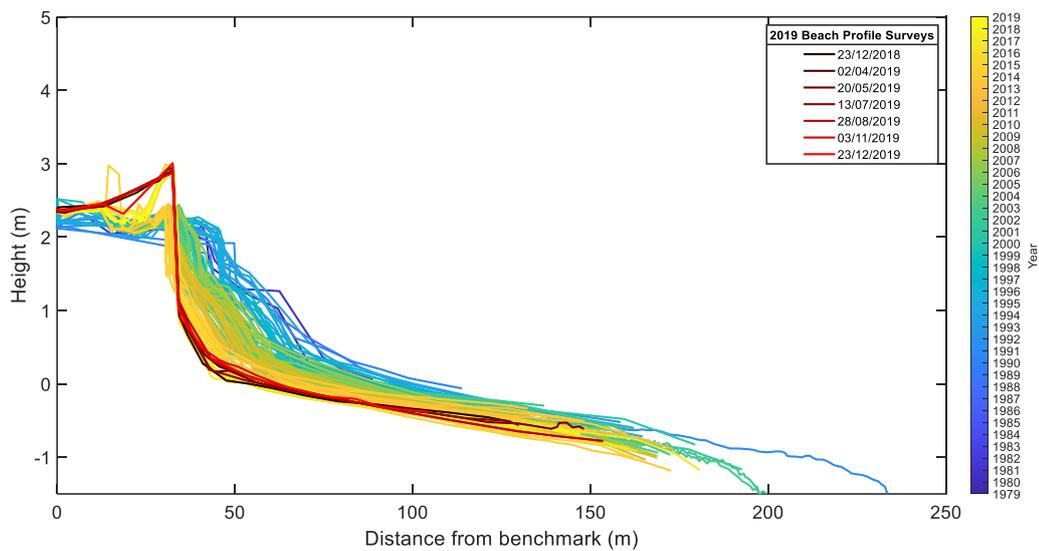
Figure B.25. Beach profile of CCS24, Buffalo Beach. Field surveys were taken 23rd December 2018, 2nd April 2019, 20th May 2019, 13th July 2019, 28th August 2019, 3rd November 2019 and 23rd December 2019.
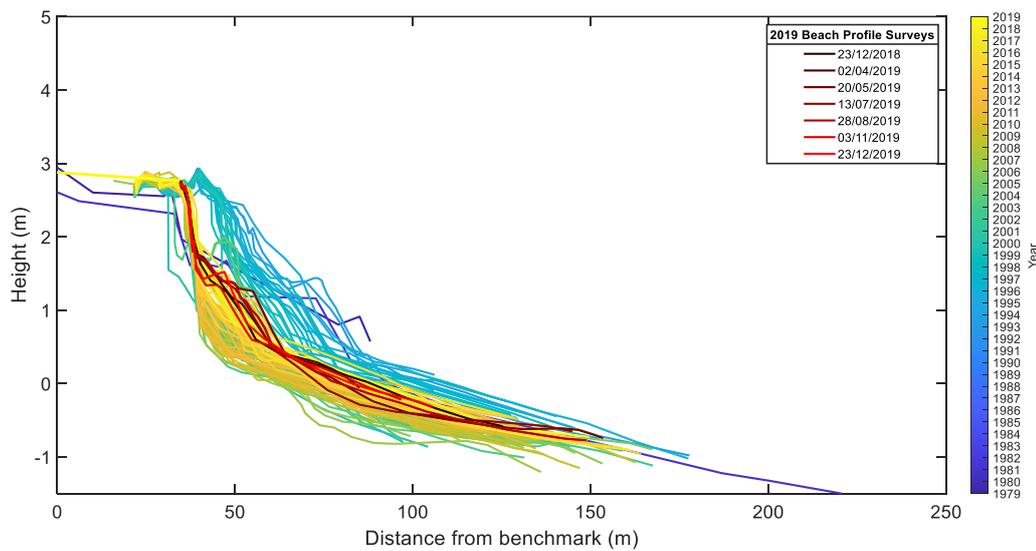
Figure B.26. Beach profile of CCS25, Buffalo Beach. Field surveys were taken 23rd December 2018, 2nd April 2019, 20th May 2019, 13th July 2019, 28th August 2019, 3rd November 2019 and 23rd December 2019.
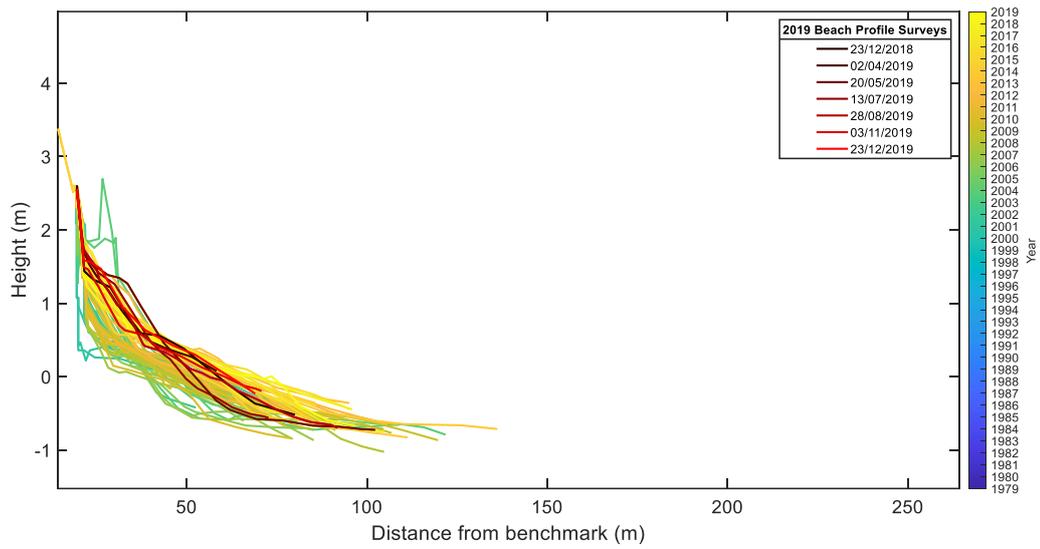
Figure B.27. Beach profile of CCS25-2, Buffalo Beach. Field surveys were taken 23rd December 2018, 2nd April 2019, 20th May 2019, 13th July 2019, 28th August 2019, 3rd November 2019 and 23rd December 2019.
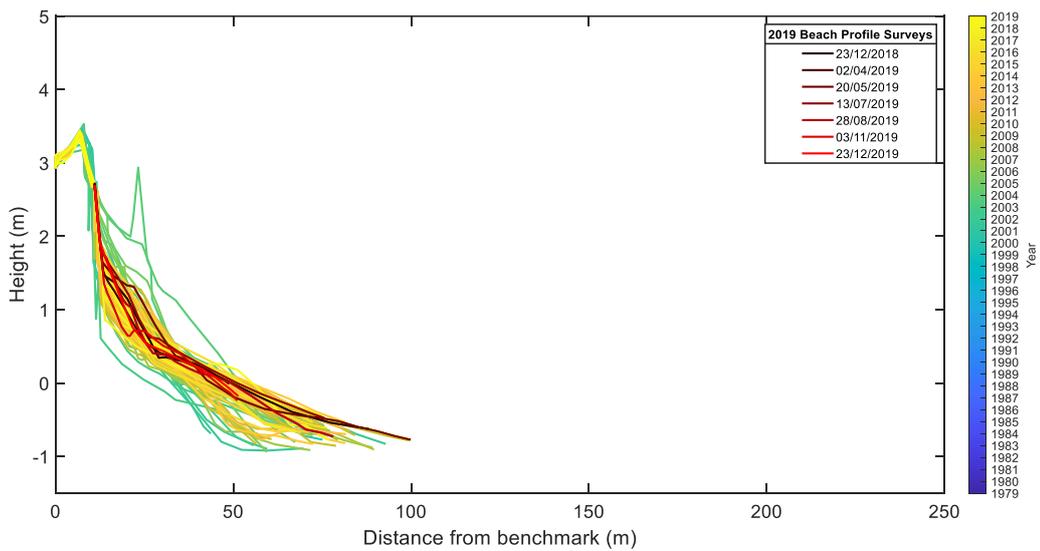
Figure B.28. Beach profile of CCS25-3, Buffalo Beach. Field surveys were taken 23rd December 2018, 2nd April 2019, 20th May 2019, 13th July 2019, 28th August 2019, 3rd November 2019 and 23rd December 2019.
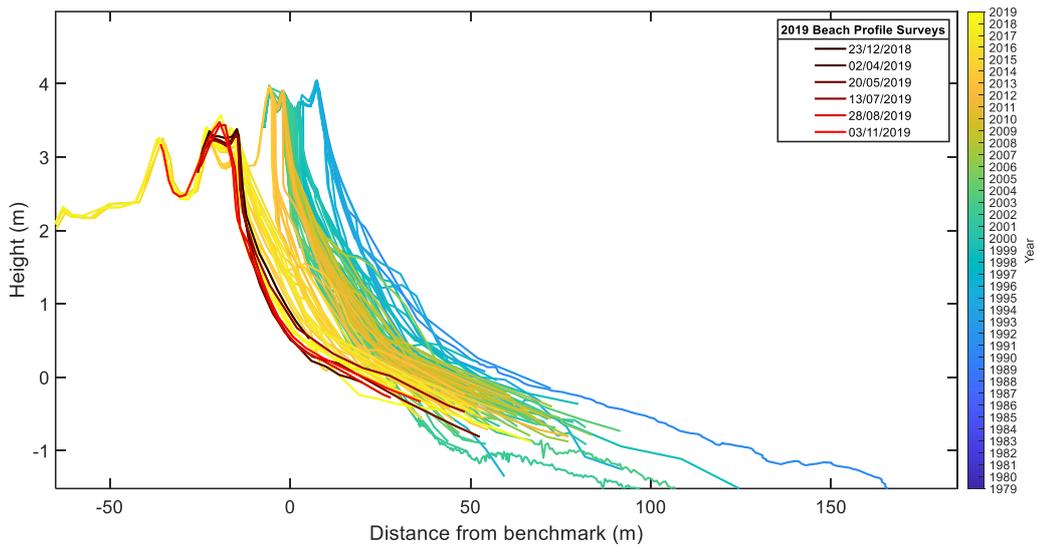
Figure B.29. Beach profile of CCS25-1, Buffalo Beach. Field surveys were taken 23rd December 2018, 2nd April 2019, 20th May 2019, 13th July 2019, 28th August 2019, 3rd November 2019 and 23rd December 2019.
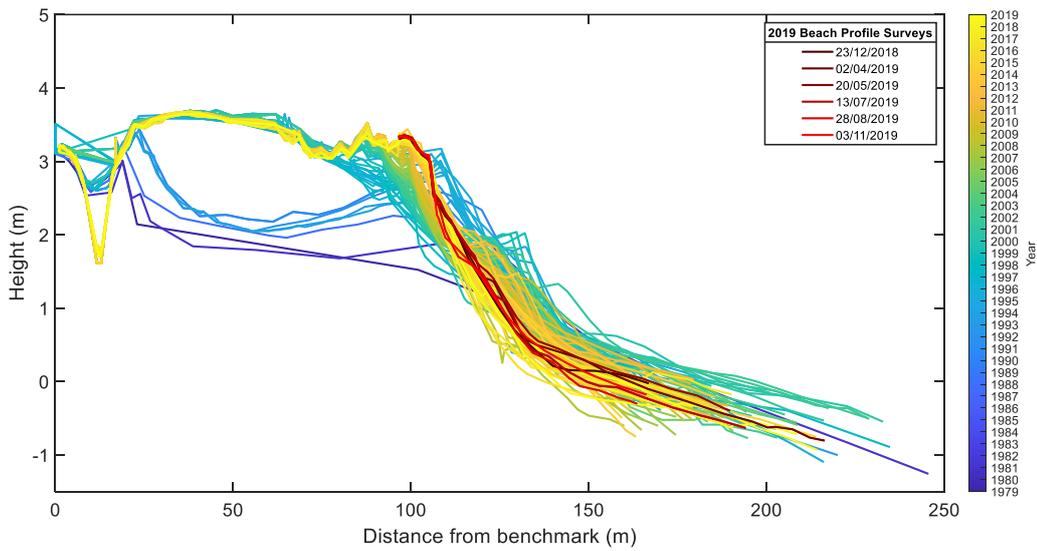
Figure B.30. Beach profile of CCS26, Buffalo Beach. Field surveys were taken 23rd December 2018, 2nd April 2019, 20th May 2019, 13th July 2019, 28th August 2019, 3rd November 2019 and 23rd December 2019.
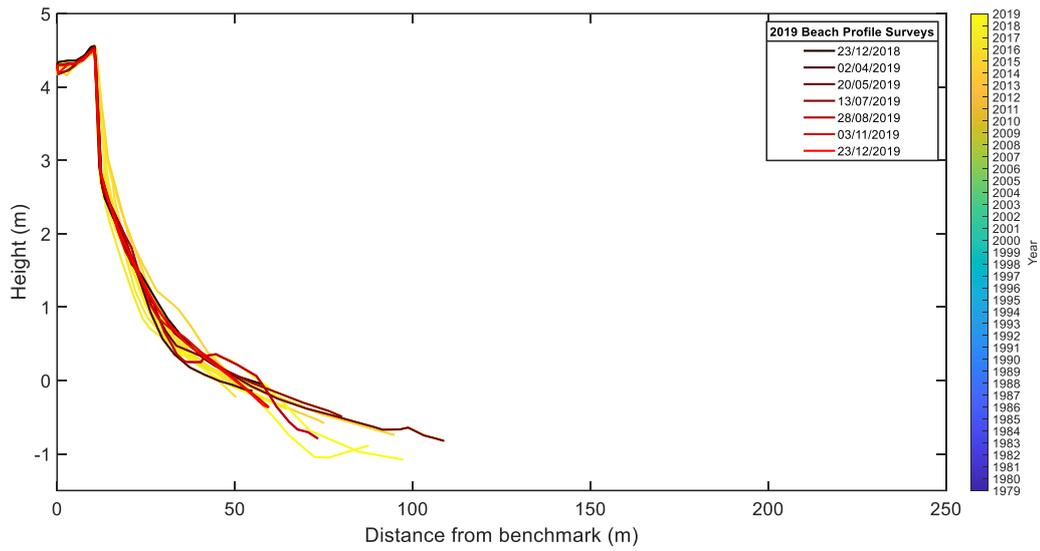
Figure B.31. Beach profile of CCS26/1, Buffalo Beach. Field surveys were taken 23rd December 2018, 2nd April 2019, 20th May 2019, 13th July 2019, 28th August 2019, 3rd November 2019 and 23rd December 2019.
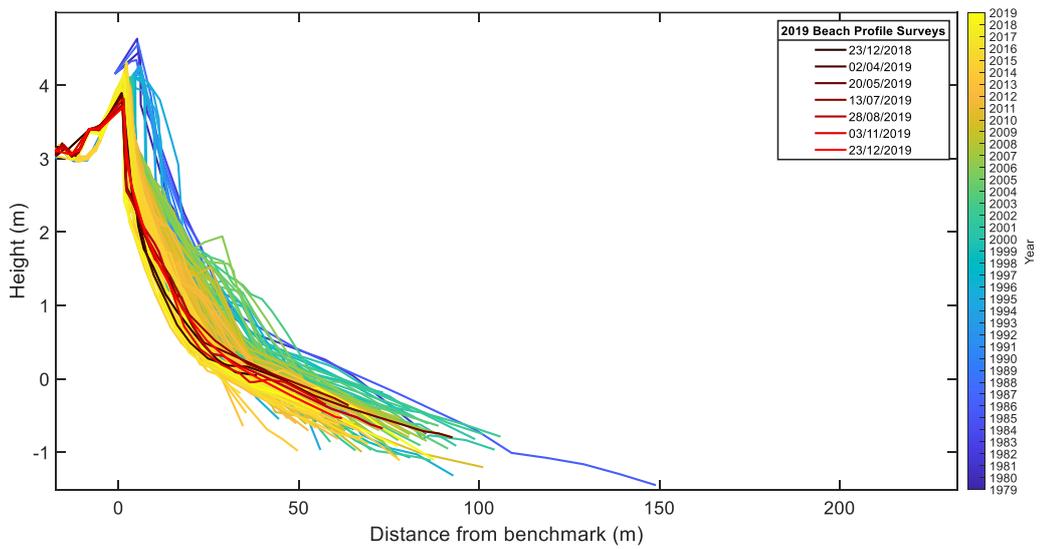
Figure B.32. Beach profile of CCS27, Buffalo Beach. Field surveys were taken 23rd December 2018, 2nd April 2019, 20th May 2019, 13th July 2019, 28th August 2019, 3rd November 2019 and 23rd December 2019.
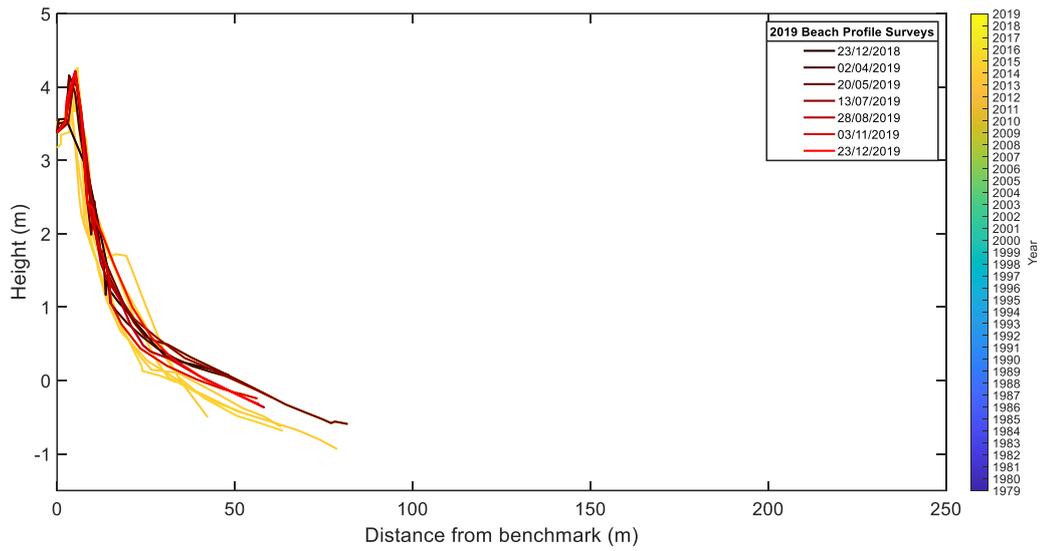
Figure B.33. Beach profile of CCS27/10, Buffalo Beach. Field surveys were taken 23rd December 2018, 2nd April 2019, 20th May 2019, 13th July 2019, 28th August 2019, 3rd November 2019 and 23rd December 2019.
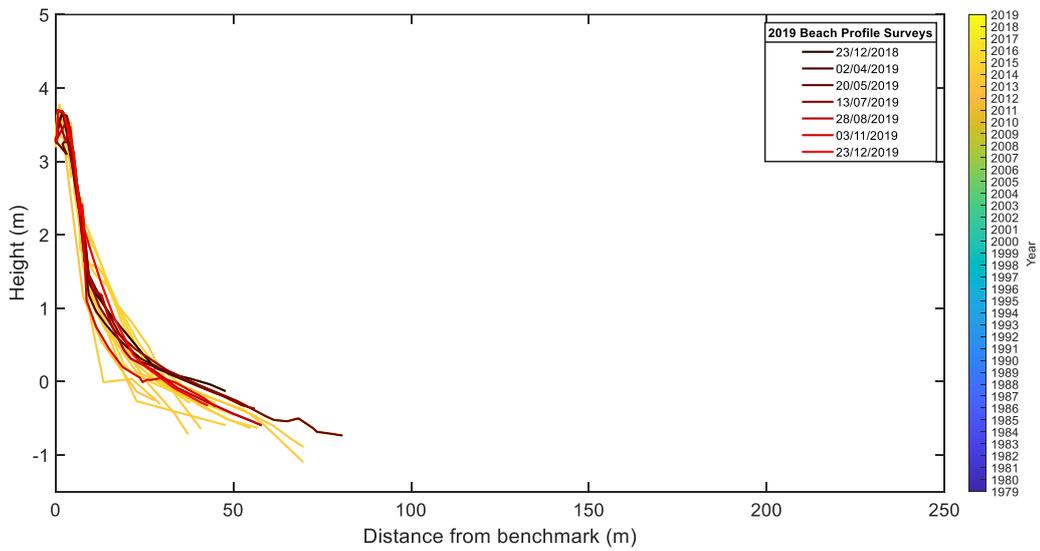
Figure B.34. Beach profile of CCS27/8, Buffalo Beach. Field surveys were taken 23rd December 2018, 2nd April 2019, 20th May 2019, 13th July 2019, 28th August 2019, 3rd November 2019 and 23rd December 2019.
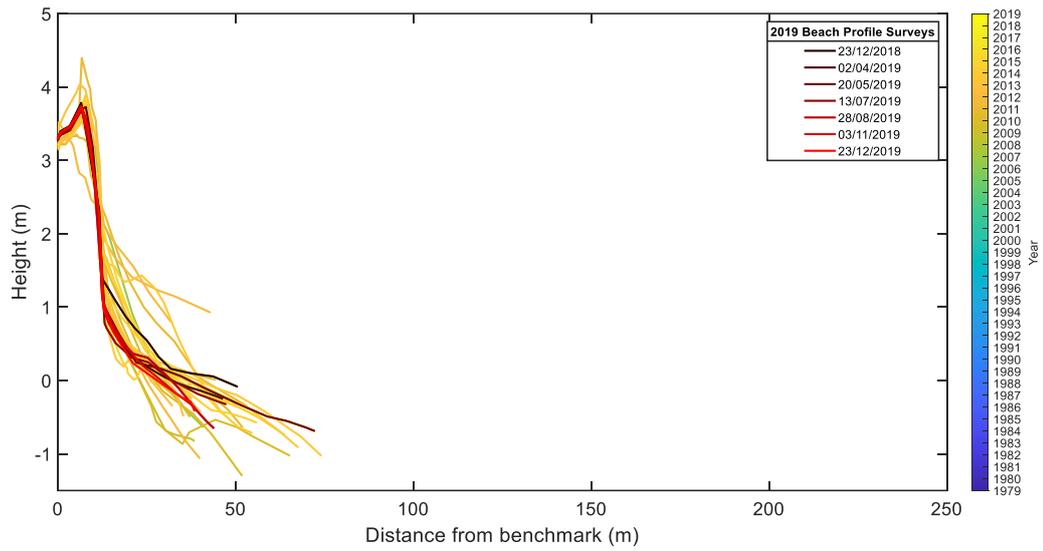
Figure B.35. Beach profile of CCS27/6, Buffalo Beach. Field surveys were taken 23rd December 2018, 2nd April 2019, 20th May 2019, 13th July 2019, 28th August 2019, 3rd November 2019 and 23rd December 2019.
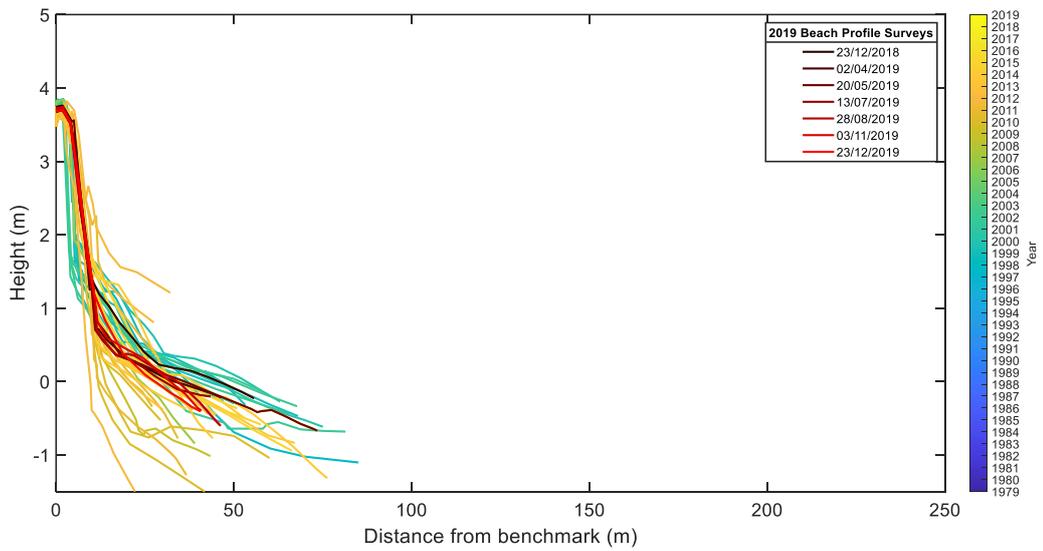
Figure B.36. Beach profile of CCS27/2, Buffalo Beach. Field surveys were taken 23rd December 2018, 2nd April 2019, 20th May 2019, 13th July 2019, 28th August 2019, 3rd November 2019 and 23rd December 2019.
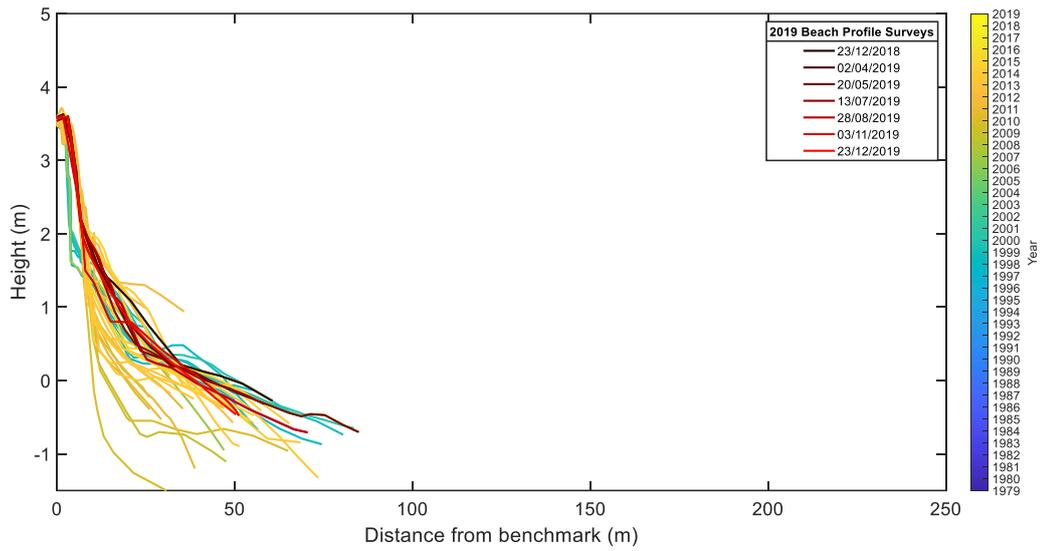
Figure B.37. Beach profile of CCS27/3, Buffalo Beach. Field surveys were taken 23rd December 2018, 2nd April 2019, 20th May 2019, 13th July 2019, 28th August 2019, 3rd November 2019 and 23rd December 2019.
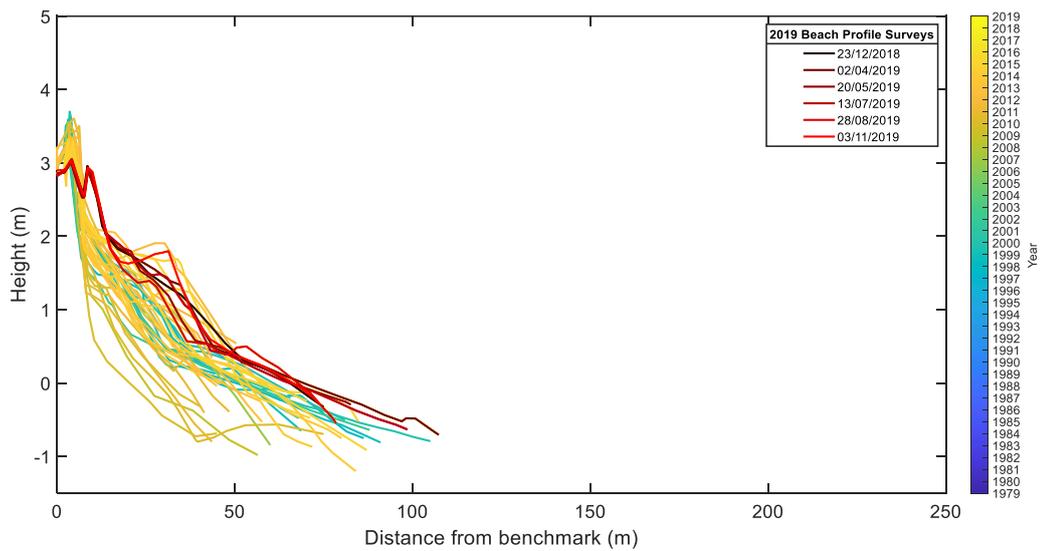
Figure B.38. Beach profile of CCS27/4, Buffalo Beach. Field surveys were taken 23rd December 2018, 2nd April 2019, 20th May 2019, 13th July 2019, 28th August 2019, 3rd November 2019 and 23rd December 2019.
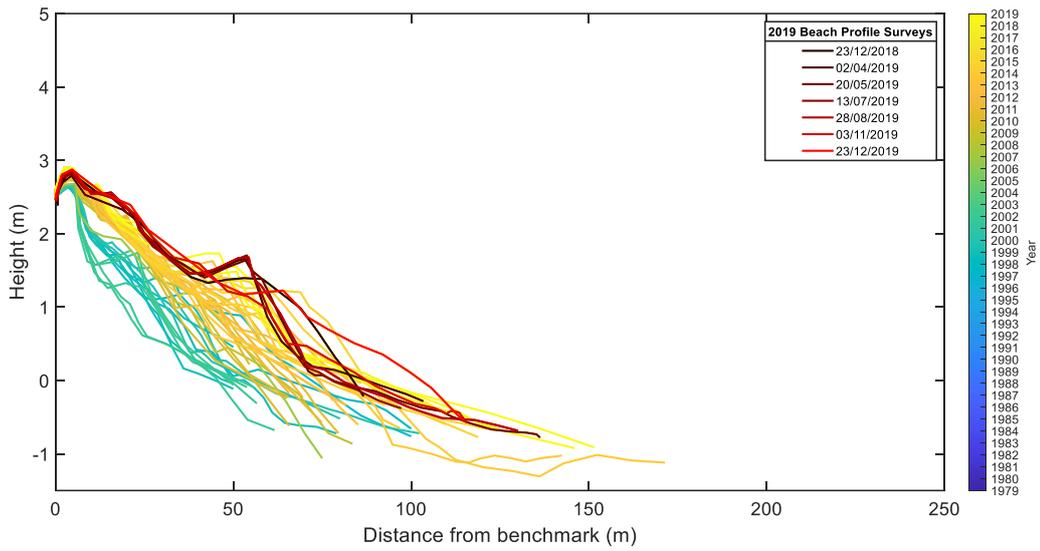
Figure B.39. Beach profile of CCS27/5, Buffalo Beach. Field surveys were taken 23rd December 2018, 2nd April 2019, 20th May 2019, 13th July 2019, 28th August 2019, 3rd November 2019 and 23rd December 2019.

Maramaratotara Beach
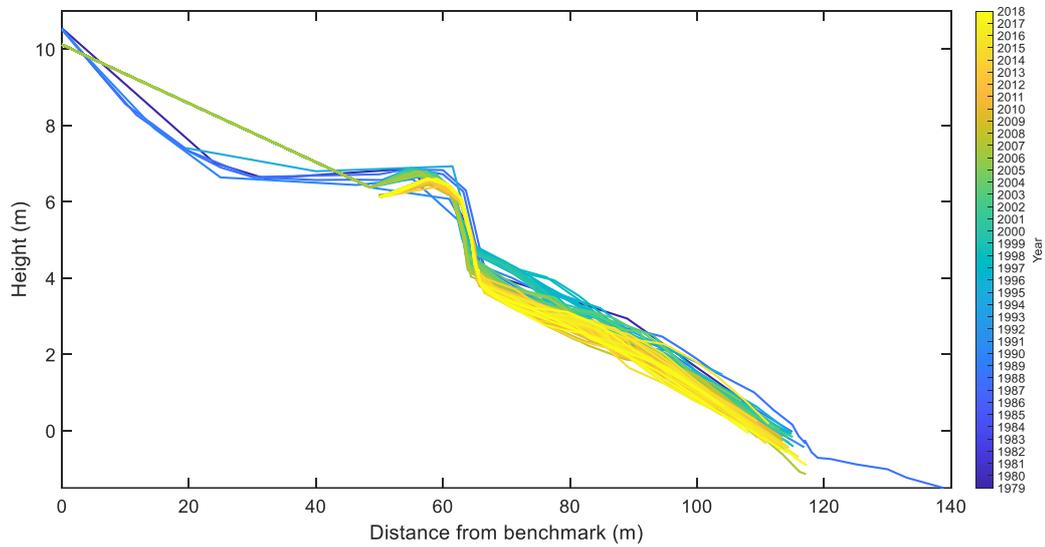
Figure B.40. Beach profile at CCS28, Maramaratotara Beach.
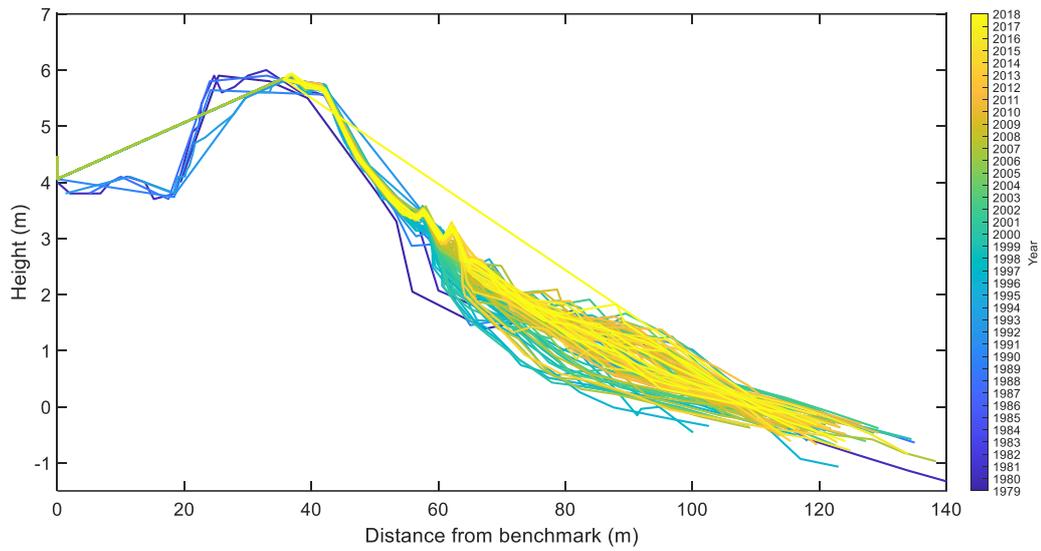
Cooks Beach

Figure B.41. Beach profile of CCS29, Cooks Beach.
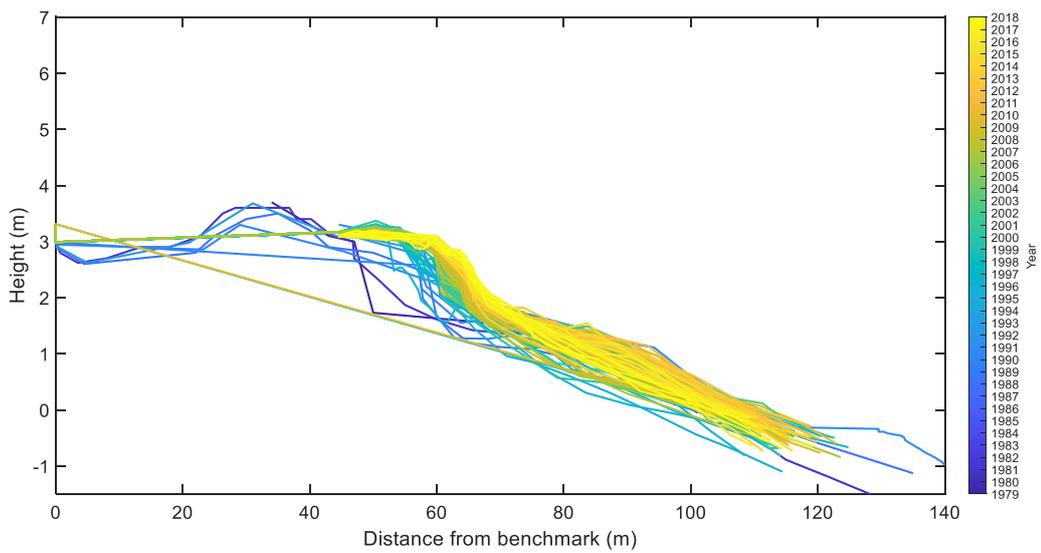
Figure B.42. Beach profile of CCS30, Cooks Beach.
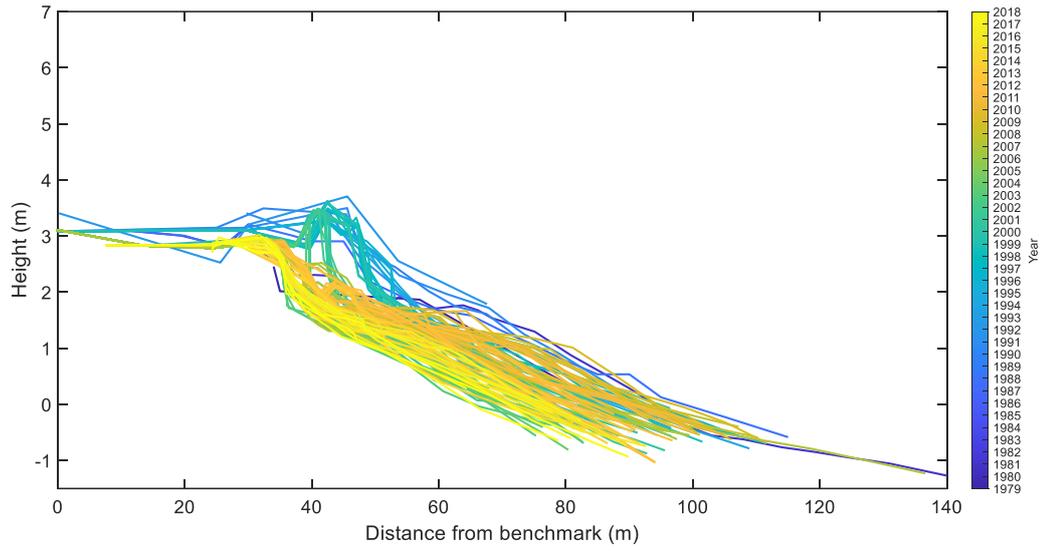
Figure B.43. Beach profile of CCS31, Cooks Beach.
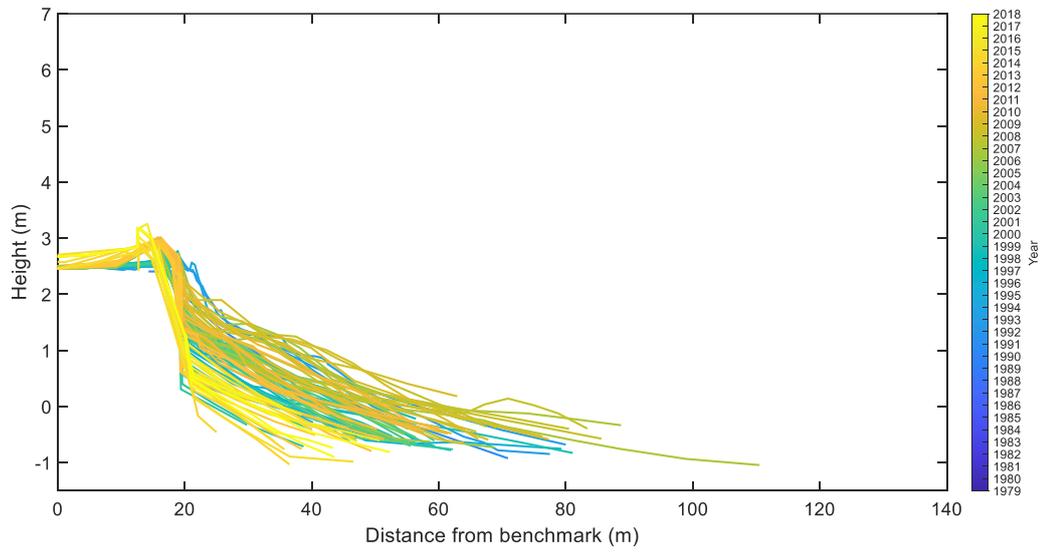
Figure B.44. Beach profile of CCS31-1, Cooks Beach.
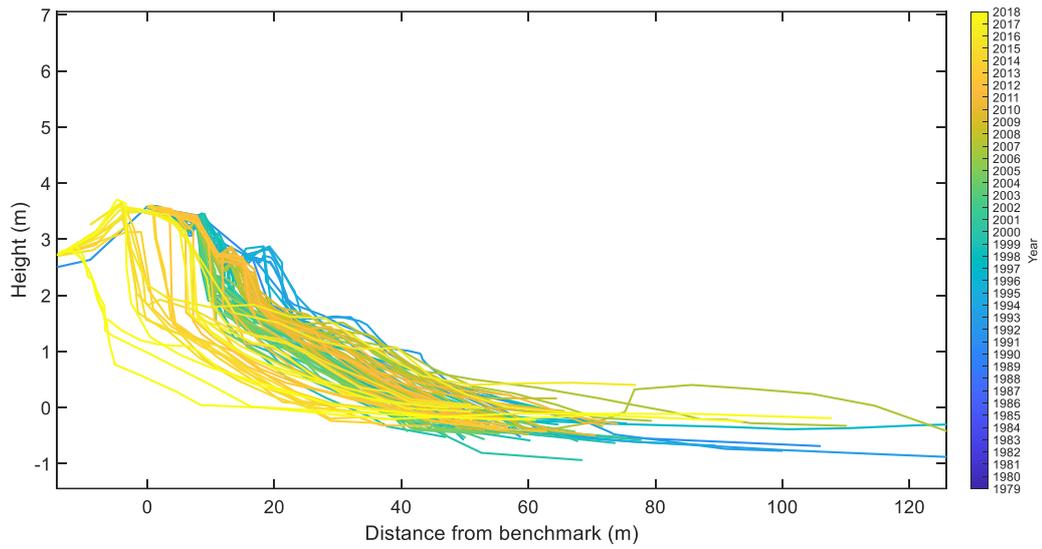
Figure B.45. Beach profile of CCS31-2, Cooks Beach.

Hahei Beach
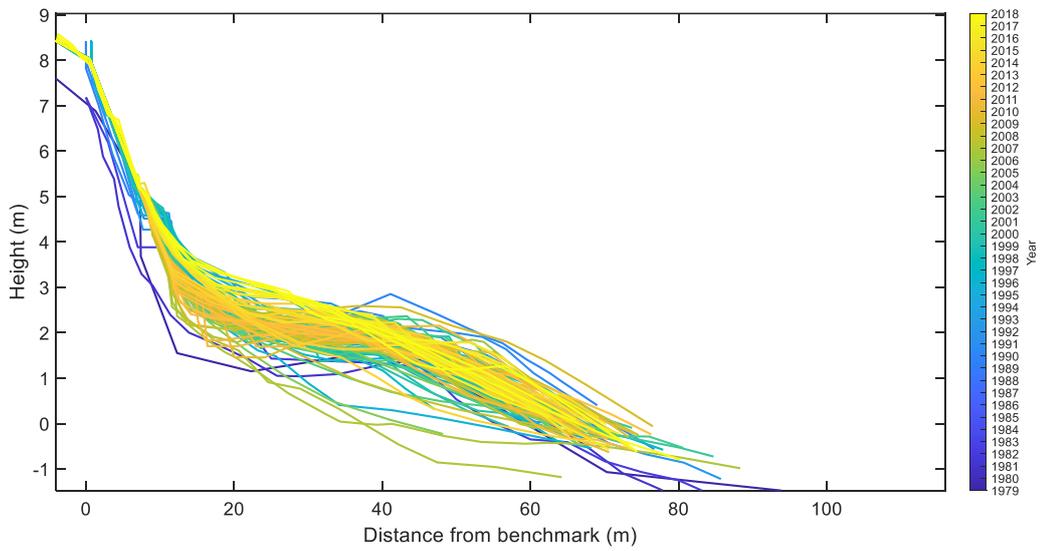
Figure B.46. Beach profile of CCS32, Hahei Beach. Note the x-axis and y-axis scale is different.
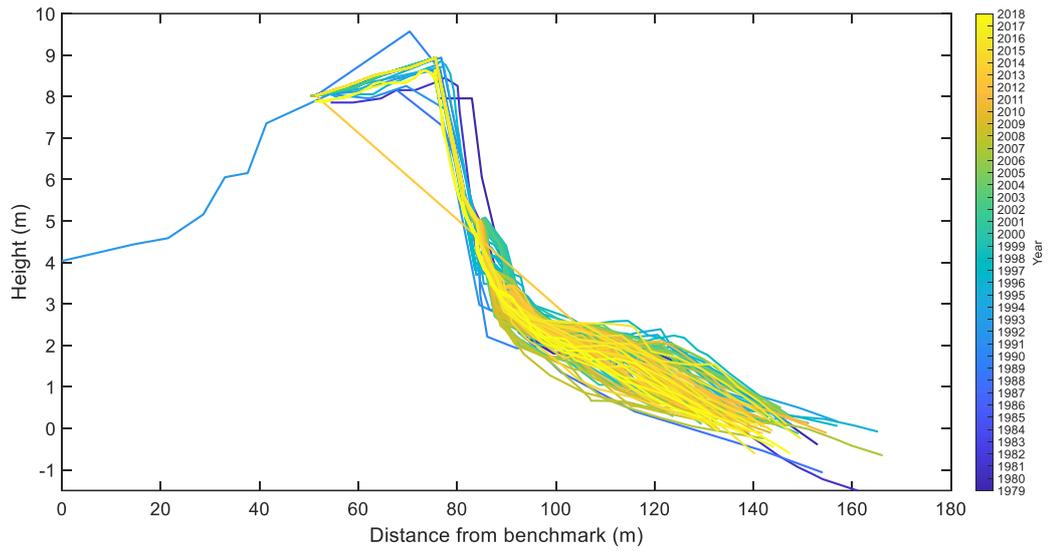
Figure B.47. Beach profile of CCS33, Hahei Beach. Not the x-axis and y-axis scale is different.

Hot Water Beach
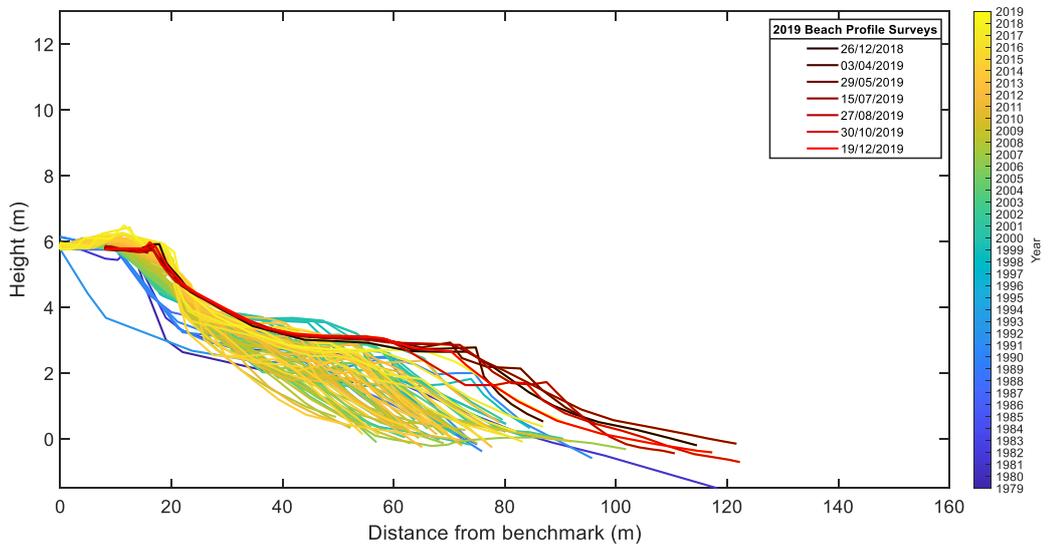
Figure B.48. Beach profile of CC34, Hot Water Beach. Field surveys were taken 26th December 2018, 3rd April 2019, 29th May 2019, 15th July 2019, 27th August 2019, 30th October 2019 and 19th December 2019.
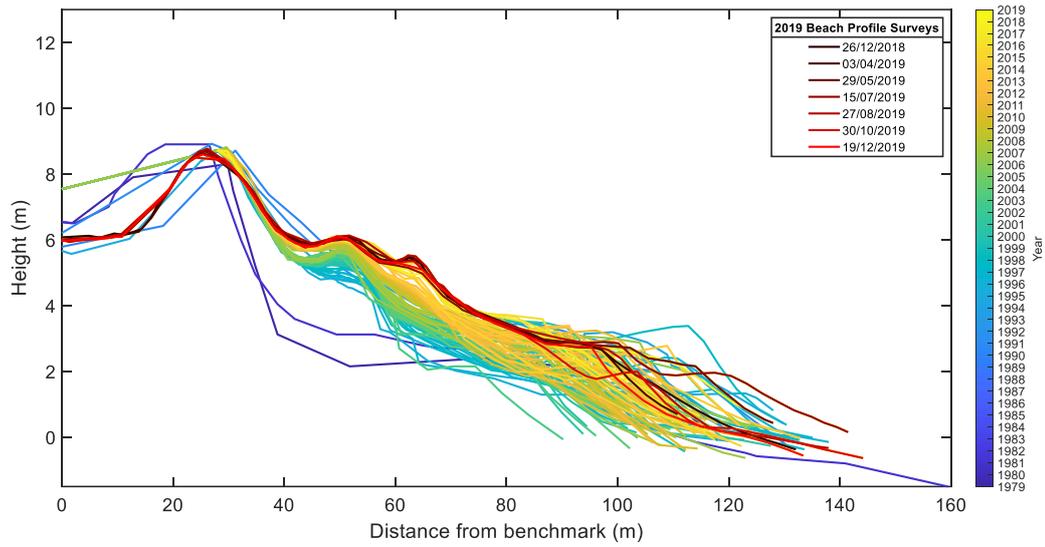
Figure B.49. Beach profile of CC35, Hot Water Beach. Field surveys were taken 26th December 2018, 3rd April 2019, 29th May 2019, 15th July 2019, 27th August 2019, 30th October 2019 and 19th December 2019.
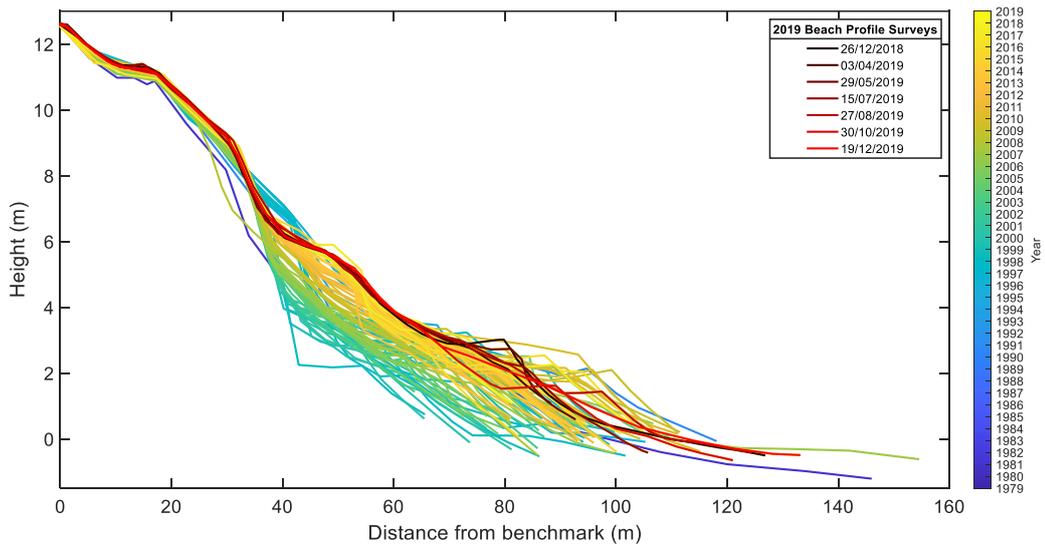
Figure B.51. Beach profile of CC35-1, Hot Water Beach. Field surveys were taken 26th December 2018, 3rd April 2019, 29th May 2019, 15th July 2019, 27th August 2019, 30th October 2019 and 19th December 2019.
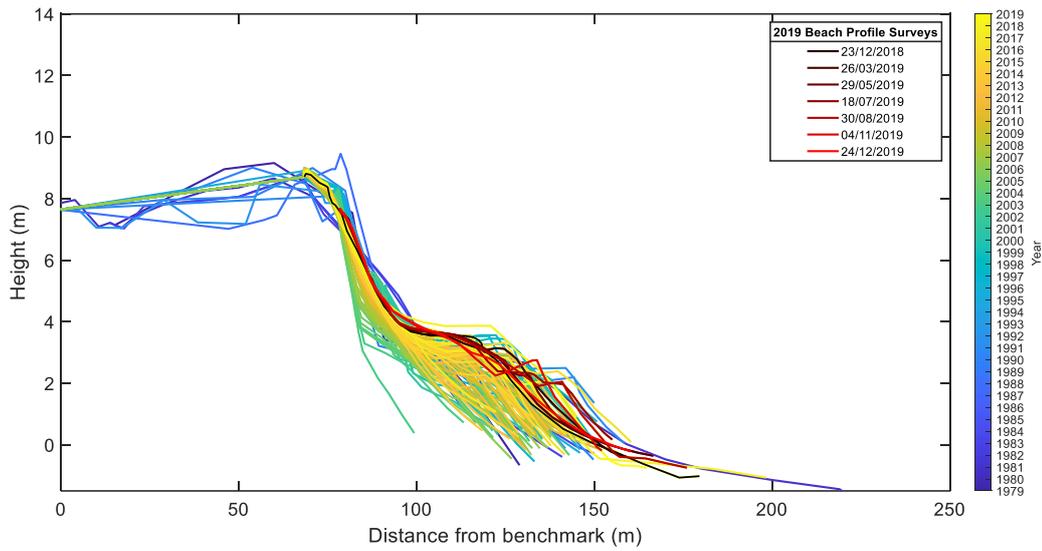
Tairua Beach

Figure B.52. Beach profile of CCS36, Tairua Beach. Field surveys were taken 23rd December 2018, 26th March 2019, 29th May 2019, 18th July 2019, 30th August 2019, 4th November 2019 and 24th December 2019.
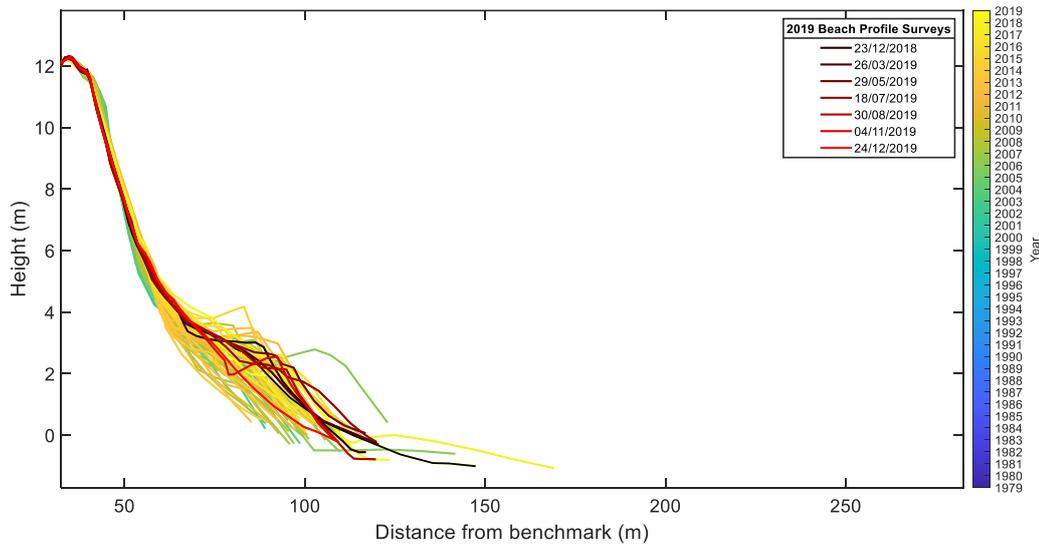
Figure B.53. Beach profile of CCS36-2, Tairua Beach. Field surveys were taken 23rd December 2018, 26th March 2019, 29th May 2019, 18th July 2019, 30th August 2019, 4th November 2019 and 24th December 2019.

212
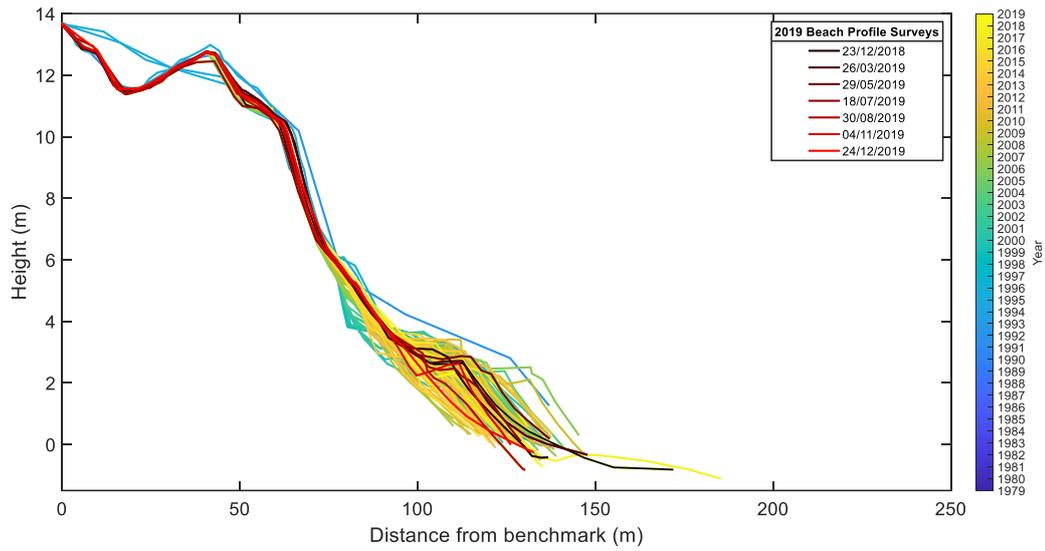
Figure B.54. Beach profile of CCS36-1, Tairua Beach. Field surveys were taken 23rd December 2018, 26th March 2019, 29th May 2019, 18th July 2019, 30th August 2019, 4th November 2019 and 24th December 2019.
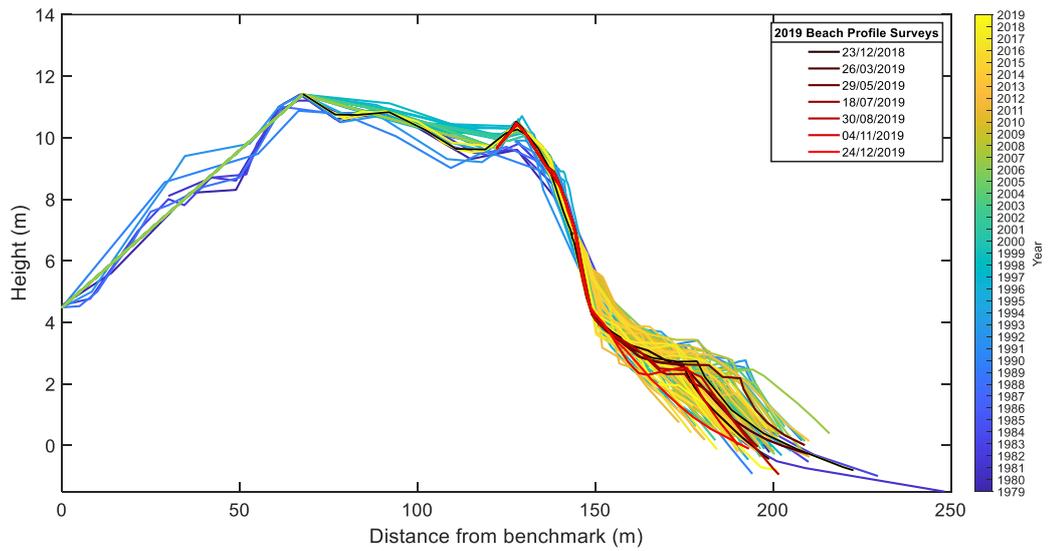
Figure B.55. Beach profile of CCS37, Tairua Beach. Field surveys were taken 23rd December 2018, 26th March 2019, 29th May 2019, 18th July 2019, 30th August 2019, 4th November 2019 and 24th December 2019.

Pauanui Beach
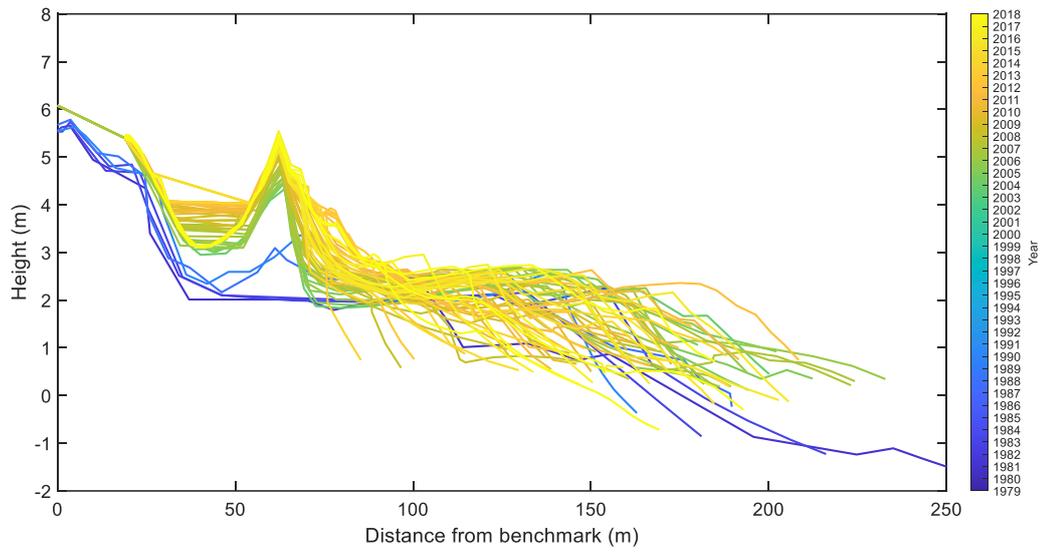
Figure B.56. Beach profile of CCS38, Pauanui Beach.
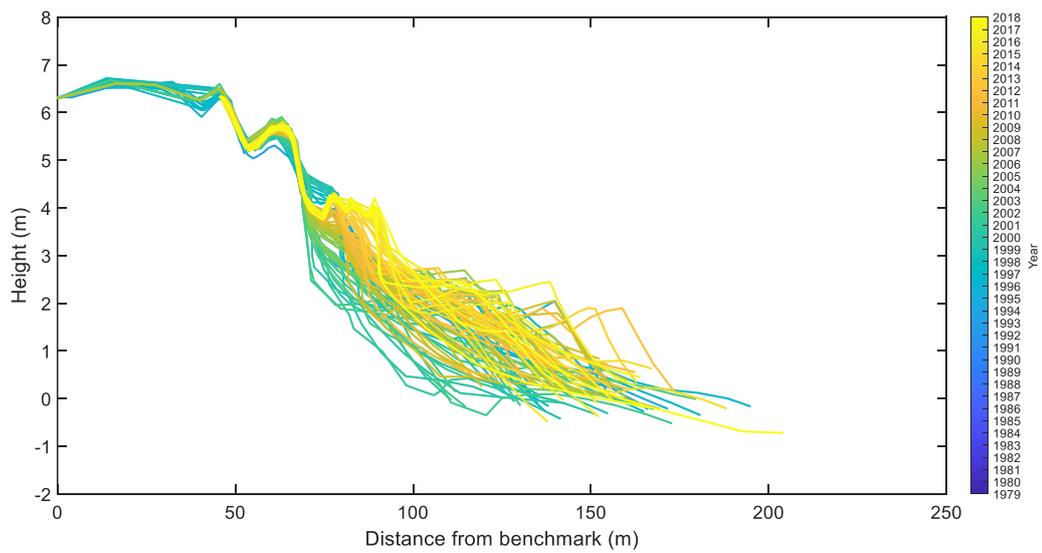
Figure B.57. Beach profile of CCS38-1, Pauanui Beach.

214
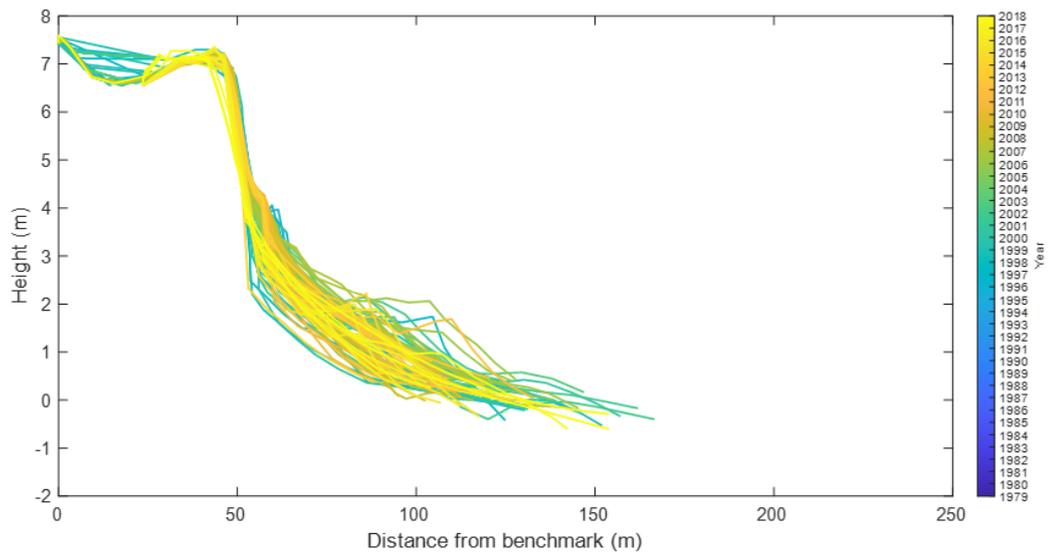
Figure B.58. Beach profile of CCS39-1, Pauanui Beach.
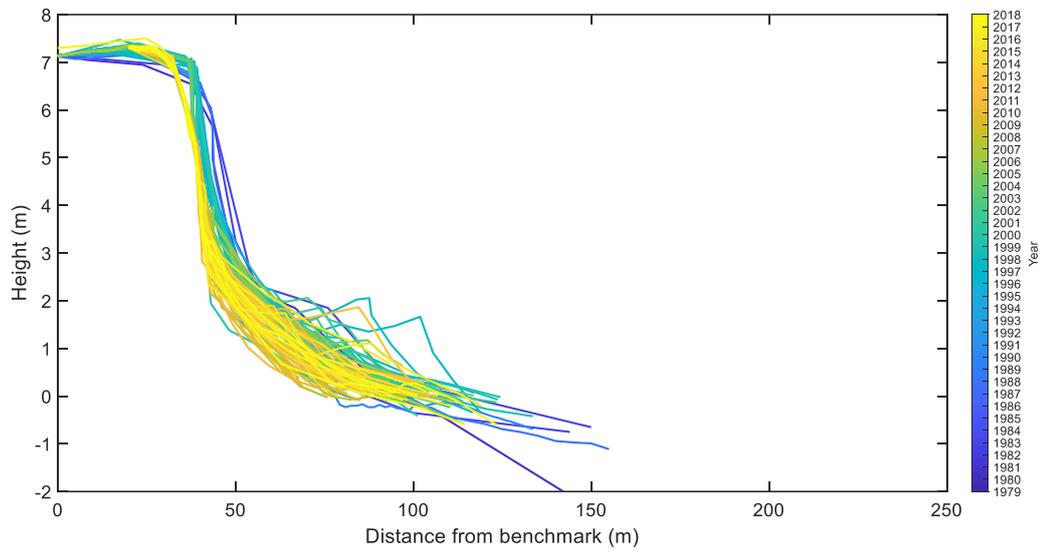
Figure B.59. Beach profile of CCS39-2, Pauanui Beach.
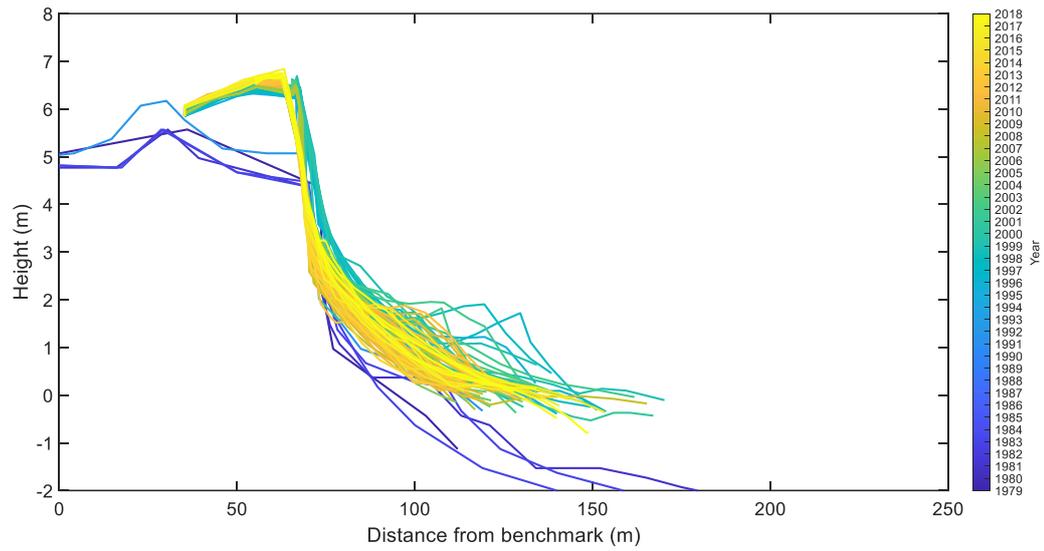
Figure B.60. Beach profile of CCS40-1, Pauanui Beach.

Opoutere Beach
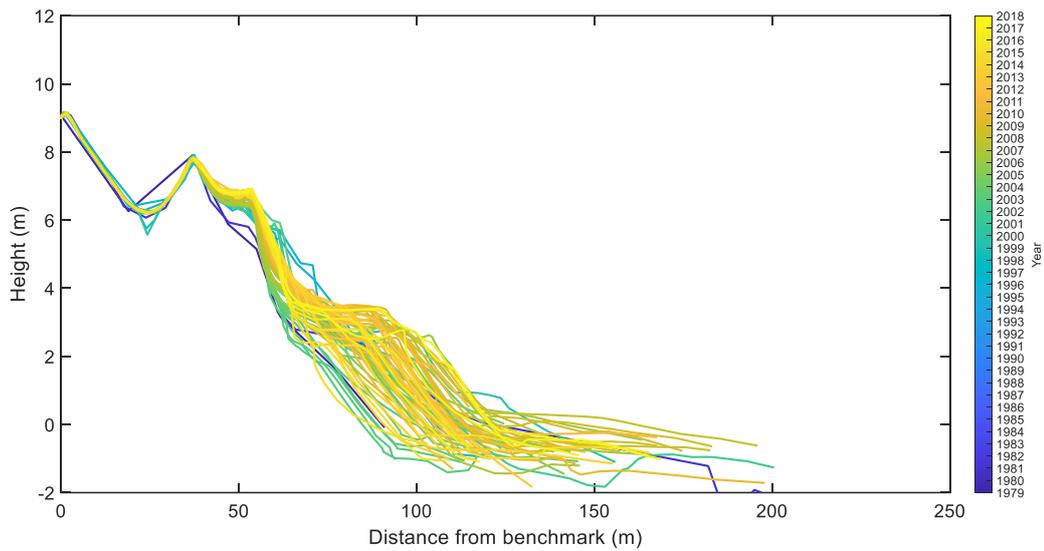
Figure B.61. Beach profile of CCS41, Opoutere Beach.
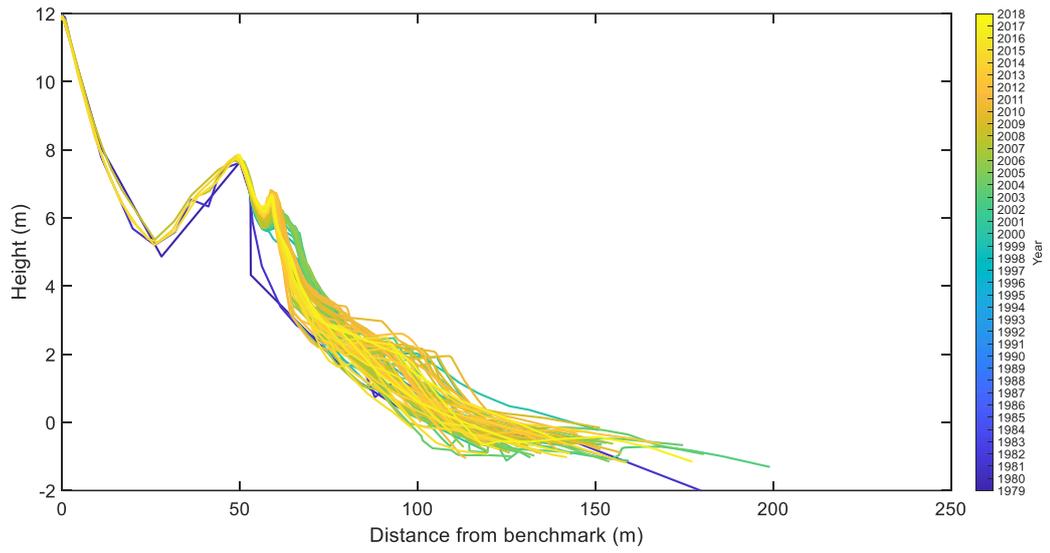
Figure B.62. Beach profile of CCS42, Opoutere Beach.
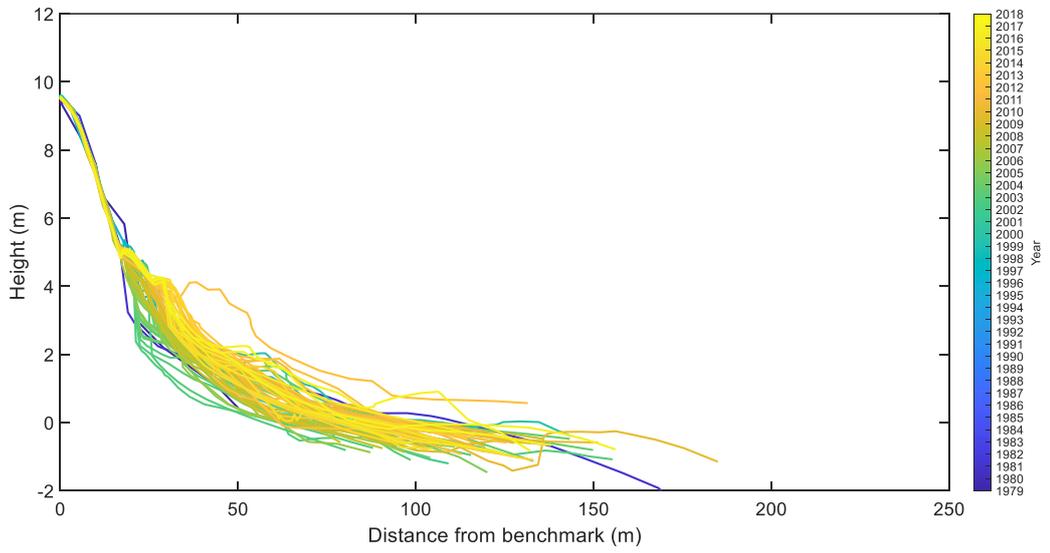
Figure B.63. Beach profile of CCS43, Opoutere Beach.
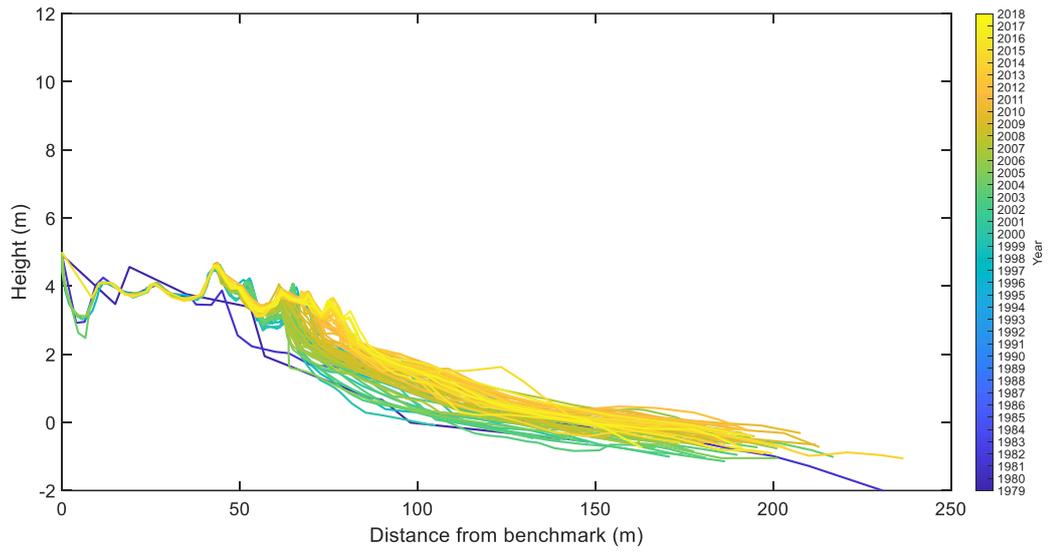
Figure B.64. Beach profile of CCS44, Opoutere Beach.

Onemana
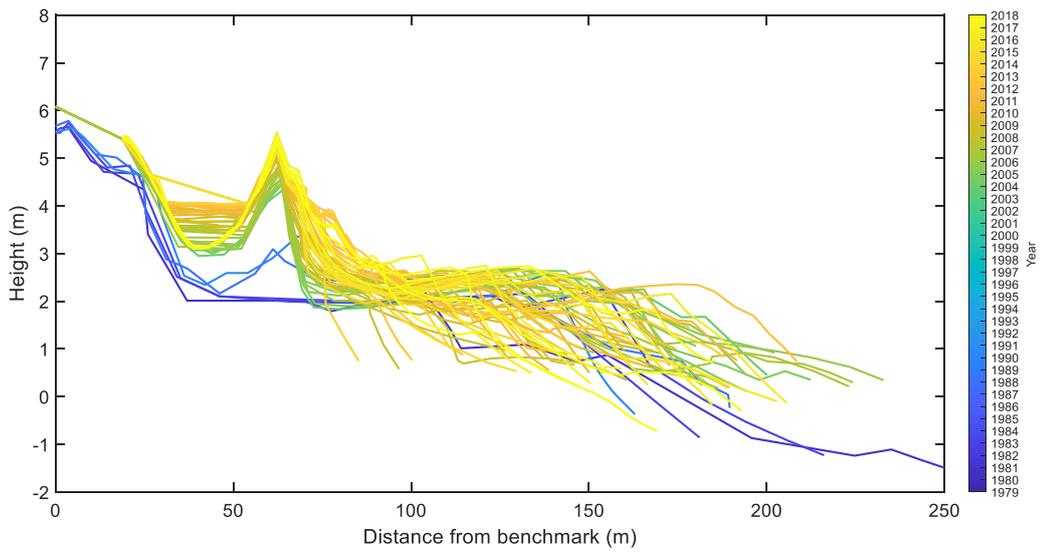
Figure B.65. Beach profile of CCS53, Onemana Beach.

218
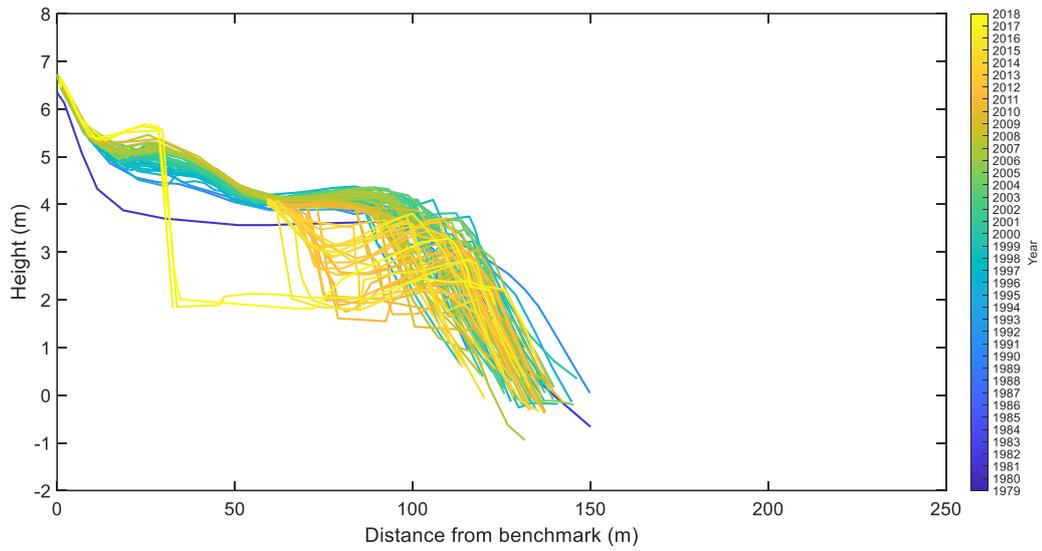
Figure B.66. Beach profile of CCS54, Onemana Beach.

Whangamata Beach
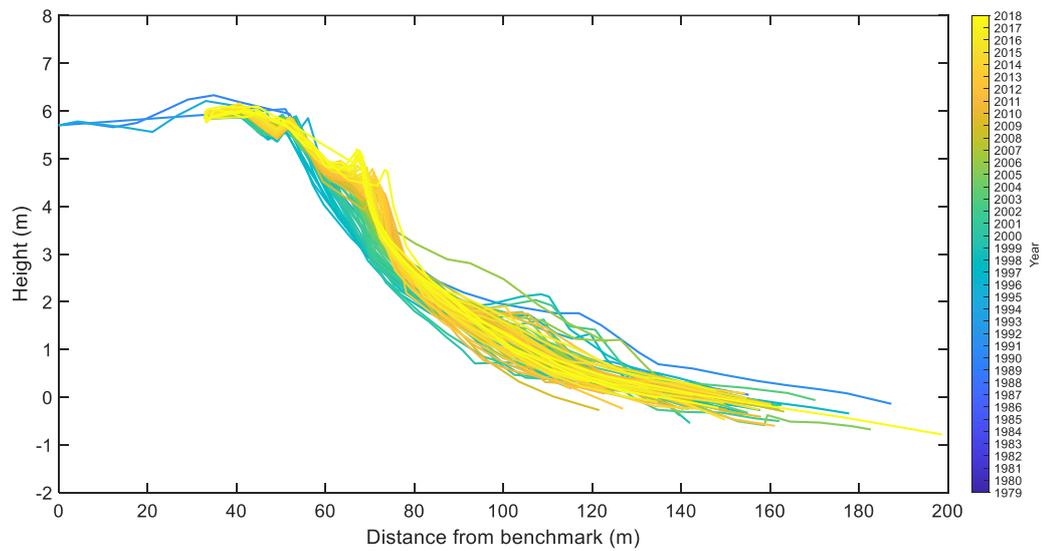
Figure B.67. Beach profile of CCS56, Whangamata Beach.
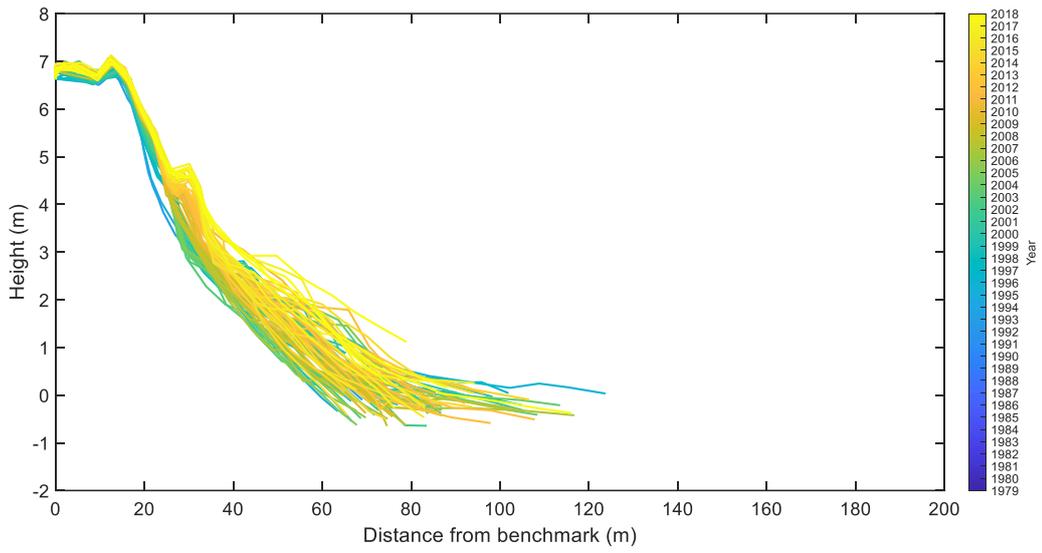
Figure B.68. Beach profile of CCS55-1, Whangamata Beach.
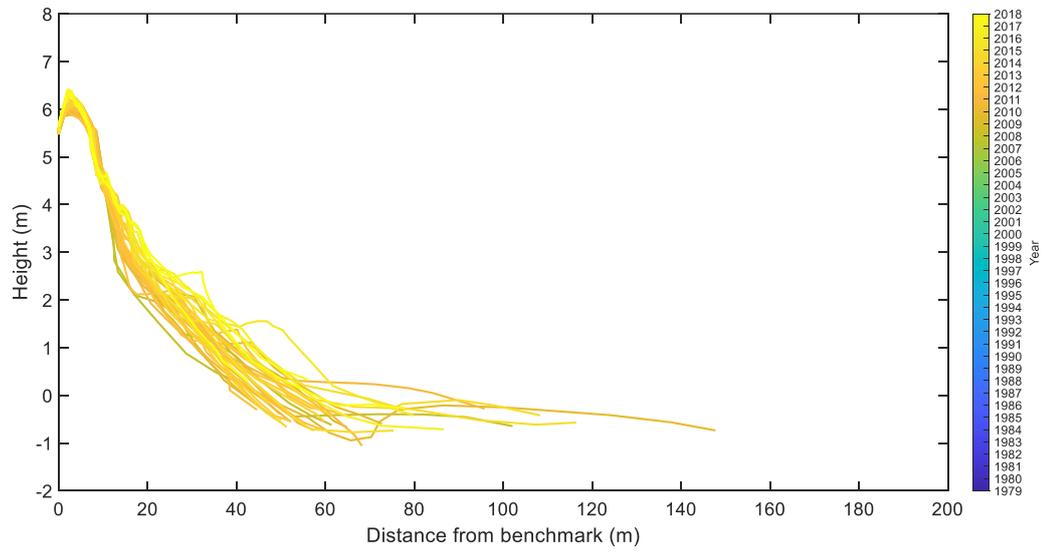
Figure B.69. Beach profile of CCS55-2, Whangamata Beach.
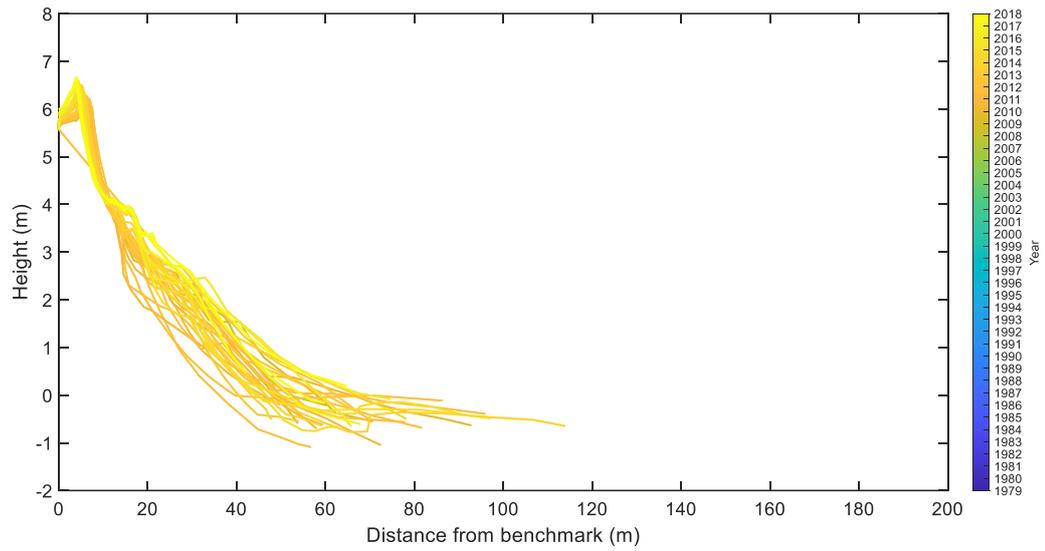
Figure B.70. Beach profile of CCS55-3, Whangamata Beach.
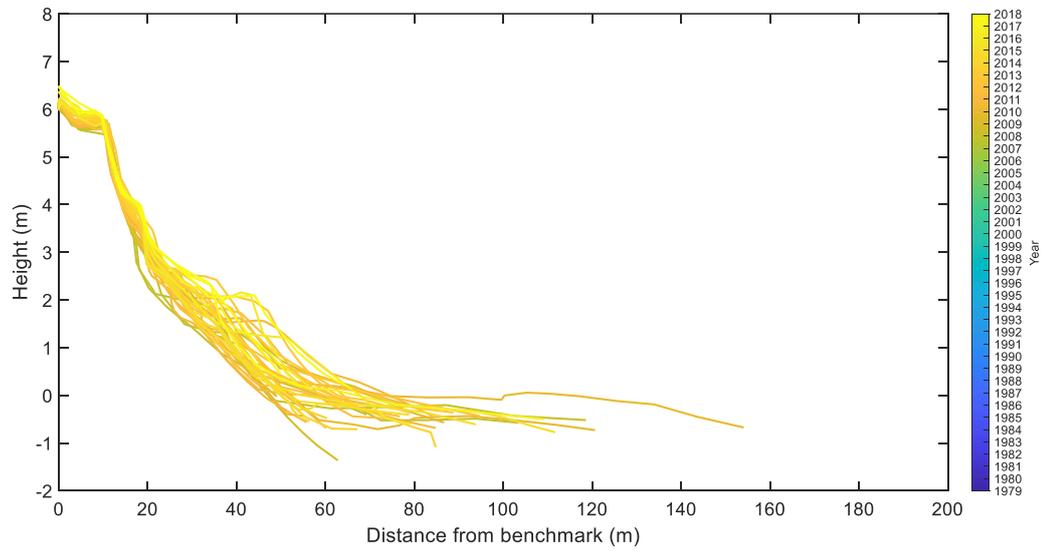
Figure B.71. Beach profile of CCS55-4, Whangmata Beach.
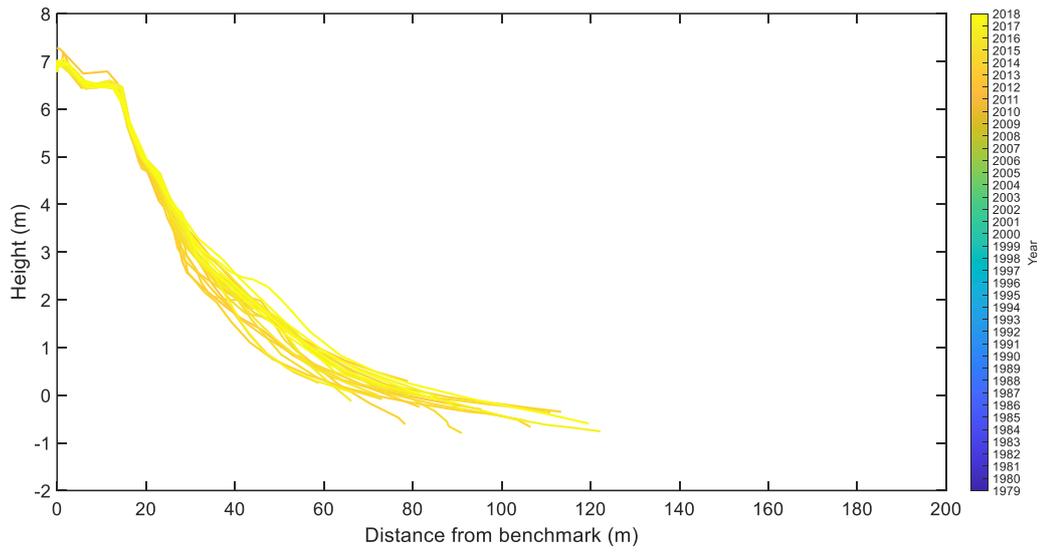
Figure B.72. Beach profile of CCS55-6, Whangamata Beach.
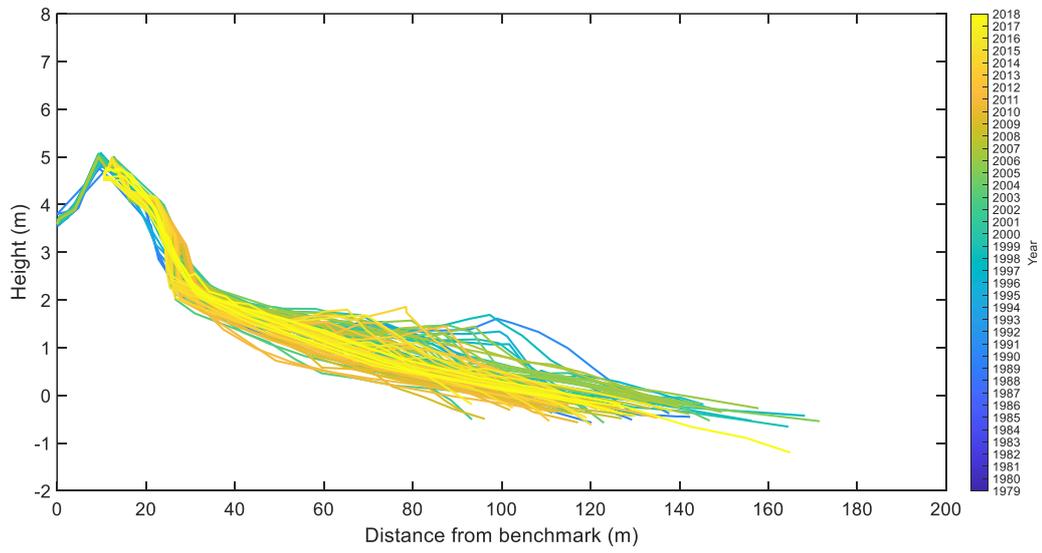
Figure B.73. Beach profile of CCS57, Whangamata Beach.
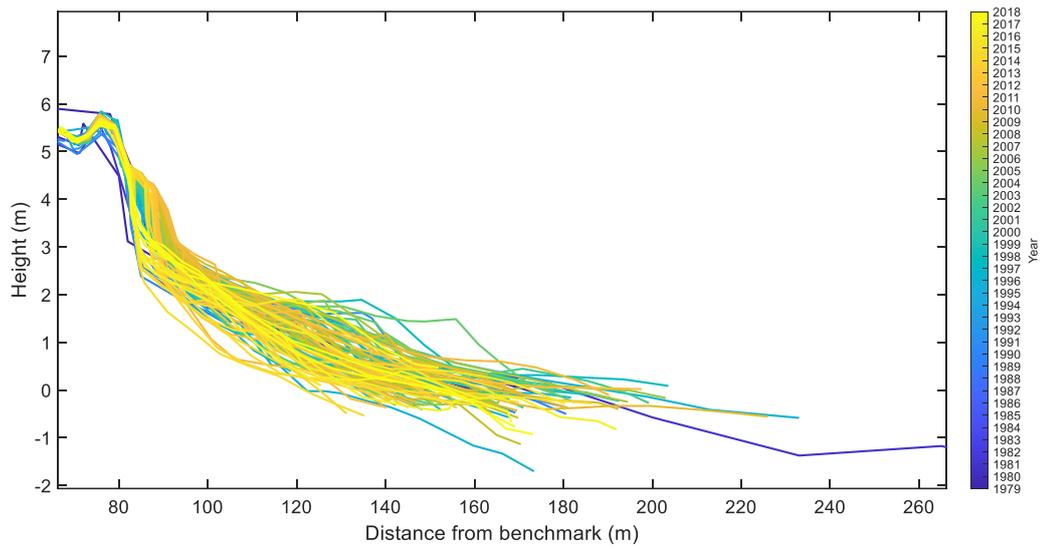
Figure B.74. Beach profile for CCS58, Whangamata Beach.
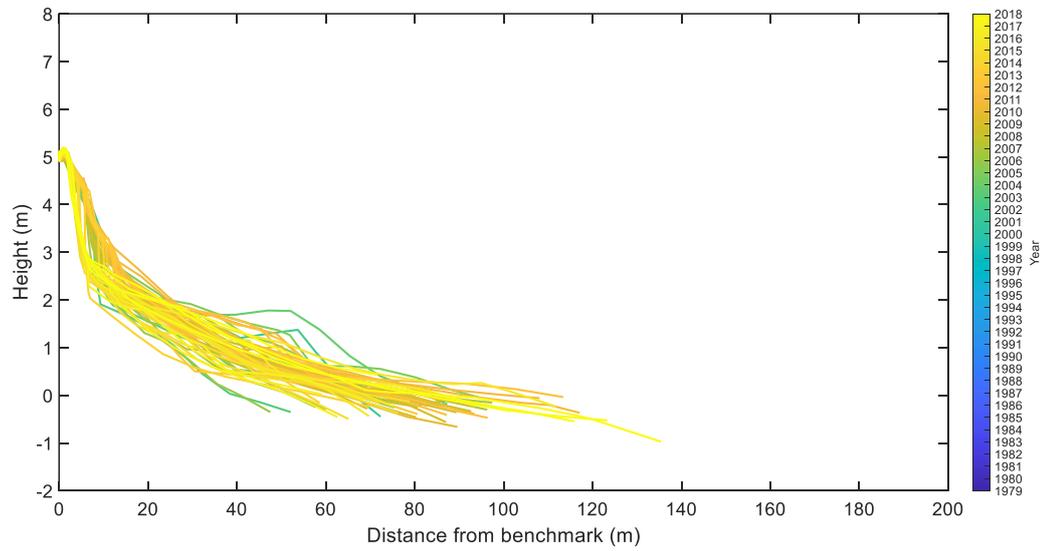
Figure B.75. Beach profile for CCS57-2, Whangamata Beach.

223
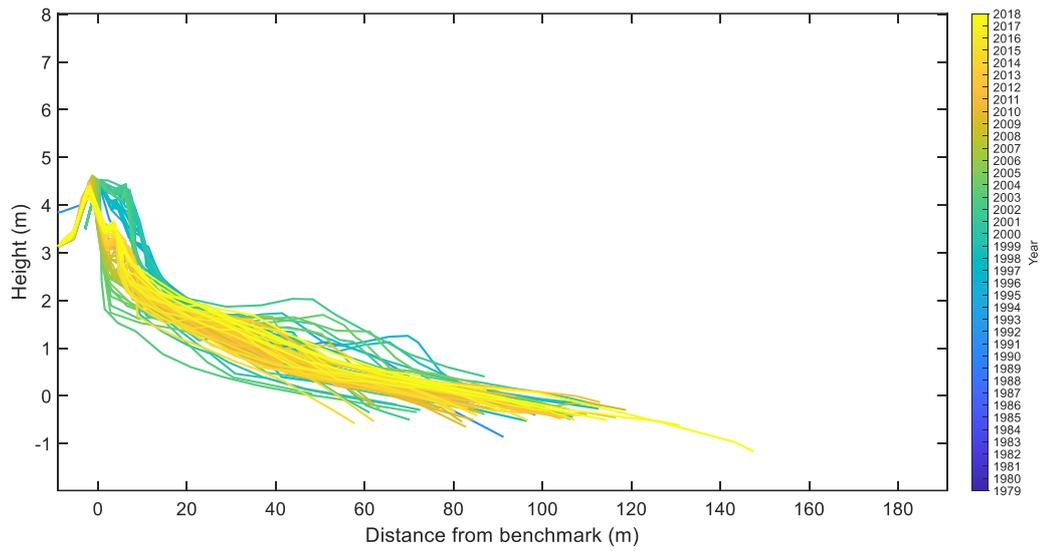
Figure B.76. Beach profile for CCS57-3, Whangamata Beach.

Whiritoa
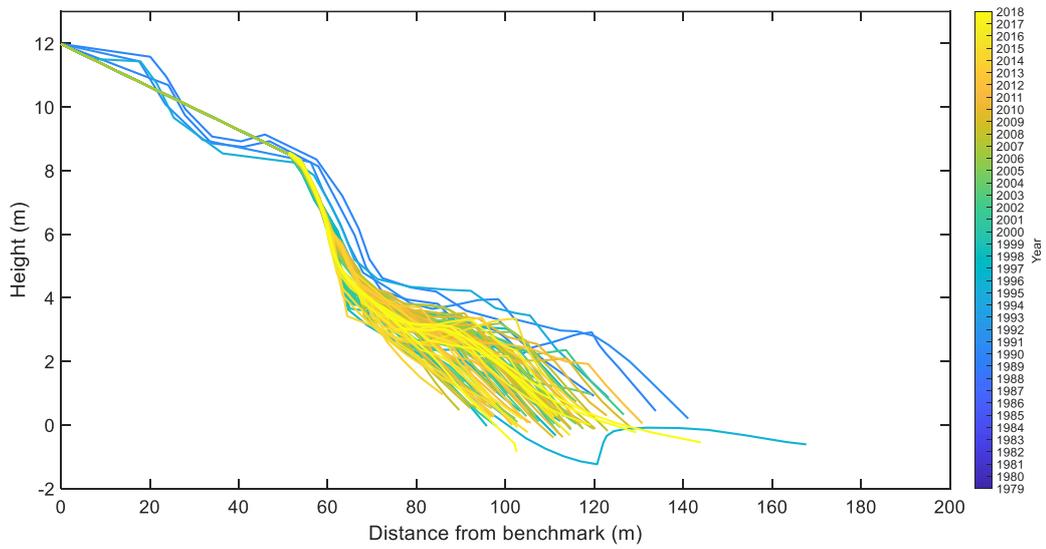
Figure B.77. Beach profile for CCS59, Whiritoa Beach.

224
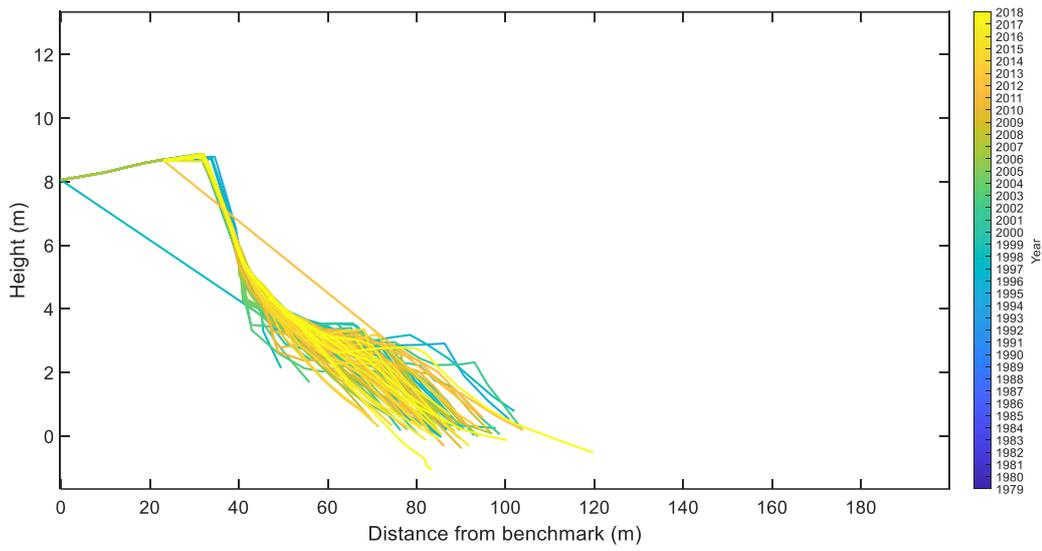
Figure B.78. Beach profile for CCS61, Whiritoa Beach.
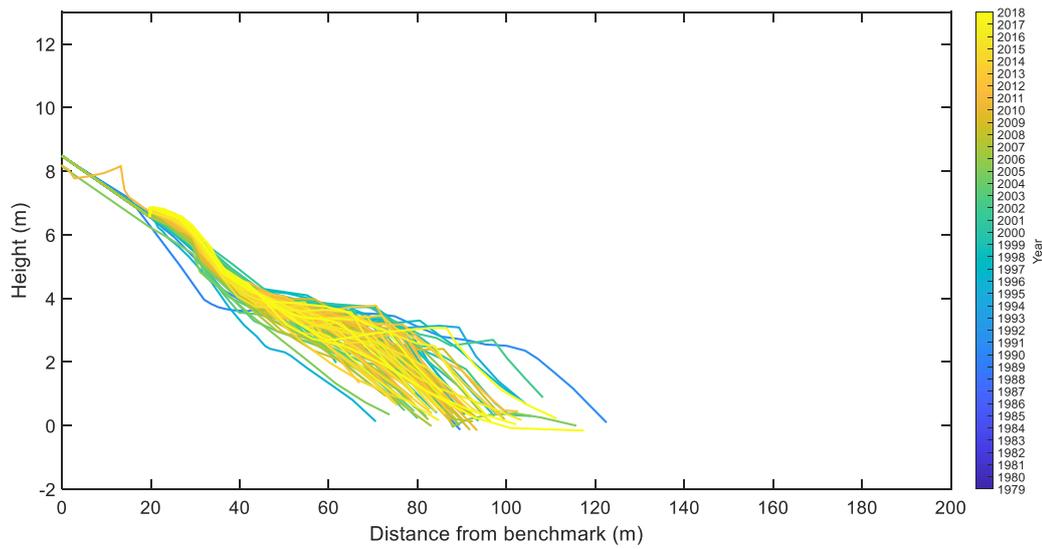
Figure B.79. Beach profile for CCS62, Whiritoa Beach.

225
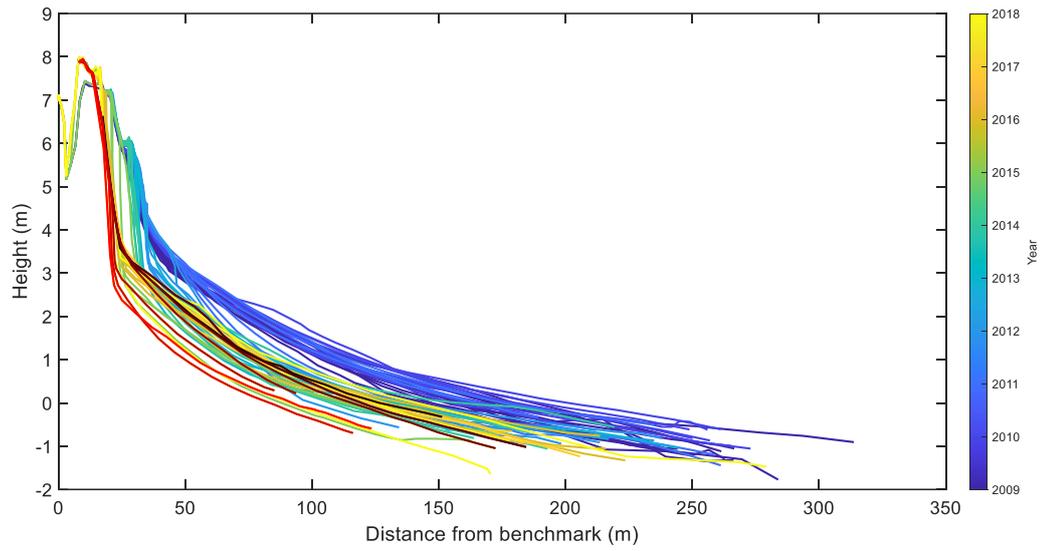
Figure B.80. Beach profile for RGN1, Ngarunui Beach, Raglan.
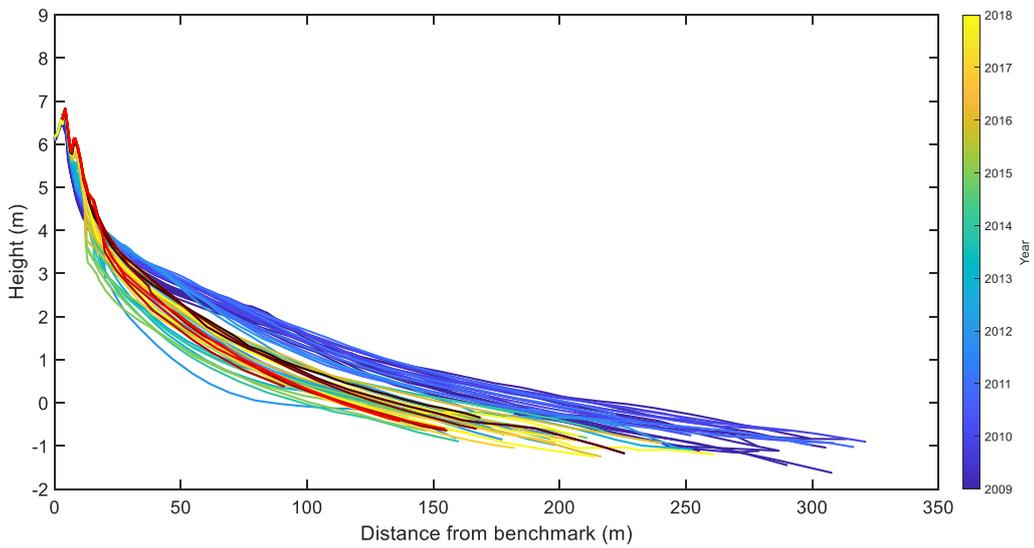
Figure B.81. Beach profile for RGN2, Ngarunui Beach, Raglan.
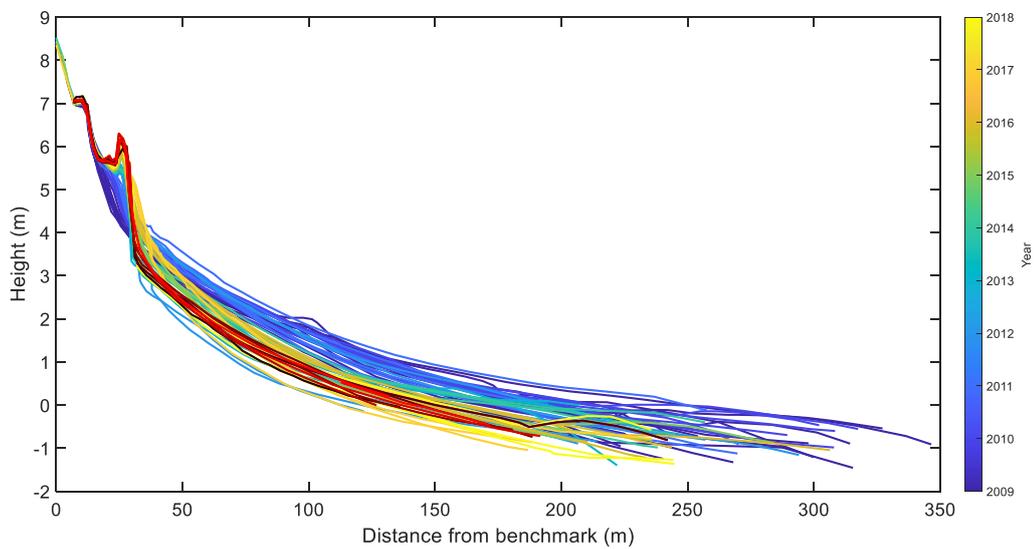
Figure B.82. Beach profile for RGN3, Ngarunui Beach, Raglan.
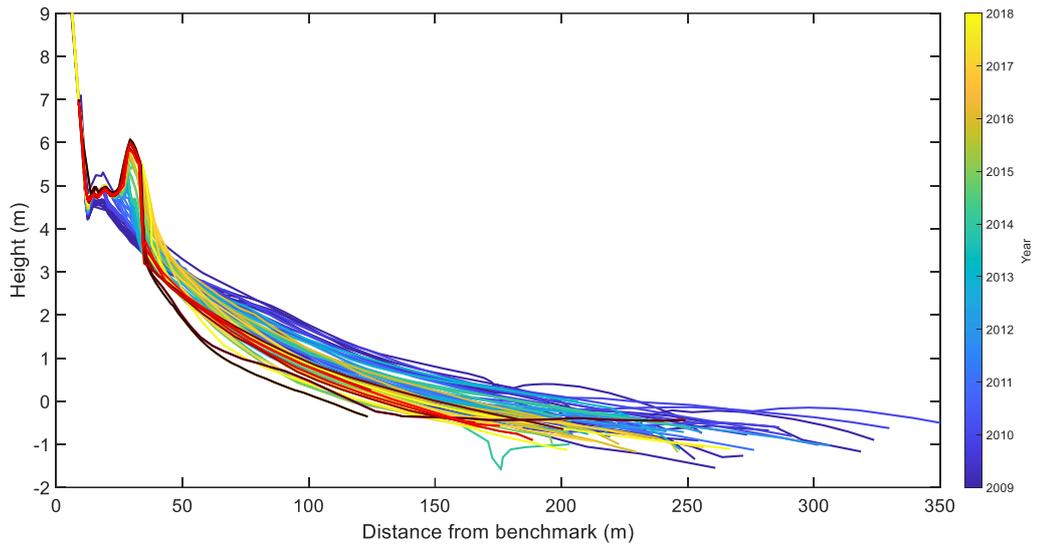
Figure B.83. Beach profile for RGN4, Ngarunui Beach, Raglan.
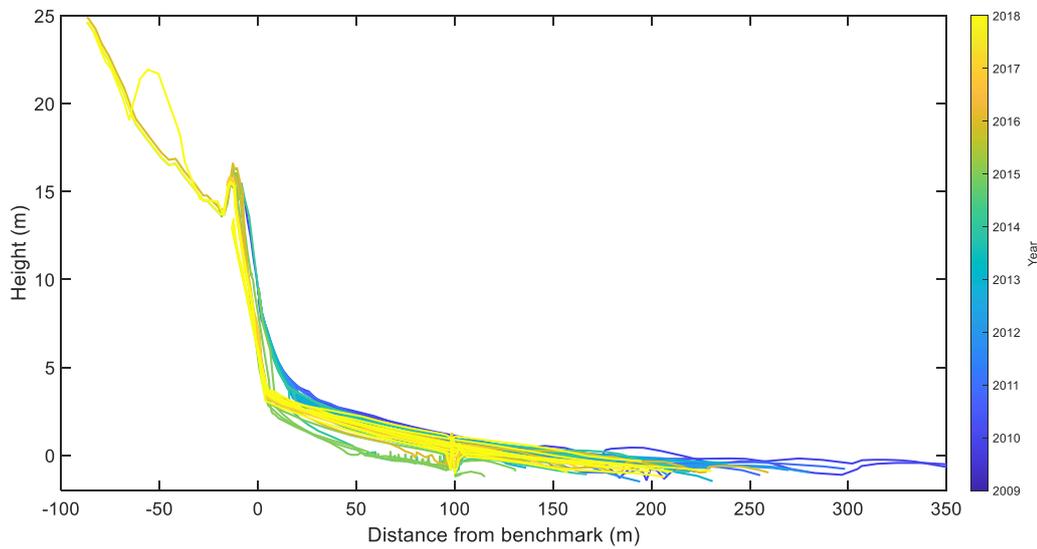
Figure B.84. Beach profile for RGN5, Ngarunui Beach, Raglan.
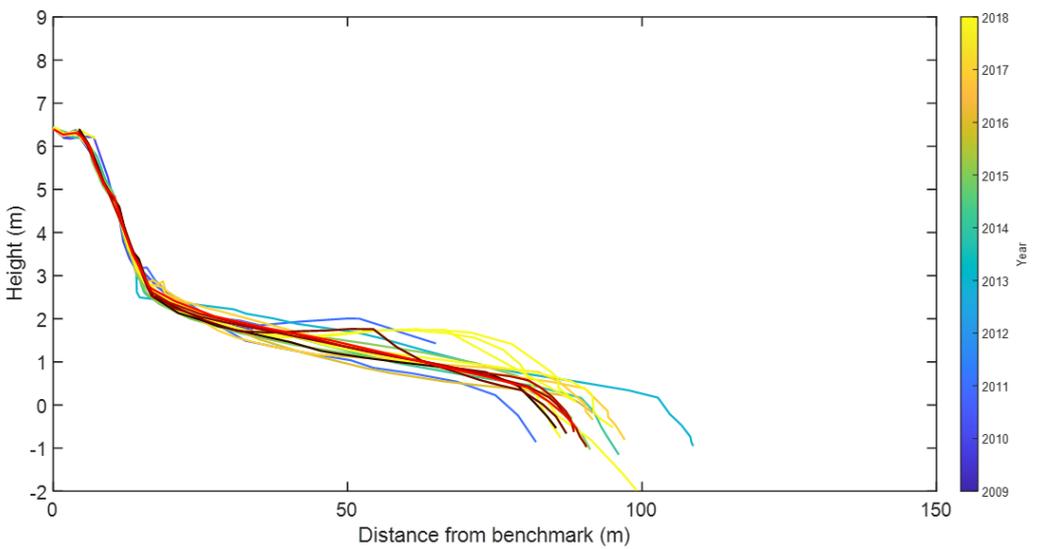
Figure B.85. Beach profile for RGNKS, Ngarunui Beach, Raglan.

227

Appendix C: Horizontal and Vertical Positions of Dune Toe and Vegetation Line

Appendix C showed the vertical height of the dune toe and vegetation line for the field survey beaches and the historic horizontal and vertical vegetation line and dune toe, along with the distribution of the dune toe and vegetation line. The height of the dune toe position for the field survey beaches were also included.

Table C.1. Reference distance (m) and height (m) for the relative distance and height of dune toe and vegetation line throughout time.

Profile Site	Date of survey	Distance (m)	Height (m)
Rings Beach			
CCS18	4th December 1991	42.40	3.63
Kuaotunu West			
CCS19-4	15th March 1995	32.00	2.92
CCS19-1	10th August 1996	36.28	5.65
CCS19-5	23 March 1997	48.30	3.47
Kuaotunu East			
CCS20	10th August 1996	23.55	3.18
CCS21	4th July 1990	106.90	3.24
Otama			
CCS45	4th December 1991	146.90	3.10
CCS46	10th September 2000	216.25	2.78
Opito			
CCS48	16th April 2000	24.55	1.97
CCS49	4th July 1996	129.60	2.27
CCS47-1	10th September 2000	8.80	2.36
CCS48-1	29th August 1999	22.31	2.30
CCS49-1	29th August 1999	31.90	3.50
Wharekaho			
CCS22	4th December 1991	49.30	4.58
CCS22-1	4th July 1996	13.30	2.78
CCS23	4th December 1991	104.80	1.43
Maramaratotara			
CCS28	22nd November 1992	86.28	2.68
Cooks Beach			
CCS29	22nd November 1992	62.90	2.36
CCS30	22nd November 1992	57.60	2.45
CCS31	4th December 1994	42.40	3.28
CCS31-1	23rd March 1997	19.10	2.42
CCS31-2	2nd December 1991	19.10	1.85
Hahei			
CCS32	22nd November 1992	11.20	4.63
CCS33	8th September 1995	83.90	3.70

Table C.2. Reference distance (m) and height (m) for the relative distance and height of dune toe and vegetation line throughout time.

Profile Site	Date of survey	Distance (m)	Height (m)
Pauanui			
CCS38	10th December 2004	64.50	4.37
CCS39	7th December 2007	80.60	4.08
CCS38-1	27th July 1995	82.40	3.06
CCS39-1	27th July 1995	63.50	3.09
CCS39-2			
CCS40-1			
Opoutere			
CCS41	8th September 2006	56.35	5.54
CCS42	17th January 1996	58.70	5.70
CCS43	2nd February 2000	29.35	2.57
CCS44	8th September 2006	62.35	3.49
Onemana			
CCS53	29th July 1996	58.60	4.28
CCS54	9th August 1998	48.50	4.23
Whangamata North			
CCS55-1	10th August 1996	23.55	3.18
CCS56	1st December 1991	71.20	3.50
CCS55-2	1st August 2008	12.30	3.45
CCS55-3	12th December 2009	7.55	5.97
CCS55-4	14th June 2008	20.30	2.97
CCS55-6	6th June 2013	26.60	3.79
Whangamata South			
CCS57	1st December 1990	33.30	1.95
CCS57-3	1st December 1991	5.30	3.24
CCS57-2	8th September 2002	10.90	2.90
CCS58	27th July 1995	86.60	3.40
Whiritoa			
CCS59	29th March 1995	66.00	5.20
CCS61	29th March 1995	42.10	4.87
CCS62	29th March 1995	35.80	4.55

Whangapoua Beach
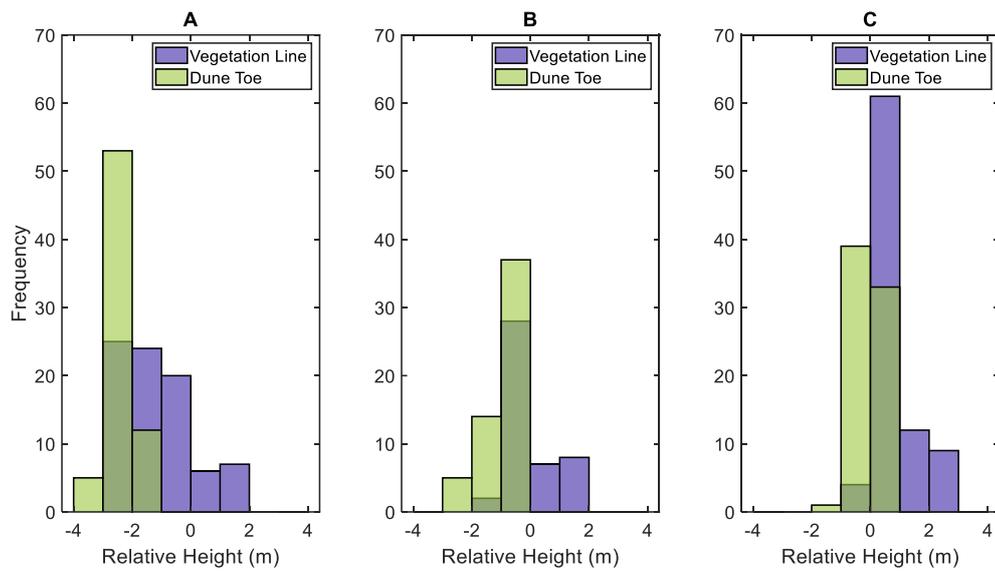
Figure C.1. The frequency of relative height position of the vegetation line and dune toe, Whangapoua Beach. The vegetation line (blue line) and dune toe (green line) for at the beach profile sites of CCS11 (A), CCS11-1 (B), CCS12 (C).
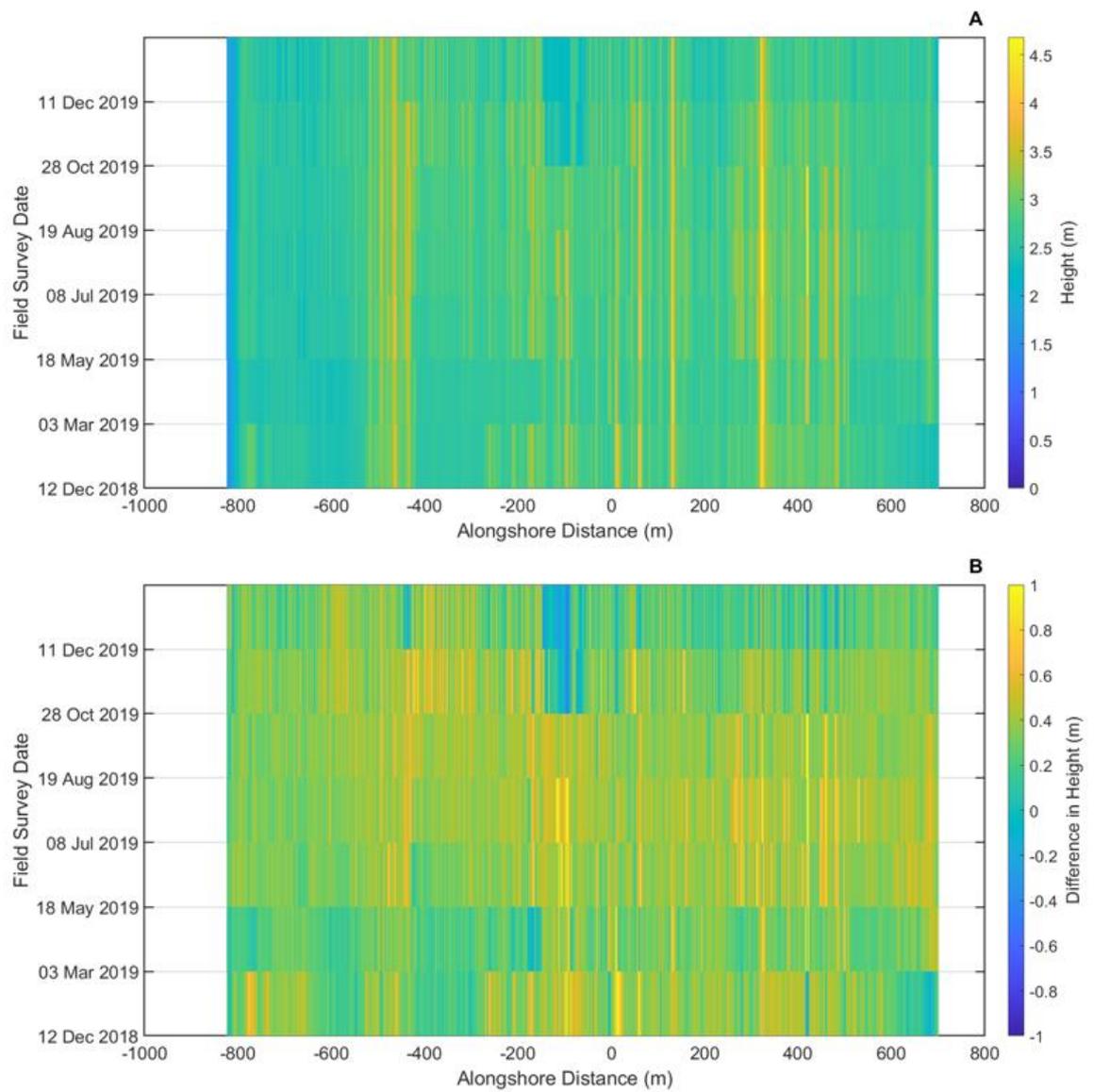
Figure C.2. The height of the dune toe and the difference in height of the dune toe from the mean height of the dune toe, Whangapoua Beach. Each bar represents a field survey of the dune toe and the colour represents the height of the dune toe (A) and the difference in height from the mean height of the dune toe (B). Field surveys were taken 9th December 2018, 3rd March 2019, 18th May 2019, 8th July 2019, 19th August 2019, 28th October 2019 and 11th December 2019.
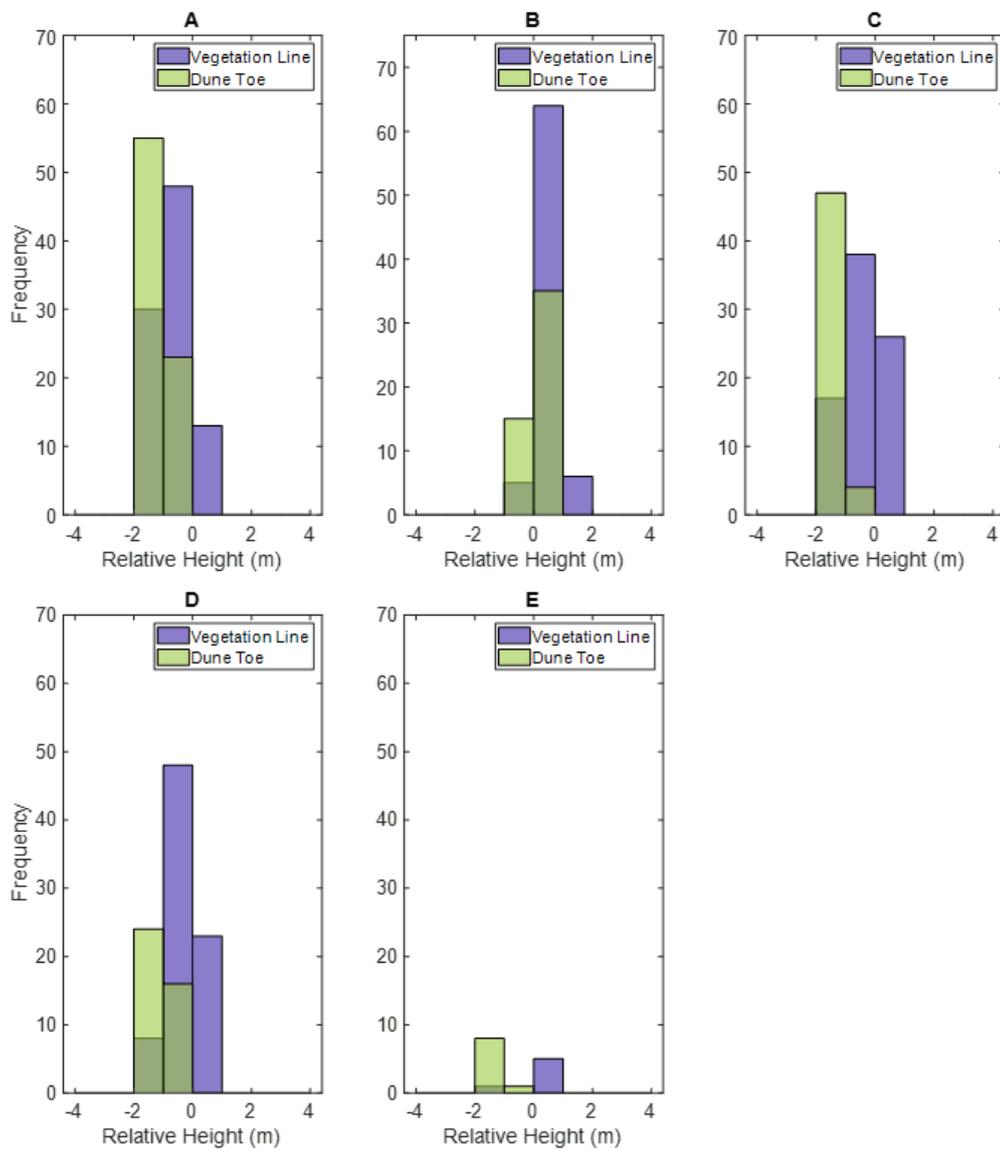
Matarangi Beach

Figure C.3. The frequency of relative height position of the vegetation line and dune toe, Matarangi Beach. The vegetation line (blue line) and dune toe (green line) for at the beach profile sites of CCS13 (A), CCS14 (B), CCS15 (C), CCS16 (D), CCS17 (E).
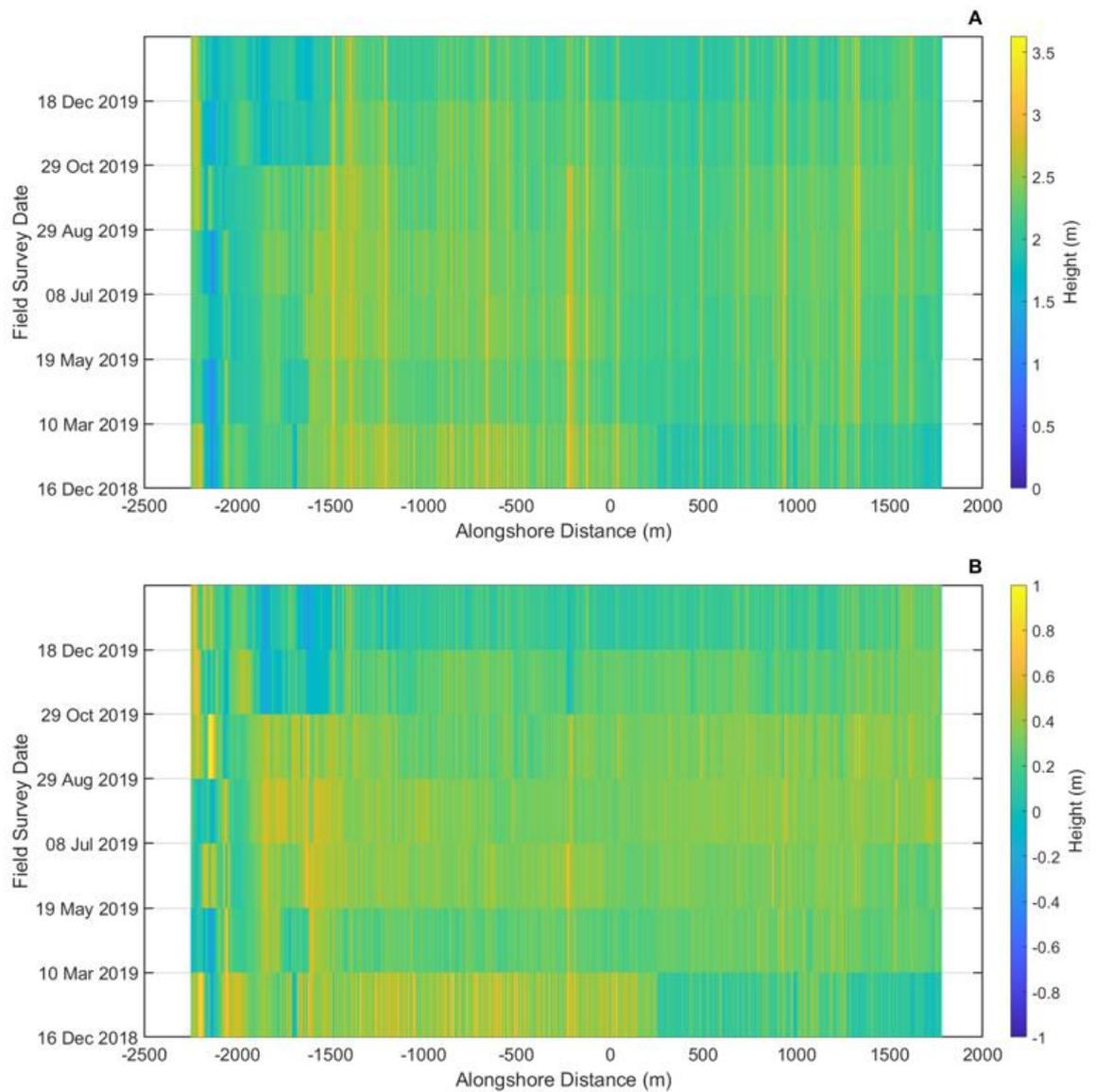
Figure C.4. The height of the dune toe and the difference in height of the dune toe from the mean height of the dune toe, Matarangi Beach. Each bar represents a field survey of the dune toe and the colour represents the height of the dune toe (A) and the difference in height from the mean height of the dune toe (B). Field surveys were taken on 16th December 2018, 10th March 2019, 19th May 2019, 8th July 2019, 29th August 2019, 29th October 2019 and 18th December 2019.

Buffalo Beach
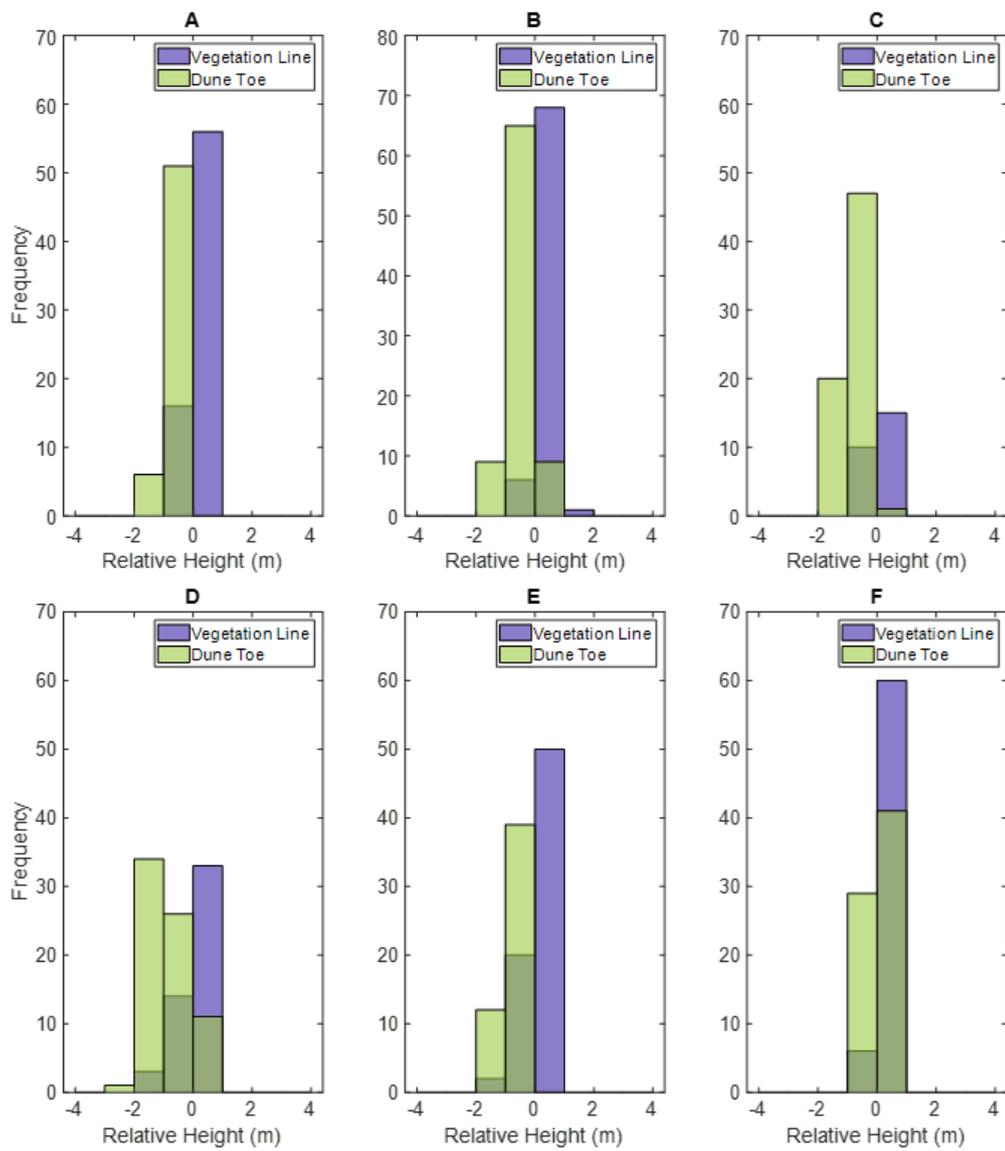
Figure C.5. The frequency of relative height position of the vegetation line and dune toe, Buffalo Beach. The vegetation line (blue line) and dune toe (green line) for at the beach profile sites of CCS24 (A), CCS25 (B), CCS25-2 (C), CCS25-3 (D), CCS25/1 (E) and CCS26 (F).
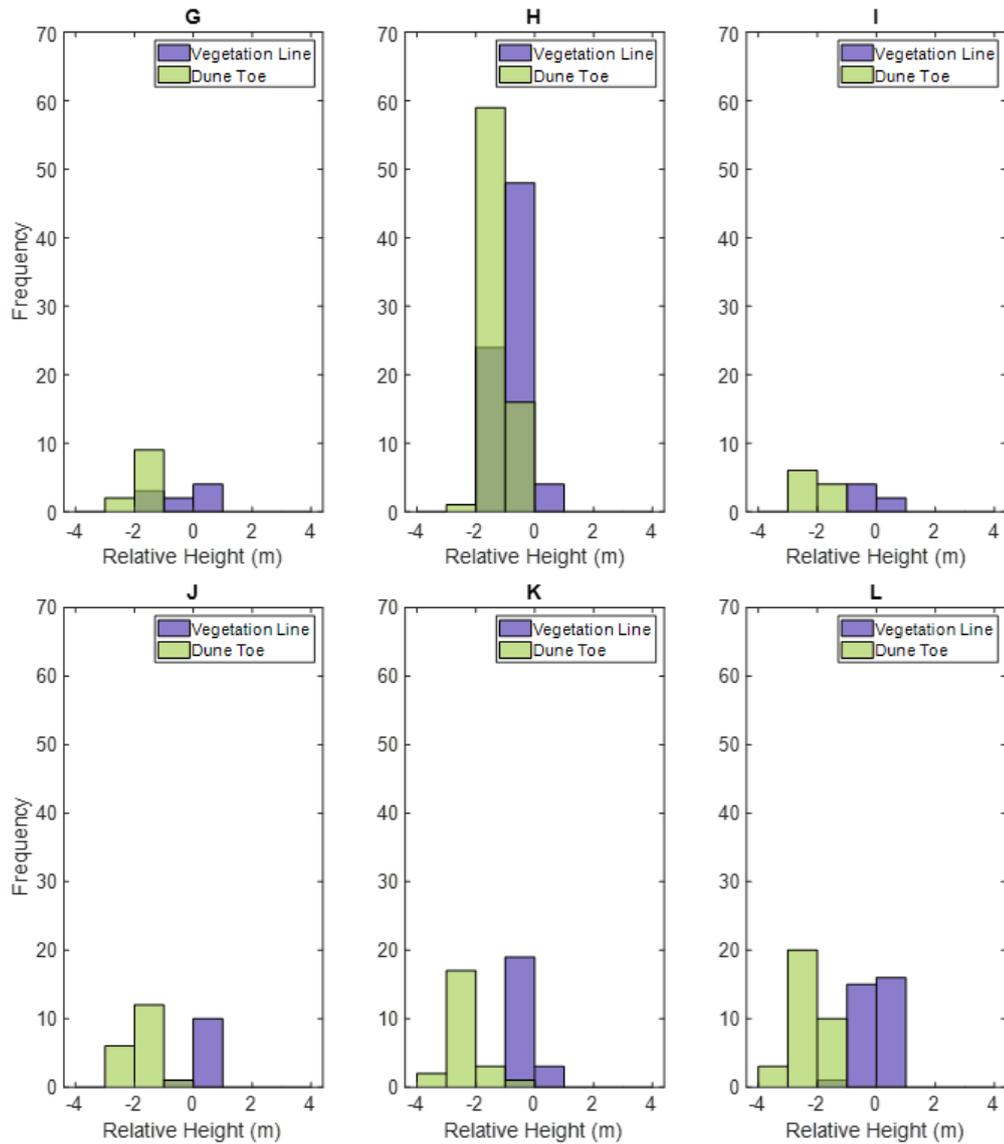
Figure C.6. The frequency of relative height position of the vegetation line and dune toe, Buffalo Beach. The vegetation line (blue line) and dune toe (green line) for at the beach profile sites of CCS26/1 (G), CCS27 (H), CCS27/10 (I), CCS27/8(J), CCS27/6 (K) and CCS27/2 (L).
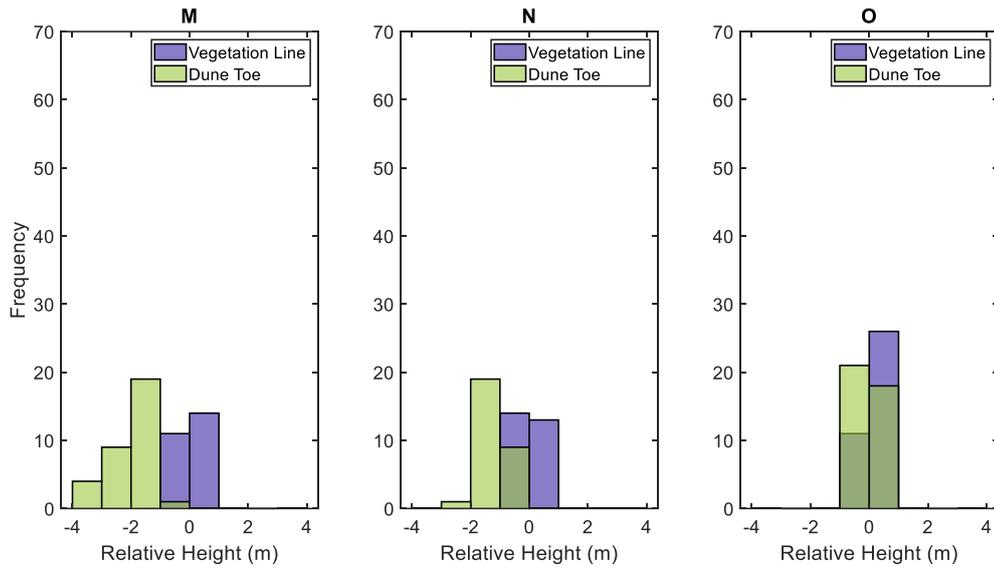
Figure C.7. The frequency of relative height position of the vegetation line and dune toe, Buffalo Beach. The vegetation line (blue line) and dune toe (green line) for at the beach profile sites of CCS27/3 (M), CCS27/4 (N) and CCS27/5 (O).

North Buffalo Beach
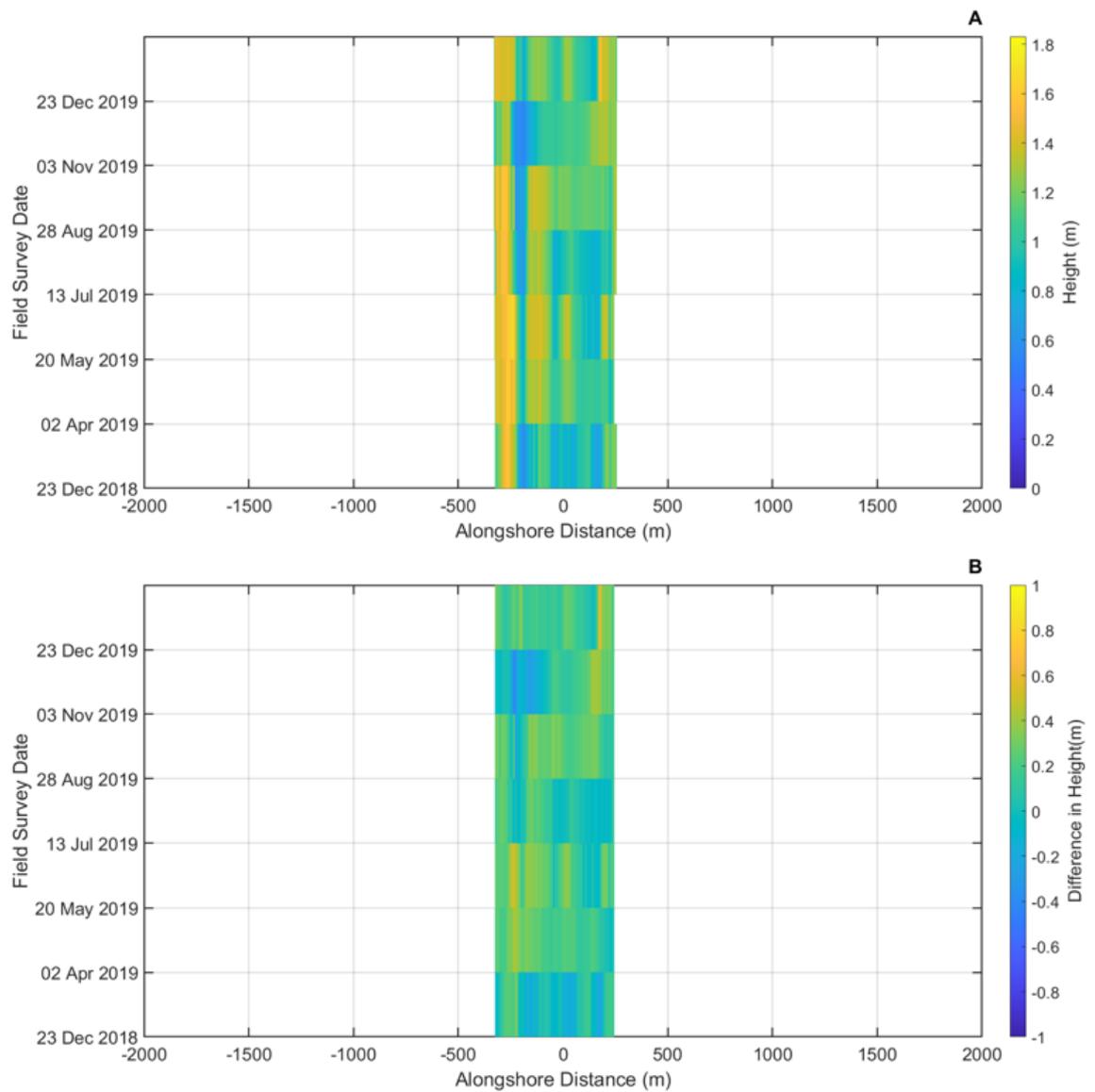
Figure C.8. The height of the dune toe and the difference in height of the dune toe from the mean height of the dune toe, North Buffalo Beach. Each bar represents a field survey of the dune toe and the colour represents the height of the dune toe (A) and the difference in height from the mean height of the dune toe (B). Field surveys were taken on 23rd December 2018, 2nd April 2019, 20th May 2019, 13th July 2019, 23rd August 2019, 3rd November 2019 and 23rd December 2019.

Middle Buffalo Beach
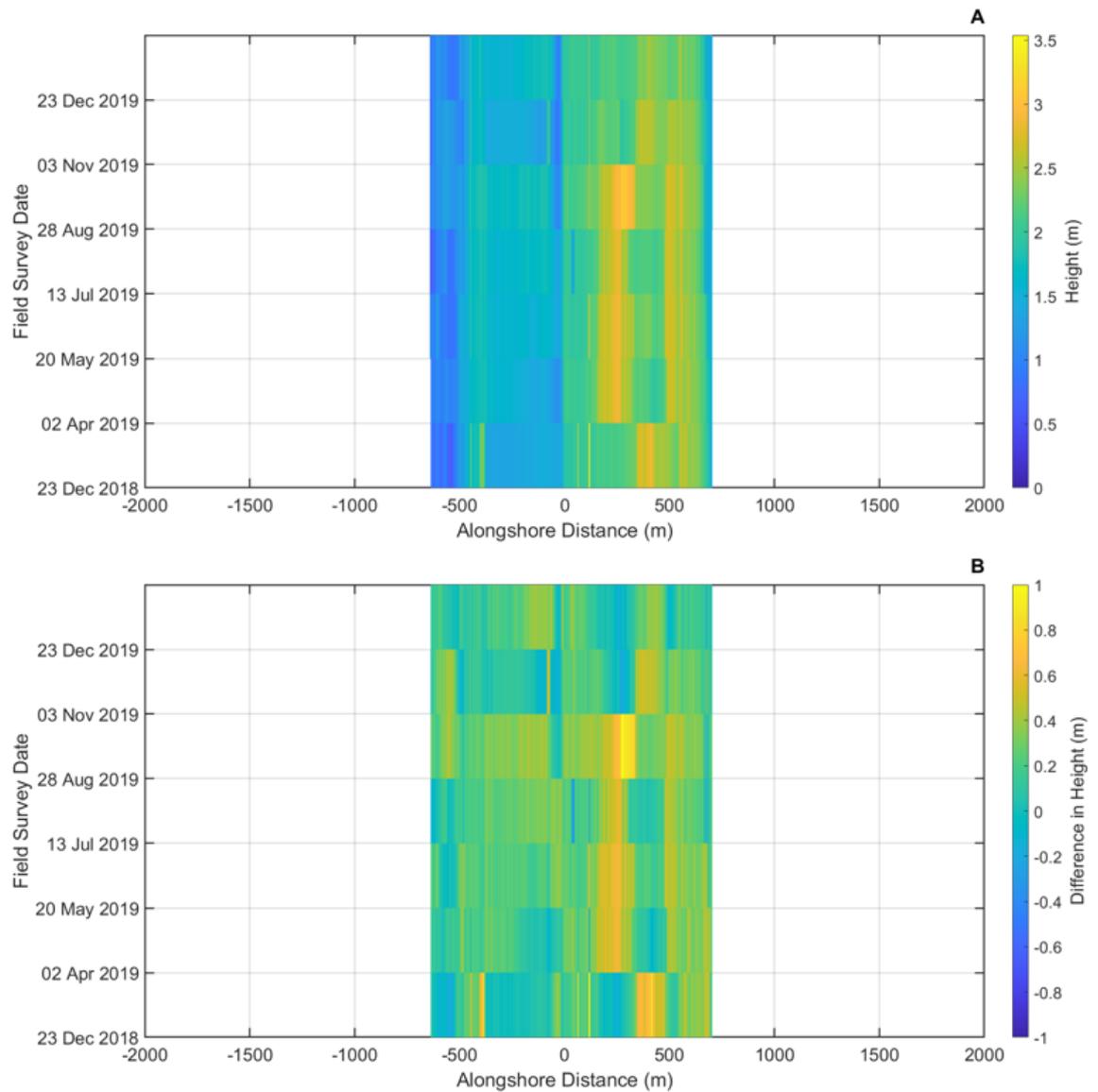
Figure C.9. The height of the dune toe and the difference in height of the dune toe from the mean height of the dune toe, Middle Buffalo Beach. Each bar represents a field survey of the dune toe and the colour represents the height of the dune toe (A) and the difference in height from the mean height of the dune toe (B). Field surveys were taken on 23rd December 2018, 2nd April 2019, 20th May 2019, 13th July 2019, 23rd August 2019, 3rd November 2019 and 23rd December 2019.

South Buffalo Beach
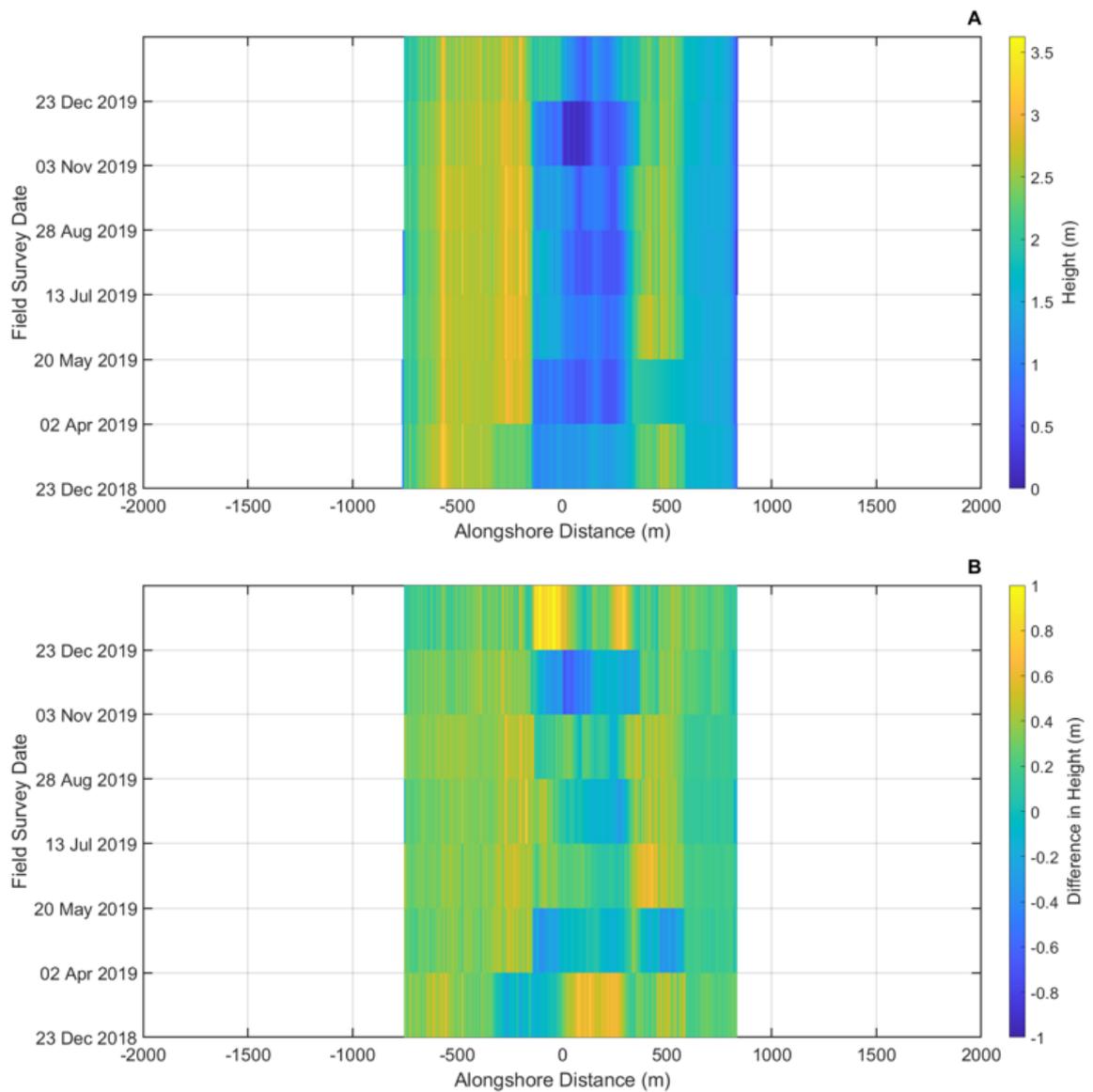
Figure C.10. The height of the dune toe and the difference in height of the dune toe from the mean height of the dune toe, South Buffalo Beach. Each bar represents a field survey of the dune toe and the colour represents the height of the dune toe (A) and the difference in height from the mean height of the dune toe (B). Field surveys were taken on 23rd December 2018, 2nd April 2019, 20th May 2019, 13th July 2019, 23rd August 2019, 3rd November 2019 and 23rd December 2019.

Hot Water Beach
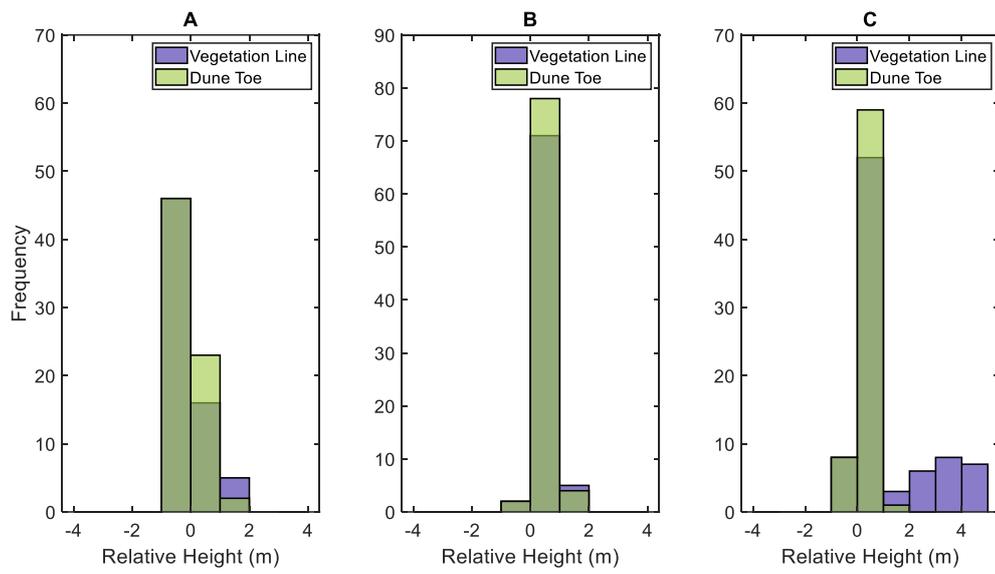
Figure C.11. The frequency of relative height position of the vegetation line and dune toe, Buffalo Beach. The vegetation line (blue line) and dune toe (green line) for at the beach profile sites of CCS34 (A), CCS35 (B) and CCS35-1 (C).
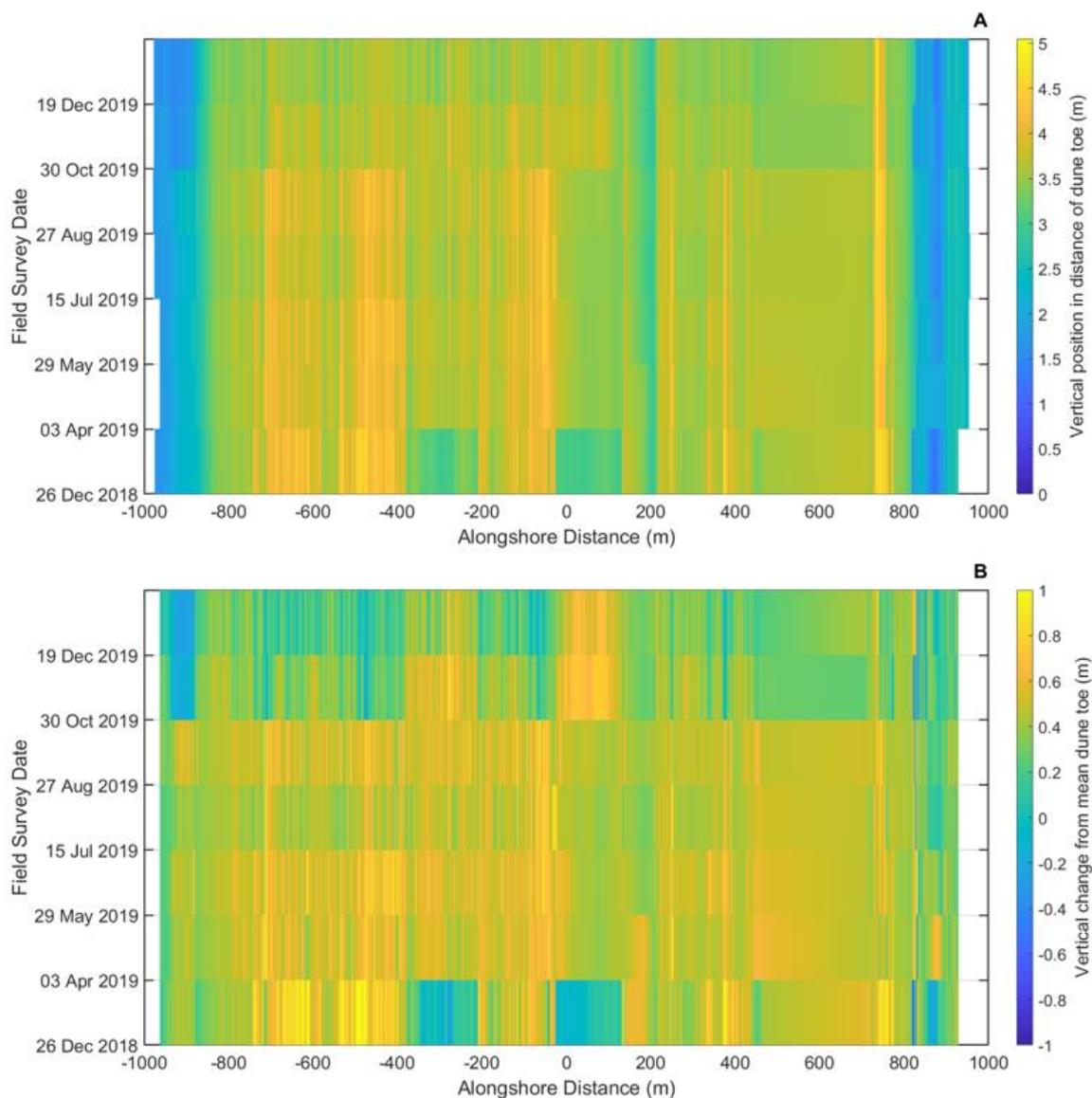
Figure C.12. The height of the dune toe and the difference in height of the dune toe from the mean height of the dune toe, Hot Water Beach. Each bar represents a field survey of the dune toe and the colour represents the height of the dune toe (A) and the difference in height from the mean height of the dune toe (B). Field surveys were taken on 26th December 2018, 3rd April 2019, 29th May 2019, 15th July 2019, 27th August 2019, 30th October 2019 and 19th December 2019.

Tairua Beach
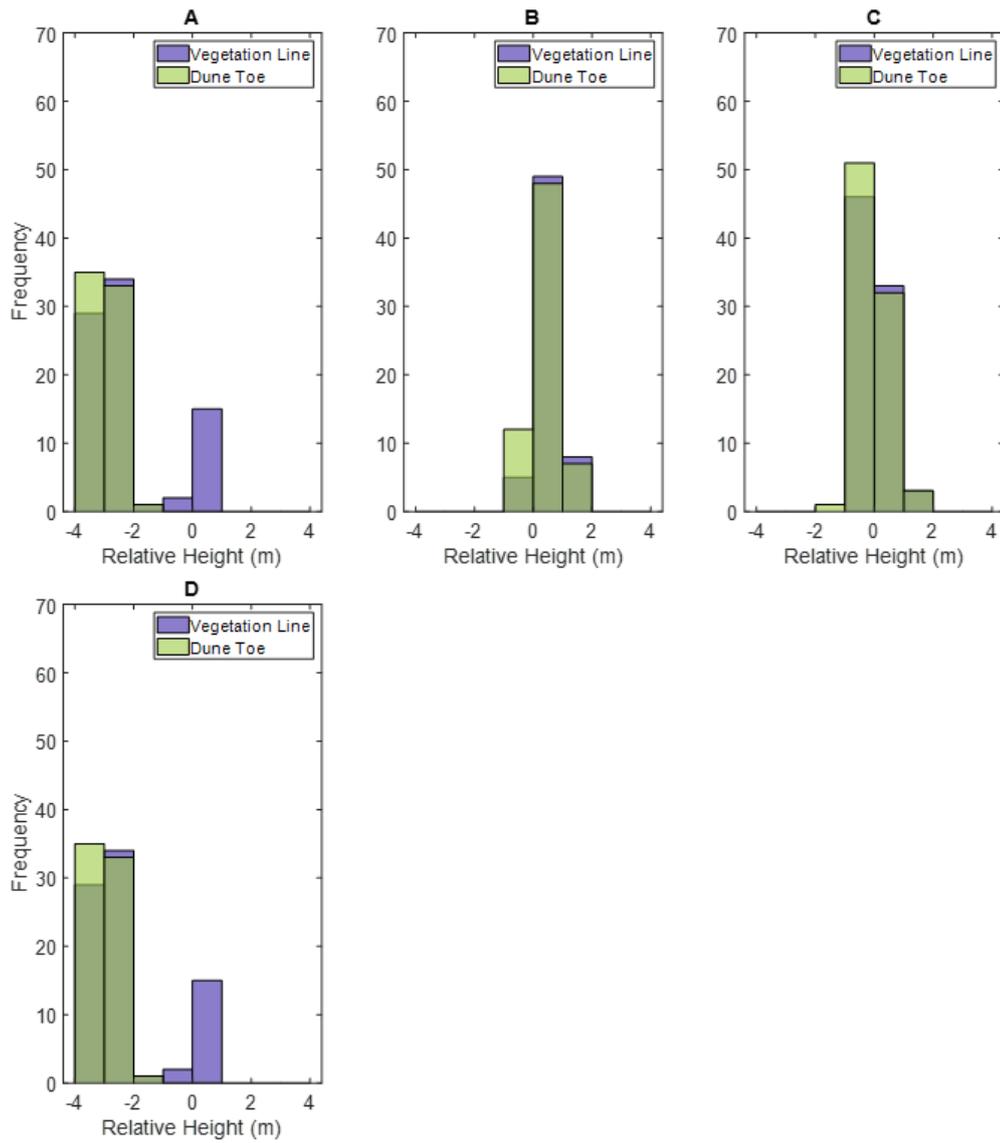
Figure C.13. The frequency of relative height position of the vegetation line and dune toe, Buffalo Beach. The vegetation line (blue line) and dune toe (green line) for at the beach profile sites of CCS36 (A), CCS36-2 (B), CCS36-1 (C) and CCS37 (D).
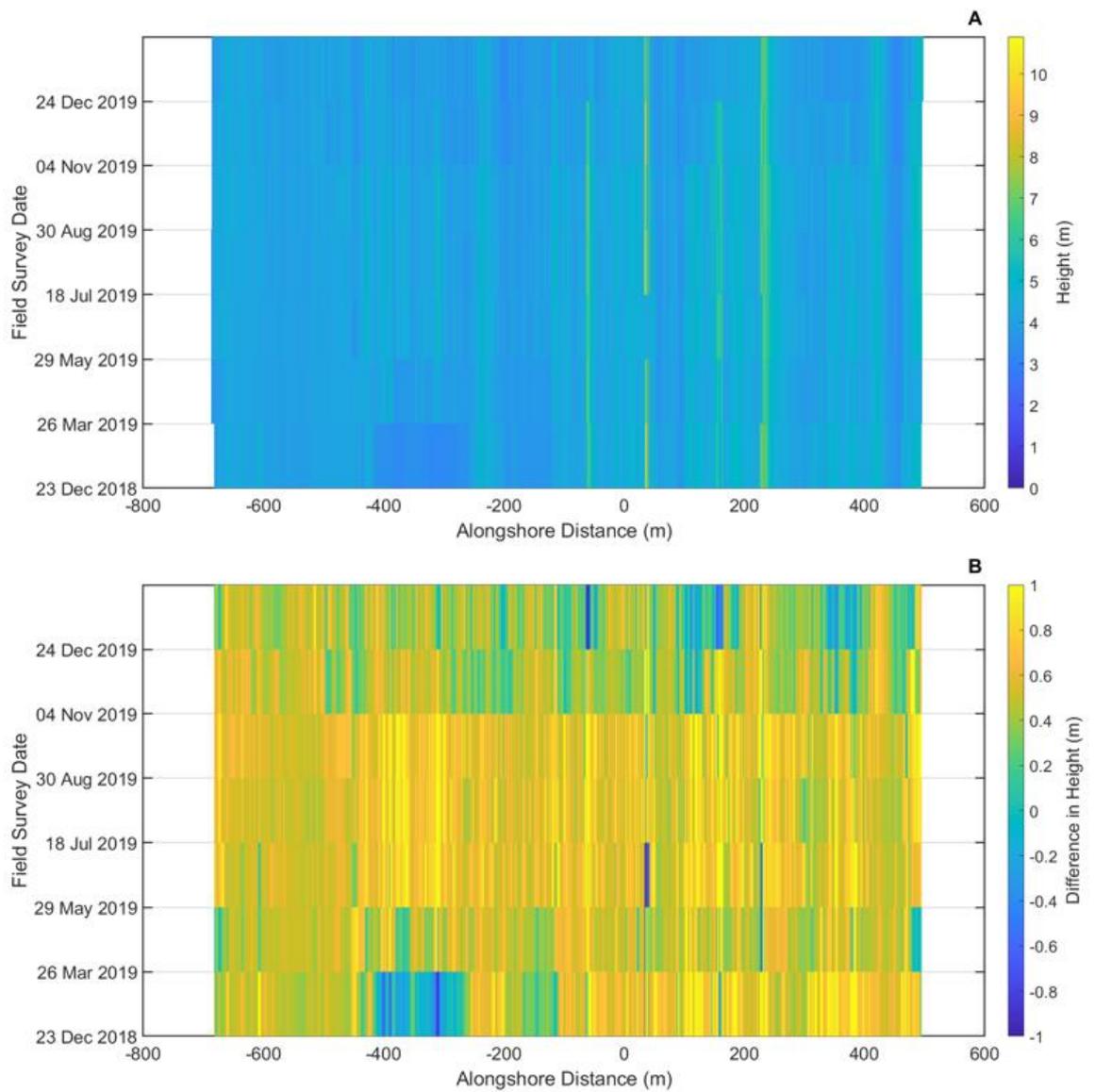
Figure C.14. The height of the dune toe and the difference in height of the dune toe from the mean height of the dune toe, Tairua Beach. Each bar represents a field survey of the dune toe and the colour represents the height of the dune toe (A) and the difference in height from the mean height of the dune toe (B). Field surveys were taken on 23rd December 2018, 26th March 2019, 18th July 2019, 30th August 2019, 4th November 2019 and 24th December 2019.